BMI/ONWI-624

Brine Migration Test Report: Asse Salt Mine, Federal Republic of Germany

Technical Report

January 1987

A. J. Coyle
J. Eckert
H. Kalia

Office of Nuclear Waste Isolation
Battelle Memorial Institute
505 King Avenue
Columbus, OH 43201-2693

ONWI
Office of Nuclear Waste Isolation

BATTELLE Project Management Division

BIBLIOGRAPHIC DATA

Coyle, A. J., J. Eckert, and H. Kalia, 1987. *Brine Migration Test Report: Asse Salt Mine, Federal Republic of Germany*, BMI/ONWI-624, Office of Nuclear Waste Isolation, Battelle Memorial Institute, Columbus, OH.

NOTICE

Printed in the United States of America
Available from
National Technical Information Service
U.S. Department of Commerce
5285 Port Royal Road
Springfield, VA 22161

NTIS price codes
Printed copy: A13
Microfiche copy: A01

BMI/ONWI-624
Distribution Category UC-70

BMI/ONWI--624

DE87 004144

Brine Migration Test Report: Asse Salt Mine, Federal Republic of Germany

Technical Report

January 1987

A. J. Coyle
J. Eckert
H. Kalia

Office of Nuclear Waste Isolation
Battelle Memorial Institute
505 King Avenue
Columbus, OH 43201-2693

The content of this report was effective as of June 1986. The report was prepared by Battelle Project Management Division, Office of Nuclear Waste Isolation, under Contract No. DE-AC02-83CH10140 with the U.S. Department of Energy.

DISCLAIMER

ABSTRACT

This report presents a summary of Brine Migration Tests which were undertaken at the Asse mine of the Federal Republic of Germany (FRG) under a bilateral U.S./FRG agreement. This experiment simulates a nuclear waste repository at the 800-m (2,624-ft) level of the Asse salt mine in the Federal Republic of Germany. This report describes the Asse salt mine, the test equipment, and the pretest properties of the salt in the mine and in the vicinity of the test area. Also included are selected test data (for the first 28 months of operation) on the following: brine migration rates, thermomechanical behavior of the salt (including room closure, stress reading, and thermal profiles), borehole gas pressures, and borehole gas analyses. In addition to field data, laboratory analyses of pretest salt properties are included in this report. The operational phase of these experiments was completed on October 4, 1985, with the commencement of cooldown and the start of posttest activities.

FOREWORD

The National Waste Terminal Storage Program was established in 1976 by the U.S. Department of Energy's (DOE) predecessor, the Energy Research and Development Administration. In September 1983, this program became the Civilian Radioactive Waste Management (CRWM) Program. Its purpose is to develop technology and provide facilities for the safe, environmentally acceptable, permanent disposal of high-level nuclear waste (HLW). HLW includes wastes from both commercial and defense sources, such as spent (used) fuel from nuclear power reactors, accumulations of wastes from the production of nuclear weapons, and solidified wastes from fuel reprocessing.

The information in this report pertains to the test facilities studies of the Salt Repository Project of the Office of Geologic Repositories in the CRWM Program.

SUMMARY

This report provides preliminary results of the joint Brine Migration Tests conducted by the U.S. Department of Energy (DOE) and the Federal Republic of Germany (FRG) at the Asse mine in the Federal Republic of Germany to determine the impact of heat on salt. When a heat source is placed in salt, traces of water contained in the salt migrate to the heat source. Since laboratory tests do not completely represent the in situ environment, a large-scale brine migration test is being performed in the Asse salt mine to obtain an understanding of the brine migration mechanisms at depth.

The primary objectives of the test are the observation of the effects of heat and gamma radiation on brine migration, the types of gases produced in the boreholes, the temperature distribution, and the thermomechanical behavior of the salt formation. The data obtained will be used to verify the validity of numerical models. The tests are performed in the main halite ($Na_2\beta$) of the Asse salt mine that is considered to be a typical FRG repository-type salt. The complete experiment, composed of four nearly identical test sites, is designed to be performed at a maximum salt temperature of 210°C (410°F) having a 3°C/cm (13.72°F/in) temperature gradient at the borehole wall.

Test sites 1 and 3 were originally pressurized while test sites 2 and 4 are maintained at atmospheric pressure. The vapor and gases in the latter boreholes are circulated by diaphragm pump through a cold trap that removes any moisture and gives a measure of brine migration rates. Noncondensable vapors and gases are recirculated to and through the boreholes. In addition, test sites 1 and 2 are nonradioactive while test sites 3 and 4 are radioactive. At the radioactive sites, the radiation of the waste is simulated by cobalt-60 sources which subject the boreholes to 3×10^8 rads per year.

During and after completion of test site mining, a number of samples were taken to determine the chemical-mineralogical composition and the water content of the salt. The salt is composed of 94.0 wt % halite, 4.0 wt % polyhalite, and 2.0 wt % anhydrite. These values represent an overall average of about 200 samples.

After installation and checkout of the test equipment, the nonradioactive sites 1 and 2 were started on May 25, 1983, and the radioactive sites 3 and 4 were started on December 15, 1983. All the tests are scheduled to end in December 1985. Within this report are the data obtained in the years 1983 through September 1985. Also included are descriptions of cooldown and post-test activities along with preliminary observations of interest.

Central heaters and guard heaters are used to maintain the designed borehole wall temperature and the correct thermal gradient. Temperature data are taken at various locations out to a radial distance of 2.2 m (7.2 ft). Within 7 months after start-up, it became necessary to increase the central heater power and the guard heater at certain sites to achieve the designed borehole wall temperature of 210°C (410°F) and thermal gradient of 3°C/cm (13.7°F/in).

The collected brine, which was measured in a cold trap, was 0.122 l (0.032 gal) after 838 days at test site 2 and 0.135 l (0.035 gal) after

654 days at test site 4. Starting on October 24, 1984, brine was collected at test site 3 because a leak developed in the test volume, resulting in a decision to allow test site 3 to become a nonpressurized site. Test site 1, which was still under pressurized conditions, accumulated brine until the end of the testing period when the brine was then collected in the cold trap.

In gas samples taken from the boreholes, hydrogen was found in both the nonradioactive and the radioactive sites. It is assumed that hydrogen is produced mainly by a corrosion reaction between the brine and the waste package under heated conditions. Another source of hydrogen is the hydrocarbons that are known to occur in rock salt.

Four independent methods are used to measure the room closure and rock mass displacements. The most interesting result of these measurements is the floor heave of about 87 mm (3.43 in) within 838 days after start-up of operation.

Stress measurements are being performed using two different gages: flat cells at test site 2 and strain-gaged stress meters at test sites 1 and 2. By the end of the testing period, all the flat cells had failed, except for one in the central borehole. Laboratory calibrations of the stress gages indicated that the direct readings of the flat cells are to be corrected by approximately 2 MPa (290 psi) and additional calibrations are necessary to convert the voltage readings of the strain-gaged stress meters to bars of pressure.

Conclusions derived from the operational phase are as follows:

1. Most of the test equipment and instrumentation worked satisfactorily for the entire testing period. The major problems encountered were the failure of the flat cells and the leakage in test site 3.

2. The measured results for temperature and room closure are very close to the predicted results.

3. The brine migration is much less than predicted. This discrepancy is mainly due to using a standard laboratory-determined permeability. In situ permeability measurements of Avery Island and Asse salt are several orders of magnitude less than those used in the predictive models (liquid and vapor transport models).

4. The initial measurement of brine accumulation at test site 3, after depressurization, was much less than one-half of the quantity collected at nonpressurized sites 2 and 4 after equal periods of exposure to heat. Therefore, the pressurized borehole apparently retarded the vapor transport mode of brine migration.

5. Analyses of gas samples from the boreholes do not reflect any noticeable effects of intense gamma radiation, i.e., chlorine ions, hydrogen, or hydrogen chloride.

6. The effects of intense gamma radiation were not reflected in any major differences in brine migration rates.

7. Posttest laboratory analyses will be conducted to thoroughly investigate the effects of gamma radiation on brine migration rates, gas content, corrosion, and salt properties.

TABLE OF CONTENTS

TABLE OF CONTENTS
(Continued)

LIST OF TABLES

LIST OF TABLES
(Continued)

LIST OF FIGURES

LIST OF FIGURES
(Continued)

1.0 INTRODUCTION

This document is the Asse mine test report on the Cooperative German-American Brine Migration Tests that were completed at the Asse salt mine in the Federal Republic of Germany (FRG). This FRG government-supported mine serves as an underground test facility for research and development work in the field of nuclear waste repository research and for simulation experiments.

The project represents a cooperative effort between the Office of Nuclear Waste Isolation (ONWI) of the Battelle Memorial Institute at Columbus, Ohio, and the German Institut für Tieflagerung (IfT), Braunschweig, of the Gesellschaft für Strahlen- und Umweltforschung mbH München (GSF).

In the United States, the test program is part of the Civilian Radioactive Waste Management (CRWM) Program funded by the U.S. Department of Energy (DOE) through ONWI and operated by Battelle Project Management Division. In the FRG, the program is funded by the Bundesministerium für Forschung und Technologie (BMFT) at the request of the Physikalisch-Technische Bundesanstalt (PTB). The project is operated by the Institut für Tieflagerung of the Gesellschaft für Strahlen- und Umweltforschung (GSF-IfT). The test plan (ONWI and GSF, 1981) was issued in April 1981.

The tests were designed to simulate the waste package and near-field behavior of a nuclear waste repository to measure the effects of heat and gamma radiation on brine migration, salt decrepitation, disassociation of brine, and collected gases. The thermomechanical behavior of salt, such as room closure, stresses, and changes in the properties of salt, are being measured and compared with predicted behavior. The performance of an array of candidate waste package materials, test equipment, and procedures under repository conditions will be evaluated with a view toward future at-depth testing of potential repository sites.

This report documents the progress and status of field work and associated laboratory test work for these experiments. It updates earlier test results documented in the first and second joint annual reports (Rothfuchs et al., 1984, 1986).

2.0 ISSUES AND OBJECTIVES

The issues and objectives of the Asse brine migration tests are as described below.

2.1 ISSUES

Results of laboratory and field tests indicate that when a heat source is placed in salt, the intergranular water in the salt and in the accessory minerals [e.g., polyhalite, $K_2MgCa_2(SO_4)_4 \cdot 2H_2O$] migrates to the heat source. If this liquid accumulates around the heat-producing waste canister, it may corrode the container, and thus release the radioactive material. Since laboratory tests do not completely represent the in situ environment, these brine migration tests are designed to simulate an actual repository environment at the repository horizon level.

The parameters that influence the brine migration rates are temperature distribution, thermal gradient, and borehole pressure. All of these parameters are time dependent. Numerical models indicate that the brine migrates to the heat source for approximately the first 100 years.

The Asse brine migration tests were performed to obtain an understanding of the brine migration mechanism and the effects of an intense gamma radiation field on salt. In addition, they will provide data for the validation of numerical models, and they will aid in determining the chemical composition of the brine produced.

2.2 OBJECTIVES

Primary objectives of the brine migration tests are to

- Observe the migration of water in salt available for testing at the Asse mine
- Qualify test methods and equipment to be used to obtain brine migration-related data and to validate numerical models at potential U.S. and FRG repository sites
- Observe conditions in the boreholes resulting from the arrival of brine water, including radiolysis, corrosion, gas generation, pressure, and other synergistic effects
- Observe the thermal and mechanical behavior of salt in the presence of heat, brine, and radiation to validate and refine finite element codes used to predict room closure and salt behavior in a simulated repository environment.

3.0 ASSE MINE

The tests were conducted at the 800-m (2,624-ft) level of the Asse mine. The Asse mine is approximately 1.5 km (1 mi) north of the village of Remlingen, 10 km (6 mi) southeast of Wolfenbüttel, and about 18 km (11 mi) southeast of Braunschweig within the Federal State of Lower Saxony (Figure 3-1). The Asse mine can be reached by road or rail.

3.1 MINING HISTORY

The beginning of mineral exploitation of the Asse region dates back to the 19th century. The first shaft, Asse 1*, was sunk to a depth of 375 m (1,230 ft) in 1899 and 1900. Potash salt was mined in the Asse I mine from three levels just beneath the surface. Major mining occurred in the Asse region in Asse II after the sinking of the Asse 2 shaft, and the mine operated until 1925. During this phase of mining, 26 rooms were mined in the northern flank of the Asse anticline (Figure 3-2). All of the rooms were backfilled and are no longer accessible. Mining resumed in 1927 and continued until 1964.

A total of 134 rooms on 13 different levels were mined in the younger halite between the 750-m (2,460-ft) and 490-m (1,607-ft) levels. The rooms averaged in size from a length of 40 to 60 m (131 to 197 ft), a width of 20 to 40 m (66 to 131 ft), and a height of 10 to 15 m (33 to 49 ft). During the period of 1927 to 1963, salt was also mined from older halite. A total of 19 rooms were excavated at the 775-, 750-, and 725-m (2,542-, 2,460-, and 2,378-ft) levels. Approximately 50 percent of the mined void was backfilled.

The Asse II mine was acquired by Gesellschaft für Strahlen- und Umweltforschung (GSF) in 1965 for the purpose of conducting research and development work for the disposal of radioactive waste in salt. For the brine migration tests, a new area at the 800-m (2,624-ft) level was accessed and developed.

3.2 GEOLOGY OF 800-m LEVEL

Figure 3-3 shows the general geology of the test area at the 800-m (2,624-ft) level and the location of the test room. This drawing is based on the mapping of the accessed drifts and subsurface drilling operations. A general stratigraphic sequence of the 800-m (2,624-ft) level is presented in Table 3-1. The sodium chloride content of the beds is presented in Table 3-2. The brine migration test area is situated at the border of the central part of the Asse mine anticline to the east of the gallery to the blind shaft No. 4 (Figure 3-3). In this area, both pure halite (Na_2S) and main halite ($Na_{2\beta}$)

---

* Arabic numerals refer to shaft identification while roman numerals refer to mines. For example, shafts Asse 2 and Asse 4 provide access to the Asse II mine.

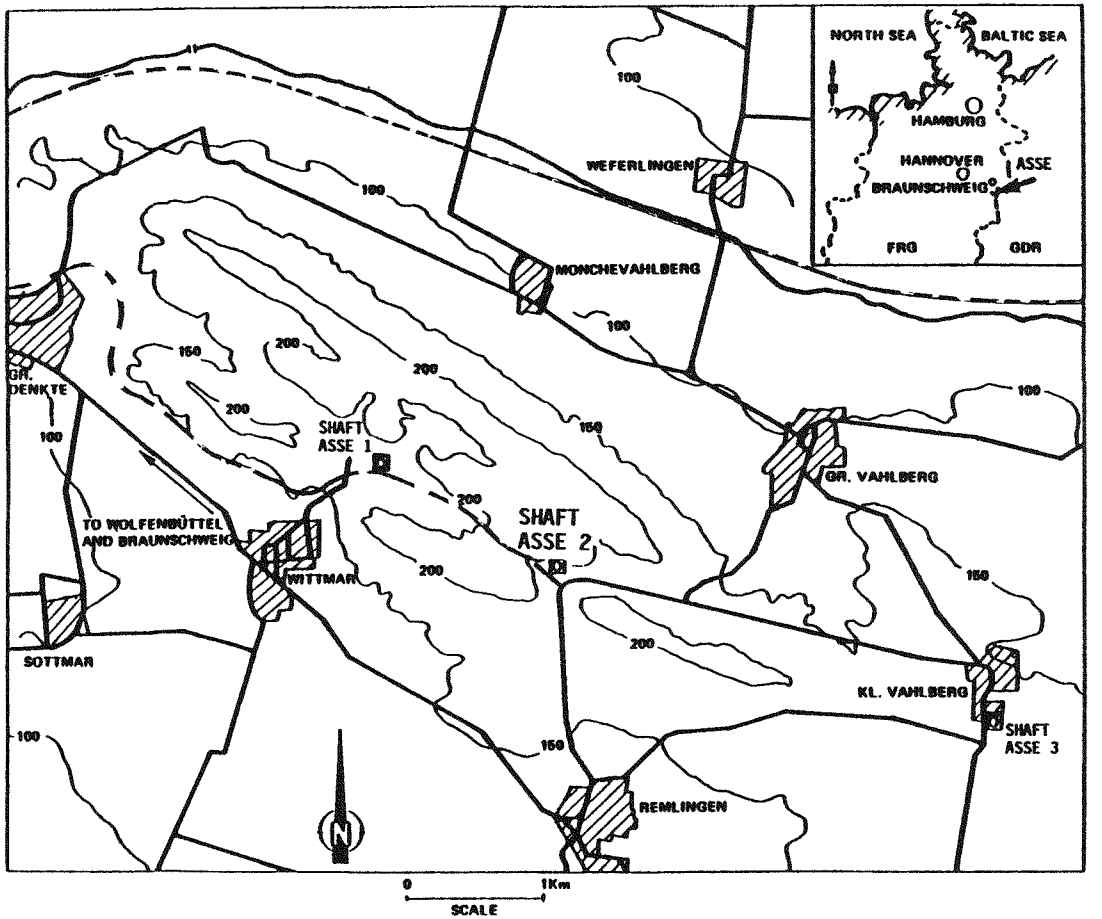

LEGEND:

- HIGHWAY AND/OR LOCAL ROAD
- RAILROAD
- MINE SHAFT
- 200 GROUND SURFACE CONTOUR LINE (METERS ABOVE MEAN SEA LEVEL)

Asse Mine Location

Figure 3-1

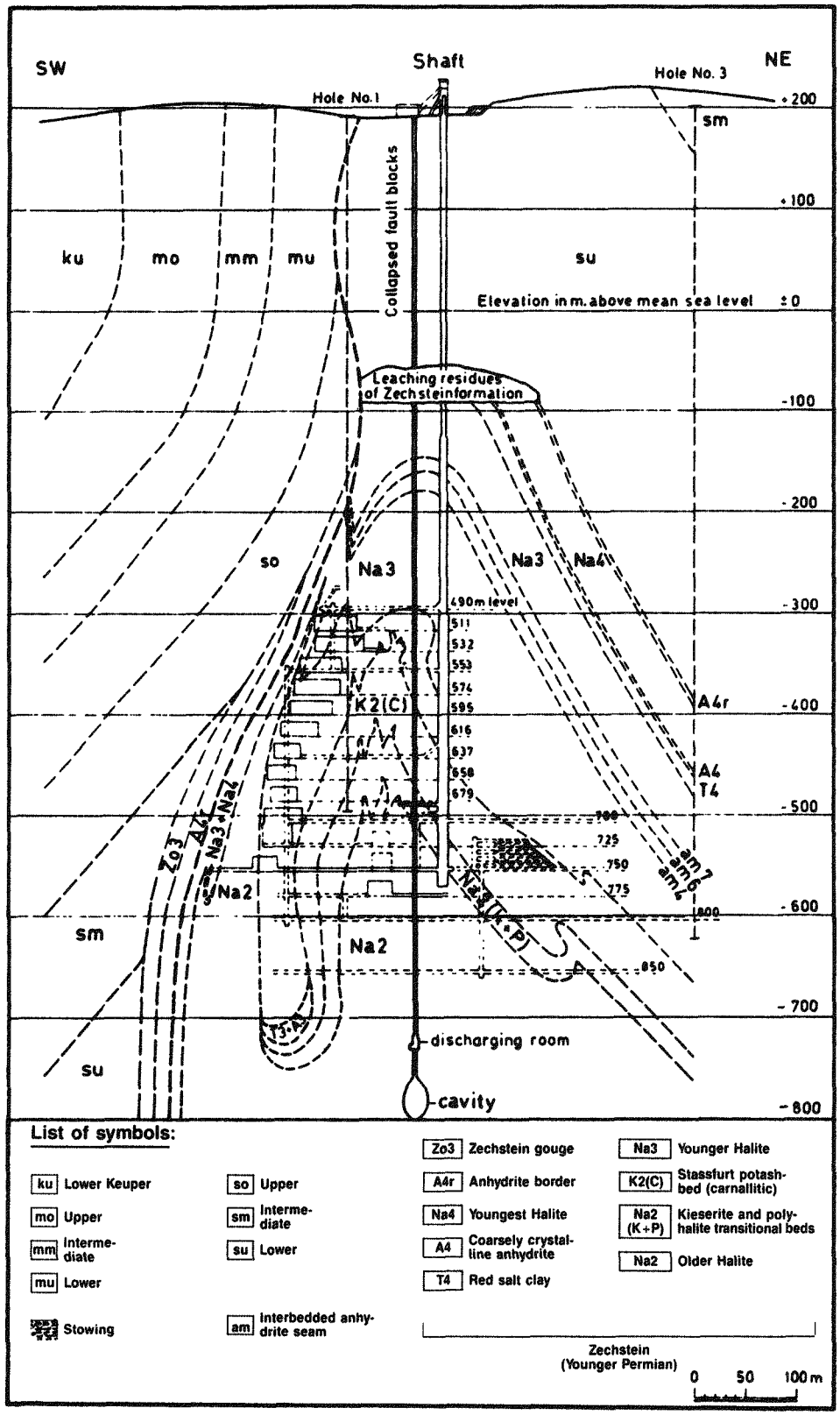

Asse II Mine Cross Section

Figure 3-2

Table 3-1. Stratigraphic Sequence at 800-m (2,624-ft) Level at Asse

Zone	Symbol	Thickness
Roof: Layered Halite	Younger Halite Na_3	Randomly distributed in the south
Potash-Seam Stassfurt, Carnallite	K_2	30 ± 20 m (98 ± 66 ft)
Kieseritic Transition Salt	Na_2K	Maximum 5 m (16 ft)
Halite With Clay Layers	Na_2T	In outermost north only
Halite With Polyhalite Beds	Na_2P	Maximum 16 m (52 ft)
Pure Halite	Na_2S	Approximately 8 to 10 m (26 to 33 ft)
Test Layer - Main Halite	$Na_2\beta$	800-m (2,624-ft) level and below to a much greater and unknown depth

Table 3-2. Sodium Chloride Content of 800-m (2,624-ft) Level at Asse

Bed	Symbol	Average(a)	Maximum(a)	Minimum(a)
Main Halite	$Na_2\beta$	89.64	97.80	82.40
Pure Halite	Na_2S	98.38	99.40	97.70
Halite With Polyhalite Beds	Na_2P	94.02	97.80	88.60
Kieseritic Transitional Salt	Na_2K	78.33	86.40	68.20

(a) Units in weight percent.

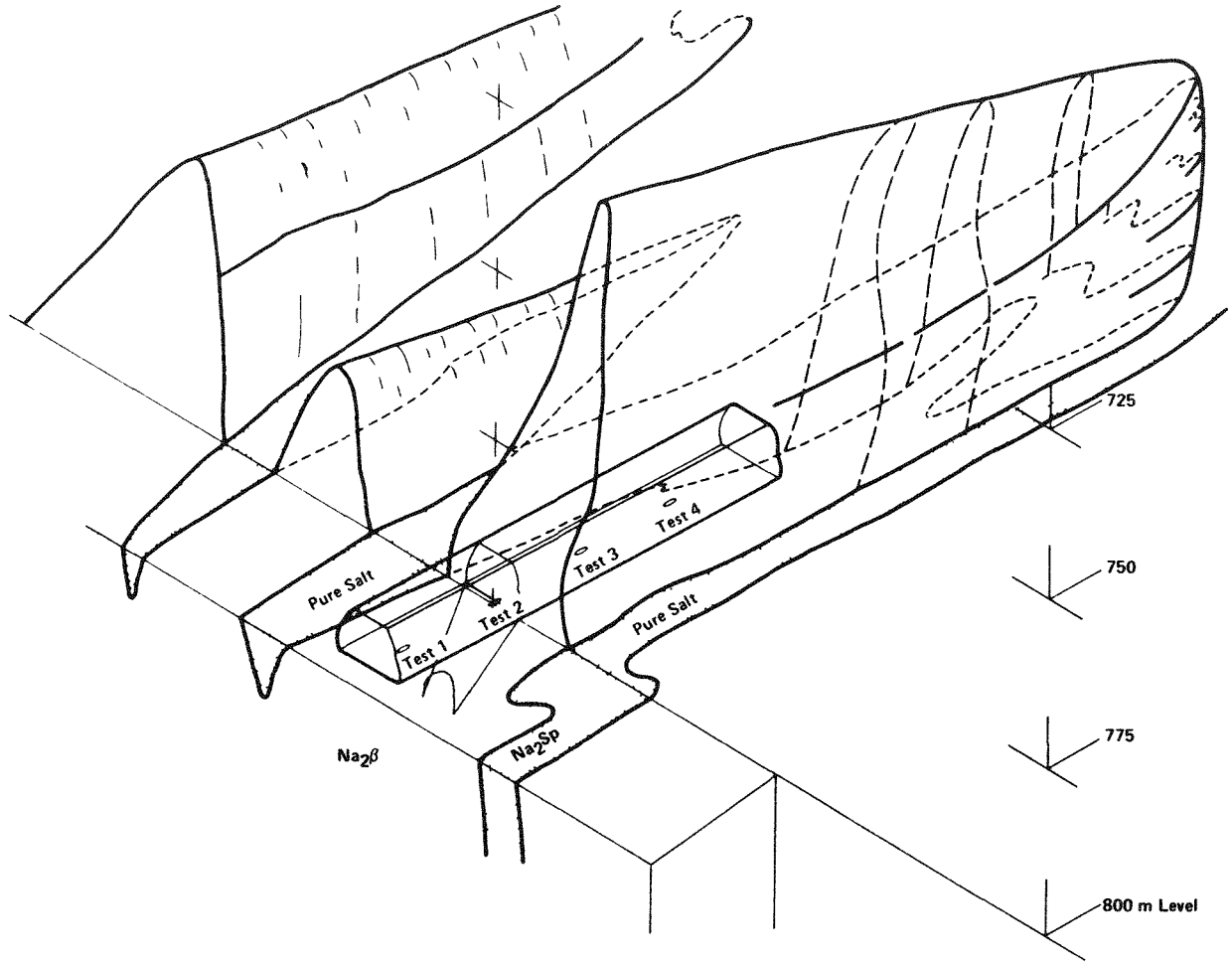

Geology of Test Area and Location of Test Room

Figure 3-3

layers are present. A total of four brine migration tests were completed. All four of these tests were located in main halite ($Na_2\beta$) (Figure 3-3). Main halite was chosen because it has considerably more water than the pure halite (Na_2S) and would therefore provide sufficient water for the brine migration tests.

4.0 BRINE MIGRATION TEST

The Asse brine migration tests were performed to obtain an understanding of the brine migration mechanism and the effects of gamma radiation. In addition, data collected will be used for the validation of numerical models and information will be obtained to determine the chemical composition of the brine produced.

4.1 DESIGN OF EXPERIMENT

The four tests (Figure 4-1) were all located in main halite (Na_2B) and were designed to be performed at a maximum salt temperature of 210°C (410°F) having 3°C/cm (13.7°F/in) thermal gradient at the borehole wall. Test sites 1 and 3 were pressurized at the beginning of the testing period, but test site 3 developed a leak in July 1984. As a result, only test site 1 was pressurized during the last years of the experiment, while test sites 2, 3, and 4 were all at atmospheric pressure.

A test setup consists of a central borehole 43.5 cm (17.1 in) in diameter. It contains a sleeve 5.0 m (16.4 ft) long. The lower 2.0 m (6.6 ft) is electrically heated. In two of the tests (test sites 3 and 4), to simulate the effect of radiation, cobalt-60 was placed in the lower 2-m- (6.6-ft-) long heated portion of the borehole.

The void between the heated sleeve and the borehole wall, which is 5 cm (2 in) wide, was filled with alumina beads. The brine vapors that migrated to the alumina beads were transported to collection points by a circulation pump. The vapors were condensed using a cold trap, and the brine was collected for analysis. The noncondensable gases and vapors were returned to the boreholes. This process took place continuously at test sites 2, 3, and 4, but only at the end of the testing period at test site 1. Figure 4-2 shows a vertical cross section of the test setup.

The lower sleeve protected the heaters and the radiation source from the brine, the lithostatic stresses, and the thermal stresses. Since the radiation source (cobalt-60) had to be removed after the completion of the tests, it was necessary that the sleeves remained intact. Because of this, the sleeves' integrity was continually monitored by checking for collapse or leakage.

The test sites are 15 m (50 ft) apart to avoid any interaction. Figure 4-3 shows the plan view of the test drift and the location of the test sites. Each of the test sites and the mined entry were monitored for heat flux, stress, room closure, and brine produced. The tests were designed to subject the test assemblies and the instrumentation to the environment that is expected to exist in an actual repository. The basic design parameters considered were

- Cobalt-60, used to produce radiation
- Tubular electrical resistance heaters, used to produce heat over the entire test length

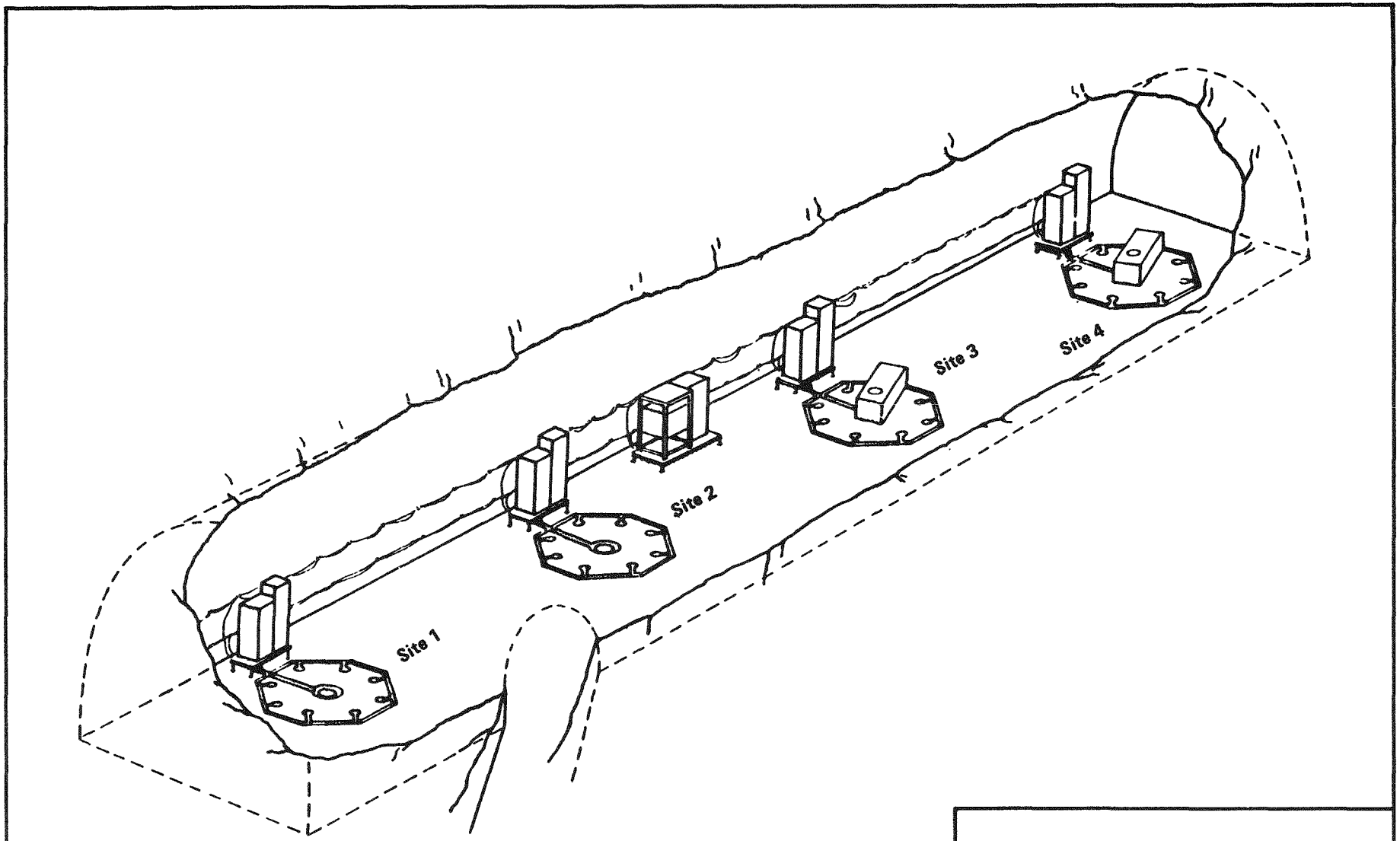

Test Gallery

Figure 4-1

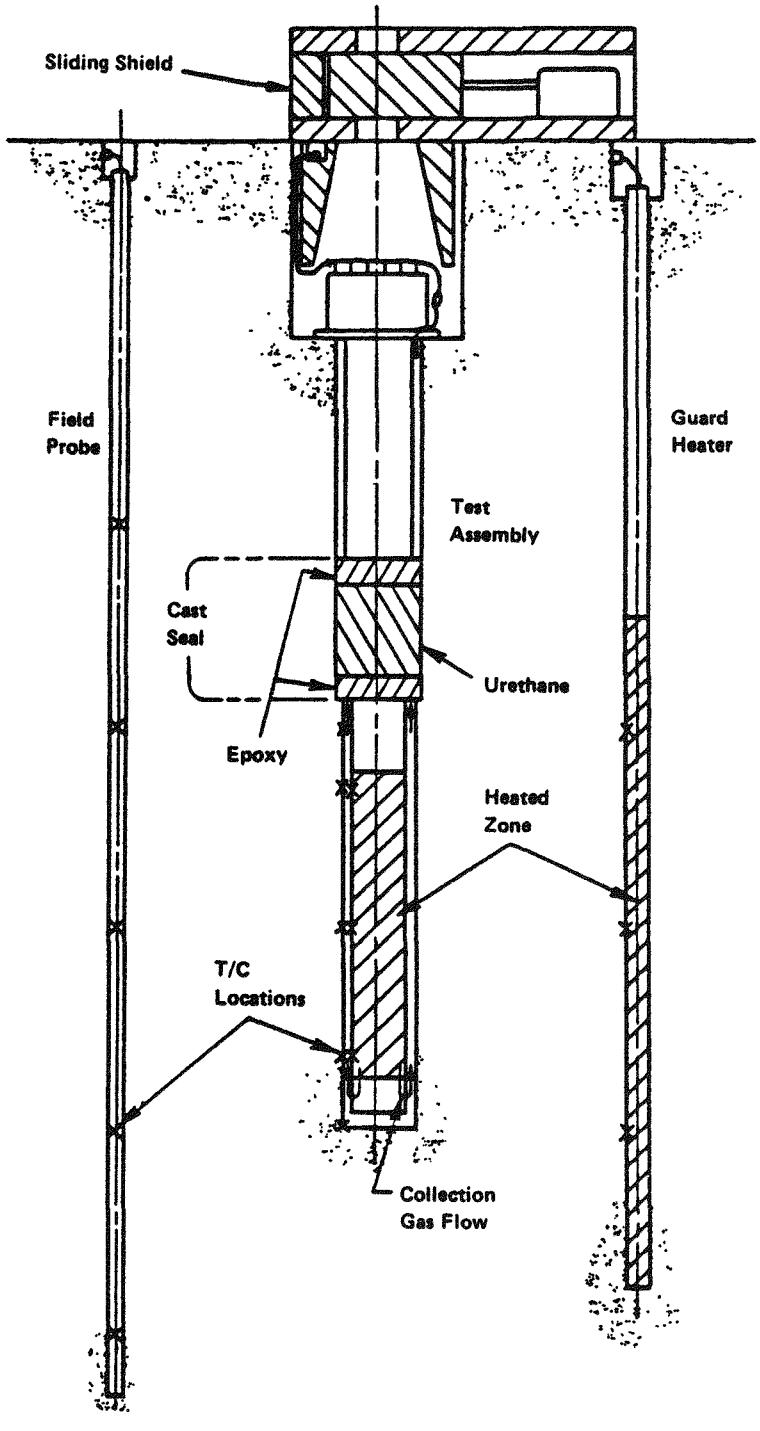

Vertical Cross Section of Test Setup

Figure 4-2

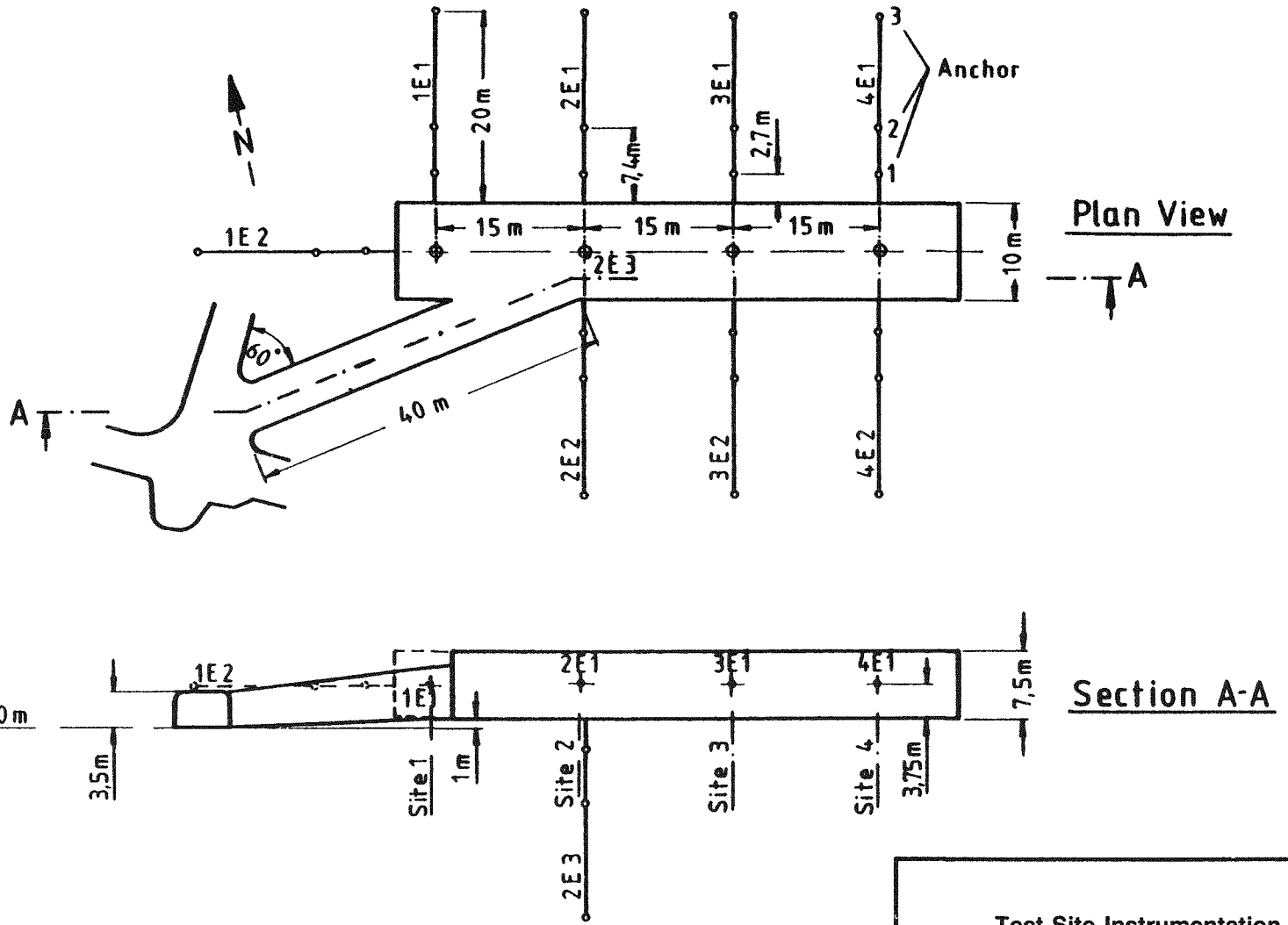

Test Site Instrumentation

Figure 4-3

- High quality and previously tested thermocouples, used to obtain temperature of the heat source, axial and vertical temperature of the outer sleeve, and thermal gradient at the test site
- Closure of the room along the ribs along the floor and roof, obtained by extensometer and wall-to-wall measurement
- Pressure gages, used to obtain pressure in the test area
- Brine, collected by circulating nitrogen and noncondensable gases through the alumina beads and by condensing the moisture in cold traps
- Test assembly, designed to provide sufficient radiation shielding to limit the average dose rate of 2.5 mrem/h at the gallery floor.

4.1.1 Test Assembly

The test assembly (Figure 4-4) is composed of an upper and lower sleeve assembly joined to an enlarged seal section to form the primary boundary to protect the test material from the pressure and corrosive effects of the salt environment. The sleeves are joined by welded joints at the seal section to form a continuous tubular assembly.

Surrounding the upper sleeve and seal section is a caisson that is sealed and bonded to the salt borehole. A series of O-ring elastomer seals provides a seal between the caisson and the sleeve assembly seal section to isolate the lower test zone.

The upper closure provides external termination of the interconnecting instrumentation: electrical lines, gas lines, and fill lines between the lower sleeve and upper closure. Within the test assembly lower sleeve are two canisters containing the cobalt-60 sources. Surrounding the canisters is an electrical heater assembly consisting of two redundant sets of six tubular heaters, each extending approximately 15 cm (6 in) beyond the upper end of the stacked canisters. Above the top canister is an assembly containing thermal insulation and shielding to protect the elastomer seals and to limit heat transfer to the upper sleeve. Thermocouple instrumentation extending from the upper sleeve closure measures temperatures on the outside diameter (OD) of the lower sleeve at three elevations and three azimuthal positions. Thermocouples extending from the caisson contact the borehole wall to measure test zone temperatures at six elevations and three azimuthal positions. The surface of the test assembly is shielded by a shield ring surrounding the upper sleeve closure transition and by an integral shield plug that limits the radiation to a low level at the mine floor. The sleeve and heater assemblies were delivered as a single unit approximately 5 m (16.4 ft) long and weighing 1,270 kg (2,800 lb). They were designed for insertion into the caisson lining the 43.5-cm- (17.1-in-) diameter borehole. Following insertion, the annulus between the borehole and the lower sleeve was filled with alumina beads through fill tubes routed from the upper closure.

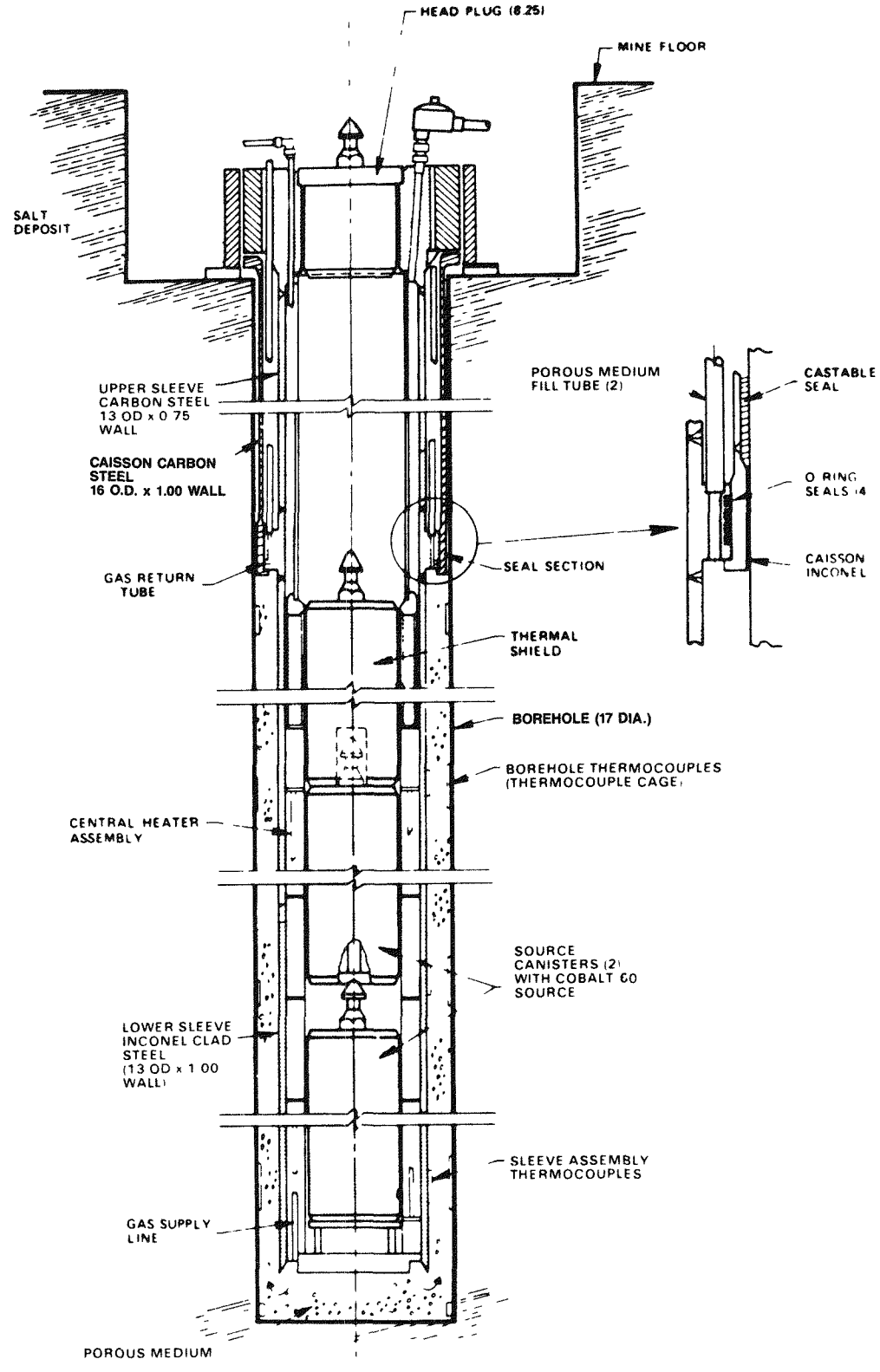

Cross Section of Brine Migration Test Assembly
(Conversion Factor: 1 in = 2.5 cm.)

Figure 4-4

4.1.2 Sleeve Assembly

The sleeve assembly (Figure 4-4), consisting of a lower sleeve, an upper sleeve, and a closure, provides the containment housing for the source canisters, tubular heaters, internal shield, and thermal baffle. The sleeves are 33 cm (13 in) in diameter with a 1.9-cm (0.75-in) wall. The lower sleeve tube, seal section, and lower end gas manifold are constructed of high-strength steel with a cladding of Inconel 600. The upper sleeve and closure are also high-strength steel. The transition weld is above the elastomer seals and is, therefore, protected from potential galvanic corrosion. Inconel 600 was chosen for this application because it is resistant to brine corrosion, is readily available, is easy to fabricate, and is inexpensive when compared to other potential materials. The lower sleeve assembly includes an end plate containing the gas inlet manifold to the porous medium and the structural support for the heater assembly.

Extending from the closure, down the outside diameter of the upper sleeve, and terminating at axially drilled passages in the center seal section are two porous medium fill tubes, three thermocouple guide tubes, and one gas exit sampling tube. The fill tubes are straight lengths of 1.6-cm (0.63-in) inside diameter (ID) Schedule 40 pipe, and the gas and thermocouple tubes are 0.9-cm (0.35-in) ID Schedule 40 pipe. The Inconel 600 tubes are socket welded to the seal sections. The zone pressure isolation is maintained at the closure end by compression seal fittings for the thermocouple sheaths and compression caps for the fill tubes. The seal section is 39.0 cm (15.4 in) in diameter, 9.2 cm (3.6 in) long with four 5.3-mm (0.21-in) diameter O-ring seals. The candidate material for the O-ring seals is an elastomer seal which meets the service requirements for temperature, radiation environment, and low compression set.

4.1.3 Heater Assembly

Contained within the inner periphery of the lower sleeve is a tubular heater assembly (Figure 4-4). This assembly consists of two sets of six 0.8-cm- (0.3-in-) diameter heaters for redundant operation. The heaters are approximately 1.9 m (75 in) long, and each has a thermal rating of 3,000 W. Several thermal baffles along the length of the assembly restrict natural convection and reduce distortion of the thermal profile. The heater assembly support tube also serves as a guide for the radioactive source canisters. The annulus above the heaters, which extends to the seal section area, contains thermal insulation and shielding. This, along with a center assembly containing insulation and shielding resting on top of the canisters, protects the external elastomer seals and limits heat transfer to the upper sleeve volume. Located at the midplane of the heater assembly is a deformation gage. This gage detects possible deformation of the sleeve due to the lithostatic pressure of the salt, permitting removal of the source canisters before sleeve deformation becomes excessive.

4.1.4 Seal and Seal Caisson

Surrounding the test assembly upper sleeve and seal section is a caisson (Figure 4-4) which is sealed and structurally bonded to the salt borehole.

The caisson is 2.2 m (87 in) long, extending from near the entrance to the borehole, and has an outside diameter of 41.6 cm (16.4 in) and an internal sealing diameter of 39.0 cm (15.4 in). The lower 15.2 cm (6.0 in) of the caisson is enlarged to a diameter of 43.2 cm (17.0 in) to provide additional rigidity for the internal seals and to restrict the flow of the castable seal material. The enlarged seal section is made from Inconel 600 while the remainder of the caisson is carbon steel.

The annulus between the borehole and caisson is filled with two 15-cm (6-in) layers of epoxy that sandwich a 61-cm (24-in) layer of urethane elastomer. The seal is required to retain the 0.4-MPa (58-psi) test zone gas pressure and support the total borehole axial pressure load. The epoxy provides the shear strength required, and the more pliable urethane provides the sealing required. A flange section at the upper end of the caisson provides a bolted connection to connect the test assembly and caisson. Extending below the caisson are thermocouples which will contact the test zone borehole wall at five elevations and three azimuthal positions. The thermocouple sheaths pass through the castable seal and terminate at the test assembly closure.

4.1.5 Closure

The test assembly closure (Figure 4-4) consists of the outer shield ring, upper sleeve transition, and shield plug. These carbon steel components, along with the internal shield, are intended to reduce the surface radiation dose rate to a maximum of 2.5 mrem/h under normal canister storage conditions. The shield plug has a diameter of 21 cm (8 in) and a standard handling pintle for grappling and handling by the surface transfer cask.

4.1.6 Canister and Source

The canisters containing the radiation sources (Figure 4-5) are approximately 1 m (39 in) long, due to constraints imposed by the transport vehicle. They were fabricated from 19.7-cm (7.8-in) OD by 3-mm (0.01-in) wall carbon steel pipe with tapered end plates and handling pintle. The sources are located in the canister by a concentric cylinder, 1.5 cm (0.6 in) ID. The source is cobalt-60. The empty volume of the canister is filled with fiberglass insulation and baffles to reduce convection within the test assembly. The sources were loaded into canisters in a hot cell area by the source manufacturer, Amersham Buchler, and the canisters were closed by simple mechanized closures.

4.1.7 Porous Medium

As described in previous sections, the annulus between the borehole wall and lower sleeve was filled with a porous medium (Figure 4-6) for the collection of water and gases generated during the test and for the support of the borehole wall. The material selected, alumina (Al_2O_3), is such that it can meet the following requirements:

- Good compressive strength at 300°C (572°F) after exposure to brine, radiation, and heat

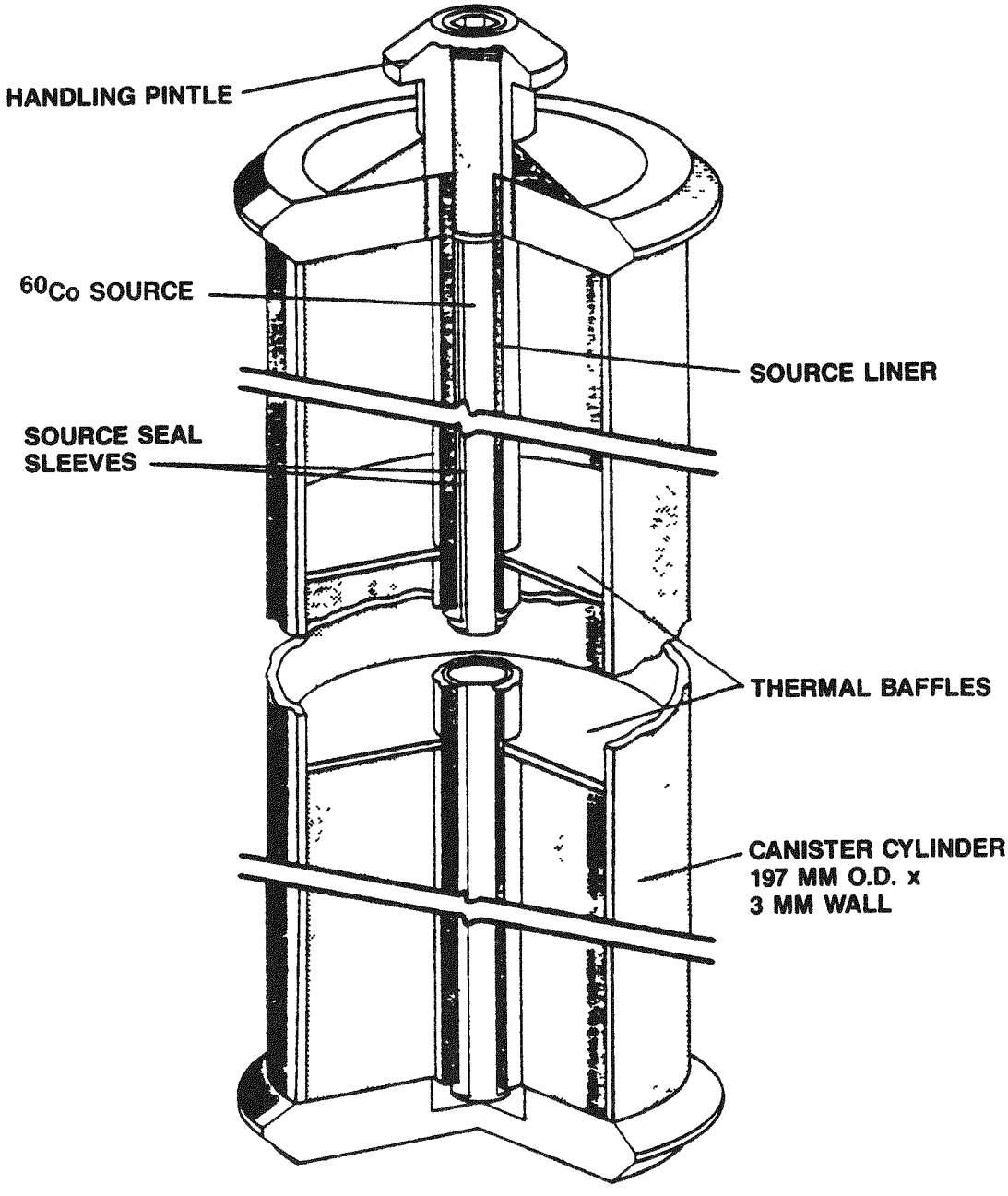

Radioactive Source Canister Assembly

Figure 4-5

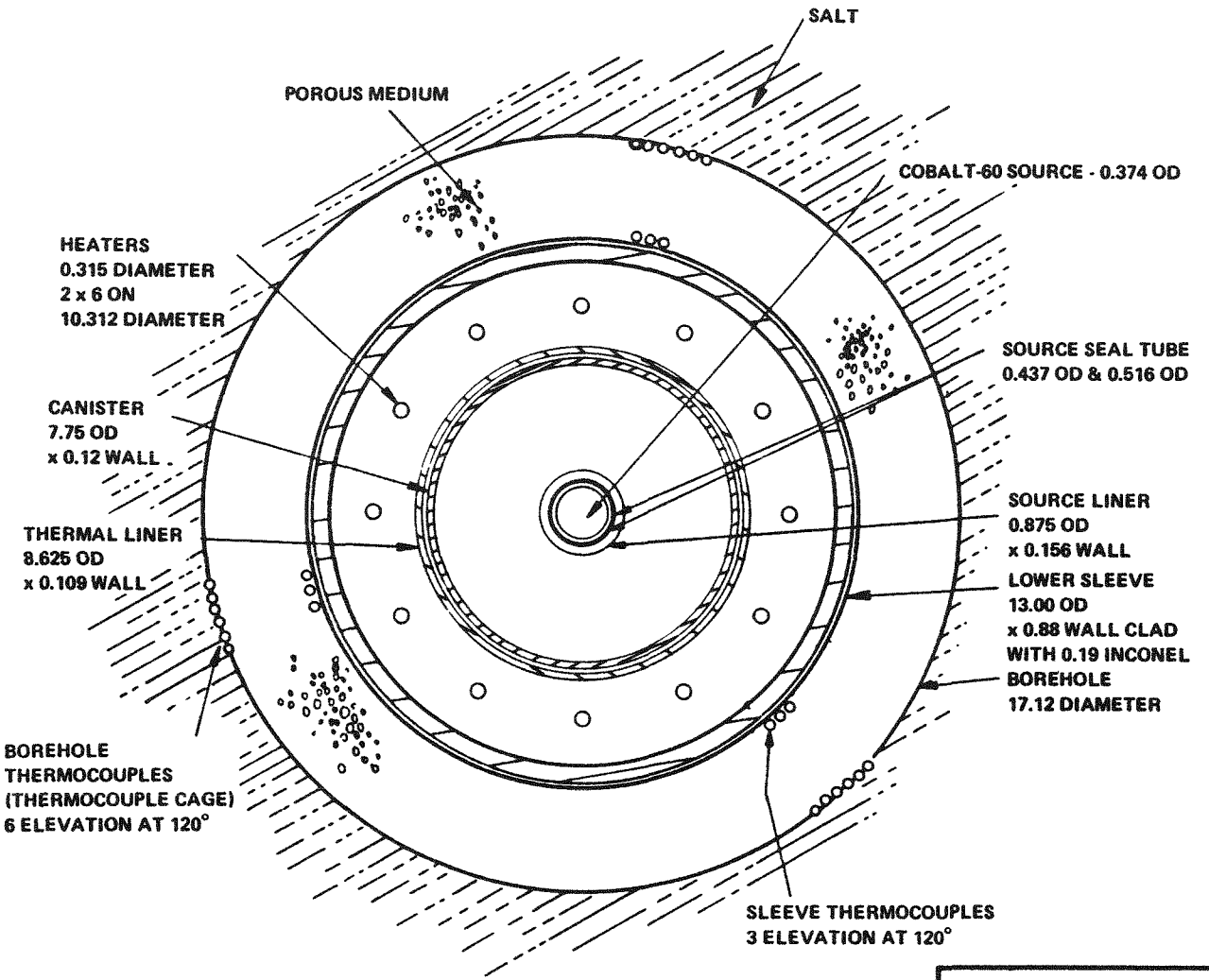

*Measurement in inches

Horizontal Section of Test Assembly Near Heater Midline

Figure 4-6

- High thermal conductivity to enhance heat transfer to the borehole wall
- Nonreactive with water and brine at the design conditions
- Good pourability
- No compaction under load
- Nonclogging with residue from evaporated brine
- Low density to limit radiation attenuation to the geologic salt.

4.1.8 Guard Heaters

Peripheral heaters (Figure 4-7) were placed in an octagonal pattern around the canister, 1.5 m (59 in) from the centerline of the test assembly. The guard heaters extended approximately 0.8 m (2.6 ft) below and above the active region of the lower sleeve. These heaters were intended to modify the thermal gradient around the lower sleeve to simulate the effect of the waste canister placed in the repository.

4.1.9 Placement and Retrieval

To prevent radiation exposure to personnel during emplacement or retrieval of the source canisters at the test site, it was necessary to use a transport cask (Figure 4-8). Separate shields with sliding valves were installed over the test assemblies of sites 3 and 4. This equipment was provided by the Federal Republic of Germany (FRG).

Sliding shields mate with the transportation cask and prevent the radiation from streaming through the closure during installation or removal and during the interval when the closure shield plug is not in place.

A transport vehicle was used to place the transportation casks containing the source over the sliding shields. The bottom of the transport cask and the valves in the shields were opened and the canisters were lowered into the test positions. Each canister was released by the grapple and the grapple was withdrawn through the transport cask. To avoid streaming, the sliding shield valve was closed before the transporter cask was removed.

The second canister was emplaced in the same manner. The thermal baffle and internal shield, and then the closure shield plug (Figure 4-4) were emplaced using the transport cask and grapple with a similar sequencing of the valves. After the shield plugs were in place, the transportation cask was removed. The sliding shields remained in place to facilitate rapid source retrieval in the event of a mine accident, but they could be removed if access to the test assemblies were required during the test. Retrieval was in the reverse order of the above procedure.

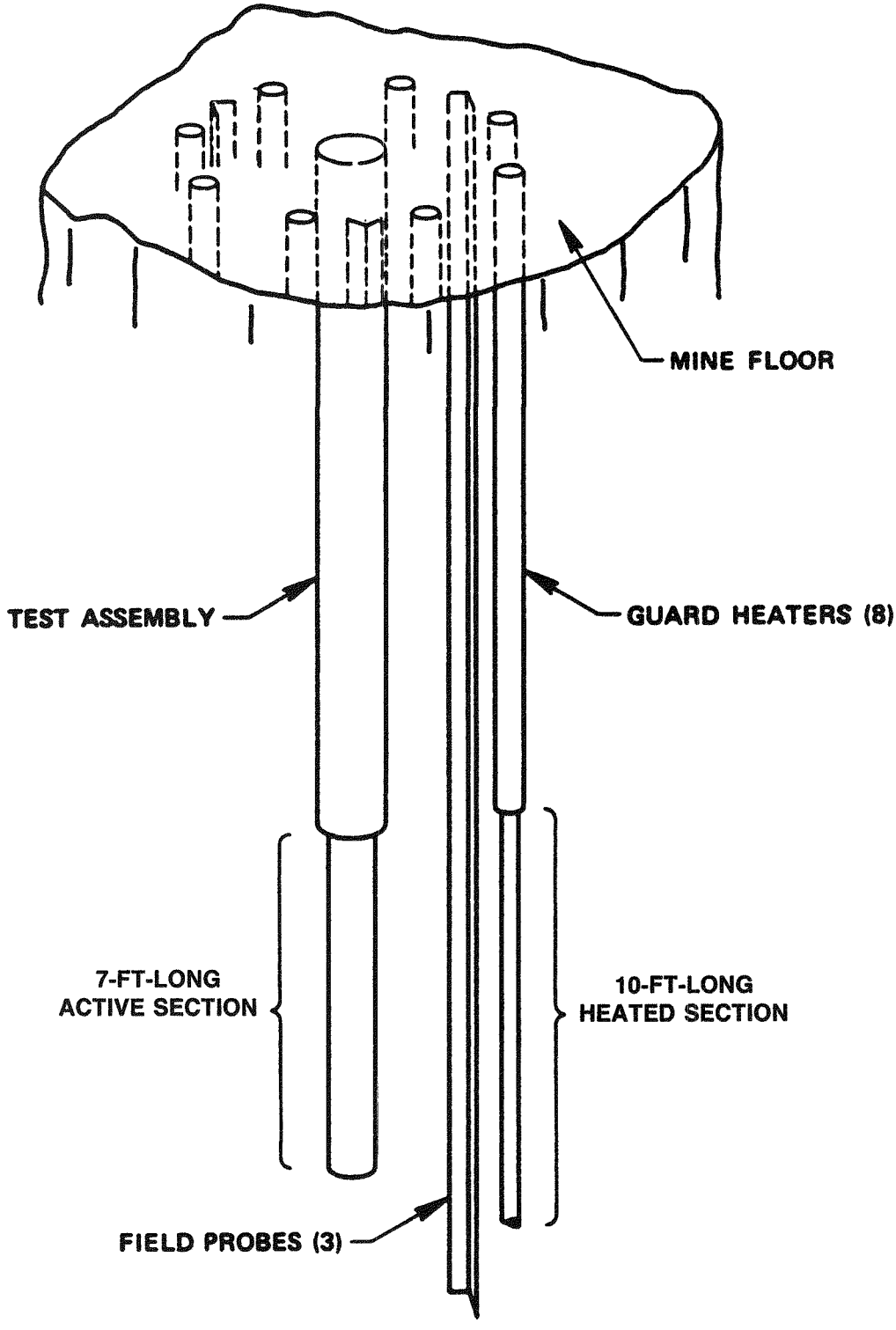

Test Site Overview

Figure 4-7

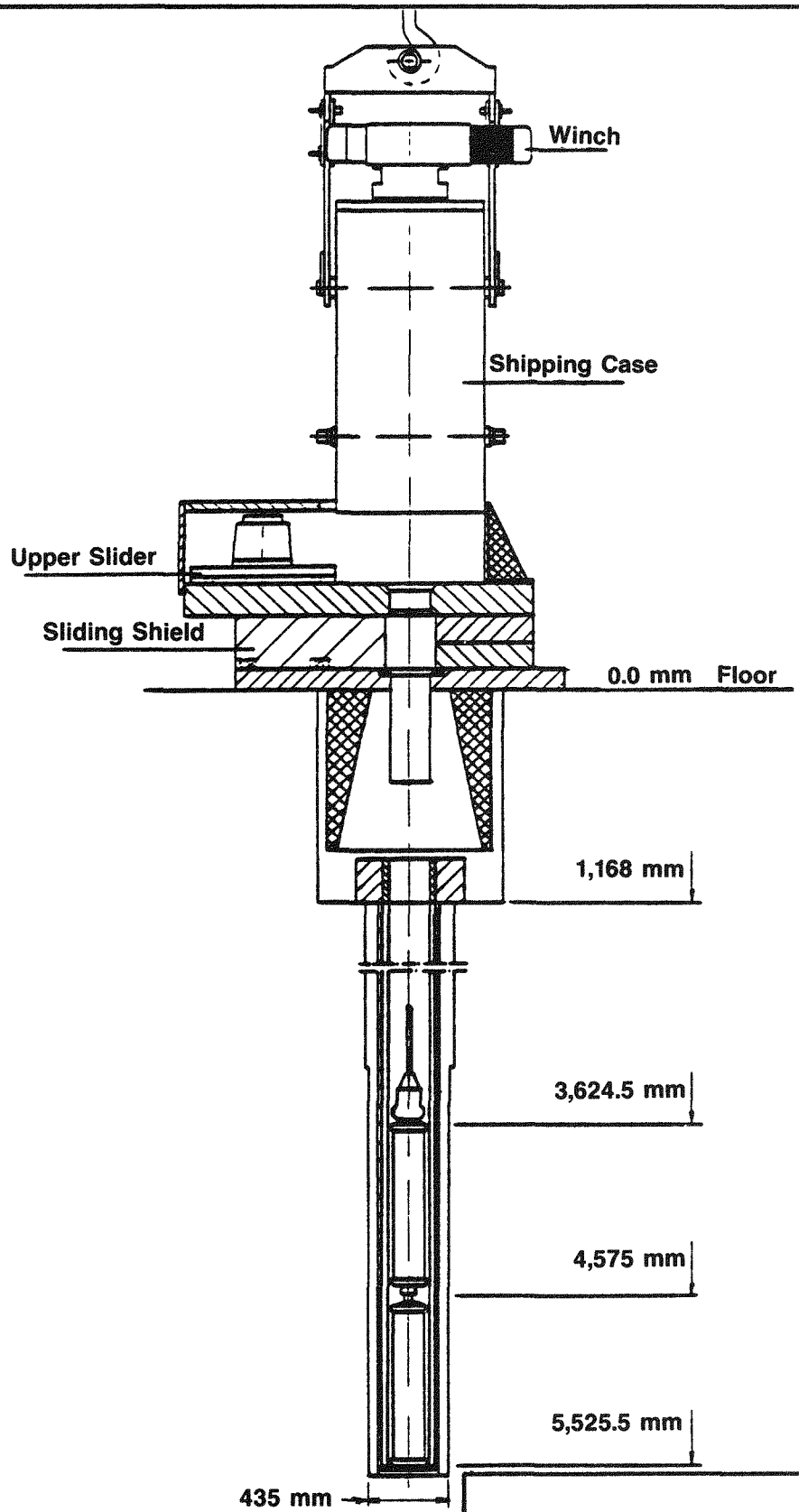

Arrangement for Installing and Removing Radioactive Source Canisters

Figure 4-8

4.1.10 Removal of Test Hardware

On conclusion of the tests and removal of the source canisters, the test assembly was removed as a unit to provide access to the porous media and to the salt in contact with the active zone during the test. The closure outer shield ring was removed and the bolts attaching the test assembly to the seal caisson disconnected. A support ring was placed around the test assembly with a support beam extending across the centerline of the test position. Tension bolts were connected to the top surface of the test assembly closure and passed through clearance holes in the support beam. Nuts placed on the tension bolts were connected to the top surface of the test assembly closure and passed through clearance holes in the support beam. Nuts placed on the tension bolts were activated to apply a tension load on the test assembly and break it free. A hoist was then used to lift the test assembly free of the hole in the floor of the salt mine. The seal caisson will not be removed. This process was successful at sites 1, 2, and 4. However, the test assembly at site 3 has not yet been removed because stronger jacking tools are necessary to break this test assembly free (see Chapter 7).

4.2 INSTRUMENTATION

Borehole wall temperature measurements inside the central borehole were made at five elevations and three azimuthal locations for a total of 15 measurements per site.

Lower inner sleeve temperature measurements were made at three elevations, and three azimuthal locations for a total of nine measurements per site. Temperature probe measurements were made at three azimuthal locations around the center of each test site and at five elevations, for a total of 15 measurements per site.

The temperature on the outside of four of the guard heaters was measured at three elevations. The probes and the guard heaters are all located at the same radial distance from the test site center. There were four current measurements per test site. Two instruments monitored power to the central borehole heater rods while the others monitored power to the guard heaters. This measurement was to detect heater failure. Displacement sensor or switches are placed inside the lower sleeve to monitor for the initiation of collapse. Sleeve deflection is monitored at one elevation, but at six stations 60 degrees apart. At each station there are three switches that are triggered at the same time to indicate assembly collapse. The borehole gap pressure, pump outlet pressure, and gas pressure measurements, and the flow switch and level switch are all associated with the moisture collection system (Figure 4-9).

The deformational behavior of the test room is measured with horizontal three-anchor extensometers at each test site and one vertical extensometer at test site 2 (Figure 4-3). The room closure is also measured in horizontal and vertical directions at each test site. Floor heave measurements are performed at 25 leveling points in a longitudinal and crosswise extension of the test room.

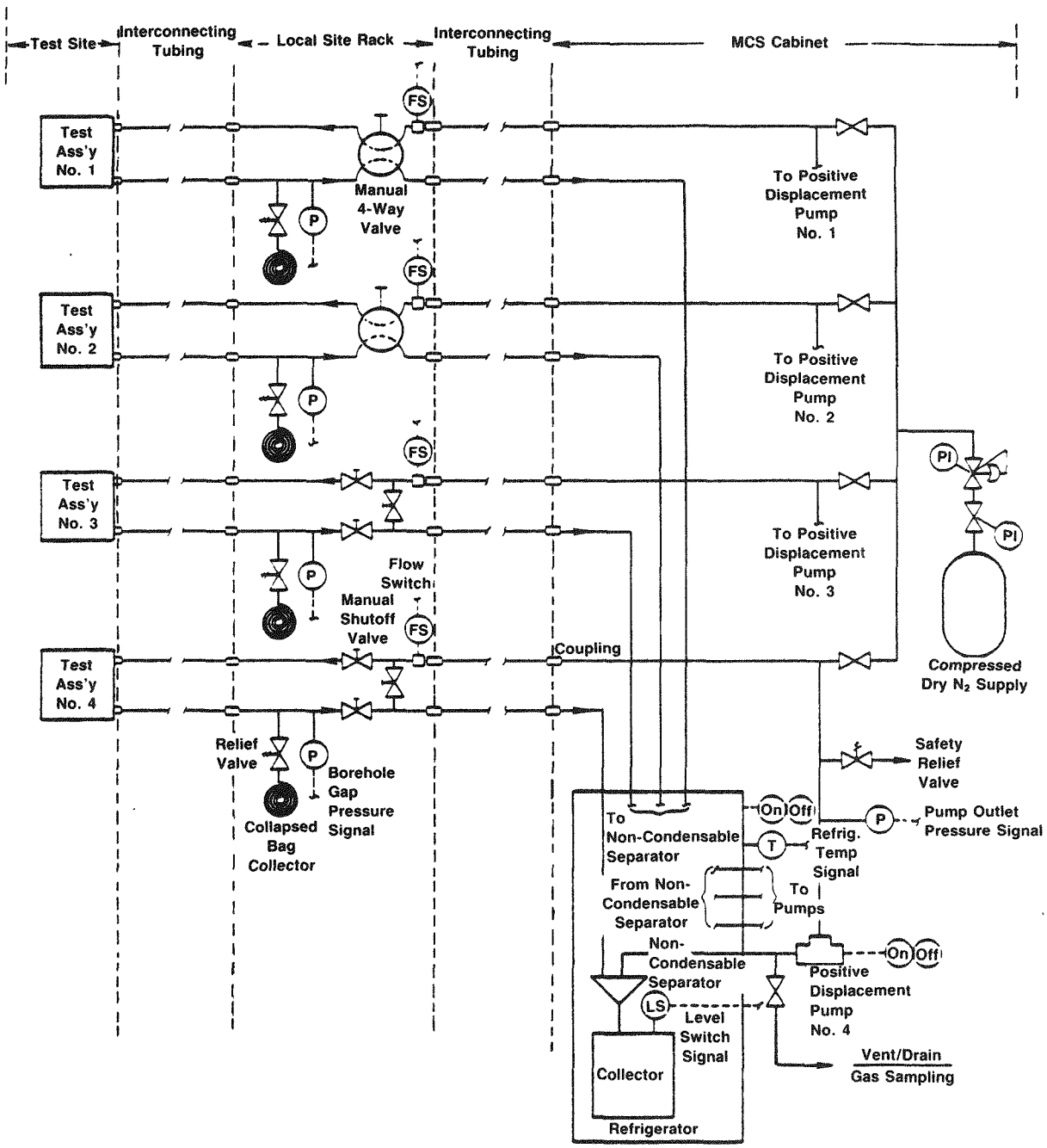

Schematic of Moisture Collection System

Figure 4-9

4.2.1 Temperature

The general environment consists of steam, saturated brine, and salt, with a temperature range of 25°C to about 350°C (77°F to 662°F). The chromel-alumel (Type K) metal sheathed and grounded junction thermocouples were fabricated with premium grade thermocouple wire and insulated with magnesium oxide inside an Inconel 600 sheath.

Thermocouples on the outer sleeve were routed down a groove in the external surface of the outer sleeve to the point of measurement. A cover plate, welded along one side only, covers the cables in the groove and protects them from damage.

Thermocouples to monitor borehole wall temperatures were attached to a support structure in the caisson. This structure supports three vertical bundles of thermocouples (at circumferential intervals of 120 degrees). One thermocouple bundle is located at each of the five measurement elevations. A spring clip provides spring loading to assure firm contact between the thermocouple and the borehole wall. This structure was installed prior to installing the test assembly and filling the annulus with beads.

Three carbon steel probes were assembled with five thermocouples to monitor the temperature field around each test site at five levels. These Inconel-clad thermocouples were also encased in Teflon to avoid corrosive incompatibility with the carbon steel. This structure provides spring loading to assure that the thermocouples make firm contact with the salt in the temperature probe borehole. Thermocouples on the guard heaters were attached to the heater assembly at three elevations. To avoid corrosion problems these Inconel-clad thermocouples were also jacketed in Teflon.

4.2.2 Pressure

Pressure measurements were taken for the borehole gap, the test assembly internal volume, and the moisture collection system (MCS) pump outlet (Figure 4-9). In each of these cases, the actual environment for the sensor electronics was mine ambient conditions. The borehole gap pressure measurement for the pressurized sites exposed the pressure sensors to 200°C (392°F) temperatures and steam; however, this is not regarded as very severe.

Local pressure gages were provided on the compressed dry nitrogen gas cylinder along with shutoff and throttling valves. This gas was used for purging and filling the MCS, including tubing and borehole gap, prior to start-up. It was used for repurging the pressure lines to the pressurized sites immediately prior to terminating the experiments.

4.2.3 Corrosion

For testing corrosion behavior of different materials under the general environment inside the test volume, several corrosion specimens were selected and attached to the spring clips that were used for borehole wall temperature measurements. The specimens were distributed at circumferential intervals of 120 degrees at three elevations in the heated and radiated zone. Table 4-1

gives an overview of the materials used and their distribution to the different test sites.

Table 4-1. Distribution of Corrosion Specimens and Material Condition

Test Site No.	Material (Material Condition)(a)	Number of Specimens(b)
1 and 3	Si Steel Casting (A)	2
	Ti-Pd/3.7025 (A, S)	4
	Mild Steel/1.0566 (S, A)	4
2 and 4	Hastelloy C4/2.4610 (A, WS, SW)	6
	Spheroidal Graphite Iron	2
	Ni-Resist. D4/O, 7680 (A)	2
	Close-Grained Gas Iron	2

(a) Material Condition: A = as-delivered condition SW = welded and annealed
S = welded WS = annealed and welded

(b) All specimens were selected and provided by Kernforschungszentrum Karlsruhe - Institut für nukleare Entsorgungstechnik.

4.2.4 Displacement Switches

The displacement switches are positive deflection indicators, made up of three conductors, which could be cut by a preset guillotine activated by sleeve collapse or yield. Six switches are 60 degrees apart at the point of maximum sleeve deflection. If and when the guillotines cut conductors, an alarm is sounded. If conductors are cut 180 degrees apart, which presents the worst case of sleeve deflection, the alarms will provide time to remove the cobalt-60 source canisters before major collapse of sleeves can occur, thereby preventing the removal of the source canisters.

This location requires sensors that can remain reliable over a 2-year period while exposed to ambient temperatures as high as 350°C (662°F). Shielding is provided for radiant heat from the heater elements, which may operate at up to 600°C (1,112°F). The environment also includes gamma radiation of 6×10^8 rads integrated dose over a 2-year period.

4.2.5 Current

There are eight current measurements per test site. Two measurements are made on each power controller output. One measurement is output to the data acquisition system to monitor changes in the output power (failure detection); the other measurement outputs to a panel-mounted kilowatt/kilowatt-hour meter.

4.2.6 Gamma Radiation Dose

No compact radiation detector has been located that can withstand the temperatures and doses anticipated for this test. Since the dose can be calculated reasonably well and there is no need for high accuracy measurements, no radiation dose measurements were made in the test zone during the tests. However, prior to removing the cobalt-60 sources, radiation intensity measurements were obtained at 1 m (3.3 ft) and 1.5 m (4.9 ft) of 1.5 and 1.2 mrem/h, respectively. These readings were taken at a depth for most intense radiation, 4.57 m (15.0 ft) below the test floor.

4.2.7 Rock Mass Deformation

To obtain the long-term and test-induced deformation of the rock mass surrounding all four test sites, nine three-anchor extensometers were installed. These are customized versions of multiple-point coaxial steel tube extensometers modified for rock salt stratum, manufactured by Stitz Corporation, Gehrden, FRG.

The extensometers to the north of the test site are identified as 1E1, 1E2, 1E3, and 1E4. The extensometers to the south of the test site are designated as 2E2, 2E3, and 2E4. Extensometer station 1E2 is located to the west side of the test site 1 and the extensometer 2E3 is installed vertically down near test site 2 (Figure 4-3).

At each of the horizontal extensometers, a wedge-type anchor is fixed at 2.7-m (8.9-ft), 7.4-m (24.3-ft), and 20.0-m (65.6-ft) depths, a distance of 3.75 m (12.3 ft) above the floor.

The one vertical extensometer (2E3) is installed into the floor at test site 2, 1.5 m (4.9 ft) from the borehole axis. The change in distance with time between the extensometer head (reference plate at wall or floor surface) and the individual downhole anchor is monitored with linear variable displacement transducer- (LVDT-) type transducers, which are attached to the various coaxial extensometer tubes at the borehole collars.

These passive transducers produce a DC output voltage change proportional to the displacement between the downhole anchors and the extensometer head, which is monitored by the Data Acquisition System (DAS).

Horizontal room closure measurements are performed manually between the heads of the horizontal extensometers. For the vertical room closure measurements, special reference points are installed at roof and floor of the test room. Each test site is measured in the same manner using steel tapes and a dial-type, closure-measuring device for measuring the time-dependent change of the wall-to-wall distance.

Floor heave measurements are made with mine surveying methods (leveling). The measurements are evaluated with regard to a reference point located at the mine surface. A total number of 25 leveling points are installed in the test room floor, 15 of them in a longitudinal direction crossing the four test sites, and 10 of them distributed crosswise at the four test sites.

4.3 DATA ACQUISITION SYSTEM

Figure 4-10 shows a block diagram of the DAS. The front end of the DAS provides input module cards, each of which can accept eight or more input channels. These cards provide the basic signal conditioning necessary to convert each type of input (volts, millivolts, milliamps, and ohms) into a precisely scaled DC voltage. A temperature reference junction is provided for thermocouple inputs to permit correction for ambient temperature.

The remote scanner card frame provides slots for up to 10 input multiplexer cards. Each remote scanner is controlled by the DAS to sequence through all of the multiplexer channels and output each to the data logger.

At the data logger, the analog signal level is converted to a digital signal, processed for any required mathematical manipulations (e.g., conversion to engineering units), and transferred to a buffer. Data can be output in engineering units on a paper or foil-type tape, output to a remote printer, or stored on magnetic tape for further evaluation.

The data logger is directly programmed at an integral keyboard, with the ability to have portions of the program remotely modified (at a remote keyboard). The data logger system is located within the test room. The data logger is equipped with an RS 232C communication port that will transmit and receive data and commands to and from the surface. The communications link includes modems to permit data transmittal over one or more twisted, shielded wire pair cables or telephone lines. The remote keyboard, printer, and magnetic tape system are located in the above-ground facility.

4.4 MOISTURE COLLECTION SYSTEM

The MCS (Figure 4-9) consists of the following items for each test site:

- A positive displacement pump to circulate the moisture carrier gases through the collection loop
- A noncondensable separator that permits liquids to drain into a collector while noncondensables continue to circulate through the system
- A collector container
- A level switch installed on each collector container
- A flow switch
- A four-way valve or three-way manual shutoff valves
- A relief valve
- A manual valve for a gas sampling line

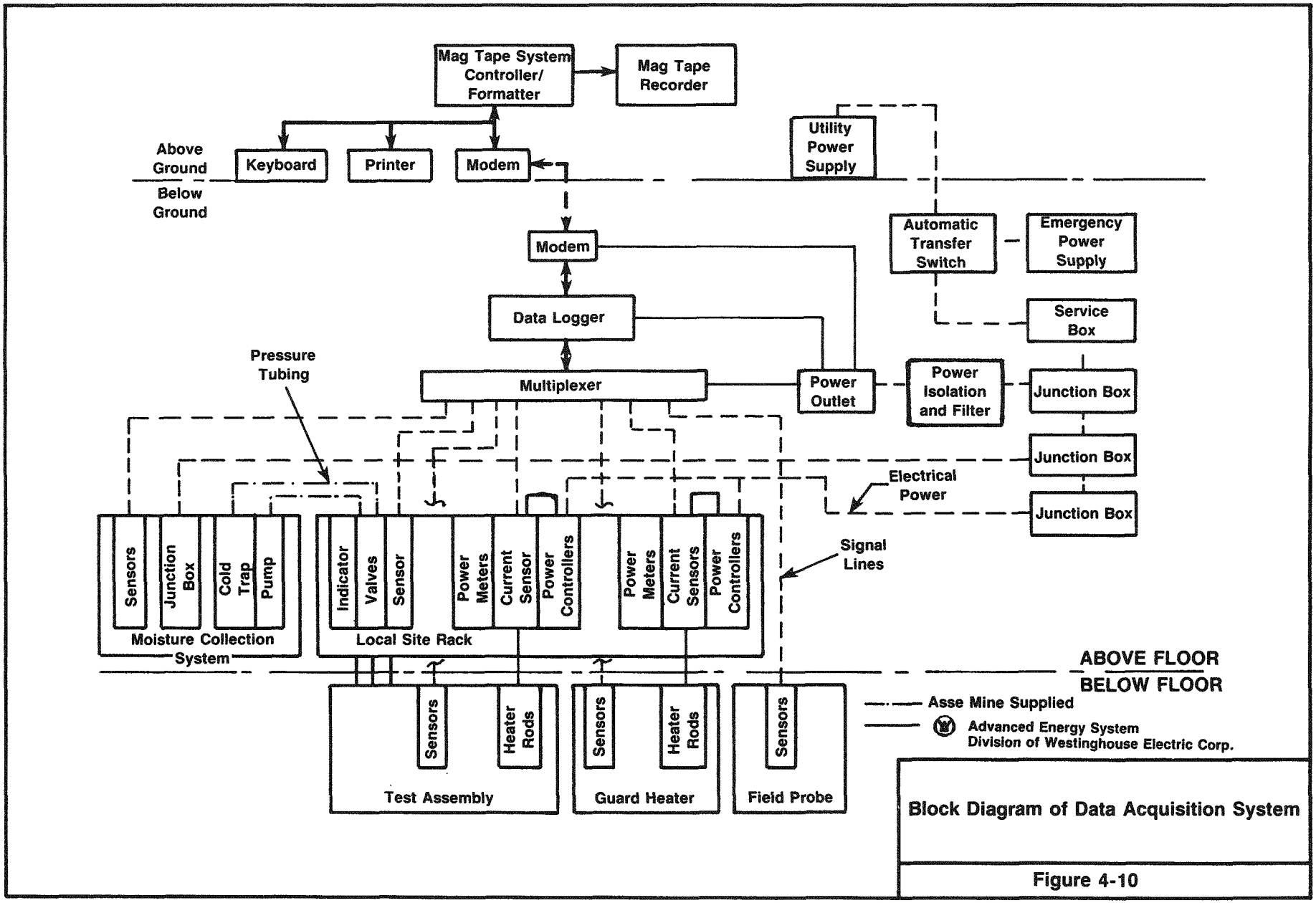

Block Diagram of Data Acquisition System

Figure 4-10

- Two pressure transducers - one on the test assembly outlet line and the other monitoring pump outlet pressure.

The overall system also includes

- A cold trap with sufficient capacity to refrigerate all four collection loops
- A thermostatic temperature control on the refrigerator
- A control panel and electrical switches for applying power to the cold traps as well as the process pump motors
- A cylinder of compressed dry nitrogen gas (for flushing and charging operations).

A moisture collection capability is required for each test site. Accordingly, two pressure lines (input and output) are built into each test assembly. The lines are discharged at the bottom of the lower sleeve and at the bottom of the caisson, respectively. The lines pass through a seal block at the top of the test assembly and are routed to an adjacent local site rack. For nonpressurized sites, the rack supports a relief valve, a pressure transducer, and a manual four-way valve. An emergency container is also provided on the relief valve outlet so that exhaust gas and water are not lost. Pressurized sites have a similar rack, except for using a three-way manual shutoff valve arrangement instead of the four-way valve. Long pressure lines join each of these racks with the central moisture collector rack.

4.5 HEATER POWER CONTROL

Four heater power controllers are used for each test site. One controller regulates the power to the six heater rods located in the test assembly (heater rods are wired in parallel), while the second regulates power to the eight guard heater rods (also wired in parallel). Similarly, the remaining two controllers regulated power to backup heater rod groups that are built into the test assembly and guard heaters. The backup system is only used in the event of a failure in the primary system.

The heater power controllers use two phase-angle fired power thyristors, which are fired alternately each half cycle. The controllers are equipped with voltage feedback control, which automatically adjusts the output for any change in input voltage. This is accomplished by adjusting the timing of the power conduction trigger pulses. For instance, if operated at 50 percent power (90 degrees conduction angle) output, with 220 input voltage alternating current (VAC), and the input voltage drops to 190 VAC, the timing of the trigger pulses increases the conduction angle to keep the output voltage the same. Adjustments for variations in heater resistance that can occur during heatup are performed manually by observing power meter indications.

4.6 RADIATION SOURCE

The radiation spectrum from spent fuel peaks in the range of 0.6 to 0.9 MeV. Cesium-137, which emits 0.66 MeV photons, is the dominant gamma emitter among fission products that have cooled more than 3 years.

High-level waste (HLW) has similar radiation properties. There is a low level of neutron emission from spent fuel (less from HLW), but this is not considered to be significant to brine migration. Alpha and beta radiation do not penetrate the waste package.

An available and convenient source of radiation is cobalt-60, which is obtained from neutron activation of cobalt and has a half-life of 5.3 years. Cobalt-60 produces gamma rays whose energies are 1.17 and 1.33 MeV (and also betas, which are not significant here). These energies are somewhat higher than the energies produced by waste forms, but it is considered that cobalt-60 will provide an acceptable simulation of the effects of radiation in the salt.

4.6.1 Thermal Output of Source

The heat output from cobalt-60 is 1 kW per 65,000 curie (Ci). Using two 9,430 Ci sources per test site yields an initial heat output of 290 W per site from the radioactive source. The Asse test sites are estimated to require 2.6 kW to produce the desired temperature.

Thus, electrical heating is required to add the additional heat and to compensate for the decrease in heat produced by the source as it decays. The half-life of the source is 5.3 years. It should be noted that the heat released by a cobalt-60 source occurs where the gamma rays are absorbed. Most of the gamma rays were absorbed in the test apparatus, but some were absorbed in the salt. This slightly reduced the peak salt temperature and temperature gradient, due to the reduced heat flux near the borehole wall. This was judged to be an insignificant perturbation.

4.6.2 Description of Radioactive Sources

Radioactive sources are used at two of the test locations. Two source assemblies are used in each of these test locations, and these source assemblies are contained in canisters for handling purposes. The source material is cobalt-60, having a strength of 9,430 Ci per assembly. A source assembly consists of five subsources shown in Figure 4-11.

Each subsource is 152 mm (5.98 in) long and 9.5 mm (0.37 in) in diameter. This subsource is encapsulated first in a stainless steel tube having an outside diameter of 11.1 mm (0.44 in) and a length of 159 mm (6.26 in), and second in a stainless steel tube with an outside diameter of 13.1 mm (0.52 in) and a length of 172 mm (6.8 in), so that the total length of cobalt-60 in the canister is 860 mm (33.9 in).

The subsources are contained in a source holder, which is a tube with an outside diameter of about 20 mm (0.79 in) and is long enough to hold the entire source with a mechanical closure at its top. The source holder is

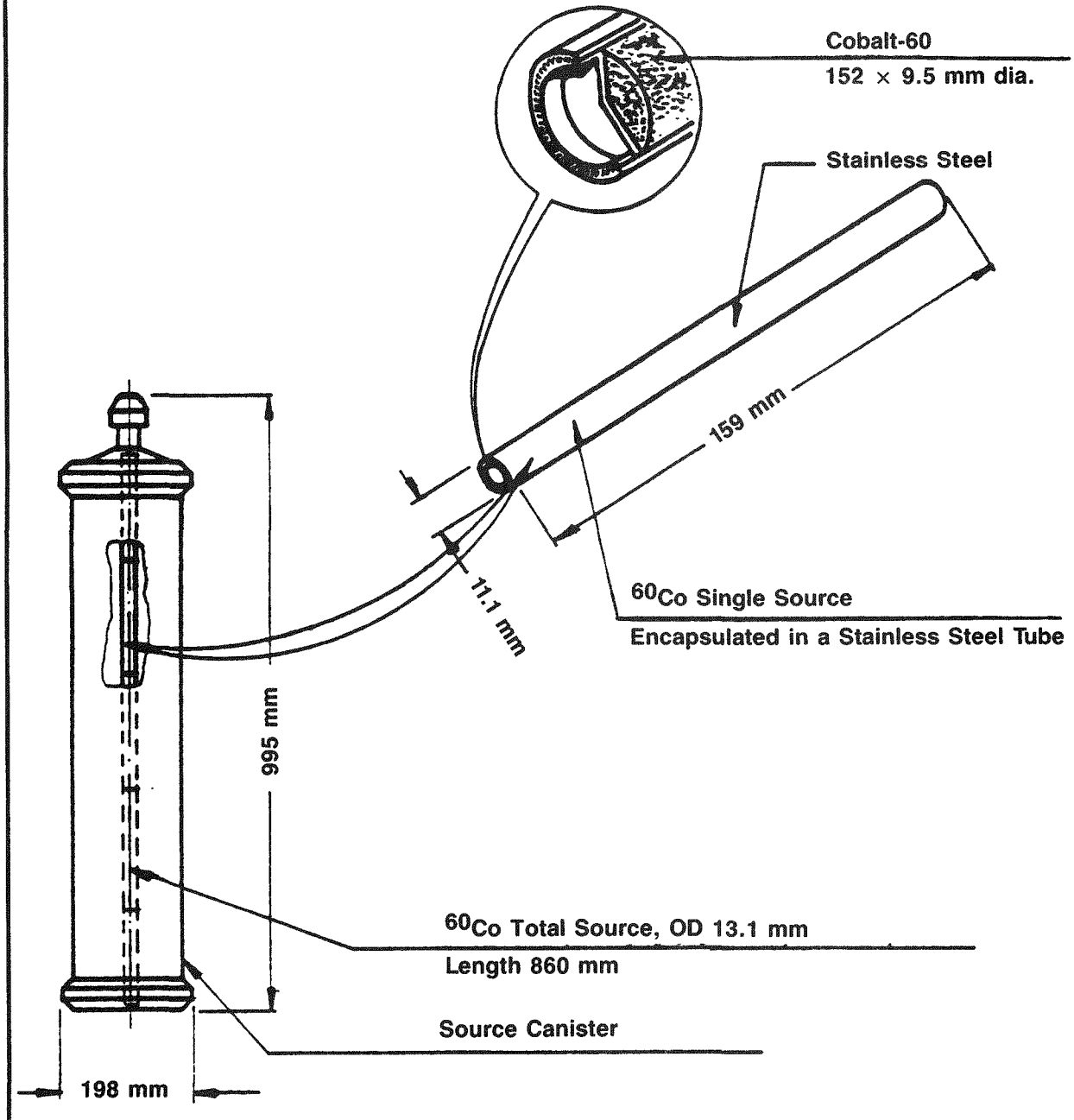

Cobalt-60 Radioactive Source Element Double Encapsulated and Inserted Into Source Canister

Figure 4-11

finned so that the source will be centrally located when the source holder is installed into the canister. The canister is 1 m (39.4 in) long, including the pintle on its top end, and it has an outside diameter of 198 mm (7.80 in). The top of the canister has a mechanical closure with a pintle to allow for grappling. Two radioactive canisters and one shielding canister per radioactive test are used.

4.6.3 Handling of Cobalt-60 Radiation Sources

The problems arising during handling and shipping of the cobalt-60 sources were not significantly different from those previously encountered when handling and shipping material of this nature.

Regulations governing shipment over land and by sea of this type of material have been established by the International Atomic Energy Agency.

The sources used were double encapsulated and manufactured in the United Kingdom. Canisters were manufactured in the United States and shipped to the source vendor who installed the sources in the canisters. Each canister contains source material having a strength of 9,430 Ci. The source vendor installed the loaded canisters into a licensed shipping cask and shipped the canisters to the Asse mine hot cell. All of the above operations regarding source manufacture, source installation into canisters, and subsequent canister installation into shielding casks were conducted in accordance with established and proven procedures for personnel and environmental protection. Installation of the sources into the canisters and the canisters into the shipping casks was done by remote control in the source vendor's hot cell. The design of the canister was furnished to the source vendor to ensure compatibility of the source with the canister and also to ensure the vendor's capability to handle the canister. A dummy canister was supplied to the source vendor to permit the development of procedures for canister operations and also to afford the opportunity for the source vendor to practice prior to the actual operations. Handling of the sources and the loaded canisters was monitored to ensure compliance with proven procedures.

The loaded cask was shipped to the Asse mine site. Here, the canisters were transferred from the shielding cask into the hot cell at the mine. The cask had capacity for one canister at a time. This operation was repeated for each of the sources and, subsequently, the sources were reinserted into the shielding cask for transfer underground. The loaded cask was transported into the mine to the experiment site, where the canister was installed in the borehole. Upon completion of the installation, the cask was returned to the hot cell to receive the next canister. This cycle of operations was performed four times to complete the transfer of all source canisters from the hot cell to the boreholes. Intermediate operations were used for the installation cask to emplace the thermal shield and the shield plug at the experimental sites.

The operations at the Asse mine were conducted in accordance with procedures which had been reviewed and rehearsed to assure maximum protection to personnel and the environment. The canister design and a dummy canister were supplied to Asse early so that operating procedures could be developed and practiced.

The shielding cask was designed and manufactured in the FRG by Ganuk mbH. The cask was designed to international standards which, on contact, allow a maximum dose rate of 200 mrem/h, and at a distance of 1 m (3.3 ft), allow a maximum dose rate of 10 mrem/h. The cask (1,792 mm [70.55 in] high, 794-mm- [31.26-in-] OD, 214-mm- [8.43-in-] ID) is made of a 240-mm- (9.45-in-) thick layer of lead, followed by a heat shield made of a 15-mm (0.59-in) layer of sand (quartz) and an outer sheath of stainless steel.

The complete handling system consists of the shielding cask with a gripping device (grapple) and a winch, and three sliding shield systems (one for the hot cell at Asse mine, two for sites 3 and 4). Figures 4-8 and 4-12 show the cask with the winch installed standing on a sliding shield system. The upper inside top of the cask is cone-shaped, and usually the grapple is fixed to a canister there. To move the grapple up and down, an electric winch is installed on top of the cask. To control movement of the grapple and/or canister and of the winch, the load attached to the grapple is measured continuously during operations. The following load steps are used:

1. Overload: The grapple is in the cone-shaped top of the transfer cask; the winch stops automatically.

2. Normal load: A source canister is hanging on the grapple and is in between the top of the cask and borehole bottom of the first canister.

3. Under load: The canister reaches the bottom of its travel, and the grapple touches the top of the canister pintle; the winch stops automatically; by lowering the grapple 40 mm (1.57 in) deeper, the canister is released and the grapple areas are mechanically locked open.

4. No load: The grapple is disconnected from the canister and retrieved into the transfer cask.

To place a source canister into the borehole, the following procedure is performed:

1. The cask with the canister inside is placed on the sliding shield.

2. The upper small slider removes the bottom plate of the cask.

3. The lower sliding shield opens the borehole.

4. The winch lowers the grapple with the canister into the borehole.

5. The grapple opens and is hauled up into the cask, leaving the source in place.

6. The sliding shield is closed.

7. The small slider moves the bottom plate closing the cask.

8. The cask can be removed.

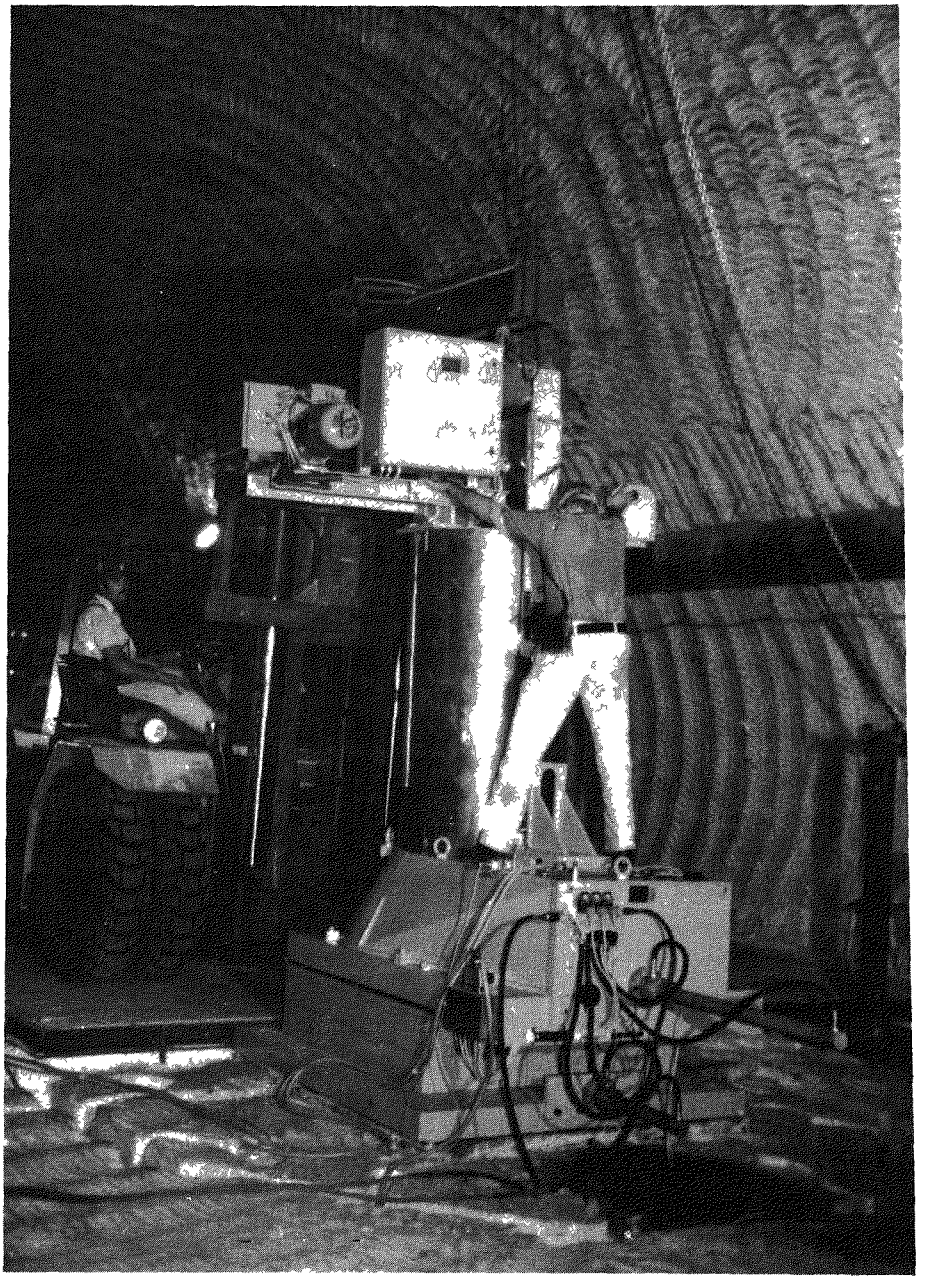

Figure 4-12 Radioactive Source Handling Equipment

At the conclusion of the experiment, the canisters will be removed from individual test sites and returned to the Asse hot cell. The cask used for installation of the canisters will be used for retrieval operations. At the hot cell, the canisters will be removed from the cask and stored, pending return to the source vendor, who will assume responsibility for the sources. It is anticipated that retrieval operations will be the reverse of the corresponding operations followed during installation.

4.7 TEST SITE PARAMETERS

Each brine migration test site contains similar hardware but has different operating parameters. The complete experiment is composed of four test sites, each consisting of a heat source, associated instrumentation, and in two cases, a radiation source. Each test site is independent of the others and has identical geometry, but each has varied parameters to attain the test objectives. The parameters to be varied are shown in Table 4-2.

Table 4-2. Matrix of Test Parameters[a]

	Site 1	Site 2	Site 3	Site 4
Salt Type	Main Halite	Main Halite	Main Halite	Main Halite
Radioactive	No	No	Yes	Yes
Pressurized Hole	Yes	No	Yes[b]	No

(a) All sites are at 210°C (410°F) maximum borehole wall temperature and 3.2°C/cm (14.6°F/in) maximum temperature gradient.

(b) On October 22, 1984, test site 3 was ventilated with nitrogen to remove approximately 30 cm^3 of brine. Since October 24, this site has been operating at atmospheric pressure.

Originally, two sites were operated with a pressurized borehole; the remaining two were nonpressurized with continuous brine (water) collection. Since October 24, 1984, only test site 1 remains as a pressurized borehole. Test site 3 developed a leak in July 1984, and in October 1984, the decision was made to allow it to become a nonpressurized test site. The borehole was then purged with nitrogen and the pressure dropped to atmospheric pressure. Each of the test sites is operated to generate a maximum borehole wall temperature of 210°C (410°F) and a maximum temperature gradient of 3.2°C/cm (14.6°F/in), which are conditions that are expected to accelerate brine migration to provide easily measurable quantities of brine inflow into the test holes.

5.0 CHRONOLOGY OF TEST PROGRESS

The complete performance of this experiment includes operations and data gathering during mining of the test field and the installation, operation, and posttest evaluation phases. Table 5-1 gives the chronology of the test progress.

Table 5-1. Chronology of Key Events

Test Site	Date	Key Event
All Sites	December 1981 - March 1982	Mining of the Test Room (Start-Up of Room Closure Measurements)
All Sites	June 1982 - December 1983	Drilling of Test Boreholes (Core Sampling)
All Sites	March - May 1983	Equipment Installation
1 and 2	May 25, 1983	Start-Up of Heating
1 and 2	September 12, 1983	Central Heater Power Increased From 2,700 W to 3,000 W
4	December 13, 1983	Radiation Source Inserted
3	December 14, 1983	Radiation Source Inserted
3 and 4	December 15, 1983	Start-Up of Heating
4	March 14, 1984	Guard Heater Power Increased From 7,220 W to 7,600 W
1	April 11, 1984	Leak Developed at Test Site 1 But Was Sealed One Week Later
4	June 12, 1984	Central Heater Power Increased From 2,700 W to 2,850 W
3	July 17, 1984	Slow Leakage Noted at Test Site 3
3	October 24, 1984	Test Site 3 Became a Nonpressurized Site
All Sites	October 4, 1985	Posttest Activities

6.0 PRELIMINARY TEST RESULTS

The following sections include preliminary data from May 25, 1983, through September, 1985.

6.1 TEMPERATURES

Figures 6-1 and 6-2 show the time-dependent temperature rise of the test assembly (outer surface) and the borehole wall, as well as the rise at the 1.5-m (4.9-ft) radius (guard heater and field probe) and at the 2.2-m (7.2-ft) radius (strain-gaged stress meter) after start-up of heating of the nonradioactive test sites 1 and 2 on May 25, 1983. The curves represent the measurement at the midplane of the test setup where the maximum temperatures are to be expected. The initial power of the central heater was adjusted to 2,530 W and that of the eight guard heaters to 7,220 W (900 W each). These heater powers, which were estimated by numerical pretest calculations, should have resulted in the desired maximum salt temperature of 210°C (410°F) at the borehole wall at the end of the 2-year heating period. However, 110 days after start-up of heating, it was observed that only a temperature of approximately 195°C (383°F) would be achieved with that power. It was then decided to increase the central heater power to 3,000 W, which would raise the borehole wall temperature as desired and would only increase the temperature gradient from the initially planned 3°C/cm (13.7°F/in) to 3.2°C/cm (14.6°F/in).

The heater power increase and the resulting change in the borehole wall temperature can be seen in both Figures 6-1 and 6-2. On heating day 230 (January 10, 1984), the maximum borehole wall temperature at both test sites reached about 210°C (410°F) and increased very little up through heating day 840 (September 9, 1985). Considering the heat output of the cobalt-60 sources inserted at test sites 3 and 4 (300 W) the initial electrical power of the central heaters was only 2,710 W.

Figures 6-3 and 6-4 show the time-dependent temperature rise at test sites 3 and 4 over the first 277 days of operation. After start-up of heating on December 15, 1983, the behavior of test site 3 was in good agreement with predictions so that the desired maximum salt temperature will be achieved. At test site 4, the temperatures were slightly low, and 90 days after start-up of heating, the guard heater power was increased from 7,220 W to 7,600 W. However, since the central borehole wall temperature did not achieve the desired temperature, the central heater power was increased to 2,850 W, 173 days after the start-up of heating. The temperatures at all four test sites were then as desired and no further heater power adjustment was expected. On September 28, 1984, the maximum borehole wall temperatures around the heater midheight were as listed in Table 6-1.

The average borehole wall temperatures measured over time at six different depths of test sites 1, 2, 3, and 4 are listed in Tables 6-2, 6-3, 6-4, and 6-5, respectively. The corresponding graphs of the axial temperature distribution along the central boreholes are presented in Figures 6-5 through 6-8. The radial temperatures measured at the 804.57-m (2,639.66-ft) level of

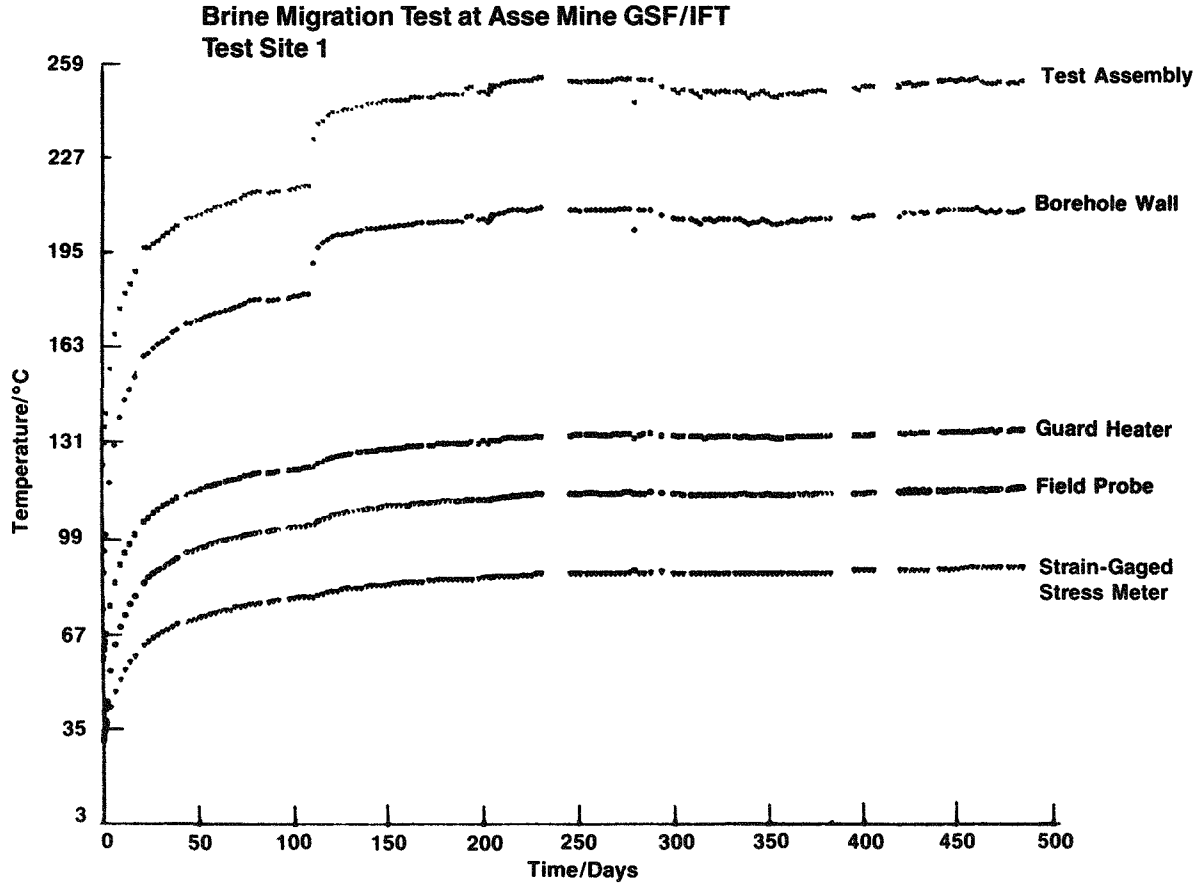

Borehole Salt Temperature
Versus Time for Test Site 1

Figure 6-1

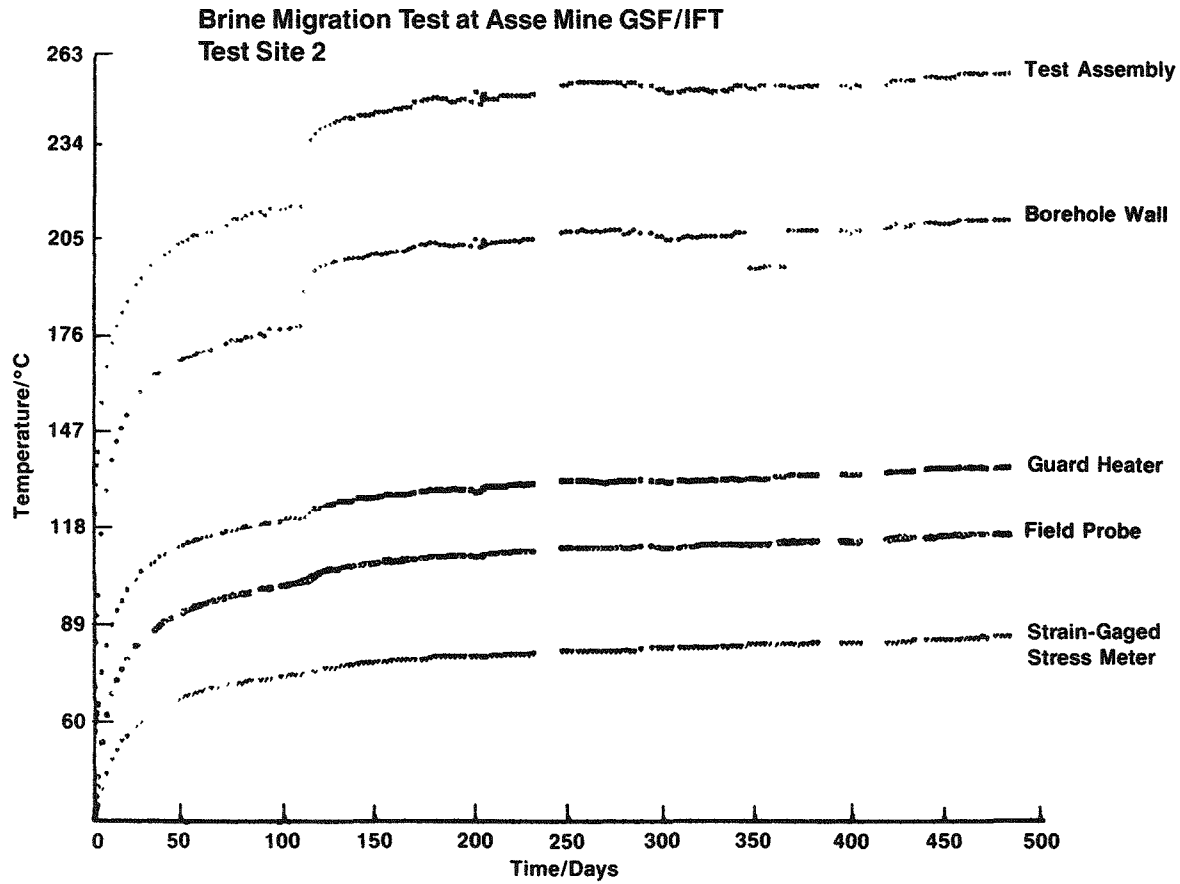

Borehole Salt Temperature Versus Time for Test Site 2

Figure 6-2

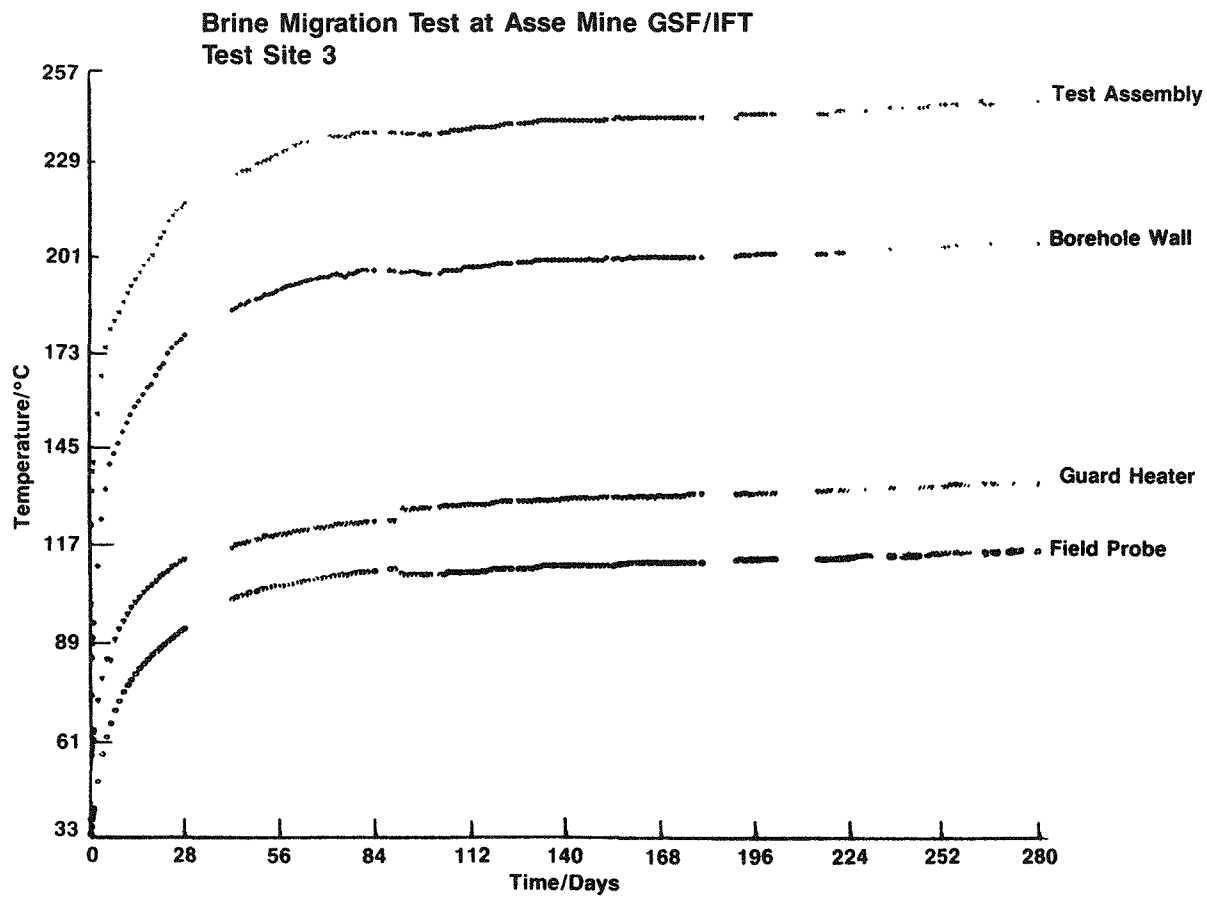

Borehole Salt Temperature
Versus Time for Test Site 3

Figure 6-3

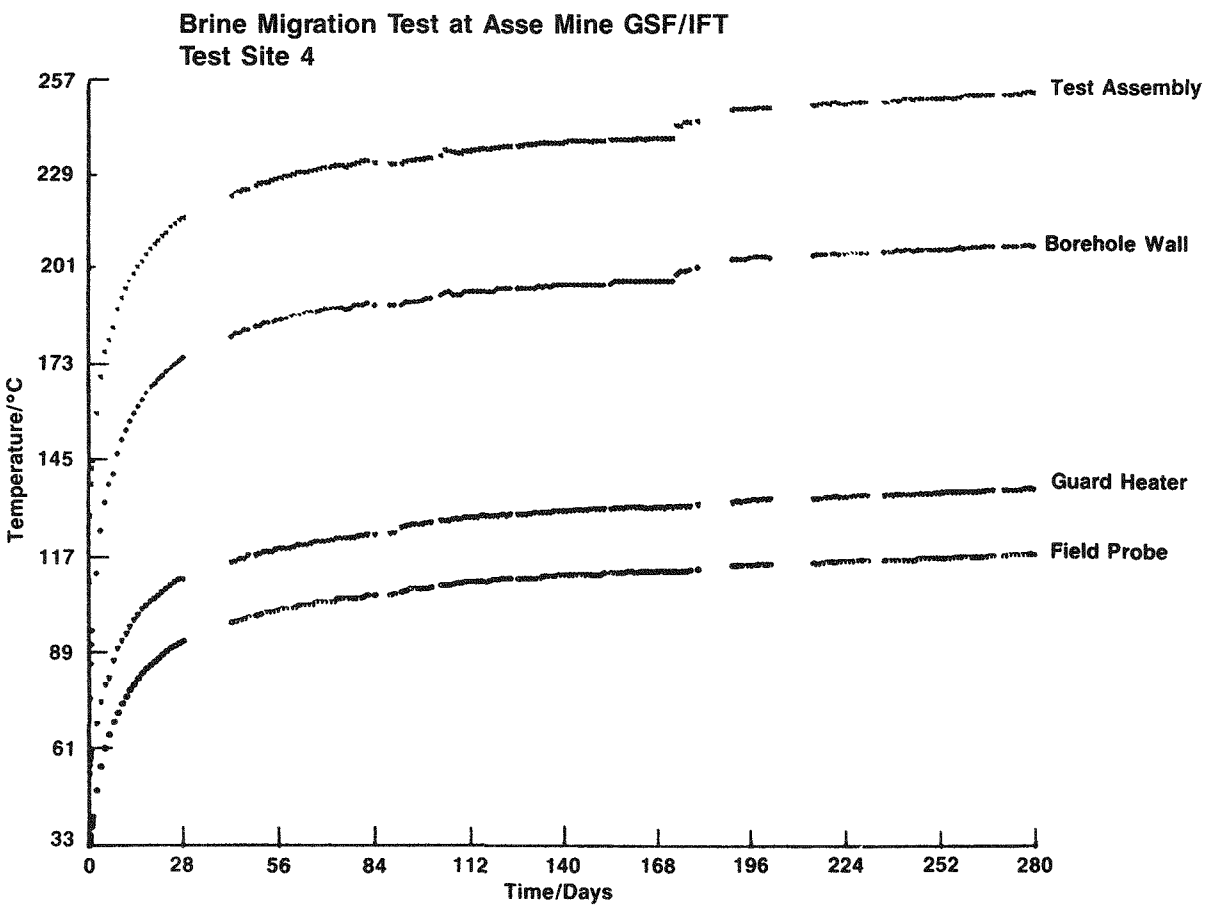

Borehole Salt Temperature
Versus Time for Test Site 4

Figure 6-4

test sites 1, 2, 3, and 4 are listed in Tables 6-6, 6-7, 6-8, and 6-9, respectively. The corresponding plots of the temperatures versus the radial distance at the 804.57-m (2,639.66-ft) level are presented in Figures 6-9 through 6-12. The temperature measurements are taken in the central borehole, the temperature probe boreholes, and at test sites 1 and 2, in the strain-gaged stress meter (SGS) boreholes, 4.57 m (15.00 ft) below the gallery floor at the midheight of the heated section.

Table 6-1. Maximum Borehole Wall Temperature

Test Site	Heating Day	Temperature (°C)
1	492	210
2	492	213
3	288	208
4	288	208

6.2 BRINE MIGRATION

As already mentioned in Section 4.7, test sites 2 and 4 were originally operated with continuous brine collection, whereas test sites 1 and 3 were closed so that brine and gases would build up pressure and react in the boreholes. Since October 24, 1984, however, test site 3 has become a nonpressurized test site. The pressurized test sites simulate the actual repository environment.

Test sites 2, 3, and 4 are currently maintained at atmospheric pressure, and the brine released to the borehole is circulated continuously by nitrogen gas and other noncondensables through the alumina beads and the moisture collection system (MCS) (Figure 4-9). The results of accumulated water up to September 23, 1985, are presented in Tables 6-10 through 6-13.

For test site 3, data of three different times (214, 314, and 649 days of operation) are presented in Table 6-10 since test site 3 developed a slow leak after 215 days of operation and then became a nonpressurized site after 313 days. Since it is not known which gas molecules (water vapor or other gases) were lost through the leakage, it is considered that the estimated amount of collected brine from test site 3 is only qualitative.

It appears that a smaller amount of brine is collected in the pressurized boreholes, indicating that the gas pressure is reducing the vapor transport mechanism (Figure 6-13). This phenomenon is explainable if vapor transport (Darcy flow) occurs parallel to liquid inclusion migration. Since the amount of water released to sites 1 and 3 is less than half of that released to sites 2 and 4 (note day 314 measurement at test site 3), it appears that both transport mechanisms have to be taken into account in the nonpressurized boreholes, whereas vapor migration is reduced in the pressurized boreholes.

Table 6-2. Average Borehole Wall Temperature (°C) for Test Site 1

Date	Depth (m)					
	803.01	803.40	803.81	804.57	805.33	805.66
5/24/83	31.00	31.00	31.00	31.00	31.00	31.00
7/23/83	93.33	116.50	147.33	175.00	148.33	119.67
8/22/83	96.00	119.50	151.33	179.33	153.00	124.33
9/21/83	102.33	129.00	165.67	199.67	168.00	134.67
10/21/83	---	---	---	---	---	---
11/20/83	106.00	133.50	170.67	205.67	173.67	140.00
12/20/83	107.33	135.50	172.67	208.33	175.67	141.67
1/19/84	---	---	---	---	---	---
2/18/84	108.00	135.50	173.00	209.67	178.67	144.00
3/19/84	107.33	134.50	171.00	207.00	176.67	143.33
4/18/84	107.00	134.50	170.67	206.67	176.00	142.67
5/18/84	107.00	133.50	169.33	205.67	175.67	142.33
6/17/84	---	---	---	---	---	---
7/17/84	108.00	134.50	171.67	208.00	178.00	144.00
8/16/84	109.00	136.00	172.67	210.00	179.67	145.00
9/15/84	109.00	136.00	172.67	209.00	179.00	145.00
10/15/84	109.33	136.00	173.67	210.33	180.00	145.67
11/14/84	109.00	136.50	173.33	210.00	180.00	147.00
12/14/84	109.33	136.50	173.67	210.00	180.00	147.67
1/13/85	109.33	136.50	173.00	209.67	180.00	145.67
2/12/85	109.33	136.50	173.67	211.00	181.00	147.67
3/13/85	109.33	136.00	172.67	209.33	180.00	147.33
4/12/85	109.33	136.00	172.67	209.67	180.00	145.67
5/12/85	109.67	136.50	173.67	210.00	180.33	148.00
6/11/85	---	---	---	---	---	---
7/11/85	110.67	137.50	174.67	211.67	181.67	149.67
8/10/85	111.00	138.00	175.00	212.33	183.00	151.00
9/9/85	111.00	138.00	174.67	211.33	182.33	150.33

Table 6-3. Average Borehole Wall Temperature (°C) for Test Site 2

Date	Depth (m)					
	803.01	803.40	803.81	804.57	805.33	805.66
5/24/83	31.67	31.67	31.50	31.67	31.33	31.33
7/23/83	92.00	115.67	146.33	173.33	146.33	118.33
8/22/83	94.00	118.67	150.67	178.67	151.00	123.00
9/21/83	100.00	128.00	165.33	198.33	166.33	133.33
10/21/83	---	---	---	---	---	---
11/20/83	104.00	133.00	171.33	205.67	172.67	139.00
12/20/83	104.33	133.33	171.33	205.67	173.00	140.00
1/19/84	---	---	---	---	---	---
2/18/84	106.00	135.67	174.33	209.67	176.67	142.33
3/19/84	106.00	134.67	173.33	207.67	175.33	142.00
4/18/84	106.67	135.33	173.33	207.67	175.33	142.00
5/18/84	107.00	133.00	168.33	198.33	162.00	136.67
6/17/84	---	---	---	---	---	---
7/17/84	107.67	135.67	173.67	210.33	181.00	146.67
8/16/84	108.67	137.00	175.00	211.33	182.00	147.67
9/15/84	109.67	137.33	175.67	212.33	183.00	148.33
10/15/84	109.67	135.33	170.67	202.33	168.33	142.00
11/14/84	114.00	139.33	174.33	206.00	177.33	151.33
12/14/84	114.00	139.67	174.67	206.33	177.67	151.33
1/13/85	114.33	140.33	176.00	208.33	180.67	152.67
2/12/85	114.00	140.00	174.67	206.67	178.33	151.33
3/13/85	114.33	140.33	175.67	208.33	178.67	152.00
4/12/85	115.00	141.33	178.00	210.67	183.00	154.33
5/12/85	115.00	141.67	179.00	212.67	186.33	155.67
6/11/85	---	---	---	---	---	---
7/11/85	115.00	142.00	178.33	212.00	184.67	154.67
8/10/85	116.33	142.33	178.33	210.67	181.00	154.33
9/9/85	116.33	145.00	183.33	220.00	196.33	161.00

Table 6-4. Average Borehole Wall Temperature (°C) for Test Site 3

	Depth (m)					
Date	803.01	803.40	803.81	804.57	805.33	805.66
12/15/83	34.00	35.00	36.33	37.33	36.67	36.00
2/13/84	101.33	128.33	166.00	195.00	163.33	133.67
3/14/84	---	---	---	---	---	---
4/13/84	105.33	132.67	169.50	200.00	170.00	138.50
5/13/84	107.00	134.00	171.50	202.33	172.00	140.50
6/12/84	107.67	134.67	172.50	203.33	173.67	141.50
7/12/84	108.00	135.67	172.50	204.00	174.67	142.50
8/11/84	109.00	136.67	174.50	205.67	176.00	143.50
9/10/84	---	---	---	---	---	---
10/10/84	111.00	138.67	176.50	207.67	178.00	145.50
11/9/84	111.00	138.67	176.50	207.67	178.67	145.50
12/9/84	111.00	138.67	176.50	207.33	178.67	146.67
1/8/85	111.00	138.67	176.50	208.00	179.33	147.33
2/7/85	111.00	138.67	176.50	207.33	178.67	146.67
3/8/85	---	---	---	---	---	---
4/7/85	111.33	138.67	176.50	207.33	179.00	147.33
5/7/85	112.00	138.67	177.00	208.00	179.67	147.33
6/6/85	108.00	135.33	179.50	204.33	169.67	137.67
7/6/85	112.67	140.00	178.50	209.33	180.67	148.33
8/5/85	113.00	140.67	179.50	210.67	182.00	149.33
9/4/85	113.00	140.67	179.50	211.00	182.33	149.33
10/4/85	113.33	141.00	179.50	211.00	182.00	149.67

Table 6-5. Average Borehole Wall Temperature (°C) for Test Site 4

Date	Depth (m)					
	803.01	803.40	803.81	804.57	805.33	805.66
12/15/83	34.33	35.67	37.67	38.33	38.00	35.33
2/13/84	99.00	125.00	159.33	187.33	156.00	126.67
3/14/84	---	---	---	---	---	---
4/13/84	105.00	132.00	166.67	194.67	164.00	134.67
5/13/84	106.33	133.00	168.33	196.33	166.00	136.00
6/12/84	115.33	141.00	174.00	201.33	174.50	153.67
7/12/84	117.00	143.33	177.00	204.67	177.50	156.33
8/11/84	118.00	144.67	178.33	206.00	179.00	158.00
9/10/84	---	---	---	---	---	---
10/10/84	119.67	146.00	179.67	207.33	180.00	160.67
11/9/84	112.00	140.00	176.67	207.33	175.00	144.00
12/9/84	111.67	139.67	176.67	207.33	175.00	143.67
1/8/85	112.00	140.00	177.33	208.00	176.00	144.33
2/7/85	112.00	140.00	177.67	208.33	176.00	144.67
3/8/85	---	---	---	---	---	---
4/7/85	112.00	140.33	178.33	209.00	177.00	144.67
5/7/85	112.00	140.00	178.00	208.33	176.50	144.67
6/6/85	111.67	139.33	177.33	208.33	175.00	142.33
7/6/85	113.00	141.00	179.33	210.00	177.50	145.67
8/5/85	113.00	141.33	179.67	210.33	178.00	146.00
9/4/85	114.00	142.00	180.33	211.00	178.50	146.67
10/4/85	114.00	142.00	180.33	211.00	178.50	146.67

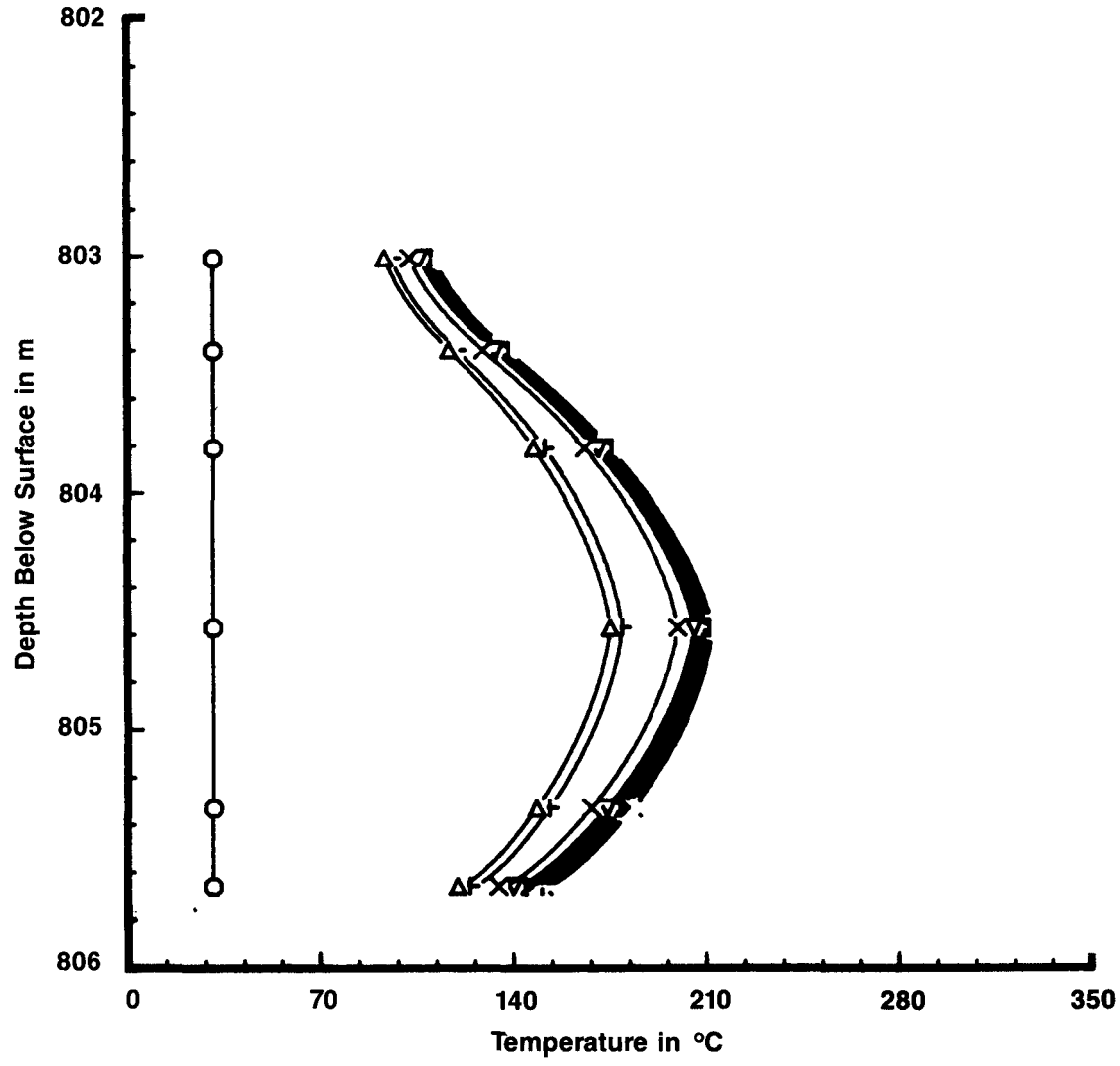

LEGEND:

○	5/24/83	○	9/15/84
△	7/23/83	□	10/15/84
+	8/22/83	■	11/14/84
×	9/21/83	□	12/14/84
▽	11/20/83	○	1/13/85
▣	12/20/83	△	2/12/85
◆	2/18/84	+	3/13/85
⊕	3/19/84	×	4/12/85
⧗	4/18/84	◇	5/12/85
⊞	5/18/84	⊠	7/11/85
◪	7/17/84	✕	8/10/85
●	8/16/84	◆	9/ 9/85

Depth Below Surface Versus Average Borehole Wall Temperature for Test Site 1

Figure 6-5

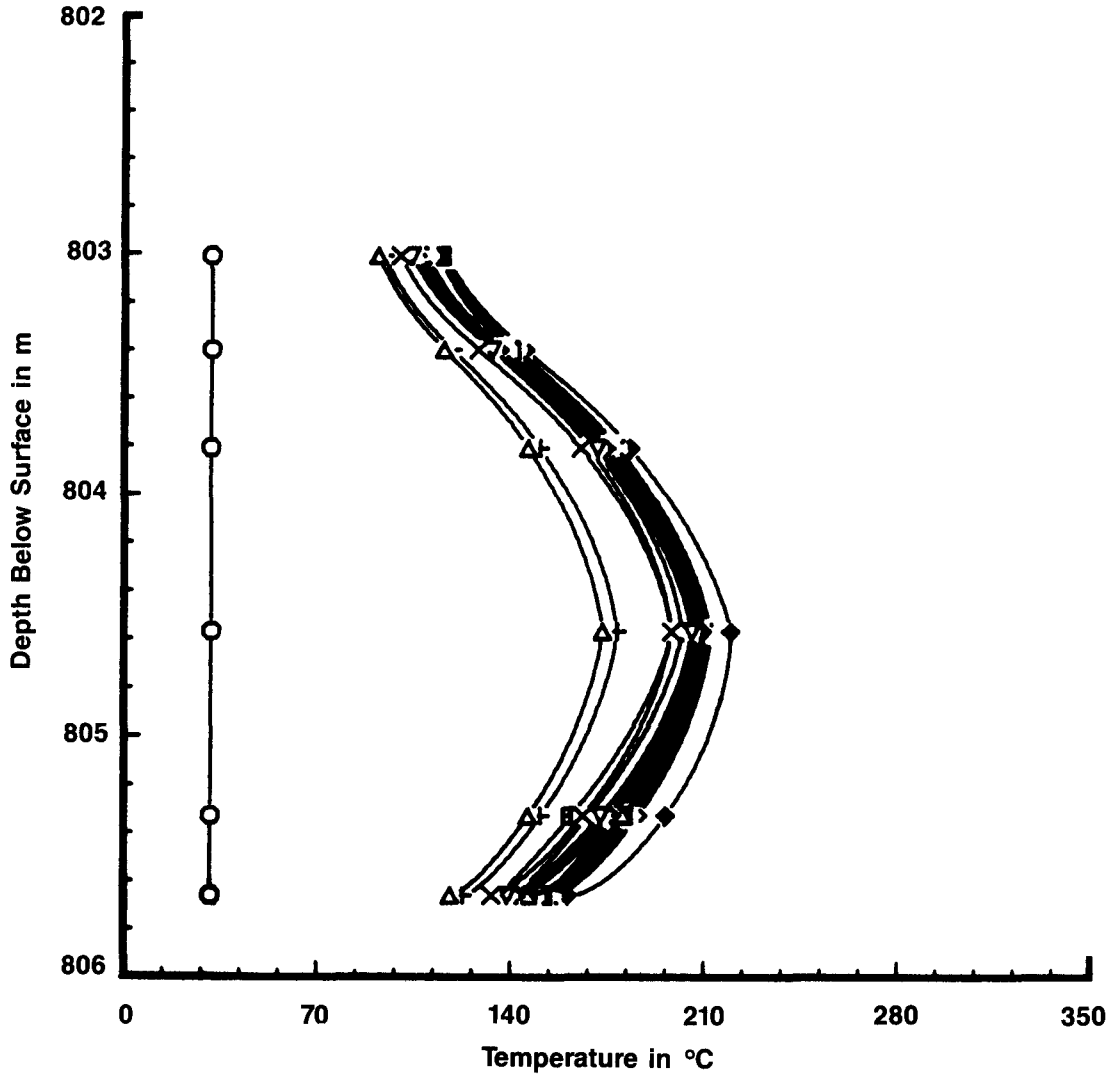

LEGEND:

5/24/83	9/15/84
7/23/83	10/15/84
8/22/83	11/14/84
9/21/83	12/14/84
11/20/83	1/13/85
12/20/83	2/12/85
2/18/84	3/13/85
3/19/84	4/12/85
4/18/84	5/12/85
5/18/84	7/11/85
7/17/84	8/10/85
8/16/84	9/ 9/85

Depth Below Surface Versus Average Borehole Wall Temperature for Test Site 2

Figure 6-6

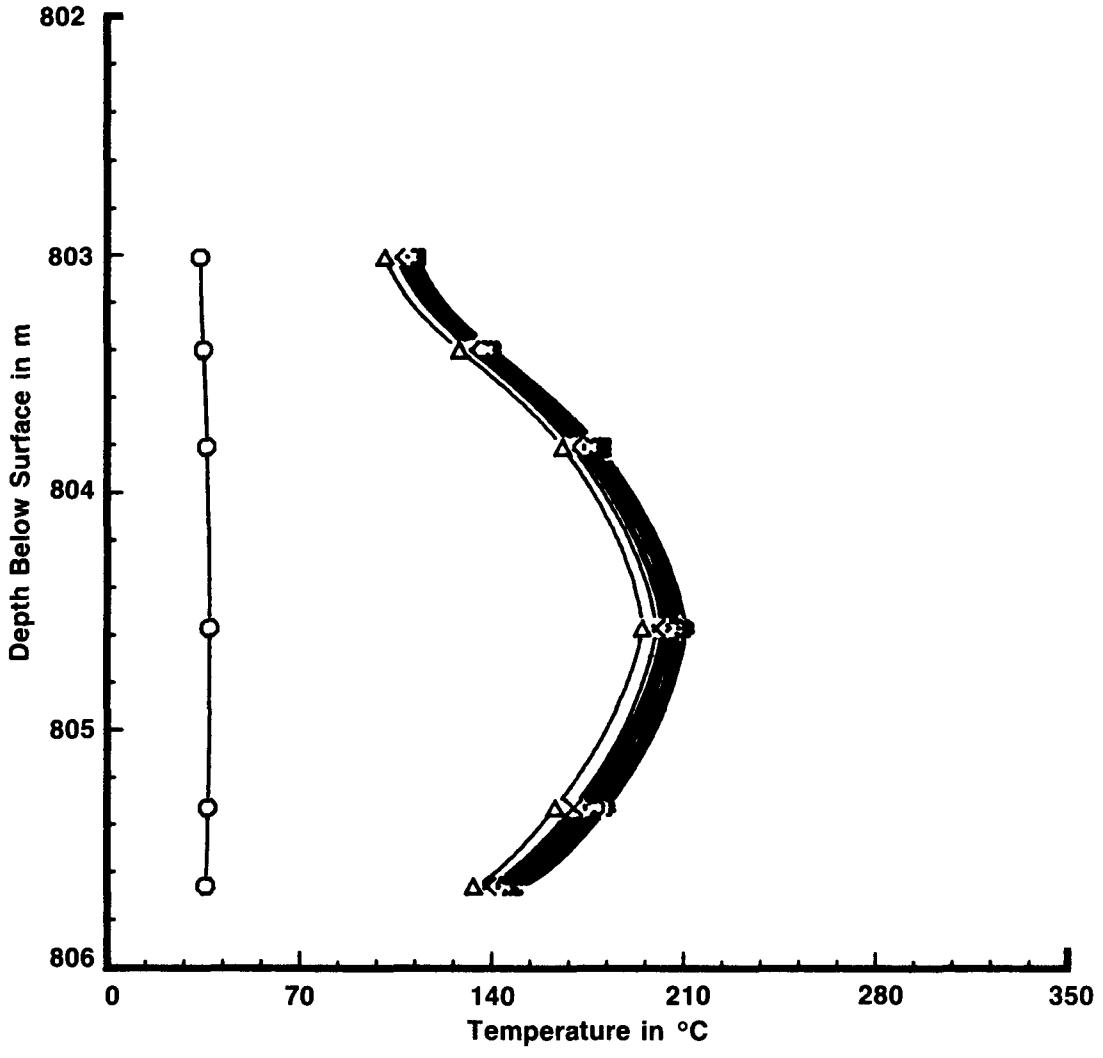

LEGEND:

○ 12/15/83	⊞ 12/ 9/84
△ 2/13/84	▩ 1/ 8/85
× 4/13/84	▨ 2/ 7/85
◇ 5/13/84	○ 4/ 7/85
▽ 6/12/84	□ 5/ 7/85
▩ 7/12/84	■ 6/ 6/85
✕ 8/11/84	□ 7/ 6/85
⊕ 10/10/84	○ 8/ 5/85
⧗ 11/ 9/84	△ 9/ 4/85
	+ 10/ 4/85

Depth Below Surface Versus Average Borehole Wall Temperature for Test Site 3

Figure 6-7

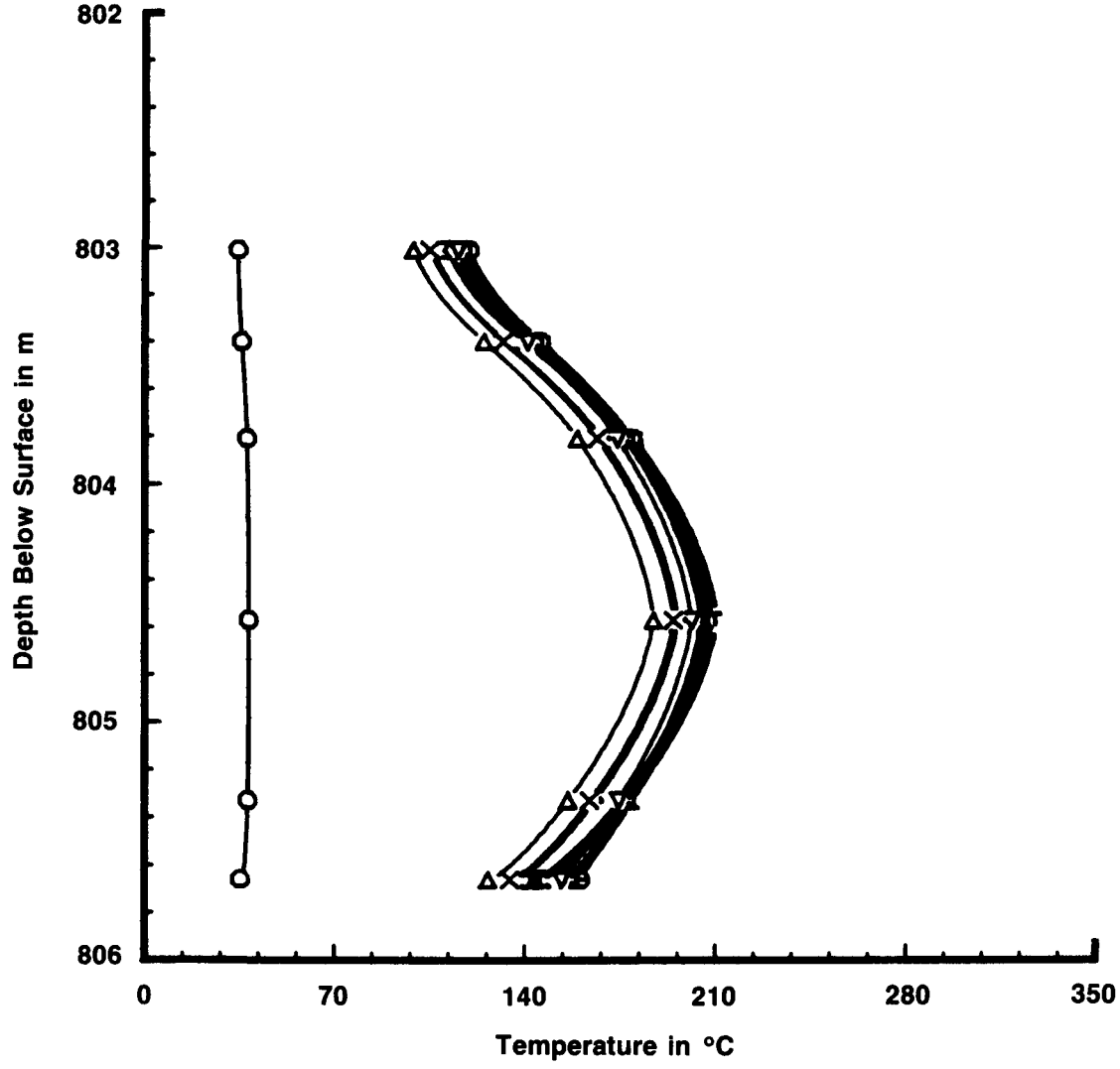

LEGEND:

○ 12/15/83	⊞ 12/ 9/84
△ 2/13/84	▣ 1/ 8/85
× 4/13/84	▨ 2/ 7/85
◇ 5/13/84	○ 4/ 7/85
▽ 6/12/84	□ 5/ 7/85
▣ 7/12/84	■ 6/ 6/85
✕ 8/11/84	□ 7/ 6/85
⊕ 10/10/84	○ 8/ 5/85
⧗ 11/ 9/84	△ 9/ 4/85
	+ 10/ 4/85

Depth Below Surface Versus Average Borehole Wall Temperature for Test Site 4

Figure 6-8

Table 6-6. Radial Temperature (°C) at 804.57 m (2,639.66 ft) From Surface for Test Site 1

Date	Radial Distance (cm)			
	16.50	21.75	150.00	220.00
5/24/83	31.00	31.00	31.00	32.33
6/23/83	199.00	164.33	88.67	66.67
7/23/83	210.33	175.00	97.67	74.33
8/22/83	215.67	179.33	102.33	78.00
9/21/83	241.67	199.67	106.67	81.33
10/21/83	---	---	---	---
11/20/83	248.33	205.67	112.00	85.67
12/20/83	251.67	208.33	113.00	86.67
1/19/84	---	---	---	---
2/18/84	253.67	209.67	114.33	87.67
3/19/84	250.00	207.00	114.33	87.67
4/18/84	250.00	206.67	114.33	87.67
5/18/84	248.00	205.67	114.00	87.67
6/17/84	---	---	---	---
7/17/84	252.00	208.00	115.00	88.67
8/16/84	253.67	210.00	115.67	89.00
9/15/84	252.67	209.00	116.33	89.67
10/15/84	254.00	210.33	116.67	90.00
11/14/84	254.00	210.00	116.67	90.00
12/14/84	253.67	210.00	117.00	90.67
1/13/85	253.67	209.67	117.00	90.67
2/12/85	255.00	211.00	117.33	90.67
3/13/85	253.33	209.33	117.33	90.67
4/12/85	253.67	209.67	117.00	90.67
5/12/85	254.00	210.00	117.33	90.67
6/11/85	---	---	---	---
7/11/85	254.67	211.67	116.33	89.67
8/10/85	256.67	212.33	118.33	91.67
9/9/85	255.67	211.33	118.67	92.00

Table 6-7. Radial Temperature (°C) at 804.57 m (2,639.66 ft) From Surface for Test Site 2

Date	Radial Distance (cm)			
	16.50	21.75	150.00	220.00
5/24/83	32.00	31.67	31.00	32.00
6/23/83	199.00	164.00	88.00	62.67
7/23/83	209.00	173.33	97.00	70.33
8/22/83	215.00	178.67	101.33	73.33
9/21/83	240.67	198.33	105.67	76.33
10/21/83	---	---	---	---
11/20/83	249.67	205.67	110.67	80.67
12/20/83	249.33	205.67	111.67	81.00
1/19/84	---	---	---	---
2/18/84	254.33	209.67	113.33	82.33
3/19/84	252.33	207.67	113.67	83.33
4/18/84	252.00	207.67	114.00	83.33
5/18/84	253.33	198.33	113.67	84.00
6/17/84	---	---	---	---
7/17/84	254.33	210.33	115.33	84.67
8/16/84	255.67	211.33	116.33	85.67
9/15/84	256.67	212.33	116.67	86.67
10/15/84	258.00	202.33	117.00	86.67
11/14/84	256.67	206.00	117.00	86.67
12/14/84	257.00	206.33	117.00	86.67
1/13/85	258.00	208.33	117.33	87.33
2/12/85	257.67	206.67	117.67	87.33
3/13/85	258.67	208.33	118.00	87.33
4/12/85	259.67	210.67	117.67	87.67
5/12/85	258.67	212.67	118.33	88.00
6/11/85	---	---	---	---
7/11/85	258.67	212.00	117.33	86.67
8/10/85	262.67	210.67	119.67	89.33
9/9/85	261.00	220.00	119.67	89.33

Table 6-8. Radial Temperature (°C) at 804.57 m (2,639.66 ft) From Surface for Test Site 3

	Radial Distance (cm)			
Date	16.50	21.75	150.00	220.00
12/15/83	41.67	37.33	33.67	---
1/14/84	---	---	---	---
2/13/84	235.67	195.00	107.67	---
3/14/84	---	---	---	---
4/13/84	241.00	200.00	111.67	---
5/13/84	243.00	202.33	112.67	---
6/12/84	244.00	203.33	113.67	---
7/12/84	245.00	204.00	114.67	---
8/11/84	247.00	205.67	115.67	---
9/10/84	---	---	---	---
10/10/84	249.00	207.67	117.67	---
11/9/84	250.00	207.67	117.67	---
12/9/84	250.00	207.33	117.67	---
1/8/85	251.00	208.00	118.67	---
2/7/85	250.00	207.33	118.67	---
3/8/85	---	---	---	---
4/7/85	250.67	207.33	118.67	---
5/7/85	251.00	208.00	119.33	---
6/6/85	234.67	204.33	102.67	---
7/6/85	252.67	209.33	120.33	---
8/5/85	254.00	210.67	120.67	---
9/4/85	254.00	211.00	120.67	---
10/4/85	254.33	211.00	121.67	---

Table 6-9. Radial Temperature (°C) at 804.57 m (2,639.66 ft) From Surface for Test Site 4

	Radial Distance (cm)			
Date	16.50	21.75	150.00	220.00
12/15/83	43.33	38.33	33.00	---
1/14/84	---	---	---	---
2/13/84	228.67	187.33	102.00	---
3/14/84	---	---	---	---
4/13/84	236.33	194.67	110.67	---
5/13/84	238.33	196.33	112.00	---
6/12/84	243.67	201.33	113.67	---
7/12/84	248.67	204.67	115.33	---
8/11/84	250.00	206.00	116.00	---
9/10/84	---	---	---	---
10/10/84	251.67	207.33	118.00	---
11/9/84	251.67	207.33	118.67	---
12/9/84	252.00	207.33	118.67	---
1/8/85	252.67	208.00	119.00	---
2/7/85	253.67	208.33	119.33	---
3/8/85	---	---	---	---
4/7/85	254.67	209.00	119.67	---
5/7/85	254.00	208.33	119.67	---
6/6/85	250.33	208.33	115.67	---
7/6/85	255.33	210.00	120.33	---
8/5/85	256.33	210.33	120.67	---
9/4/85	256.33	211.00	121.00	---
10/4/85	256.67	211.00	121.67	---

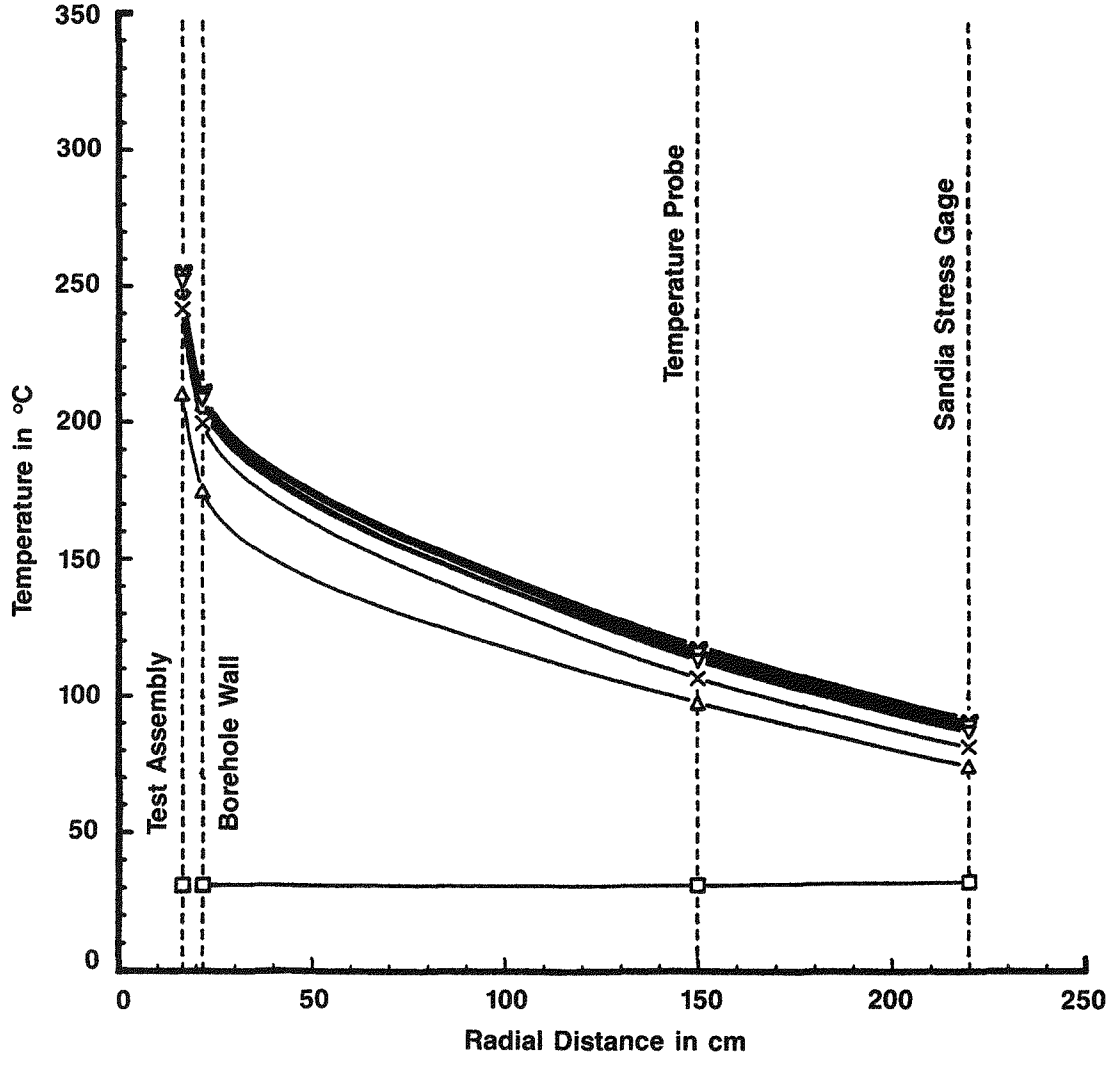

LEGEND:

□ 5/24/83	▨ 10/15/84
△ 7/23/83	○ 12/14/84
× 9/21/83	■ 2/12/85
▽ 12/20/83	○ 4/12/85
✱ 3/19/84	+ 7/11/85
⊕ 5/18/84	◇ 9/ 9/85
▦ 8/16/84	

Radial Temperature at 804.57 m (2,639.66 ft) From Surface for Test Site 1

Figure 6-9

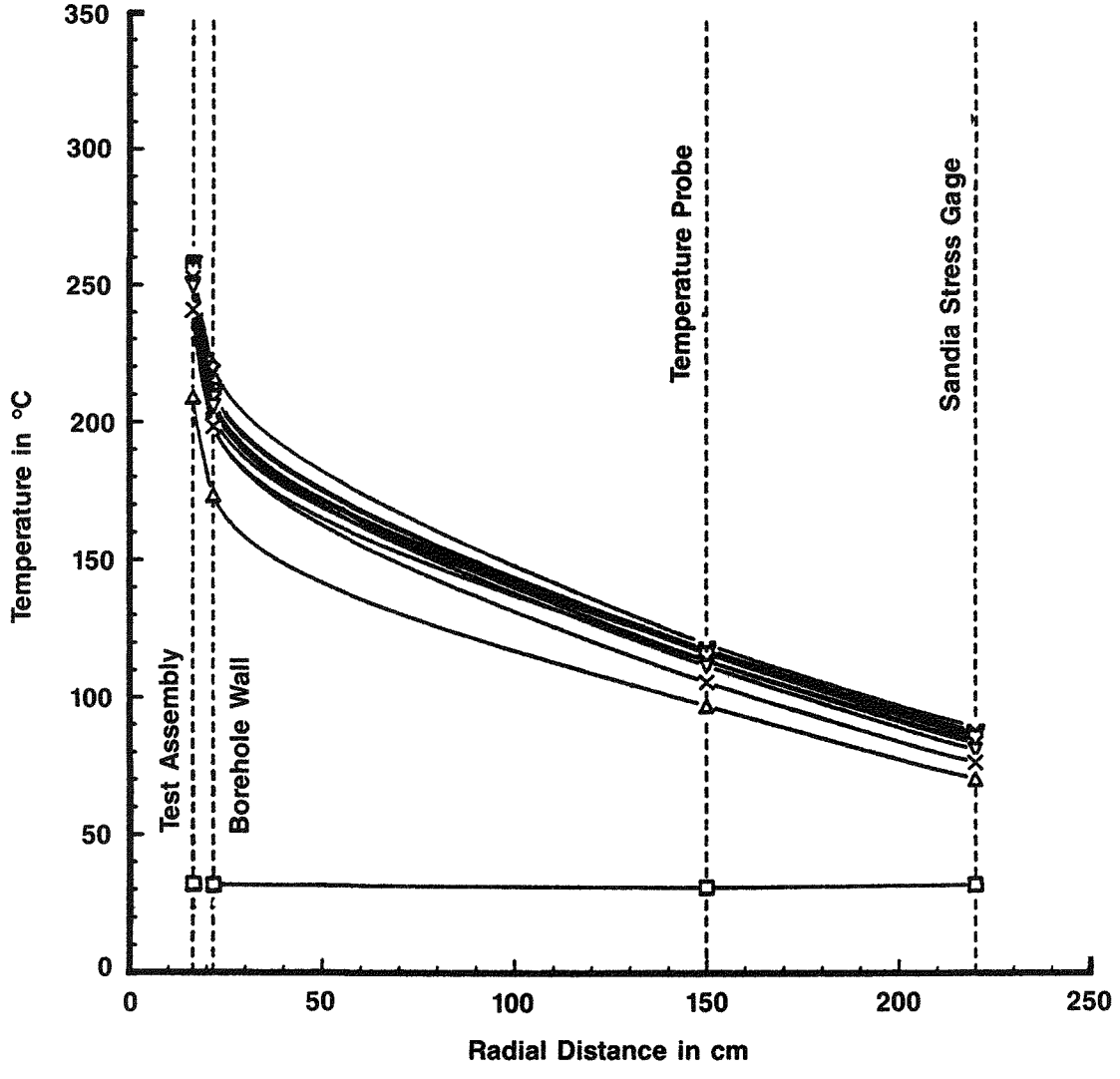

LEGEND:

5/24/83	10/15/84
7/23/83	12/14/84
9/21/83	2/12/85
12/20/83	4/12/85
3/19/84	7/11/85
5/18/84	9/ 9/85
8/16/84	

Radial Temperature at 804.57 m (2,639.66 ft) From Surface for Test Site 2

Figure 6-10

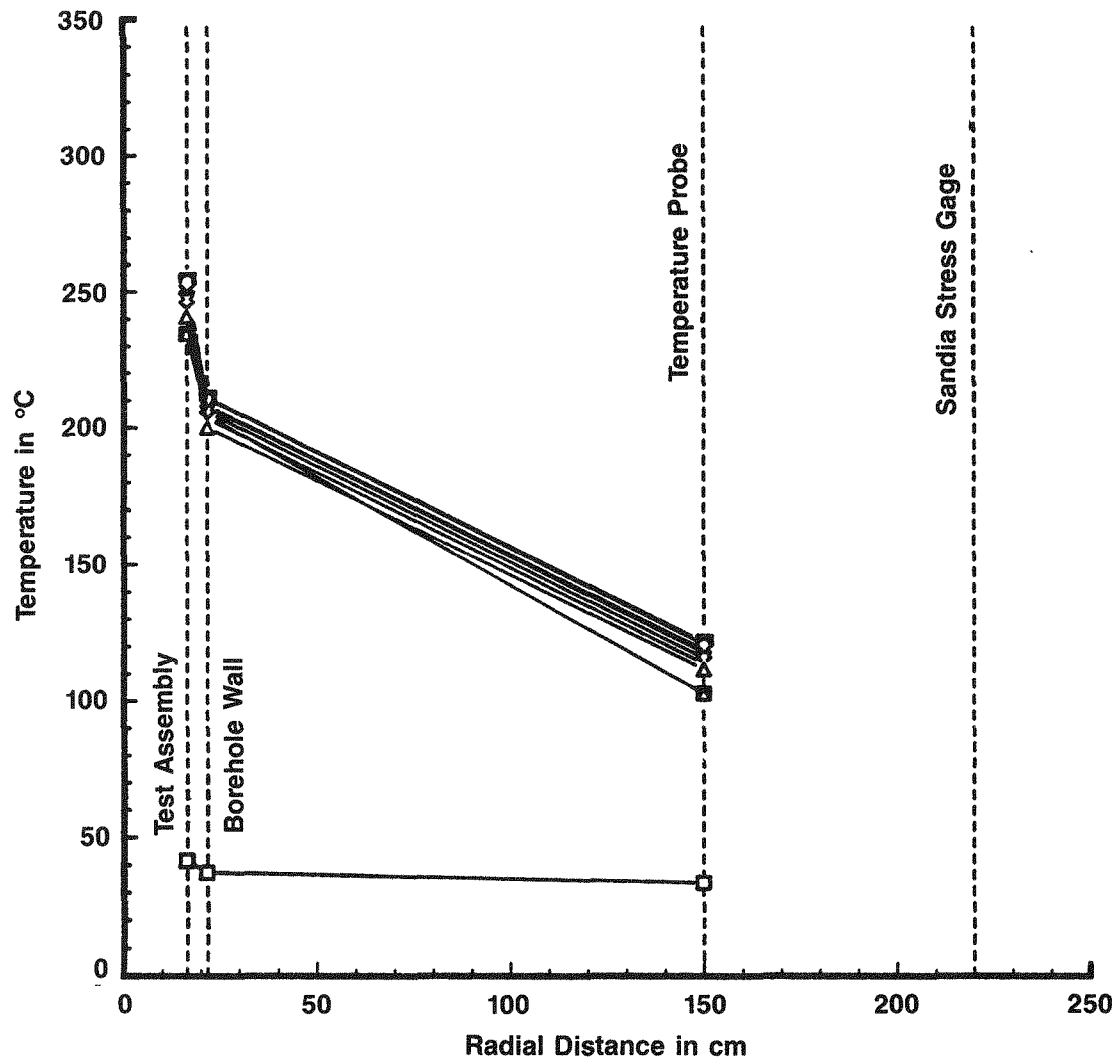

LEGEND:

□ 12/15/83	● 1/ 8/85
△ 4/13/84	▣ 4/ 7/85
× 6/12/84	◪ 6/ 6/85
▽ 8/11/84	○ 8/ 5/85
✱ 11/ 9/84	■ 10/ 4/85

Radial Temperature at 804.57 m (2,639.66 ft) From Surface for Test Site 3

Figure 6-11

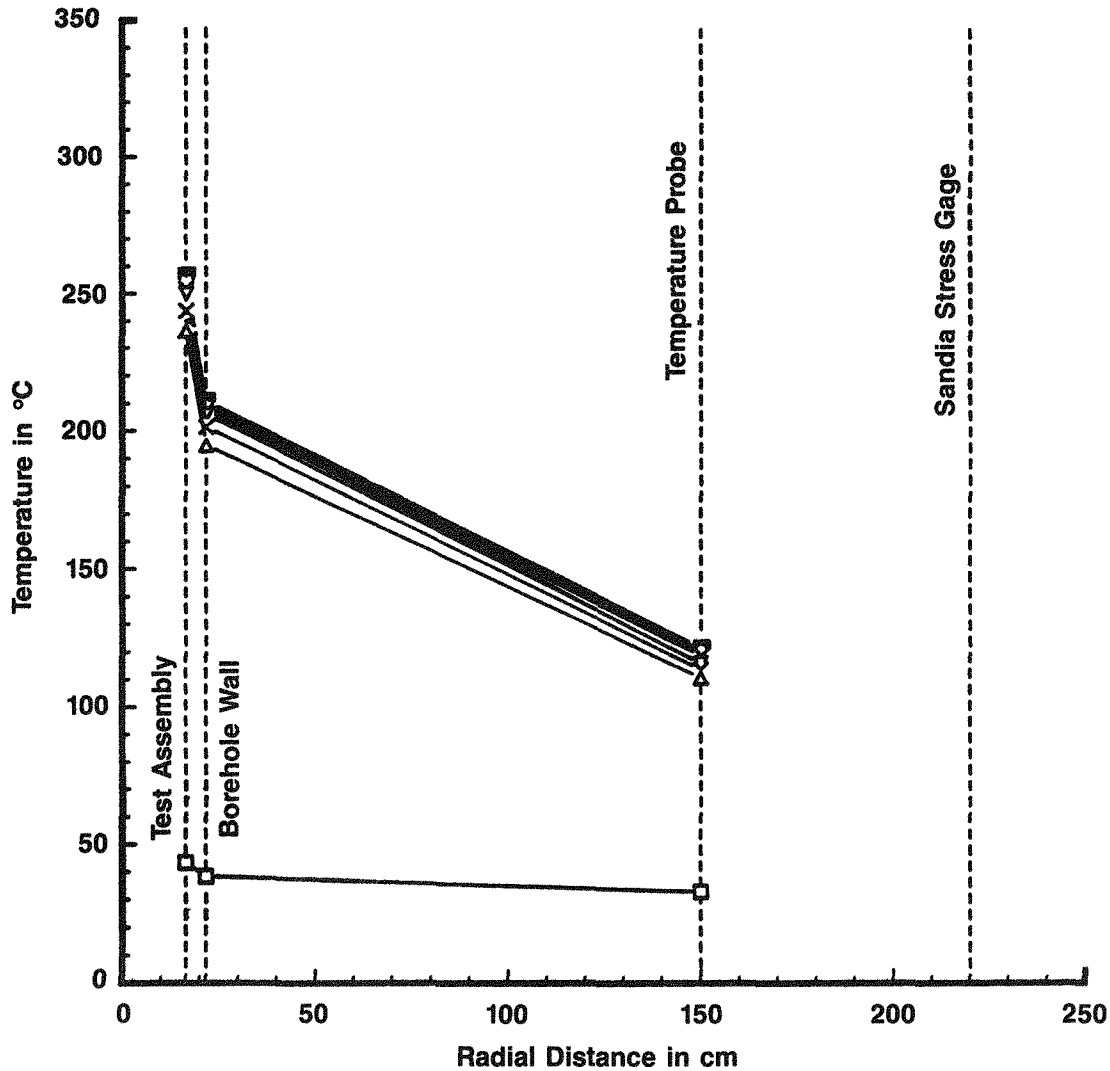

LEGEND:

□ 12/15/83	● 1/ 8/85
△ 4/13/84	■ 4/ 7/85
× 6/12/84	⊠ 6/ 6/85
▽ 8/11/84	○ 8/ 5/85
✱ 11/ 9/84	■ 10/ 4/85

Radial Temperature at 804.57 m (2,639.66 ft) From Surface for Test Site 4

Figure 6-12

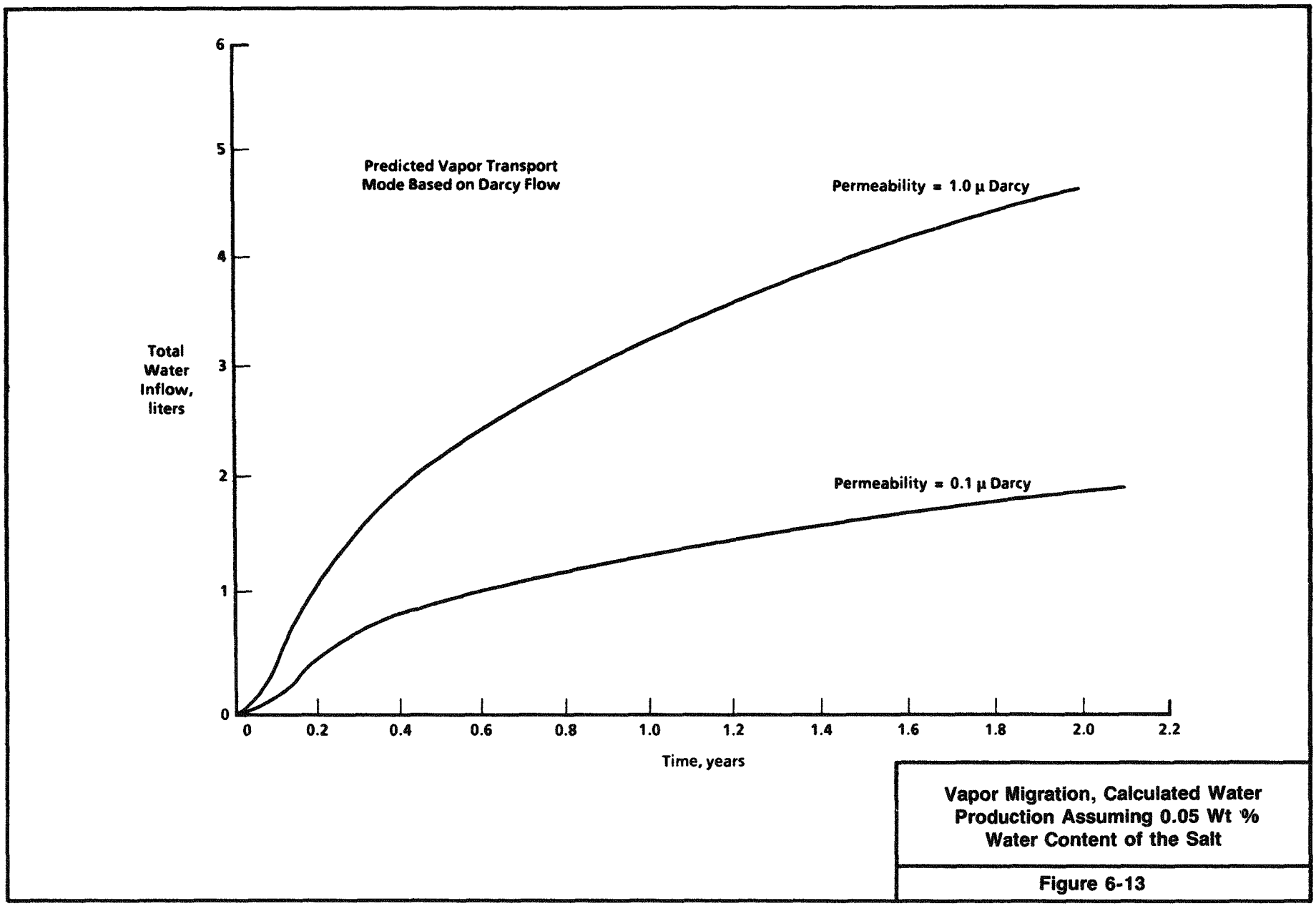

Vapor Migration, Calculated Water Production Assuming 0.05 Wt % Water Content of the Salt

Figure 6-13

Table 6-10. Brine Collection Data

Test Site No.	Days of Operation	Absolute Borehole Gas Pressure (bars)	Average Gas-Temperature (K)	Collected Brine (cm^3)	Collected After Cooldown (cm^3)
1	843	3.21	479	42(a)	1,500(b)
2	843	1.08	483	102(b)	1,775(b)
3	214	2.64	481	26(a)	
3	314	1.11	478	40(b)	725(b)
3	649	1.07	480	100(b)	
4	640	1.07	480	135(b)	1,320(b)

(a) Estimated from water vapor partial pressure.
(b) MCS measurement.

A comparison of calculated or predicted brine collection (Liquid Transport Model, Jenks, 1979) with total measured brine from sites 2 and 4 is made in Figure 6-14. As outlined in Section 5.1 of the annual report of 1983 (Rothfuchs et al., 1984), it is likely that only the adsorbed water contained in the salt (0.02 wt %) contributes to the water collected in the boreholes. Therefore, the measured amount of water is smaller than that calculated, based on an assumed 0.05 wt % liquid water in salt. Further, if the predicted vapor transport is considered, see Figure 6-13, the total brine collected in the boreholes is considerably less than predicted. However, since the average water content of the Asse salt is only one-half the amount used in the prediction, the difference becomes less. In addition, the predicted amount calculated was based on a permeability several orders of magnitude higher than one would expect from domal salt subjected to heat, which increases impermeability (Blankenship and Stickney, 1983). The continuation of the measurements and posttest analysis of moisture content of salt samples has to be made to more than the current preliminary results.

6.3 GAS PRESSURE AND GAS ANALYSIS

Measurements of gas pressure in the boreholes are made at all four sites. Since only test sites 1 and 3 were originally pressurized, and test sites 2 and 4 were operated under atmospheric pressure, only the pressure rise of test sites 1 and 3 is presented and discussed in this chapter. Prior to start-up of the experiments, all boreholes were purged with dry nitrogen gas (N_2) to remove moisture and other gas components contained in the borehole atmosphere. Measurements of borehole and test assembly pressure for test sites 1 and 3 are listed in Tables 6-14 and 6-15, respectively. The corresponding graphs

Table 6-11. Brine Migration for Test Site 2 (Nonradioactive)

Date	Brine Migration in cm^3
5/26/83	0.0
8/17/83	50.0
9/8/83	57.0
9/29/83	58.0
11/11/83	75.0
12/5/83	75.0
12/28/83	77.6
1/19/84	80.0
2/10/84	87.5
3/2/84	88.0
3/23/84	95.0
4/12/84	95.0
5/9/84	95.0
5/30/84	95.5
6/25/84	98.0
7/17/84	100.0
8/7/84	100.0
8/30/84	101.0
9/24/84	101.0
10/15/84	101.0
11/5/84	105.0
11/27/84	107.0
12/18/84	108.0
1/16/85	108.0
2/6/85	112.0
2/27/85	113.0
3/20/85	114.0
4/16/85	116.0
5/3/85	117.0
5/28/85	119.0
6/19/85	119.0
7/10/85	120.0
8/1/85	121.0
8/22/85	122.0
9/12/85	122.0

Table 6-12. Brine Migration for Test Site 3 (Radioactive)

Date	Brine Migration in cm^3
10/24/84	40.0
11/2/84	50.0
11/13/84	50.0
11/23/84	60.0
12/4/84	60.0
12/13/84	60.0
12/27/84	62.0
1/10/85	65.0
1/21/85	65.0
1/30/85	70.0
2/8/85	71.0
2/19/85	73.0
2/28/85	75.0
3/11/85	75.0
3/20/85	77.0
3/29/85	80.0
4/11/85	82.0
4/22/85	84.0
5/2/85	86.0
5/13/85	88.0
5/23/85	89.0
6/4/85	90.0
6/13/85	90.0
6/24/85	92.0
7/3/85	92.0
7/15/85	94.0
7/24/85	96.0
8/2/85	98.0
8/13/85	99.0
8/22/85	99.0
9/2/85	99.0
9/11/85	100.0
9/23/85	100.0

Table 6-13. Brine Migration for Test Site 4 (Radioactive)

Date	Brine Migration in cm^3
12/16/83	0.0
1/10/84	50.0
2/1/84	50.0
2/22/84	67.5
3/14/84	70.0
4/4/84	75.0
4/27/84	79.0
5/22/84	82.5
6/15/84	85.0
7/9/84	89.5
7/28/84	92.5
8/23/84	95.5
9/17/84	99.0
10/8/84	100.0
10/29/84	105.0
11/19/84	106.0
12/11/84	112.0
1/9/85	115.0
1/30/85	120.0
2/20/85	120.0
3/13/85	123.0
4/4/85	120.0
4/29/85	126.0
5/22/85	128.0
6/13/85	130.0
7/5/85	131.0
7/29/85	133.0
8/19/85	134.0
9/9/85	135.0

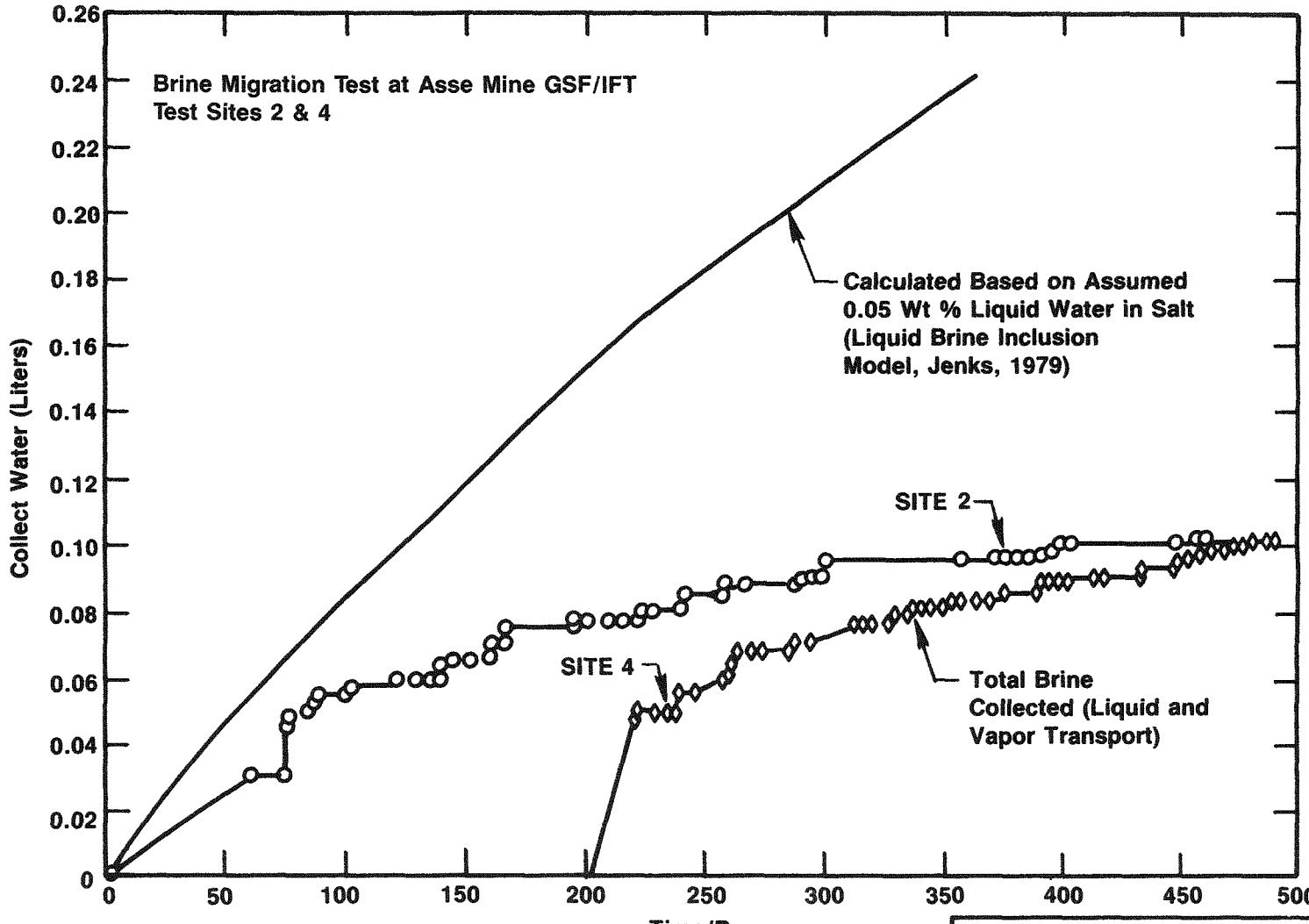

Brine Collection Versus Time
(Predicted and Measured)
for Test Sites 2 and 4

Figure 6-14

Table 6-14. Test Assembly and Borehole Pressure for Test Site 1

Date	Elapsed Days	Pressure in bars	
		Borehole	Test Assembly
5/24/83	0	1.10	1.08
6/23/83	30	1.97	1.08
7/23/83	60	2.17	1.09
8/22/83	90	2.30	1.08
9/21/83	120	2.61	1.08
10/21/83	150	---	---
11/20/83	180	3.01	1.09
12/20/83	210	3.38	1.06
1/19/84	240	3.58	1.04
2/18/84	270	3.34	1.03
3/19/84	300	3.36	1.01
4/18/84	330	3.32	1.07
5/18/84	360	3.27	1.09
6/17/84	390	---	---
7/17/84	420	3.36	1.08
8/16/84	450	3.42	1.06
9/15/84	480	3.22	1.05
10/15/84	510	3.19	1.07
11/14/84	540	3.29	1.06
12/14/84	570	3.21	1.07
1/13/85	600	3.13	1.08
2/12/85	630	3.16	1.07
3/13/85	660	3.21	1.08
4/12/85	690	3.24	1.05
5/12/85	720	3.21	1.06
6/11/85	750	---	---
7/11/85	780	3.08	1.07
8/10/85	810	3.01	1.06
9/9/85	840	2.88	1.06

Table 6-15. Test Assembly and Borehole Pressure for Test Site 3

Date	Elapsed Days	Pressure in bars	
		Borehole	Test Assembly
12/15/83	0	1.06	1.10
1/14/84	30	---	---
2/13/84	60	2.18	1.08
3/14/84	90	---	---
4/13/84	120	2.42	1.06
5/13/84	150	2.52	1.06
6/12/84	180	2.59	1.08
7/12/84	210	2.64	1.07
8/11/84	240	2.23	1.07
9/10/84	270	---	---
10/10/84	300	1.69	1.07
11/9/84	330	1.11	1.06
12/9/84	360	1.10	1.06
1/8/85	390	1.08	1.05
2/7/85	420	1.08	1.05
3/8/85	450	---	---
4/7/85	480	1.07	1.05
5/7/85	510	1.07	1.05
6/6/85	540	1.07	1.05
7/6/85	570	1.08	1.07
8/5/85	600	1.07	1.06
9/4/85	630	1.06	1.05
10/4/85	660	1.07	1.04

showing pressure rise versus time are presented in Figures 6-15 and 6-16 for test site 1 (nonradioactive) and test site 3 (radioactive), respectively. The pressure increase is a function of temperature and of the water vapor and gases released to the boreholes. The pressure decrease after operation day 215 at test site 3 is due to the leakage described in Section 6.2. Data on the gas composition at individual test sites are presented in Tables 6-16 through 6-19. A study of the gas compositions shows no marked difference between the gases in the radioactive versus the nonradioactive boreholes.

To estimate the heat-induced pressure increase of the original N_2 gas for comparison with the total pressure increase, the average gas temperature in the borehole gap was determined, using the test assembly outer surface temperature and the borehole wall temperature measured at three elevations (Section 4.2.1). Table 6-20 gives an indication of the pressure increase of the different gas components at test sites 1 and 3 (see also Tables 6-16 and 6-18).

These gases also contribute to the total pressure increase. It is of interest that hydrogen is observed in the nonradioactive sites as well as in the radioactive sites. The hydrogen in the nonradioactive sites is probably produced by corrosion reactions of the released brine. It will be of great interest to retrieve those different metal samples, which were attached to the thermocouple cage for corrosion investigations. The production of small amounts of hydrocarbons, carbon dioxide, and carbon monoxide is not surprising since it is known from former investigations that these components usually occur in rock salt. The production of hydrogen chloride (HCl), observed in four measurements at sites 1 and 2, is possibly due to hydrolysis of bischofite ($MgCl_2 \cdot 6H_2O$). This mineral could occur in small traces in the salt. In order to prove this assumption, special chemical analyses will need to be performed on salt samples of the test formation after the tests are completed.

Since hydrogen production at the nonradioactive test sites is considered to be due to corrosion reactions, it should be expected that the hydrogen production would decrease when either the brine release rates decrease or the metal surfaces are protected by oxide coatings. And in fact, it can be observed at test site 2 (Table 6-17) that the hydrogen production decreased approximately 400 days after start-up of operation when the brine release rates became very small. Since the same effect can be observed at test site 1 where the water vapor is kept in the borehole, it can be concluded that the hydrogen production is also reduced because of the oxidized metal surfaces.

A significant production of hydrogen by radiolysis at the radioactive test site 3 has not been observed within the 660 days of operation. The results of test site 4 are not representative with regard to any gas production because the test volume developed a leak soon after emplacement, causing the composition of the borehole atmosphere to become increasingly similar to normal air. This leakage is not listed in the Chronology of Key Events (Table 5-1) because there was no change in the pressure status of this site (test site 4 was already a nonpressurized site).

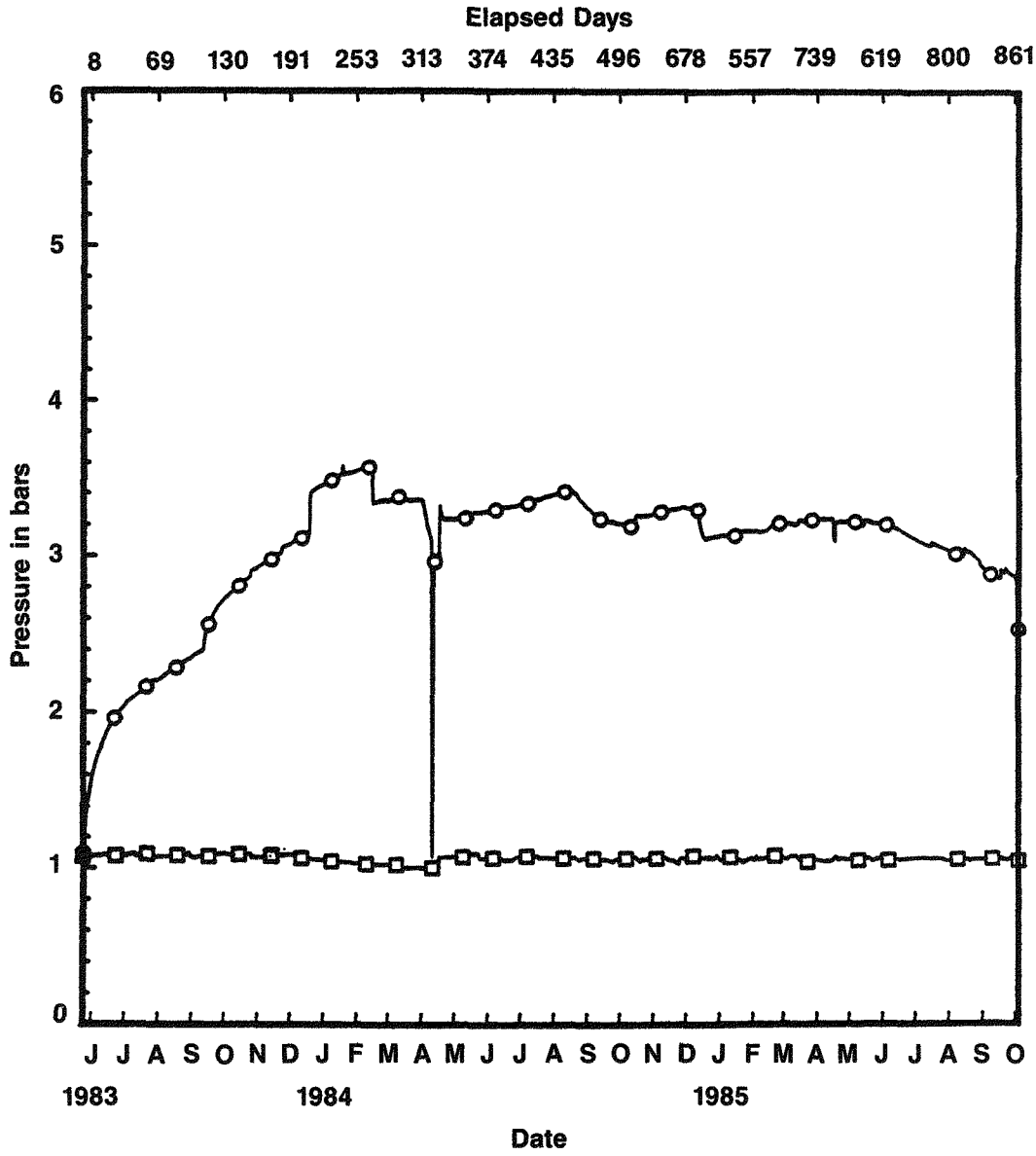

LEGEND:

- O Borehole Pressure
- □ Test Assembly Pressure

Test Assembly and Borehole Pressure Versus Time for Test Site 1

Figure 6-15

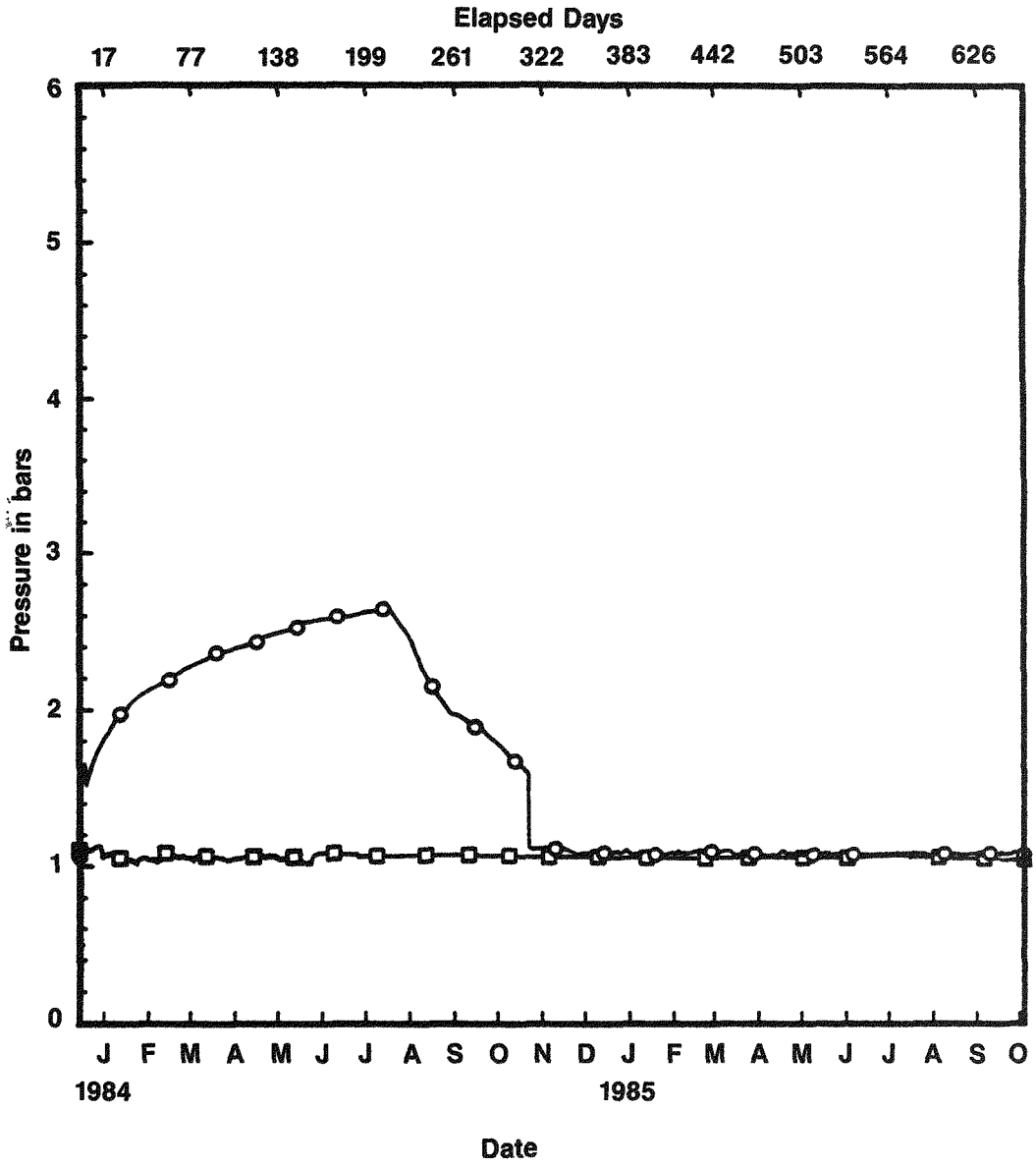

LEGEND:

- O Borehole Pressure
- □ Test Assembly Pressure

Test Assembly and Borehole Pressure Versus Time for Test Site 3

Figure 6-16

Table 6-16. Gas Analysis for Test Site 1 (Nonradioactive)
(Page 1 of 2)

Date of Sampling	Test Day	Sample No.	Component (Vol. %)							
			H_2	O_2	N_2	CO_2	CO	CH_4	C_2H_6	C_3H_8
May 25, 83	0	1/1	-	0.9	98.9	0.034	-	0.0005	-	-
June 15, 83	21	1/3	-	0.4	99.3	0.69	-	0.02	0.005	0.0063
July 20, 83	56	1/4	0.01	1.04	-	1.5	0.096	0.033	0.0027	-
Aug. 23, 83	90	1/5	0.45	2.8	94	3.1	0.052	0.06	0.0287	0.164
Sept. 23, 83	121	1/6	0.6	0.74	93.6	4.04	0.32	0.0678	0.04	0.195
Oct. 25, 83	153	1/7	1.43	0.56	91.4	7.1	0.51	0.1140	0.00495	0.216
Nov. 23, 83	182	1/8	1.34	1.1	89.9	7.0	0.27	0.123	0.073	0.163
Dec. 19, 83	208	1/9	1.94	1.1	89.8	6.8	0.31	0.167	0.0715	0.159
Jan. 17, 84	237	1/10	1.47	0.84	93.1	4.1	0.30	0.152	0.058	0.125
Feb. 15, 84	266	1/11	1.40	0.51	93.8	4.7	0.26	0.167	0.027	0.13
March 14, 84	294	1/12	1.72	0.59	90.6	6.0	0.40	0.18	0.015	0.072
April 17, 84	328	1/13	2.21	0.24	91.4	5.46	0.39	0.22	0.03	0.10
May 15, 84	357	1/14	1.84	0.72	92.7	4.30	0.24	0.185	0.024	0.075
June 16, 84	386	1/15	2.31	0.28	91.8	4.95	0.29	0.18	0.024	0.075
July 13, 84	415	1/16	1.54	0.26	92.5	4.70	0.30	0.20	0.025	0.061
Aug. 16, 84	449	1/17	1.05	0.38	92.7	4.70	0.31	0.214	0.022	0.068
Sept. 17, 84	481	1/18	0.74	0.39	92.0	5.19	0.30	0.25	0.02	0.07
Oct. 15, 84	509	1/19	0.58	0.28	93.5	5.3	0.31	0.24	0.02	0.06
Nov. 8, 84	537	1/20	0.23	2.3	93.1	4.1	0.14	0.2	0.02	0.05
Dec. 14, 84	569	1/21	0.27	0.72	93.2	4.2	0.16	0.18	0.02	0.02
Jan. 15, 85	601	1/22	0.26	0.28	93.6	4.6	0.22	0.21	0.022	0.035

Table 6-16. Gas Analysis for Test Site 1 (Nonradioactive)
(Page 2 of 2)

Date of Sampling	Test Day	Sample No.	Component (Vol. %)							
			H_2	O_2	N_2	CO_2	CO	CH_4	C_2H_6	C_3H_8
Feb. 15, 85	632	1/23	0.23	0.39	92.0	5.8	0.15	0.17	0.02	0.03
March 14, 85	659	1/24	0.14	0.30	93.7	4.1	0.09	0.17	0.013	0.016
April 15, 85	691	1/25	0.12	0.29	95.0	3.8	0.09	0.22	0.02	0.01
May 14, 85	720	1/26	0.13	0.26	93.6	4.2	0.045	0.09	0.006	0.008
June 13, 85	750	1/27	0.097	0.24	94.3	4.4	0.11	0.17	0.009	0.02
July 15, 85	782	1/28	0.115	0.54	94.2	3.14	0.071	0.12	0.009	0.021
Aug. 14, 85	812	1/29	0.112	0.33	93.4	3.16	0.065	0.11	0.01	0.019
Sept. 17, 85	846	1/30	0.11	0.43	94.3	3.23	0.047	0.11	0.014	0.016

Table 6-17. Gas Analysis for Test Site 2 (Nonradioactive)
(Page 1 of 2)

Date of Sampling	Test Day	Sample No.	Component (Vol. %)							
			H_2	O_2	N_2	CO_2	CO	CH_4	C_2H_6	C_3H_8
May 25, 83	0	2/1	-	0.8	98.6	0.021	-	0.0005	-	-
June 15, 83	21	2/3	-	0.8	99.0	0.27	-	0.022	0.0015	0.0003
July 20, 83	56	2/4	0.01	1.0	-	1.0	0.074	0.05	0.004	0.001
Aug. 23, 83	90	2/5	0.76	1.06	95.0	1.5	-	0.079	0.0074	0.003
Sept. 23, 83	121	2/6	0.68	1.22	94.4	1.8	0.043	0.076	0.008	0.0042
Oct. 25, 83	153	2/7	0.72	2.06	94.0	2.8	0.06	0.09	0.0079	0.0053
Nov. 23, 83	182	2/8	0.11	3.9	92.8	3.4	0.05	0.084	0.0082	0.0051
Dec. 19, 83	208	2/9	0.79	2.5	93.0	3.0	0.04	0.0917	0.0087	0.0054
Jan. 17, 84	237	2/10	0.92	3.3	94.8	2.3	0.08	0.111	0.0085	0.006
Feb. 15, 84	266	2/11	0.97	3.5	93.2	.8	0.075	0.104	0.006	0.007
March 14, 84	294	2/12	1.0	2.2	93.1	2.6	0.06	0.065	0.008	0.003
April 17, 84	328	2/13	1.49	1.53	94.0	2.38	0.06	0.06	0.0084	0.009
May 15, 84	357	2/14	1.61	1.5	95.2	1.70	0.005	0.074	0.004	0.004
June 16, 84	386	2/15	1.91	0.91	94.1	2.87	0.005	0.071	0.004	0.004
July 13, 84	415	2/16	1.26	0.94	94.4	2.4	0.017	0.052	0.004	0.018
Aug. 16, 84	449	2/17	0.73	1.07	94.4	2.0	0.055	0.064	0.004	0.005
Sept. 17, 84	481	2/18	0.55	1.12	94.8	2.1	0.055	0.06	0.004	0.005
Oct. 15, 84	509	2/19	0.46	0.7	95.3	2.5	0.06	0.07	0.004	0.005
Nov. 8, 84	537	2/20	0.2	3.1	94.3	2.1	0.03	0.05	0.004	0.005
Dec. 14, 84	569	2/21	0.25	1.6	95.2	1.9	0.05	0.048	0.002	<0.002
Jan. 15, 85	601	2/22	0.06	0.68	95.8	1.95	0.045	0.05	0.003	<0.002

Table 6-17. Gas Analysis for Test Site 2 (Nonradioactive)
(Page 2 of 2)

Date of Sampling	Test Day	Sample No.	Component (Vol. %)							
			H_2	O_2	N_2	CO_2	CO	CH_4	C_2H_6	C_3H_8
Feb. 15, 85	632	2/23	0.02	1.36	94.2	4.1	0.12	0.05	0.003	<0.002
March 14, 85	659	2/24	-	1.6	95.0	2.8	0.04	0.045	0.003	0.003
April 15, 85	691	2/25	<0.0005	8.8	90.4	1.8	0.026	0.027	<0.001	<0.001
May 14, 85	720	2/26	0.003	0.83	93.3	2.4	0.012	0.008	0.001	0.0015
June 13, 85	750	2/27	0.097	0.54	96.4	2.44	0.25	0.03	0.0014	0.002
July 15, 85	782	2/28	-	1.4	94.4	2.09	0.018	0.03	0.0014	0.002
Aug. 14, 85	812	2/29	0.0015	0.61	94.0	2.09	0.013	0.037	0.0014	0.002
Sept. 17, 85	846	2/30	0.003	0.88	95.7	1.97	-	0.021	0.0014	0.002

Table 6-18. Gas Analysis for Test Site 3 (Radioactive)
(Page 1 of 2)

Date of Sampling	Test Day	Sample No.	Component (Vol. %)							
			H_2	O_2	N_2	CO_2	CO	CH_4	C_2H_6	C_3H_8
Dec. 12, 83	201	3/1[a]	-	9.1	67.8	0.022	-	0.0025	0.0001	0.0001
Dec. 15, 83	204	3/2[b]	-	1.6	98.3	0.009	-	0.00015	0.0001	0.0001
Jan. 17, 84	237	3/3	0.45	1.03	98.2	0.47	0.17	0.083	0.006	0.008
Feb. 15, 84	266	3/4	0.52	0.59	96.8	2.2	0.21	0.12	0.03	0.025
March 14, 84	294	3/5	0.61	0.64	94.7	3.5	0.34	0.19	0.04	0.027
April 17, 84	328	3/6	0.70	0.28	92.9	4.05	0.36	0.23	0.048	0.03
May 15, 84	357	3/7	0.55	0.51	94.0	4.0	0.33	0.23	0.047	0.029
June 16, 84	386	3/8	0.68	0.35	91.5	6.0	0.35	0.22	0.045	0.028
July 13, 84	415	3/9	0.57	0.30	91.3	6.45	0.35	0.23	0.046	0.03
Aug. 16, 84	449	3/10	0.47	0.52	91.7	5.8	0.36	0.227	0.044	0.03
Sept. 17, 84	481	3/11	0.52	0.42	91.7	5.83	0.33	0.22	0.05	0.03
Oct. 15, 84	509	3/12	0.56	0.46	91.6	6.9	0.37	0.22	0.05	0.04
Nov. 8, 84	537	3/13	0.04	1.2	90.4	8.0	0.27	0.18	0.04	0.04
Dec. 14, 84	569	3/14	0.01	0.94	88.7	9.7	0.21	0.12	0.015	0.005
Jan. 15, 85	601	3/15	<0.01	1.6	87.8	10.0	0.26	0.06	0.005	<0.002
Feb. 15, 85	632	3/16	-	6.9	83.5	9.6	0.31	0.03	0.002	<0.002
March 14, 85	659	3/17	-	8.8	84.4	6.4	0.24	0.01	<0.002	<0.002
April 15, 85	691	3/18	<0.0005	12.8	81.6	5.5	0.27	<0.001	<0.001	<0.001

Table 6-18. Gas Analysis for Test Site 3 (Radioactive)
(Page 2 of 2)

Date of Sampling	Test Day	Sample No.	Component (Vol. %)							
			H_2	O_2	N_2	CO_2	CO	CH_4	C_2H_6	C_3H_8
May 14, 85	720	3/19	0.0005	14.8	79.6	4.4	0.135	0.001	-	-
June 13, 85	750	3/20	0.0005	16.7	79.8	3.5	0.35	0.003	0.0005	-
July 15, 85	782	3/21	0.0005	17.1	79.6	3.16	0.20	0.003	0.0005	0.0003
Aug. 14, 85	812	3/22	-	18.5	79.4	2.4	0.22	0.0092	0.0005	0.0006
Sept. 17, 85	846	3/23	-	17.5	79.9	3.08	0.21	0.0038	0.0005	0.0006

(a) Before purging with nitrogen.
(b) After purging with nitrogen.

Table 6-19. Gas Analysis for Test Site 4 (Radioactive)
(Page 1 of 2)

Date of Sampling	Test Day	Sample No.	Component (Vol. %)							
			H_2	O_2	N_2	CO_2	CO	CH_4	C_2H_6	C_3H_8
Dec. 12, 83	201	4/1[a]	-	16.8	80.0	0.03	-	0.0031	0.0001	0.0001
Dec. 15, 83	204	4/2[b]	-	2.1	97.8	0.009	-	0.00045	0.0001	0.0001
Jan. 17, 84	237	4/3	0.02	8.0	90.3	0.75	0.06	0.008	0.002	0.0016
Feb. 15, 84	266	4/4	0.02	12.6	85.5	2.1	0.03	0.005	-	-
March 14, 84	294	4/5	0.01	14.5	83.4	2.5	0.045	0.0015	-	-
April 17, 84	328	4/6	0.01	14.22	83.5	2.8	0.04	0.0017	-	-
May 15, 84	357	4/7	0.004	15.5	81.2	3.15	0.005	0.001	0.0005	0.0005
June 16, 84	386	4/8	0.006	14.8	81.4	3.0	-	0.0008	0.0005	0.0005
July 13, 84	415	4/9	-	15.08	81.2	2.9	-	0.0005	0.0005	0.0005
Aug. 16, 84	449	4/10	0.004	16.5	81.2	3.15	-	0.0005	0.0005	0.0005
Sept. 17, 84	481	4/11	0.004	16.0	81.4	3.2	-	0.0005	0.0005	0.0005
Oct. 15, 84	509	4/12	<0.004	15.3	82.5	2.8	-	<0.0005	<0.0005	<0.0005
Nov. 8, 84	537	4/13	< NG	16.5	80.6	2.5	-	<0.0005	<0.0005	<0.0005
Dec. 14, 84	569	4/14	-	17.3	79.4	2.8	-	<0.0005	<0.0005	<0.0005
Jan. 15, 85	601	4/15	-	17.0	79.8	2.93	-	<0.0005	<0.0005	<0.0005
Feb. 15, 85	632	4/16	0.04	18.2	79.6	2.14	-	<0.0005	<0.0005	<0.0005
March 14, 85	659	4/17	-	17.9	80.0	2.6	-	<0.0005	<0.0005	<0.0005
April 15, 85	691	4/18	-	17.4	79.0	2.5	-	<0.0005	<0.0005	<0.0005

Table 6-19. Gas Analysis for Test Site 4 (Radioactive)
(Page 2 of 2)

Date of Sampling	Test Day	Sample No.	Component (Vol. %)							
			H_2	O_2	N_2	CO_2	CO	CH_4	C_2H_6	C_3H_8
May 14, 85	720	4/19	0.0005	17.1	79.7	2.2	0.025	0.0005	-	-
June 13, 85	750	4/20	-	17.5	80.5	2.3	0.051	0.001	-	-
July 15, 85	782	4/21	-	18.1	79.0	2.27	0.035	0.001	-	-
Aug. 14, 85	812	4/22	-	18.1	80.1	2.07	0.041	0.0012	-	-
Sept. 17, 85	846	4/23	-	18.2	79.9	1.85	0.02	0.0004	-	-

(a) Before purging with nitrogen.
(b) After purging with nitrogen.

Table 6-20. Borehole Gas Pressure Increase

Test Site	Days of Operation	Total Gas-Pressure Increase (bar)	Heat-Induced Pressure Increase of N_2 (bar)	Water Vapor Partial Pressure (bar)	Other Gases Besides N_2 (bar)
1	492	2.15	0.6	1.45	0.1
3	214	1.58	0.6	0.92	0.06
3	288	0.74	0.6	0.13(a)	0.01

(a) This figure is based on a proportional decrease in all borehole gases. Since the vapor molecules are much larger than those of other gases present, it is believed that the partial pressure would be unchanged, but the partial pressures of other gases would decrease.

6.4 ROOM CLOSURE AND ROCK MASS DISPLACEMENTS

Four independent observation methods are applied to measure the room closure and rock mass displacements.

- Horizontal closure: Manual wall-to-wall measurements to determine the change of distance by means of steel tapes connected to diametrically opposite fixed reference points in the walls
- Vertical closure: Same as previous definition, but ceiling-to-floor
- Floor heave: Surveying
- Displacements within the surrounding rock mass: extensometer observations; continuous (electrical) measurements of the change of distance between the extensometer head (reference plate) and individual downhole anchors along the extensometer axis in the walls or floor.

In general, horizontal and vertical closure measurements are relative observations of oppositely directed displacements. In fact, these closure measurements cover in a summary way the total displacement between two usually opposite reference points, i.e., wall-to-wall or floor-to-roof of the opening. Under certain circumstances these corresponding reference points may displace with a different individual amount of displacement or displacement rate.

The observations of floor heave by means of surveying methods (leveling) can be an absolute method if the individual changes of vertical reference

point displacements are to be related to a reference point whose position is unaffected from any subsidence or uplift.

Likewise, the extensometer readings are relative observations because the relative displacements (lengthening or shortening) between the reference plate of the extensometer at the borehole collar and the individual downhole anchor will be determined. In general, the reference plate of the extensometer is recessed slightly into the face of the wall. Usually this plate at or near the wall, floor, or roof surface moves with the comparative maximum displacement rate toward the opening.

With increasing wall depth, however, the downhole anchor displacement and the rate of displacement decrease as a function of hole depth (distance to the room surface), except for special conditions. It depends on the extent of the overall displacement field around the opening, whether the deepest downhole anchor is movable with time or not. In the latter case, the absolute displacement can be determined for all other anchors in the direction of the opening and likewise of the reference plate at the borehole collar. Otherwise, by combining absolute floor heave measurement results with adjacent extensometer readings, one can determine roof sag from the total room closure, as well as the absolute rock mass displacements in the direction of the vertical extensometer axis.

6.4.1 Horizontal Closure

Figure 6-17 and Table 6-21 show the horizontal closure at sites 1 through 4, respectively. Figure 6-18 compares the predicted horizontal closure with the measured data at test site 2.

The test room, height 7.5 m (24.6 ft), was excavated with a part face heading machine called a Voest Alpine Miner AM50 (Figure 6-19). The test room was mined in two levels or steps. After the upper level was cut out in December 1981 and January 1982, the lower level of the test room was excavated in February and March 1982. The horizontal closure measurements were started as soon as the upper level of the test room was opened.

Within 30 days the wall-to-wall closure was about 8 mm (0.31 in). The corresponding average closure rate was about 0.27 mm/d (0.010 in/d). Related to a wall-to-wall distance of 10 m (32.8 ft), this closure rate corresponds to a relative horizontal closure rate of 2.7×10^{-2} mm/m/d (3.0×10^{-4} in/ft/d) or 9.9 mm/m/yr (0.11 in/ft/yr), respectively. This closure rate then doubled after the start of electric heating at test sites 1 and 2. Table 6-22 gives the horizontal closure rate per day.

6.4.2 Vertical Closure

Figure 6-20 and Table 6-23 show the vertical closure between ceiling and floor at test sites 1 through 4, respectively. Figure 6-21 compares the predicted vertical closure with the measured data at test site 2. Before the start of heating, the vertical closure rate was constant with approximately 5×10^{-2} mm/d (2×10^{-4} in/d). Compared to the horizontal closure rates, which were nearly constant after start-up of heating, the vertical closure

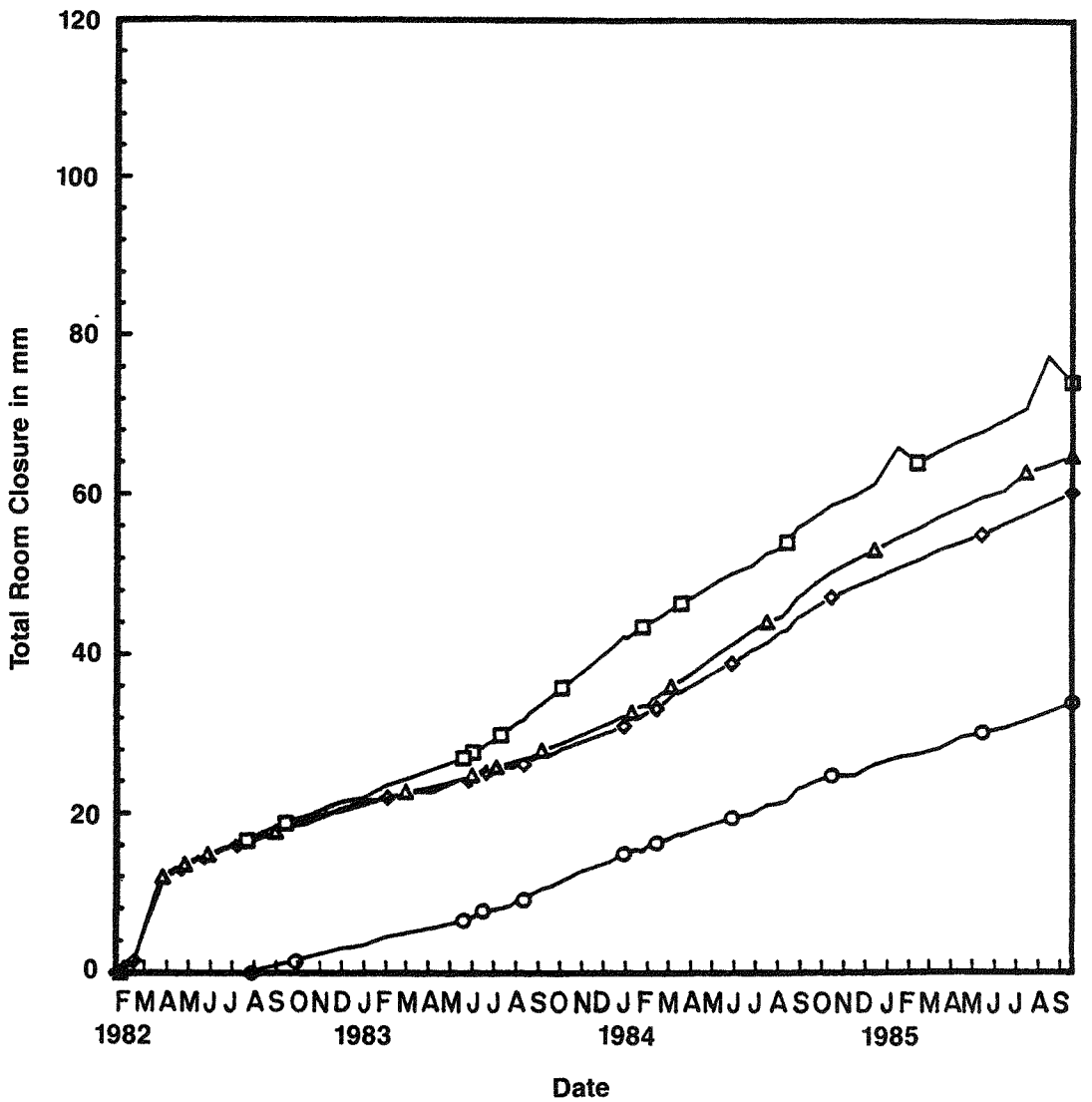

LEGEND:

- ○ 1E1/1E0
- □ 2E1/2E2
- △ 3E1/3E2
- ◇ 4E1/4E2

Total Horizontal Room Closure Versus Time for Test Sites 1 Through 4

Figure 6-17

Table 6-21. Total Horizontal Room Closure (mm) for Test Sites 1 Through 4

Date	1E1/1E0	2E1/2E2	3E1/3E2	4E1/4E2
1/20/82	---	---	---	0.00
2/1/82	---	---	---	1.39
3/17/82	---	---	10.20	---
4/1/82	---	---	12.41	11.94
5/3/82	---	---	14.02	14.16
6/7/82	---	---	15.13	15.00
7/2/82	---	---	16.06	15.66
8/2/82	0.10	17.09	16.68	16.59
9/14/82	1.30	18.78	18.03	18.42
10/13/82	1.95	19.72	18.74	19.26
11/1/82	2.39	---	19.52	19.76
12/30/82	3.47	21.95	21.58	21.06
2/3/83	4.61	23.58	21.88	22.01
3/1/83	---	24.32	22.78	22.71
4/6/83	5.66	---	22.69	23.37
5/20/83	6.59	27.03	24.48	24.42
6/1/83	7.00	27.74	24.86	24.50
7/5/83	8.01	29.52	25.89	25.28
8/2/83	9.10	31.42	26.74	26.13
9/6/83	10.55	33.88	28.02	27.33
10/4/83	11.55	35.88	28.95	28.21
11/1/83	12.77	37.72	29.98	29.10
12/8/83	13.88	40.42	31.38	30.29
1/3/84	15.09	42.06	32.33	31.26
2/1/84	15.93	43.81	33.54	32.75
3/5/84	16.99	45.68	36.03	34.72
4/4/84	17.96	47.20	37.70	36.18
5/14/84	19.06	49.48	40.40	38.27
6/26/84	19.99	51.17	43.02	40.56
7/17/84	21.11	52.72	44.15	41.53
8/6/84	21.39	53.40	44.79	42.90
9/26/84	24.19	57.49	49.21	46.21
10/15/84	24.75	58.71	50.39	47.24
11/15/84	24.76	59.85	51.85	48.54
12/14/84	26.20	61.40	53.18	49.60
1/16/85	27.12	65.97	54.68	50.92
2/13/85	27.52	64.06	55.76	51.88
3/15/85	28.25	65.54	57.29	53.22
4/15/85	29.70	66.90	58.51	54.17
5/14/85	30.21	67.93	59.74	55.10
6/14/85	30.88	69.38	60.58	56.44
7/15/85	31.83	70.86	62.93	57.62
8/14/85	32.87	77.46	63.74	58.92
9/17/85	34.01	74.16	64.94	60.31

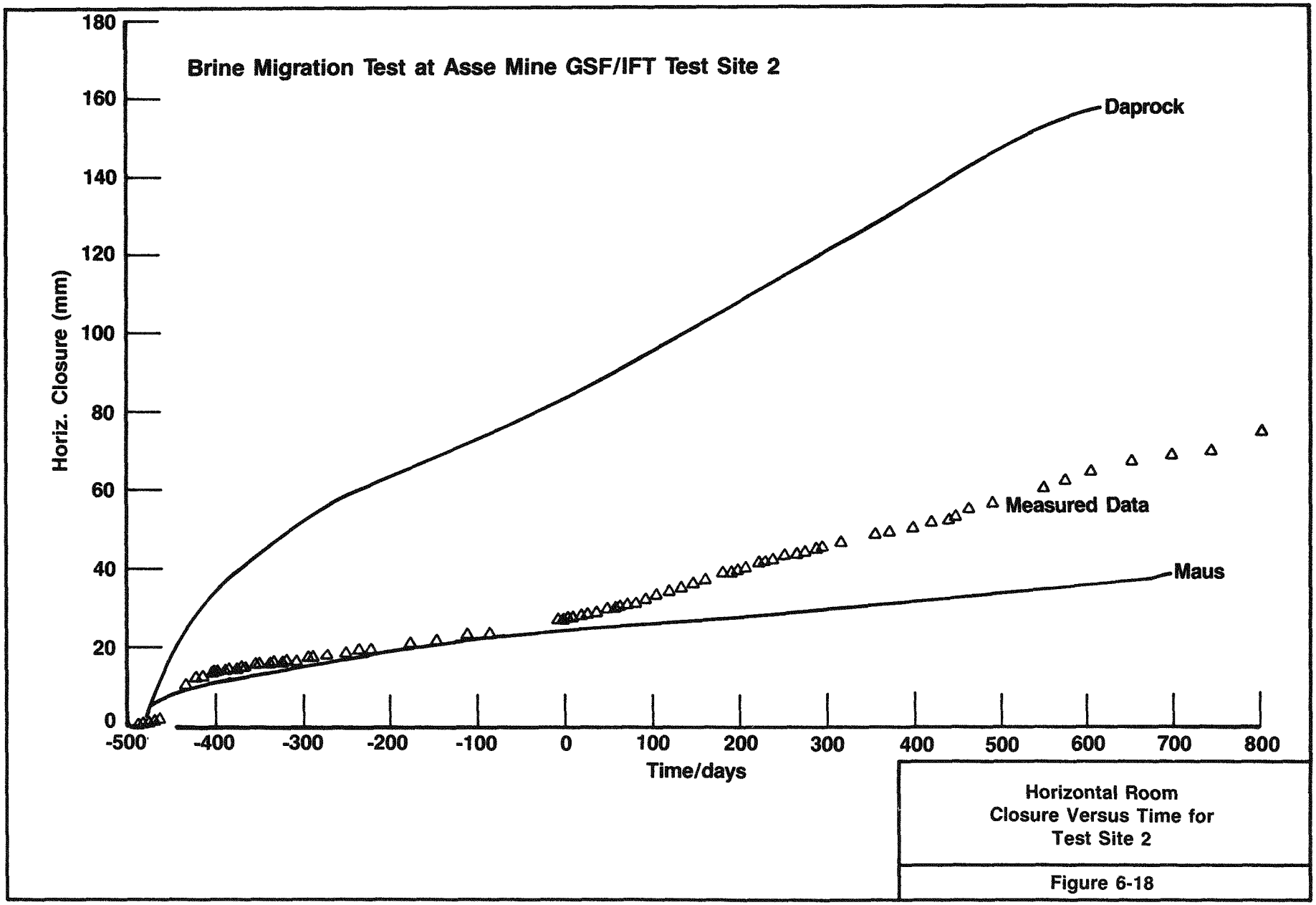

Horizontal Room
Closure Versus Time for
Test Site 2

Figure 6-18

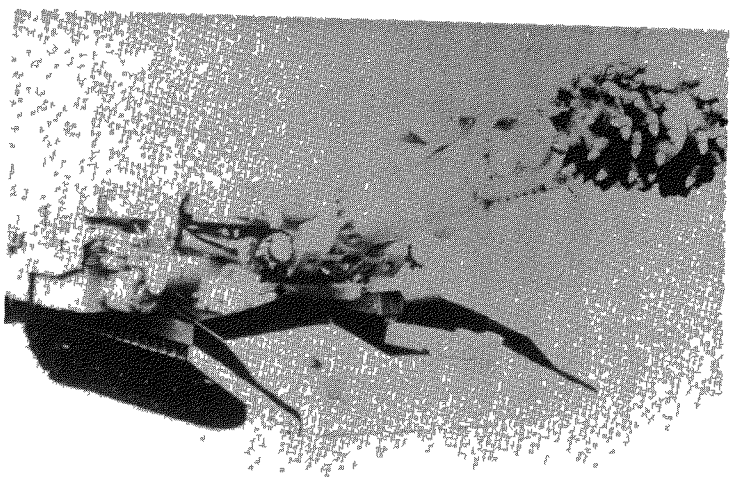

Figure 6-19 VOEST Part Face Heading Machine (Continuous Miner)

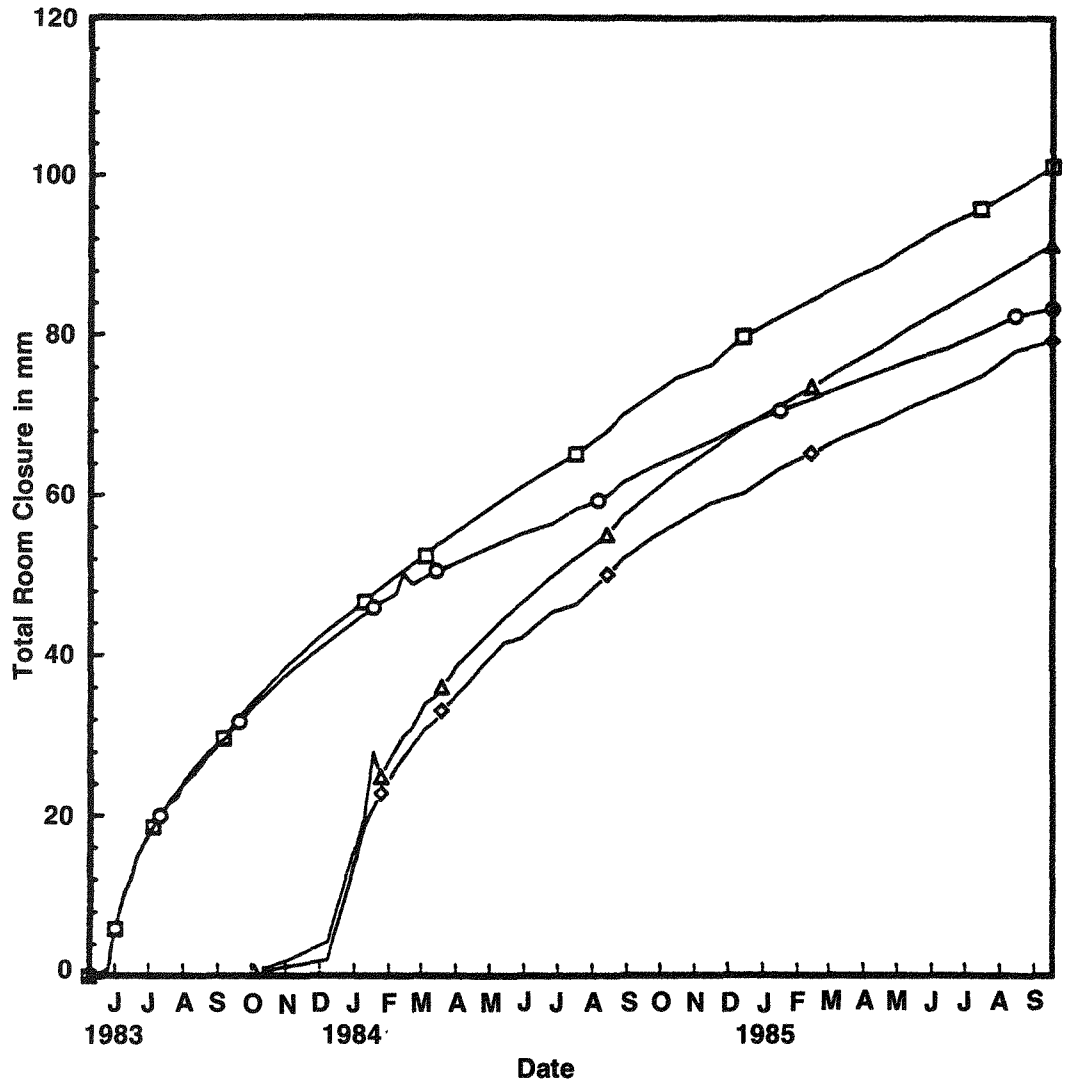

LEGEND:

- ○ VK1
- □ VK2
- △ VK3
- ◇ VK4

Total Vertical Room Closure Versus Time for Test Sites 1 Through 4

Figure 6-20

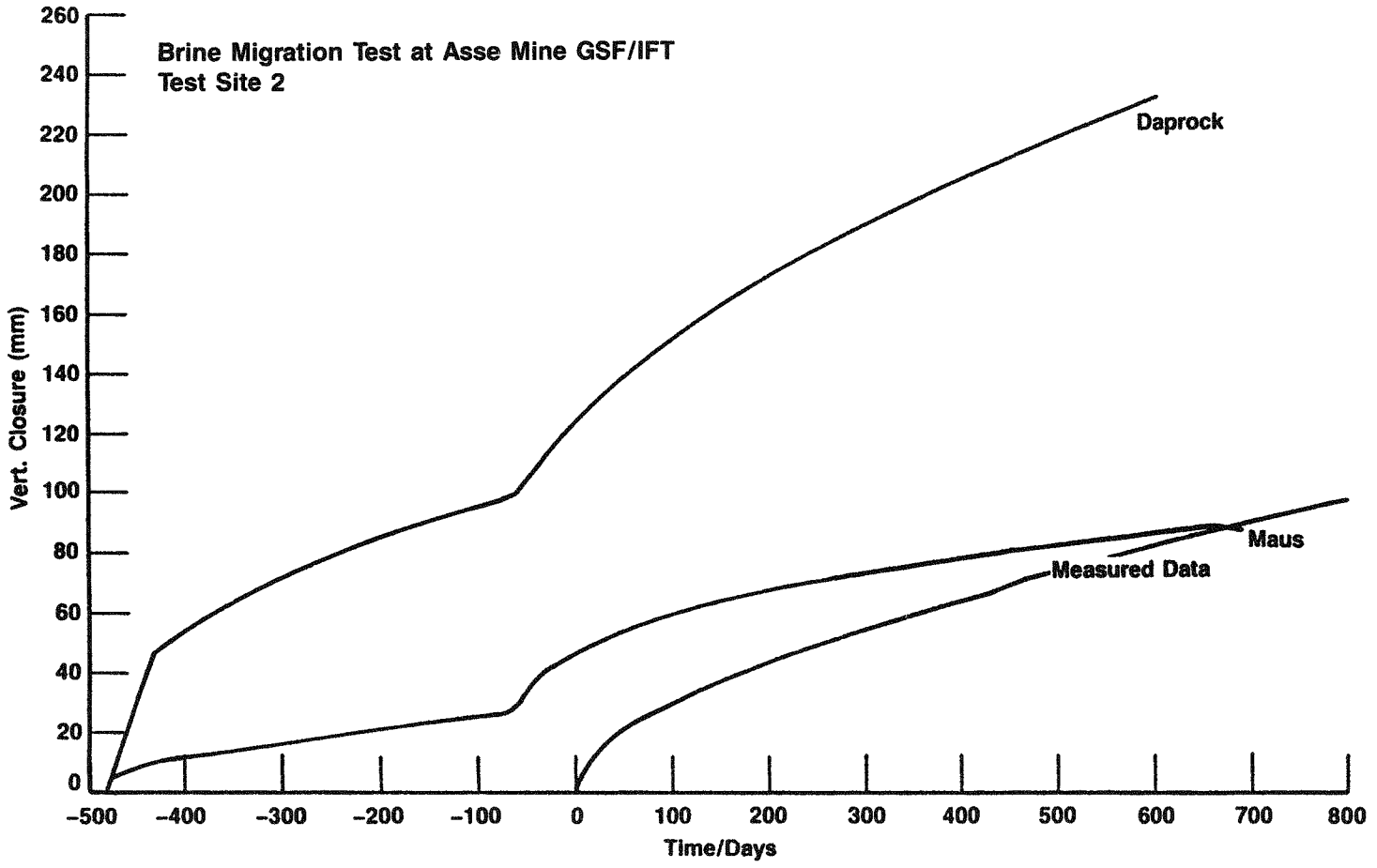

Vertical Room Closure
Versus Time for Test Site 2

Figure 6-21

Table 6-22. Horizontal Closure Rate (10^{-1} mm/day)

	Site 1	Site 2	Site 3	Site 4
Closure rate before start-up of sites 1 and 2, Aug. 2, 1982, to May 25, 1983	2.3	3.5	2.6	2.7
Closure rate after start-up of sites 1 and 2, July 5, 1983, to December 8, 1983	3.8	7.0	3.5	3.2
Closure rate after start-up of sites 3 and 4, Dec. 16, 1983, to June 26, 1984	2.8	5.3	5.9	5.2

rates behaved in a more transient way, with higher closure rates at start-up of heating. This is due to the comparatively high floor heave above the heated zone (Section 6.4.3). During the first 840 days of operation of sites 1 and 2, the vertical closure was approximately 90 mm (3.5 in) and 104 mm (4.1 in) respectively.

6.4.3 Floor Heave

Figure 6-22 shows five cross sections of the test field with measured floor heave profiles. Figure 6-23 presents the floor heave at the center of site 2 (measuring point 11) versus time.

Here, the floor heave is about 99 mm (3.9 in) in the first 844 days of operation. Since a similar value of 101.15 mm (3.98 in) was measured for the total vertical closure (Table 6-23), the roof sag is very small, with only a few millimeters difference.

6.4.4 Extensometer Readings

As described in Section 4.2, two horizontal extensometers are installed at each test site. An additional vertical extensometer is installed at test site 2. Their three anchors, A1, A2, and A3, are at fixed depths of 2.7 m (8.9 ft), 7.4 m (24.3 ft), and 20 m (65.6 ft), respectively. Table 6-24 summarizes the measured change of distance between the extensometer head (MP) and the individual anchors (A1, A2, A3) at 504 days after start-up of heating at test sites 1 and 2, and 300 days after start-up of heating at test sites 3 and 4. Tables 6-25 through 6-33 give the readings for the individual extensometers; the corresponding plots of the time-dependent movement measured by the extensometers are presented in Figures 6-24 through 6-32.

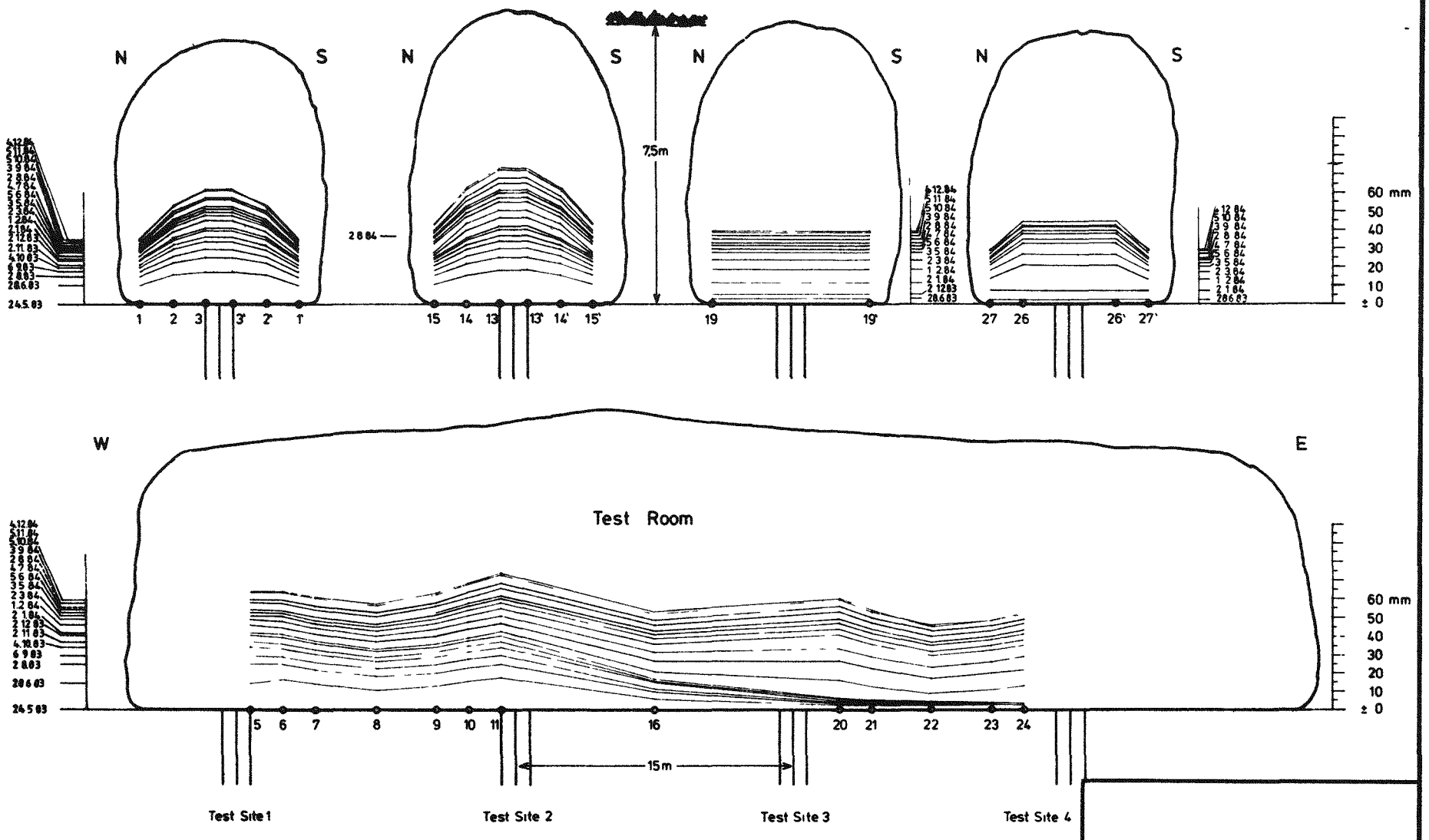

Floor Heave Profiles at Times Indicated

Figure 6-22

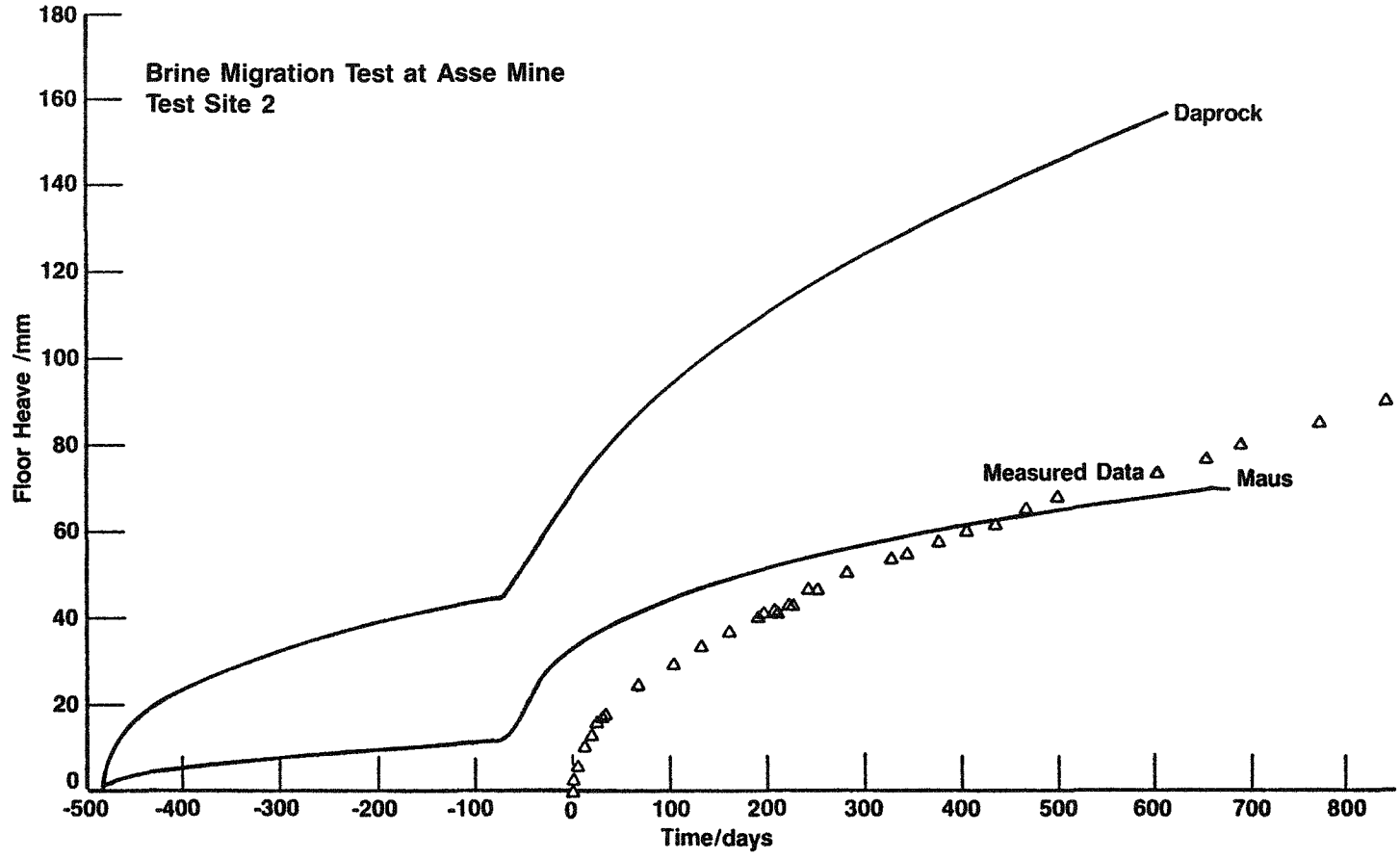

Floor Heave Versus
Time for Test Site 2

Figure 6-23

Table 6-23. Total Vertical Room Closure (mm) for Test Sites 1 Through 4

Date	VK1	VK2	VK3	VK4
5/9/83	0.00	0.00	---	---
6/1/83	5.88	5.83	---	---
7/5/83	18.50	18.53	---	---
8/2/83	24.11	24.34	---	---
9/6/83	29.45	29.65	---	---
10/4/83	33.83	34.52	0.55	0.29
11/1/83	37.54	38.51	1.87	1.13
12/8/83	41.59	43.12	4.25	2.02
1/3/84	44.38	45.95	16.18	14.58
2/1/84	47.17	49.21	26.76	24.46
3/5/84	49.78	52.31	34.07	30.89
4/4/84	51.66	55.63	38.95	35.41
5/14/84	54.21	59.59	44.62	41.55
6/26/84	56.39	63.42	49.92	45.41
7/17/84	58.26	65.12	52.12	46.33
8/6/84	59.29	67.19	54.15	48.99
9/26/84	63.77	72.86	60.69	54.92
10/15/84	64.93	74.79	62.91	56.49
11/15/84	66.85	76.36	65.77	59.08
12/14/84	68.84	79.81	68.64	60.31
1/16/85	70.65	82.32	71.29	63.51
2/13/85	72.16	84.39	73.65	65.35
3/15/85	73.82	86.72	76.14	67.46
4/15/85	75.50	88.75	78.49	69.20
5/14/85	77.06	91.35	81.16	71.24
6/14/85	78.38	93.85	83.46	72.96
7/15/85	80.29	95.86	86.10	74.97
8/14/85	82.29	98.31	88.64	78.02
9/17/85	83.27	101.15	91.38	79.31

The values in Table 6-24 can be used to calculate strain in the extensometer sections. The equation is as follows:

$$\text{Strain} = \Delta L/L_o \qquad (6\text{-}1)$$

where

ΔL = the change of distance in between extensometer anchors
L_o = the initial length of the extensometer section

Table 6-24. Change of Distance (mm) Between Extensometer Anchors

Extensometer Section	Site 1		Site 2			Site 3		Site 4	
	1E1	1E2	2E1	2E2	2E3	3E1	3E2	4E1	4E2
MP-A1	5.32	5.16	4.86	9.96	5.59	4.28	6.30	3.99	5.60
A1-A2	2.30	2.00	2.82	4.73	24.62	3.55	2.76	3.29	2.81
A2-A3	0.60	0.63	0.41	1.04	30.63	0.76	0.91	0.38	0.81

At test site 1, for example, the greatest strain is found in section MP-A1, with an average value of 1.94 mm/m (0.023 in/ft). As the distance into the rock increases, the strain decreases at each of the horizontal extensometers. The vertical extensometer 2E3, however, has its largest strain in the middle section A1-A2. This strain is calculated to be 5.24 mm/m (0.063 in/ft), a value much higher than the strain at any of the horizontal extensometers. The total change of length between the extensometer head (MP) and the deepest anchor A3 at extensometer 2E3 is 60.84 mm (2.40 in). This value compares closely with the vertical closure measurement after 504 days at test site 2 (Figure 6-21).

6.4.5 Comparison of Measured and Predicted Data

Pretest computer code (finite element [FE]) calculations have been performed to predict the order of magnitude of the thermomechanical rock mass responses and to compare them with displacements which actually occur within and around the brine migration test field. Two different FE codes, namely DAPROK (U.S. code) and MAUS (FRG code), were adapted to model and to predict the test room closure in horizontal and vertical directions as well as room floor heave above the heated zone (Rothfuchs et al., 1986).

It was known that the results of these pretest calculations would be of a preliminary character; however, they are accurate enough to use in the design of the test program, test room geometry, and the layout of rock instrumentation. For modeling-induced rock mass response the following material

Table 6-25. Extensometer Readings (mm) for Extensometer 1E1

Date	Elapsed Days	Anchor No. and Depth (m)		
		No. 1 2.7	No. 2 7.4	No. 3 20.0
5/24/83	0	0.74	0.91	1.04
6/23/83	30	1.04	1.22	1.34
7/23/83	60	1.46	1.75	1.89
8/22/83	90	1.89	2.33	2.48
9/21/83	120	2.27	2.88	3.05
10/21/83	150	---	---	---
11/20/83	180	2.92	3.88	4.07
12/20/83	210	3.16	4.14	4.56
1/19/84	240	---	---	---
2/18/84	270	3.69	5.02	5.44
3/19/84	300	3.90	5.40	5.84
4/18/84	330	4.08	5.66	6.21
5/18/84	360	4.22	5.95	6.52
6/17/84	390	---	---	---
7/17/84	420	4.55	6.45	7.02
8/16/84	450	4.85	6.86	7.44
9/15/84	480	5.12	7.29	7.87
10/15/84	510	5.35	7.67	8.29
11/14/84	540	5.46	7.90	8.70
12/14/84	570	5.64	8.16	9.03
1/13/85	600	5.77	8.39	9.31
2/12/85	630	5.88	8.63	9.58
3/13/85	660	6.04	8.83	9.83
4/12/85	690	6.22	9.11	10.12
5/12/85	720	6.34	9.35	10.41
6/11/85	750	---	---	---
7/11/85	780	6.70	9.84	10.96
8/10/85	810	6.88	10.14	11.27
9/9/85	840	7.08	10.46	11.60

Table 6-26. Extensometer Readings (mm) for Extensometer 1E2

Date	Elapsed Days	Anchor No. and Depth (m)		
		No. 1 2.7	No. 2 7.4	No. 3 20.0
5/24/83	0	1.10	1.32	1.87
6/23/83	30	1.36	1.60	2.16
7/23/83	60	1.74	2.09	2.67
8/22/83	90	2.11	2.63	3.21
9/21/83	120	2.42	3.12	3.71
10/21/83	150	---	---	---
11/20/83	180	3.01	4.02	4.64
12/20/83	210	3.28	4.44	5.07
1/19/84	240	---	---	---
2/18/84	270	3.79	5.20	5.85
3/19/84	300	3.97	5.48	6.15
4/18/84	330	4.11	5.67	6.33
5/18/84	360	4.24	5.90	6.51
6/17/84	390	---	---	---
7/17/84	420	4.52	6.30	6.93
8/16/84	450	4.75	6.62	7.23
9/15/84	480	4.99	6.91	7.54
10/15/84	510	5.19	7.21	7.84
11/14/84	540	5.32	7.44	8.08
12/14/84	570	5.46	7.69	8.31
1/13/85	600	5.58	7.90	8.52
2/12/85	630	5.68	8.11	8.74
3/13/85	660	5.81	8.29	8.93
4/12/85	690	5.96	8.50	9.13
5/12/85	720	6.10	8.69	9.34
6/11/85	750	---	---	---
7/11/85	780	6.43	9.17	9.81
8/10/85	810	6.62	9.43	10.09
9/9/85	840	6.80	9.71	10.37

Table 6-27. Extensometer Readings (mm) for Extensometer 2E1

Date	Elapsed Days	Anchor No. and Depth (m)		
		No. 1 2.7	No. 2 7.4	No. 3 20.0
5/24/83	0	---	0.97	0.86
6/23/83	30	0.82	1.25	1.14
7/23/83	60	1.20	1.79	1.67
8/22/83	90	1.57	2.35	2.26
9/21/83	120	1.91	2.90	2.82
10/21/83	150	---	---	---
11/20/83	180	2.48	3.87	3.82
12/20/83	210	2.72	4.27	4.26
1/19/84	240	---	---	---
2/18/84	270	3.18	4.99	5.06
3/19/84	300	3.40	5.36	5.44
4/18/84	330	3.60	5.67	5.80
5/18/84	360	3.76	6.00	6.19
6/17/84	390	---	---	---
7/17/84	420	4.09	6.51	6.80
8/16/84	450	4.39	6.95	7.26
9/15/84	480	4.67	7.38	7.74
10/15/84	510	4.88	7.74	8.17
11/14/84	540	4.97	7.95	8.48
12/14/84	570	5.13	8.19	8.75
1/13/85	600	5.22	8.38	9.01
2/12/85	630	5.29	8.54	9.25
3/13/85	660	5.43	8.70	9.50
4/12/85	690	5.56	8.91	9.77
5/12/85	720	5.67	9.09	10.01
6/11/85	750	---	---	---
7/11/85	780	5.94	9.50	10.53
8/10/85	810	6.11	9.73	10.79
9/9/85	840	6.28	9.99	11.09

Table 6-28. Extensometer Readings (mm) for Extensometer 2E2

Date	Elapsed Days	Anchor No. and Depth (m)		
		No. 1 2.7	No. 2 7.4	No. 3 20.0
5/24/83	0	1.67	2.46	2.50
6/23/83	30	2.11	2.98	3.02
7/23/83	60	2.79	3.92	3.93
8/22/83	90	3.46	4.89	4.88
9/21/83	120	4.08	5.82	5.80
10/21/83	150	---	---	---
11/20/83	180	5.21	7.52	7.45
12/20/83	210	5.72	8.25	8.68
1/19/84	240	---	---	---
2/18/84	270	6.61	9.61	10.01
3/19/84	300	7.09	10.32	10.70
4/18/84	330	7.56	11.01	11.37
5/18/84	360	7.96	11.69	12.34
6/17/84	390	---	---	---
7/17/84	420	8.71	12.82	13.43
8/16/84	450	9.17	13.49	14.42
9/15/84	480	9.62	14.16	15.08
10/15/84	510	10.02	14.80	15.84
11/14/84	540	10.29	15.26	16.46
12/14/84	570	10.62	15.77	17.10
1/13/85	600	10.91	16.19	17.58
2/12/85	630	11.14	16.59	18.15
3/13/85	660	11.44	16.97	18.66
4/12/85	690	11.73	17.40	19.08
5/12/85	720	11.98	17.80	19.57
6/11/85	750	---	---	---
7/11/85	780	12.57	18.63	20.65
8/10/85	810	12.85	19.05	21.06
9/9/85	840	13.17	19.52	21.51

Table 6-29. Extensometer Readings (mm) for Extensometer 2E3

Date	Elapsed Days	Anchor No. and Depth (m)		
		No. 1 2.7	No. 2 7.4	No. 3 20.0
5/24/83	0	0.04	0.17	0.21
6/23/83	30	0.85	9.37	9.93
7/23/83	60	1.44	13.62	15.46
8/22/83	90	1.77	16.45	19.59
9/21/83	120	2.09	19.10	23.43
10/21/83	150	---	---	---
11/20/83	180	2.74	23.50	30.35
12/20/83	210	3.01	24.25	33.18
1/19/84	240	---	---	---
2/18/84	270	3.55	26.55	39.63
3/19/84	300	3.84	27.54	42.68
4/18/84	330	4.09	28.51	45.47
5/18/84	360	4.37	29.15	48.32
6/17/84	390	---	---	---
7/17/84	420	4.79	29.51	53.40
8/16/84	450	5.08	29.78	56.06
9/15/84	480	5.37	30.03	58.74
10/15/84	510	5.63	30.25	61.37
11/14/84	540	5.84	30.48	63.84
12/14/84	570	6.03	30.63	66.13
1/13/85	600	6.23	30.82	68.38
2/12/85	630	6.37	30.99	70.47
3/13/85	660	6.53	31.10	72.30
4/12/85	690	6.71	31.27	74.24
5/12/85	720	6.87	31.42	76.20
6/11/85	750	---	---	---
7/11/85	780	7.23	31.75	80.12
8/10/85	810	7.45	32.01	82.20
9/9/85	840	7.65	32.16	84.33

Table 6-30. Extensometer Readings (mm) for Extensometer 3E1

Date	Elapsed Days	Anchor No. and Depth (m)		
		No. 1 2.7	No. 2 7.4	No. 3 20.0
5/24/83	0	0.45	0.94	1.08
6/23/83	30	0.57	1.10	1.27
7/23/83	60	0.72	1.34	1.50
8/22/83	90	0.84	1.58	1.75
9/21/83	120	0.98	1.84	2.02
10/21/83	150	---	---	---
11/20/83	180	1.21	2.31	2.54
12/20/83	210	1.37	2.60	2.86
1/19/84	240	---	---	---
2/18/84	270	2.01	3.68	3.99
3/19/84	300	2.36	4.37	4.68
4/18/84	330	2.67	4.90	5.25
5/18/84	360	2.91	5.46	5.88
6/17/84	390	---	---	---
7/17/84	420	3.39	6.29	6.86
8/16/84	450	3.75	6.88	7.50
9/15/84	480	4.06	7.43	8.12
10/15/84	510	4.32	7.93	8.70
11/14/84	540	4.41	8.23	9.12
12/14/84	570	4.56	8.51	9.47
1/13/85	600	4.70	8.76	9.80
2/12/85	630	4.77	8.98	10.10
3/13/85	660	4.92	9.21	10.41
4/12/85	690	5.07	9.47	10.72
5/12/85	720	5.19	9.71	11.04
6/11/85	750	---	---	---
7/11/85	780	5.49	10.20	11.62
8/10/85	810	5.64	10.46	11.92
9/9/85	840	5.76	10.66	12.20

Table 6-31. Extensometer Readings (mm) for Extensometer 3E2

Date	Elapsed Days	Anchor No. and Depth (m)		
		No. 1 2.7	No. 2 7.4	No. 3 20.0
5/24/83	0	1.01	1.42	1.51
6/23/83	30	1.17	1.63	1.71
7/23/83	60	1.35	1.89	1.98
8/22/83	90	1.54	2.17	2.26
9/21/83	120	1.72	2.46	2.54
10/21/83	150	---	---	---
11/20/83	180	2.09	3.02	3.11
12/20/83	210	2.31	3.33	3.42
1/19/84	240	---	---	---
2/18/84	270	3.21	4.55	4.64
3/19/84	300	3.73	5.32	5.42
4/18/84	330	4.16	5.91	6.26
5/18/84	360	4.54	6.53	6.96
6/17/84	390	---	---	---
7/17/84	420	5.20	7.47	8.09
8/16/84	450	5.63	8.08	8.75
9/15/84	480	6.01	8.64	9.44
10/15/84	510	6.35	9.15	10.11
11/14/84	540	6.55	9.52	10.61
12/14/84	570	6.79	9.86	11.06
1/13/85	600	6.97	10.16	11.47
2/12/85	630	7.15	10.44	11.83
3/13/85	660	7.35	10.70	12.18
4/12/85	690	7.55	11.01	12.58
5/12/85	720	7.73	11.29	12.95
6/11/85	750	---	---	---
7/11/85	780	8.12	11.83	13.59
8/10/85	810	8.32	12.11	13.96
9/9/85	840	8.50	12.38	14.32

Table 6-32. Extensometer Readings (mm) for Extensometer 4E1

Date	Elapsed Days	Anchor No. and Depth (m)		
		No. 1 2.7	No. 2 7.4	No. 3 20.0
5/24/83	0	0.38	0.78	0.65
6/23/83	30	0.49	0.97	0.84
7/23/83	60	0.61	1.18	1.04
8/22/83	90	0.72	1.39	1.25
9/21/83	120	0.84	1.61	1.48
10/21/83	150	---	---	---
11/20/83	180	1.06	1.99	2.04
12/20/83	210	1.19	2.24	2.29
1/19/84	240	---	---	---
2/18/84	270	1.89	3.35	3.39
3/19/84	300	2.21	3.97	4.06
4/18/84	330	2.47	4.45	4.58
5/18/84	360	2.67	4.92	5.12
6/17/84	390	---	---	---
7/17/84	420	3.10	5.69	5.94
8/16/84	450	3.47	6.29	6.62
9/15/84	480	3.79	6.86	7.21
10/15/84	510	4.04	7.35	7.76
11/14/84	540	4.11	7.62	8.09
12/14/84	570	4.26	7.91	8.44
1/13/85	600	4.37	8.13	8.70
2/12/85	630	1.66	3.03	3.14
3/13/85	660	1.37	4.28	5.73
4/12/85	690	1.03	3.27	4.69
5/12/85	720	1.78	5.50	7.55
6/11/85	750	---	---	---
7/11/85	780	5.06	9.50	10.54
8/10/85	810	5.21	9.76	10.82
9/9/85	840	5.34	10.01	11.08

Table 6-33. Extensometer Readings (mm) for Extensometer 4E2

Date	Elapsed Days	Anchor No. and Depth (m)		
		No. 1 2.7	No. 2 7.4	No. 3 20.0
5/24/83	0	0.98	1.47	1.44
6/23/83	30	1.13	1.68	1.66
7/23/83	60	1.28	1.92	1.90
8/22/83	90	1.43	2.13	2.13
9/21/83	120	1.57	2.36	2.36
10/21/83	150	---	---	---
11/20/83	180	1.86	2.82	2.87
12/20/83	210	2.04	3.07	3.14
1/19/84	240	---	---	---
2/18/84	270	2.83	4.15	4.26
3/19/84	300	3.29	4.85	5.00
4/18/84	330	3.63	5.38	5.60
5/18/84	360	3.92	5.90	6.24
6/17/84	390	---	---	---
7/17/84	420	4.51	6.76	7.28
8/16/84	450	4.94	7.38	8.02
9/15/84	480	5.33	7.97	8.70
10/15/84	510	5.65	8.50	9.32
11/14/84	540	5.83	8.84	9.84
12/14/84	570	6.05	9.19	10.30
1/13/85	600	6.23	9.49	10.72
2/12/85	630	6.39	9.77	11.12
3/13/85	660	6.58	10.04	11.46
4/12/85	690	6.80	10.35	11.90
5/12/85	720	6.96	10.65	12.27
6/11/85	750	---	---	---
7/11/85	780	7.35	11.24	12.99
8/10/85	810	7.55	11.53	13.38
9/9/85	840	7.75	11.84	13.77

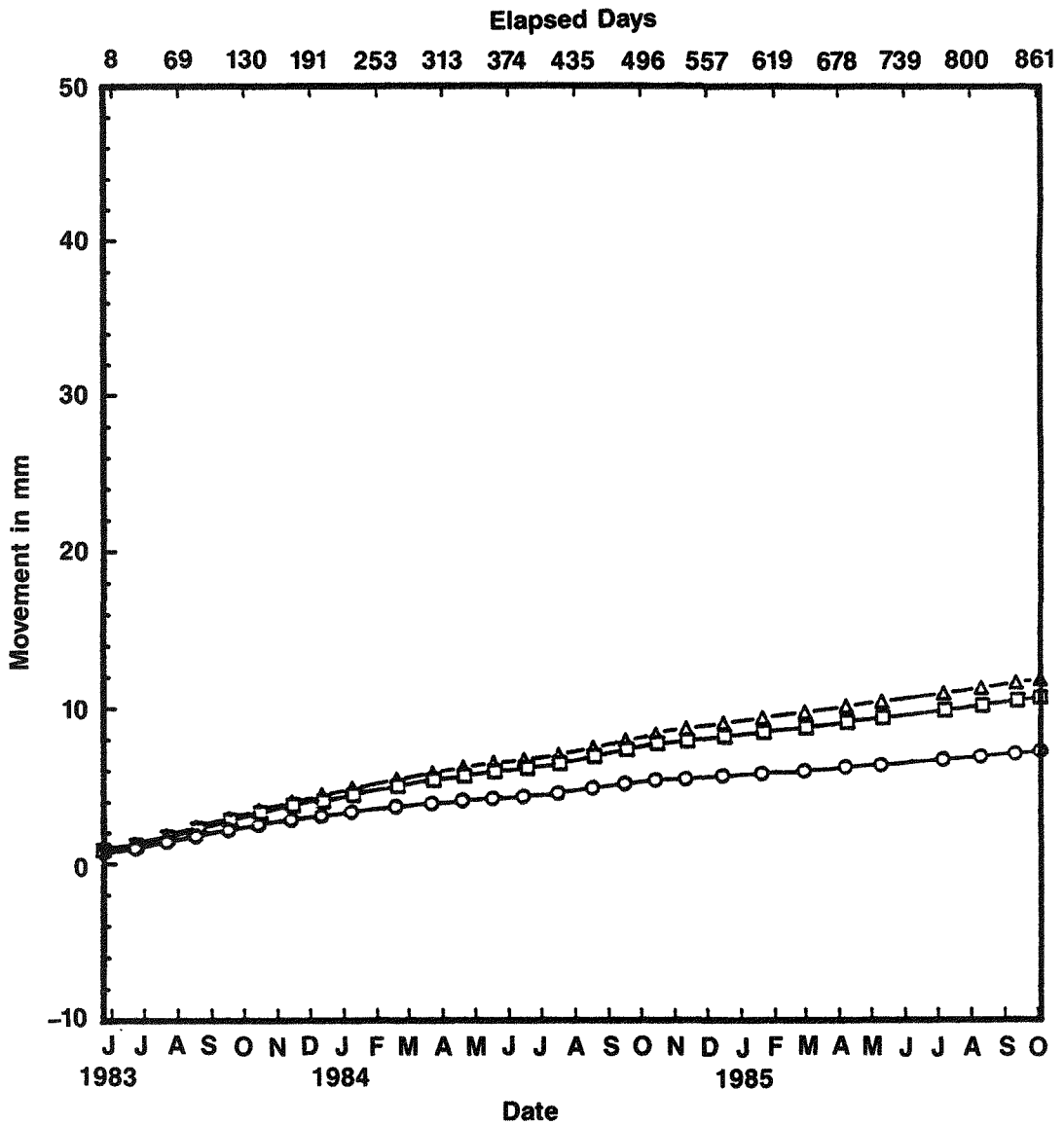

LEGEND:
- ○ 1E1-1, 2.7 m
- □ 1E1-2, 7.4 m
- △ 1E1-3, 20.0 m

Extensometer 1E1—
Movement Versus Time

Figure 6-24

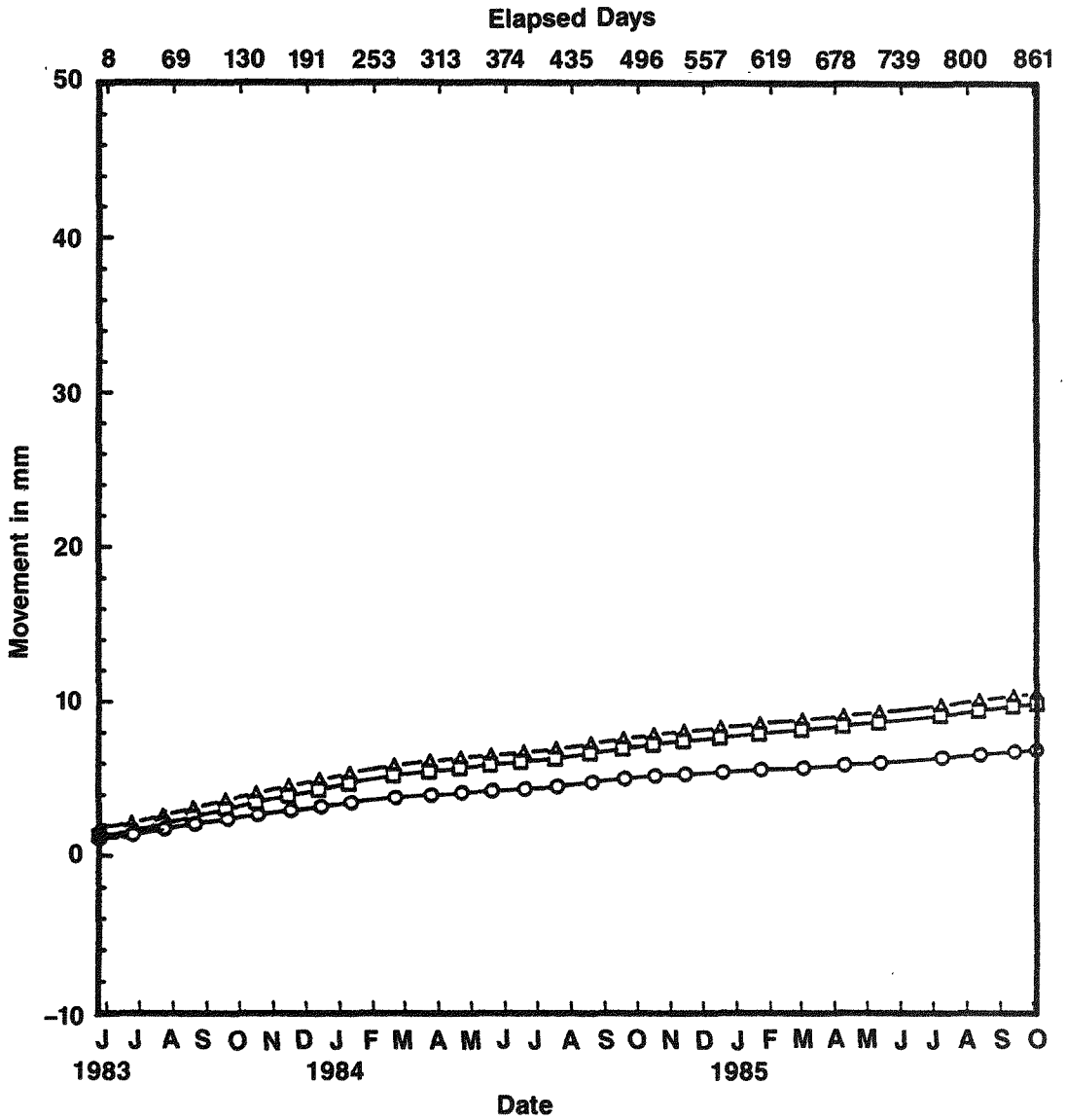

LEGEND:

- ○ 1E2-1, 2.7 m
- □ 1E2-2, 7.4 m
- △ 1E2-3, 20.0 m

Extensometer 1E2—
Movement Versus Time

Figure 6-25

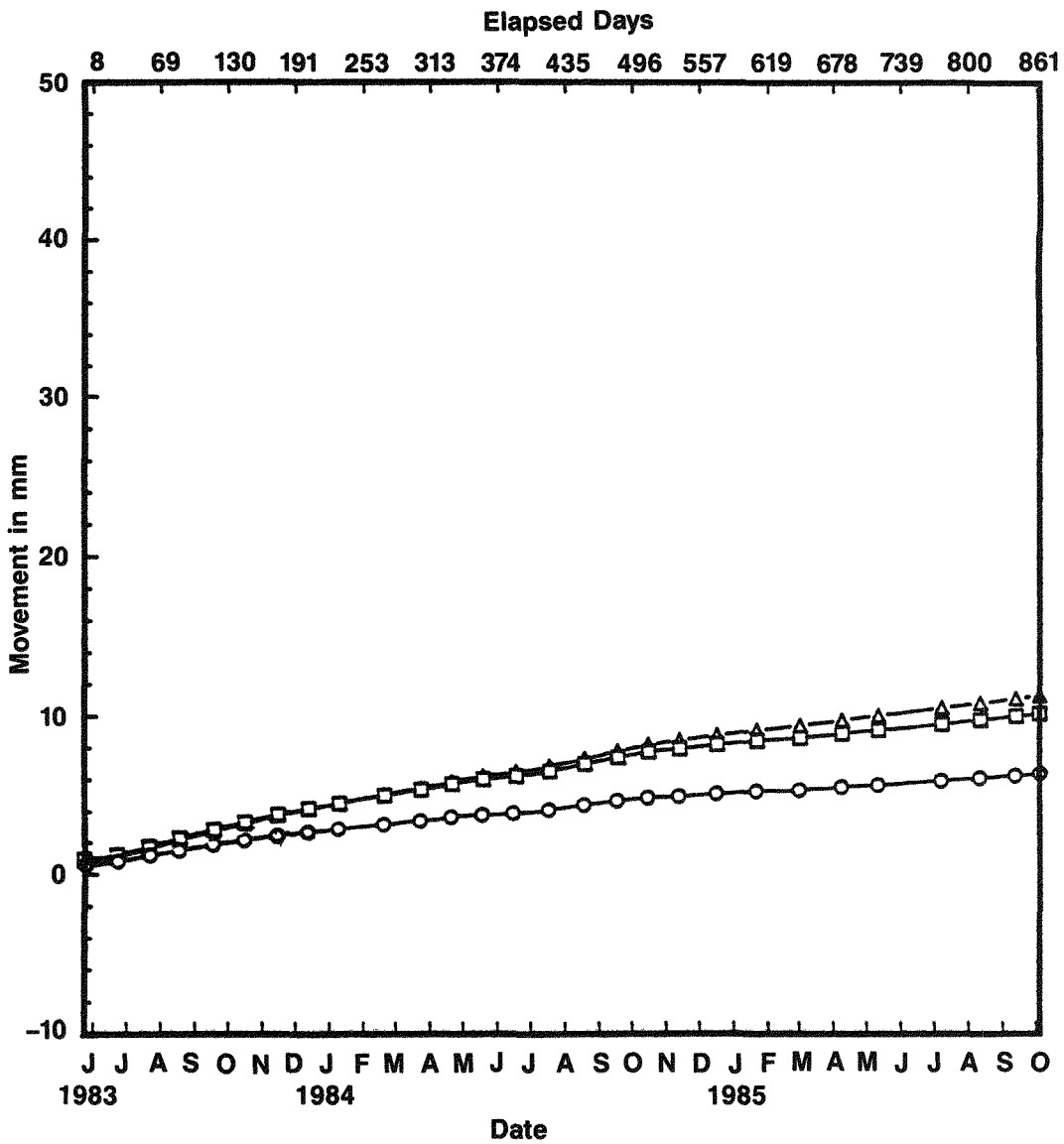

LEGEND:

- ○ 2E1-1, 2.7 m
- □ 2E1-2, 7.4 m
- △ 2E1-3, 20.0 m

Extensometer 2E1—
Movement Versus Time

Figure 6-26

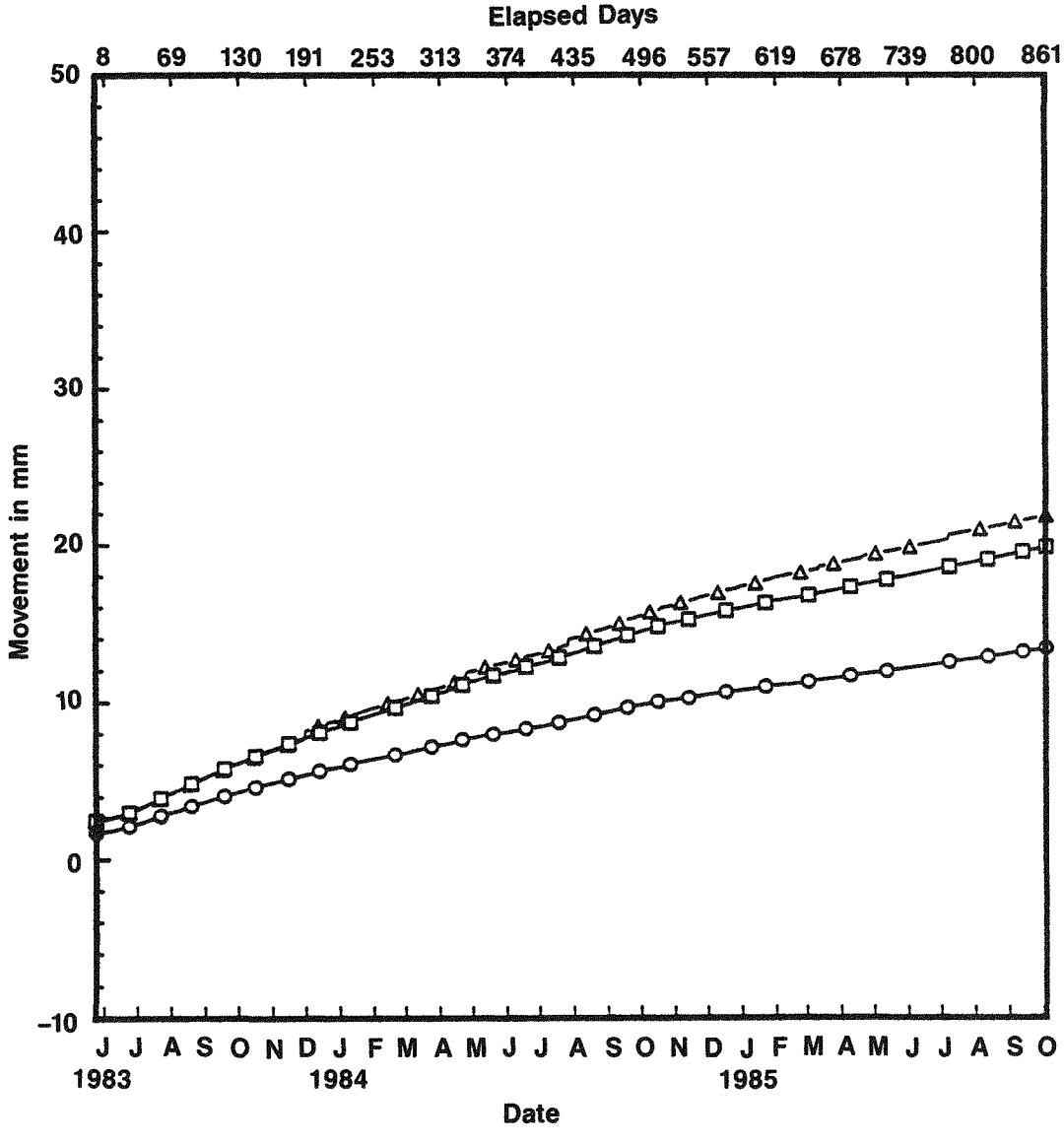

LEGEND:

- ○ 2E2-1, 2.7 m
- □ 2E2-2, 7.4 m
- △ 2E2-3, 20.0 m

Extensometer 2E2—
Movement Versus Time

Figure 6-27

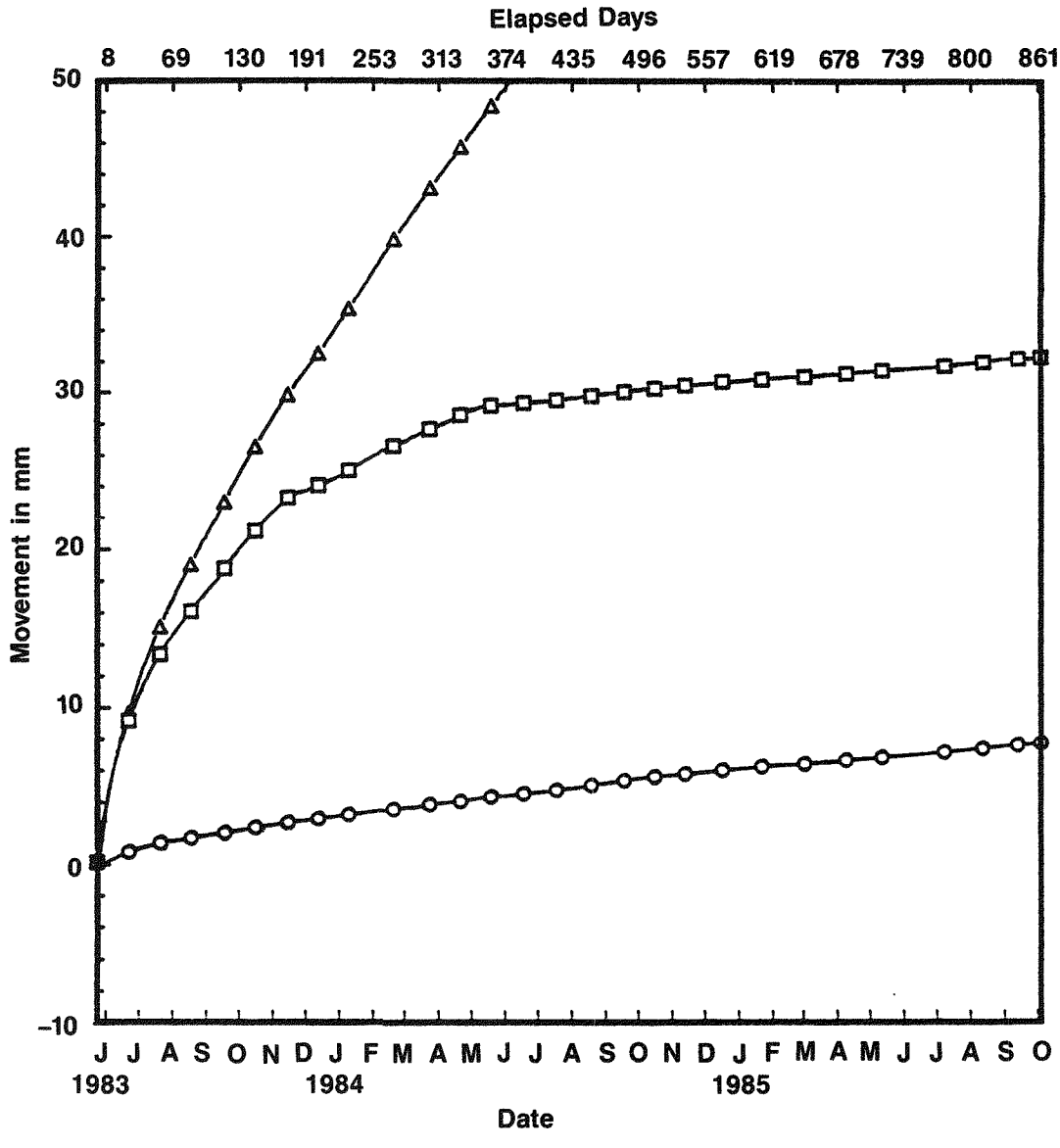

LEGEND:

- ○ 2E3-1, 2.7 m
- □ 2E3-2, 7.4 m
- △ 2E3-3, 20.0 m

**Extensometer 2E3—
Movement Versus Time**

Figure 6-28

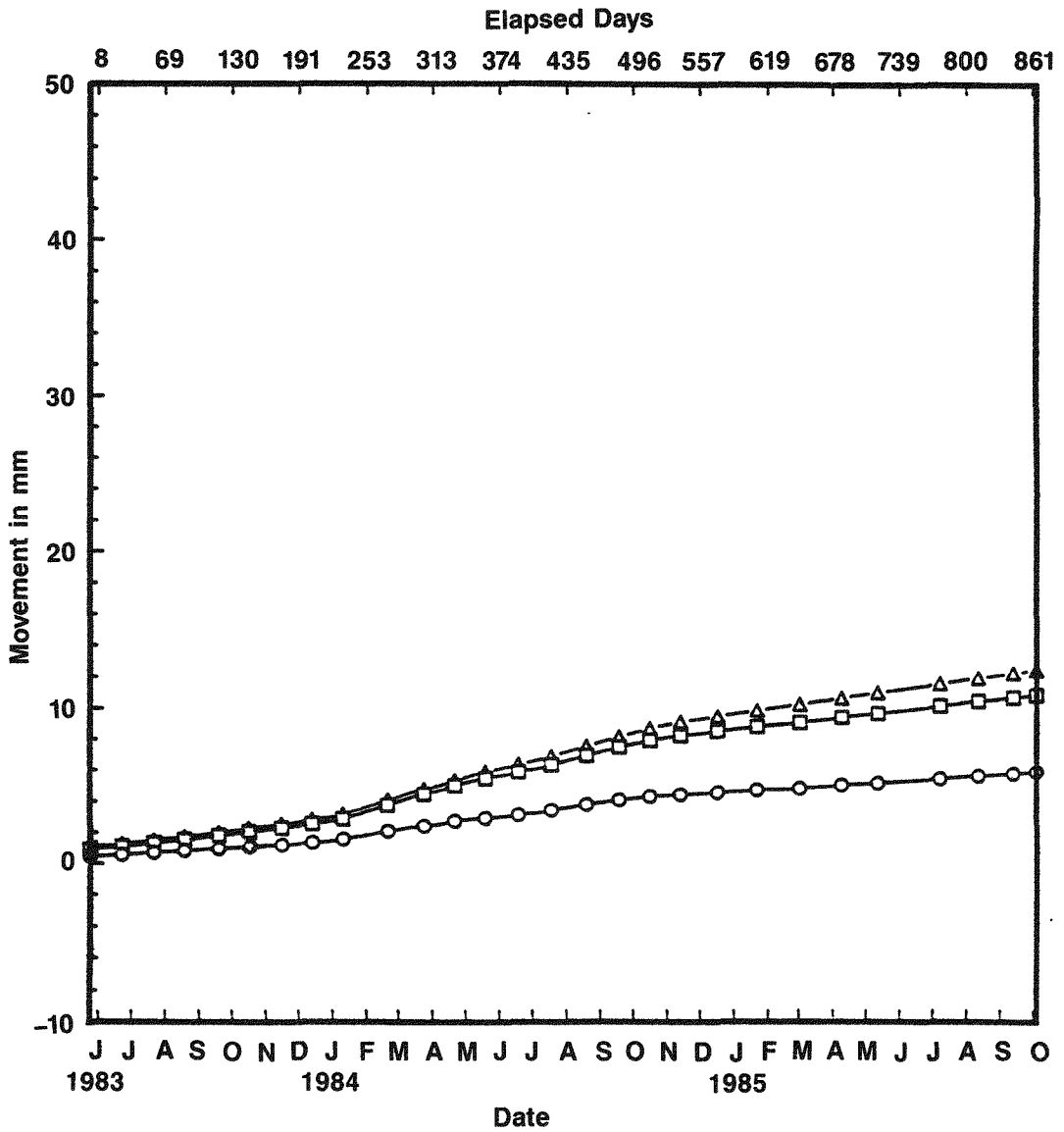

LEGEND:

- ○ 3E1-1, 2.7 m
- □ 3E1-2, 7.4 m
- △ 3E1-3, 20.0 m

Extensometer 3E1—
Movement Versus Time

Figure 6-29

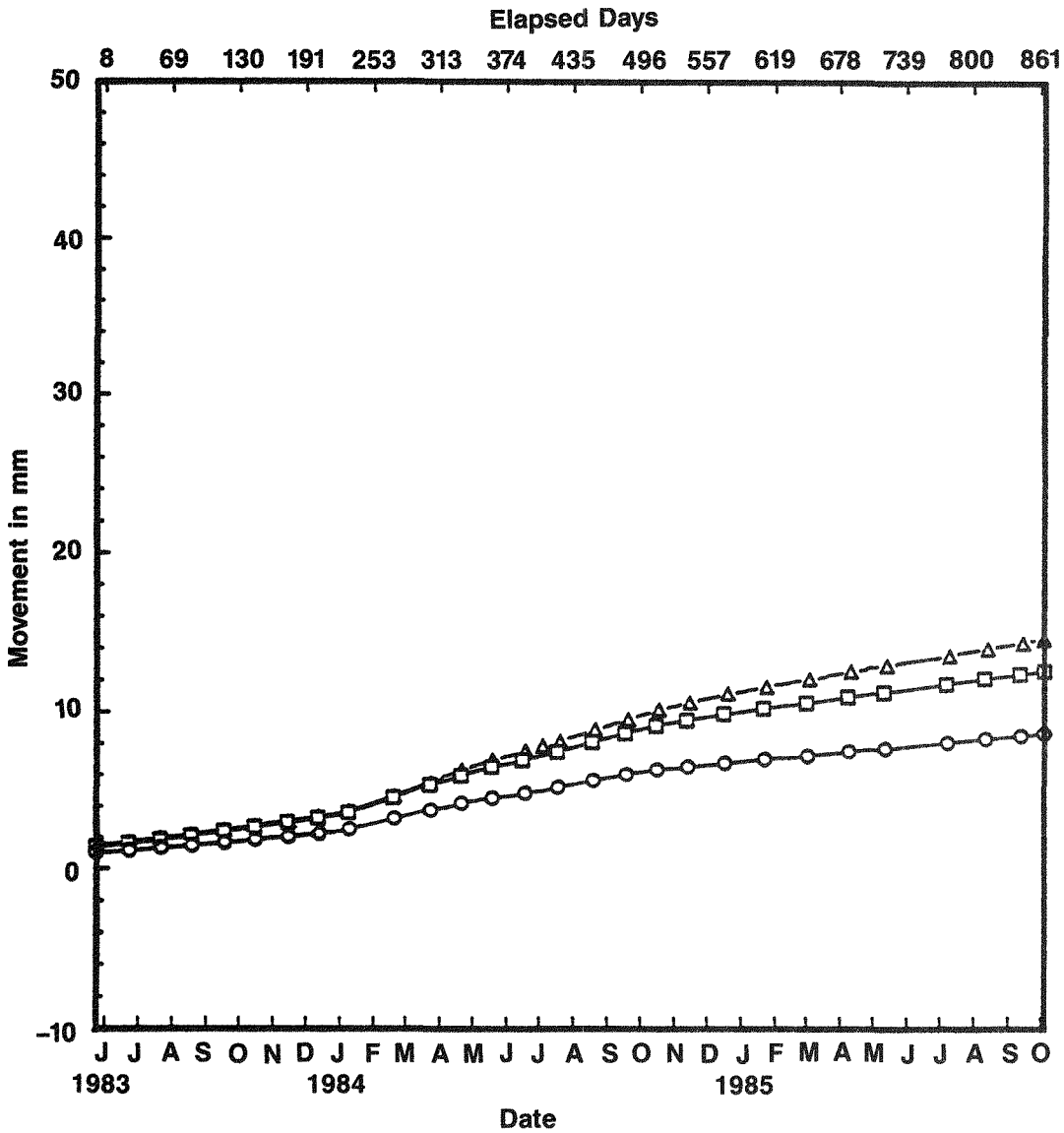

LEGEND:

- ○ 3E2-1, 2.7 m
- □ 3E2-2, 7.4 m
- △ 3E2-3, 20.0 m

**Extensometer 3E2—
Movement Versus Time**

Figure 6-30

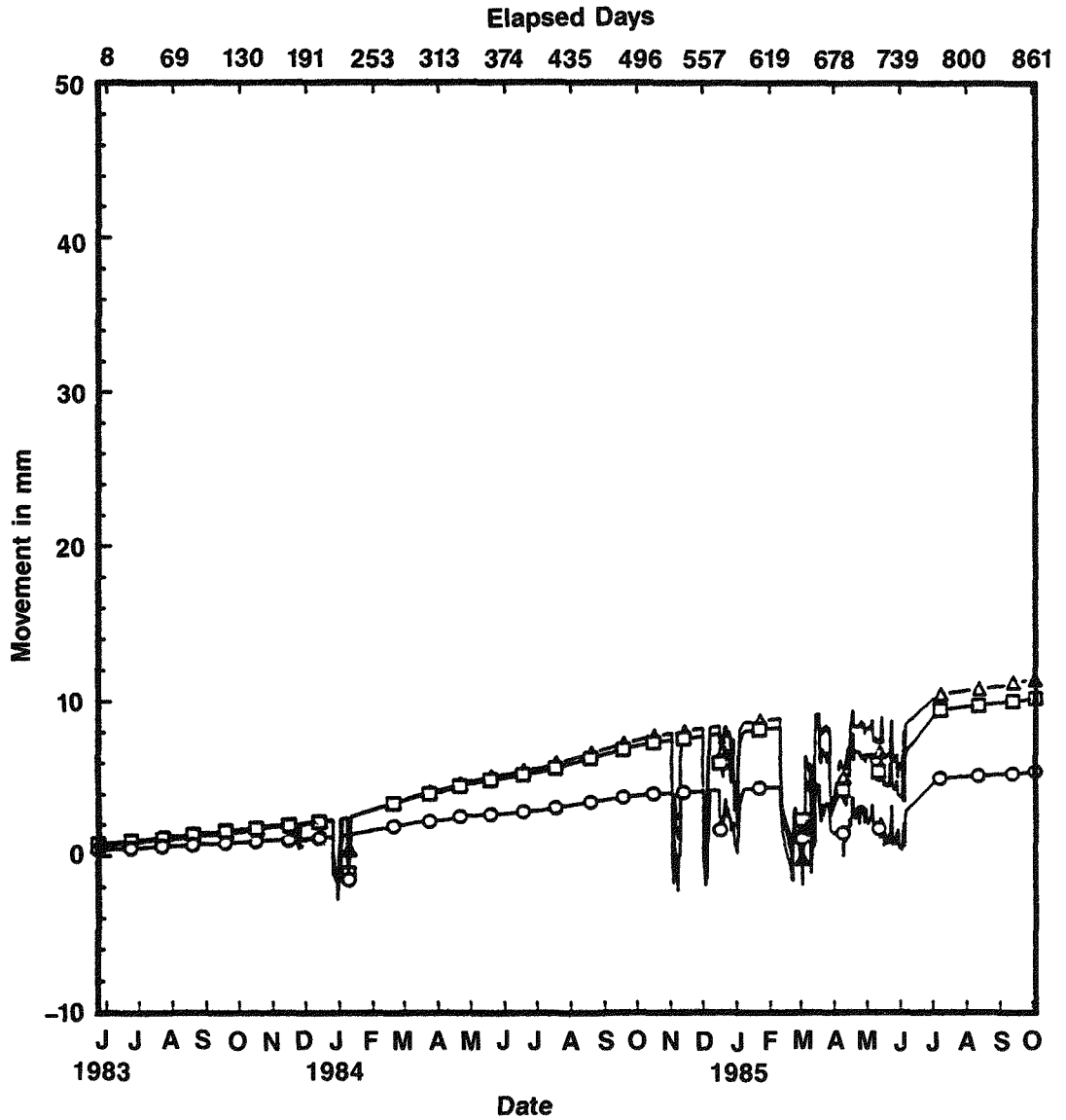

LEGEND:
- ○ 4E1-1, 2.7 m
- □ 4E1-2, 7.4 m
- △ 4E1-3, 20.0 m

Extensometer 4E1—
Movement Versus Time

Figure 6-31

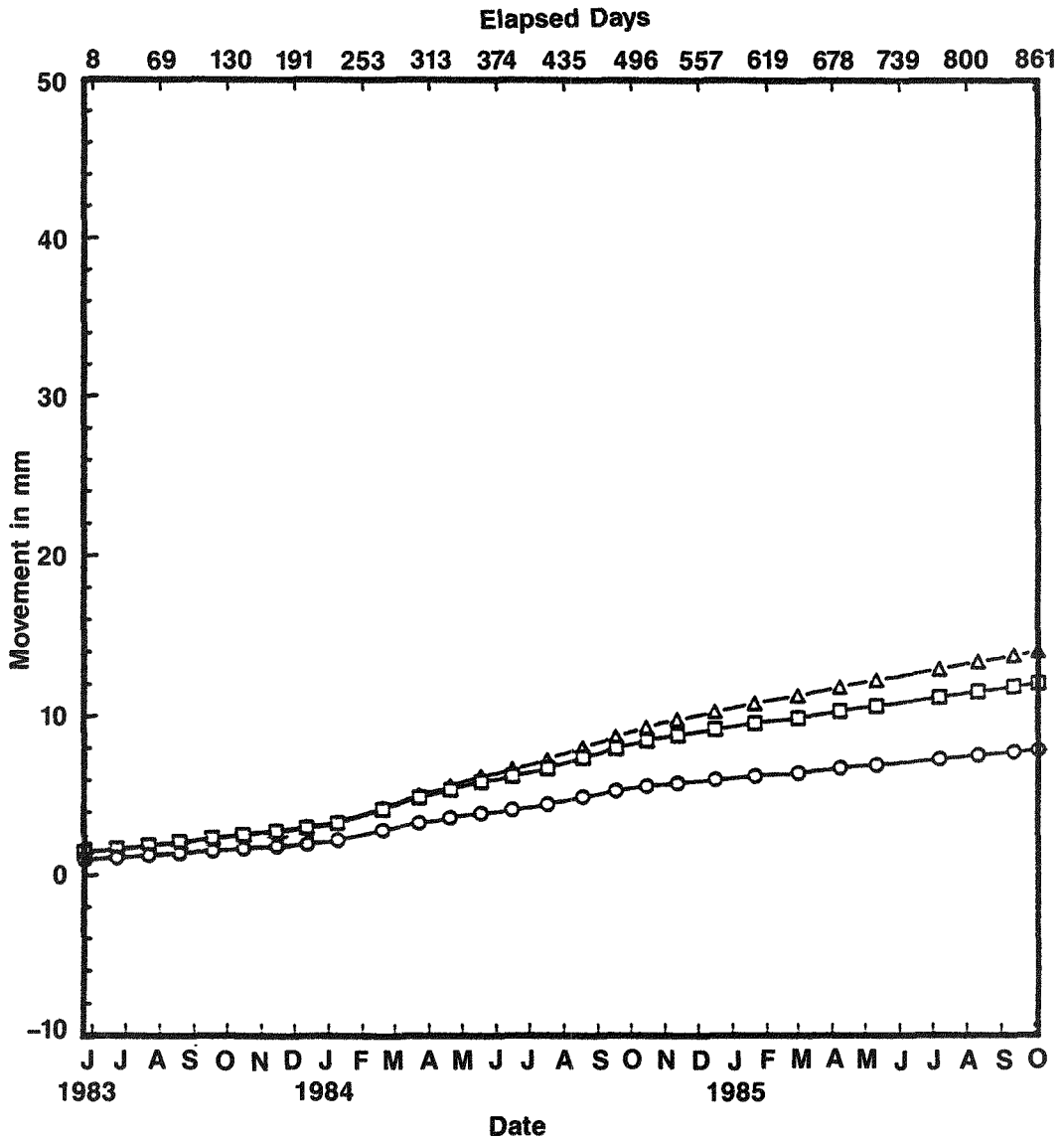

LEGEND:

- ○ 4E2-1, 2.7 m
- □ 4E2-2, 7.4 m
- △ 4E2-3, 20.0 m

**Extensometer 4E2—
Movement Versus Time**

Figure 6-32

properties of salt rock, stratum model conditions, and creep law were used in the above-mentioned numerical codes:

- Elastic material properties in both codes:

  Young's modulus E = 6.9 GPa (1.0×10^6 psi)

  Poisson's ratio $\nu = 0.4$

- Time-dependent properties:

  For long-term considerations only steady state (secondary creep) was considered; transient creep was neglected.

- Creep law adapted for secondary creep rate $\dot{\varepsilon}_s$:

  - DAPROK (U.S. Code) : $\dot{\varepsilon}_s = 2.08 \times 10^{-11} \times \frac{\sigma e^5}{bar} \times \exp \frac{-6776K}{T} \times s^{-1}$

  - MAUS (FRG Code) : $\dot{\varepsilon}_s = 4.85 \times 10^{-11} \times \frac{\sigma e^5}{bar} \times \exp \frac{-6880K}{T} \times s^{-1}$

- Assumptions for primary stresses, boundary conditions, model size, and FE-mesh pattern were as shown in Figure 6-33 for the DAPROK-code and in Figure 6-34 for the MAUS code.

More detailed information on the FE codes, modeling, and results of numerical pretest calculations is reported by Rothfuchs et al. (1986).

A comparison of the two pretest calculational results (Figures 6-18, 6-21, and 6-23) shows that DAPROK produces higher deformations than MAUS in the preheating phase, but produces nearly the same predictions after heating was started. Since both codes are similar, the differences may be due to the fact that DAPROK was applied to a much smaller rock volume than MAUS, resulting in higher stress levels and deformations.

6.5 STRESS MEASUREMENTS

Most stress measurements are carried out to determine the local stress field (primary or secondary) as an important design parameter for underground openings or constructions.

One of the significant measurements that can be performed in the brine migration test at Asse is the determination of the induced thermal stresses to get a better understanding of the resulting deformations.

Two types of "stress meters" were installed within the near-field area of the central heaters where the most temperature-influenced zone is to be expected. The stress measurement instruments adopted were direct-reading hydraulic

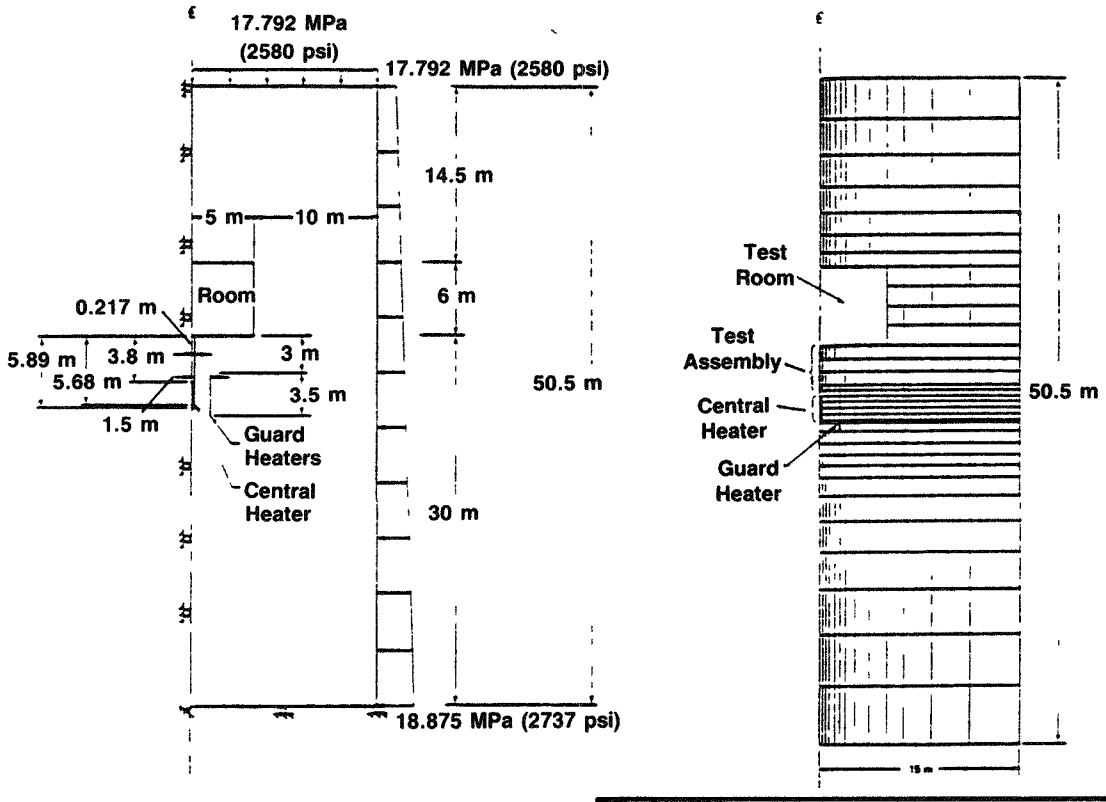

Finite Element Net (DAPROK)

Figure 6-33

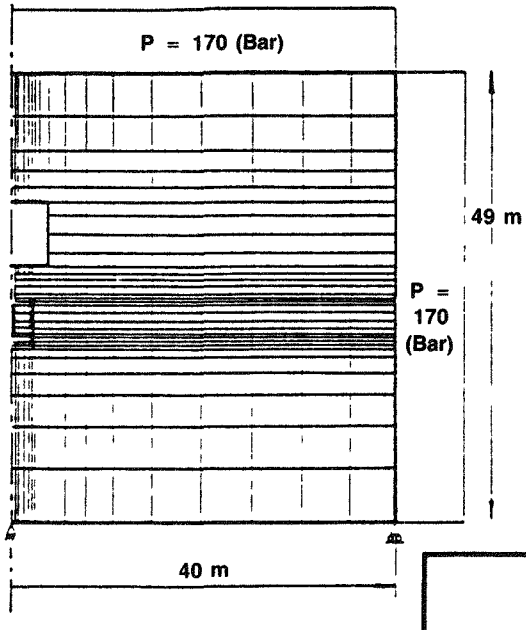

Finite Element Net (MAUS)

Figure 6-34

stress gages of the Gloetzl type (flat cells) and strain-gaged stress meters, a version of the well-known IRAD vibrating wire stress meter. The flat cells are installed only at test site 2 and the strain-gaged stress meters are only at test sites 1 and 2.

6.5.1 Location and Arrangement of Stress Gages

The stress change measurements were conducted in boreholes drilled into the floor, at a 2.2-m (7.2-ft) radial distance from the centerline of the test sites 1 and 2 of the test field. Twelve strain-gaged stress meters and six flat cells were installed in the test field. The arrangement of the stress meters and their downhole positions at both sites are similar, with the exception that the flat cells were installed only in test site 2. Figure 6-35 shows a schematic overview of test site 2. Two stress meters were placed in the individual boreholes to detect radial and tangential stress changes due to the thermal expansion of the host rock. During the setting operation, two electric wires were broken, resulting in no data being received from strain gages 1S1-2 and 2S1-2. Figure 6-36 shows the cross section through test site 2. Table 6-34 presents the detailed information regarding location of each of the stress meters in terms of its installation depth, radial distance to the heater centerline, and azimuth.

6.5.2 Calibration of Stress Gages

To evaluate the in situ data, laboratory calibrations are necessary for both types of stress gages.

6.5.2.1 Flat Cells

Theoretically, it is expected that the reading of a flat cell is equal to the external normal stress. In the case of the sandwich system used at Asse (rock salt/polyurethane/mortar/flat cell) a stress transfer factor might exist with respect to the normal stress. First, calibration tests of the system (polyurethane/mortar/flat cell) were carried out in an autoclave. The system was loaded stepwise in several cycles by fluid pressure up to 18 MPa (2,612 psi). In the autoclave calibration, it was not possible to calibrate the flat cell for fluid temperature. The resulting calibration curves for loading and unloading without a differentiation of the cycles is shown in Figures 6-37 and 6-38. The flat cell reading is about 2 MPa (290 psi) less than the applied external pressure. Creep effects from five minutes to one hour were observed, but no long-term creep effects were observed.

6.5.2.2 Calibration of Strain-Gaged Stress Meters

First, calibration tests were performed in different salt blocks at the same loading conditions in a uniaxial compression machine at ambient temperature. The salt was halite taken from the boundary of a $Na_2\beta$ and Na_2S formation at the 775-m (2,542-ft) level of the mine. This salt cannot be considered to be representative of the salt type of the test field at the 800-m (2,624-ft) level. The salt blocks were prepared from 300-mm (11.8-in) outside

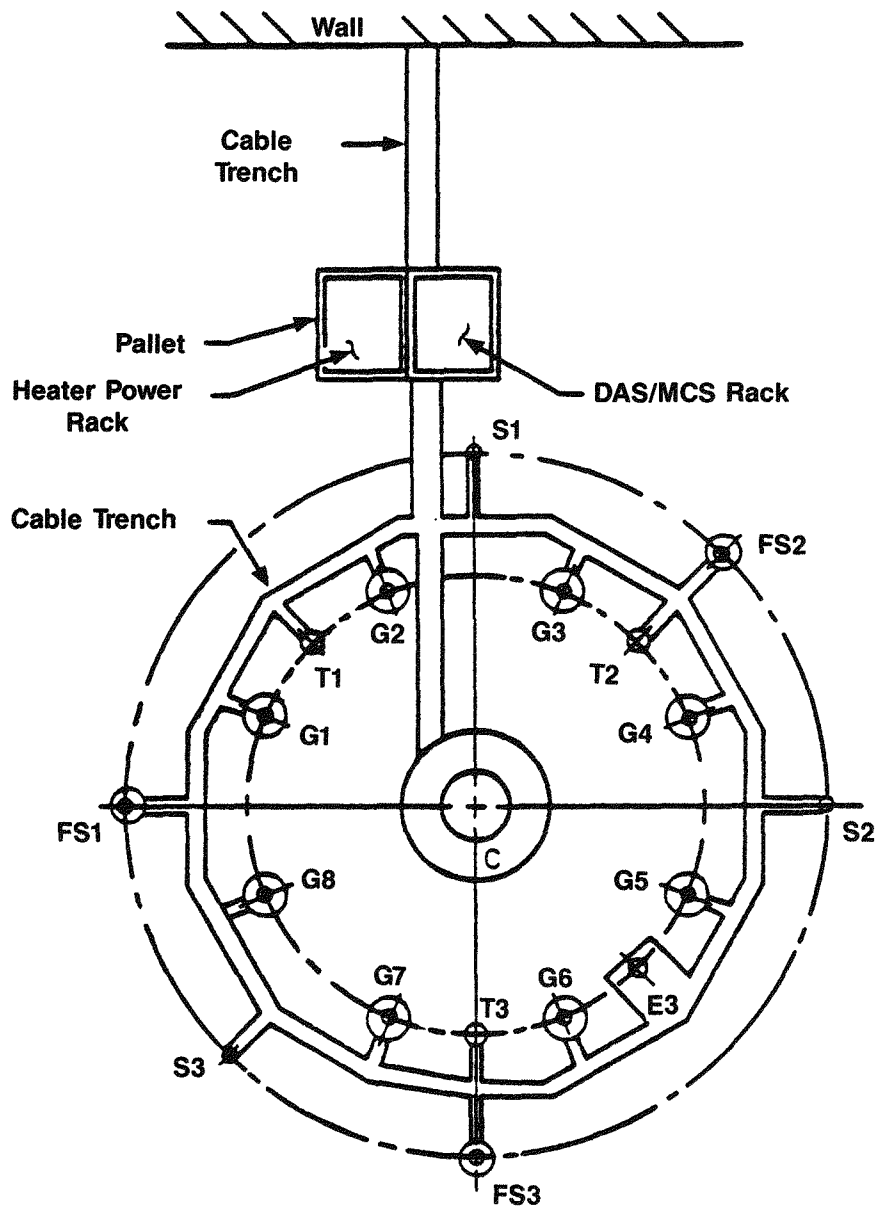

Legend

- C = Central Test Assembly
- G = Guard Heater
- T = Thermocouple Probe
- FS = Flat Cell (Gloetzl)
- S = Strain-Gaged Stress Meter
- E = Extensometer

Test Site Overview

Figure 6-35

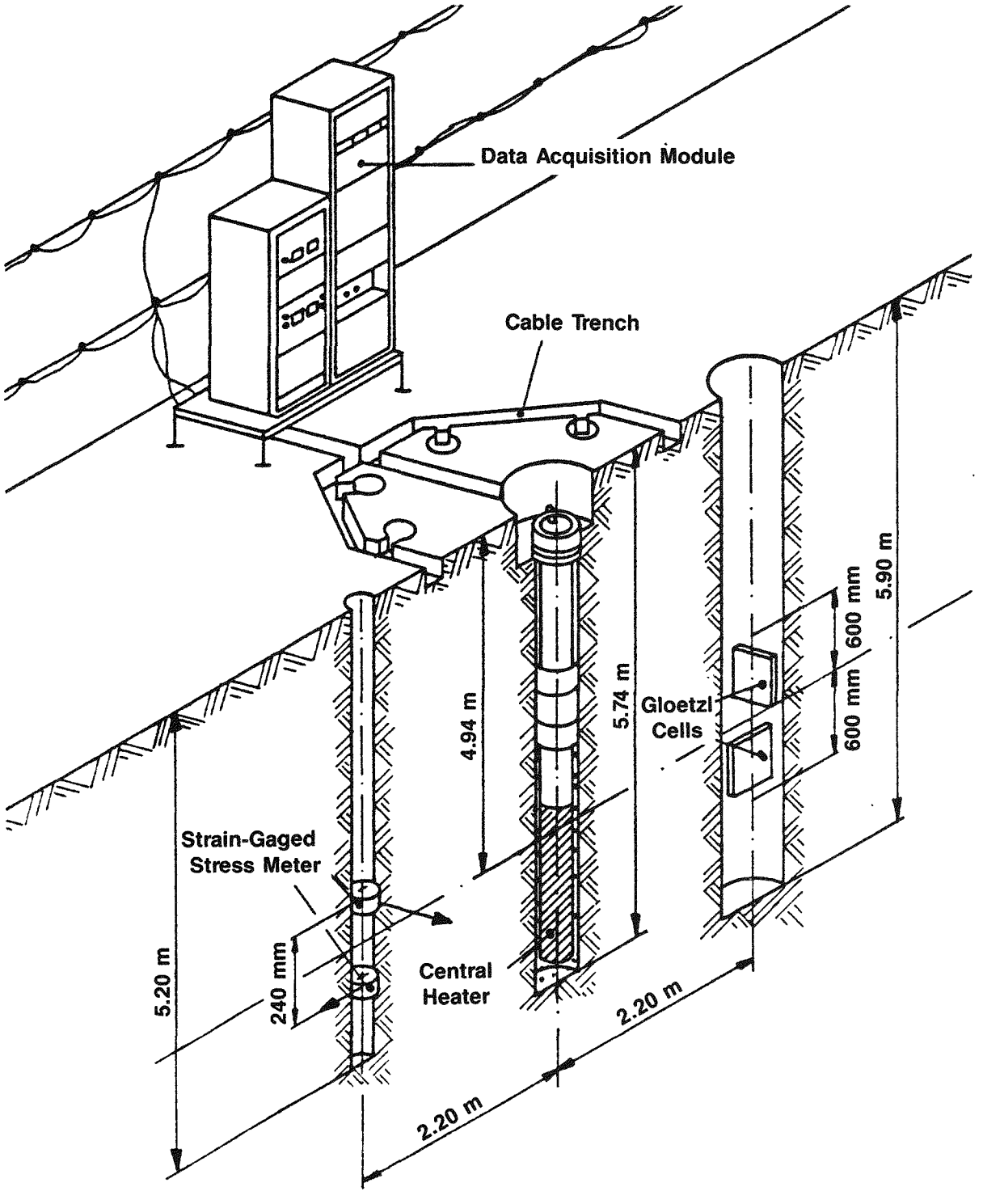

Vertical Cross Section Through Test Site 2, Showing Arrangement of Stress Meters

Figure 6-36

Table 6-34. Location and Orientation of Stress Meters

Site	Borehole	Gage	Radial Distance from Centerline (m)	Depth (m)	Azimuth	Orientation	Remarks
1	1S1[a]	1S1-1	2.2	4.82	90°	radial	T/C attached[c]
1	1S1	1S1-2	-	-	-	-	N/A
1	1S2	1S2-1	2.2	5.06	180°	radial	
1		1S2-2	2.2	4.82	180°	tangential	T/C attached
1	1S3	1S3-1	2.2	5.06	315°	radial	
1		1S3-2	2.2	4.82	315°	tangential	T/C attached
2	2S1	2S1-1	2.2	4.01	90°	radial	T/C attached
2	2S1	2S1-2	-	-	-	-	N/A
2	2S2	2S2-1	2.2	5.06	180°	radial	
		2S2-2	2.2	4.82	180°	tangential	T/C attached
2	2S3	2S3-1	2.2	5.06	315°	radial	
2		2S3-2	2.2	4.82	315°	tangential	T/C attached
2	2FS1[b]	2FS1-1	2.2	4.64	0°	radial	
2	2FS1	2FS1-2	2.2	5.24	0°	tangential	
2	2FS2	2FS2-1	2.2	4.64	135°	radial	
2	2FS2	2FS2-2	2.2	5.24	135°	tangential	
2	2FS3	2FS3-1	2.2	4.64	270°	radial	
2	2FS3	2FS3-2	2.2	5.24	270°	tangential	

(a) S - Strain-gaged Stressmeters.
(b) FS - Flat cells.
(c) T/C - Thermocouple.

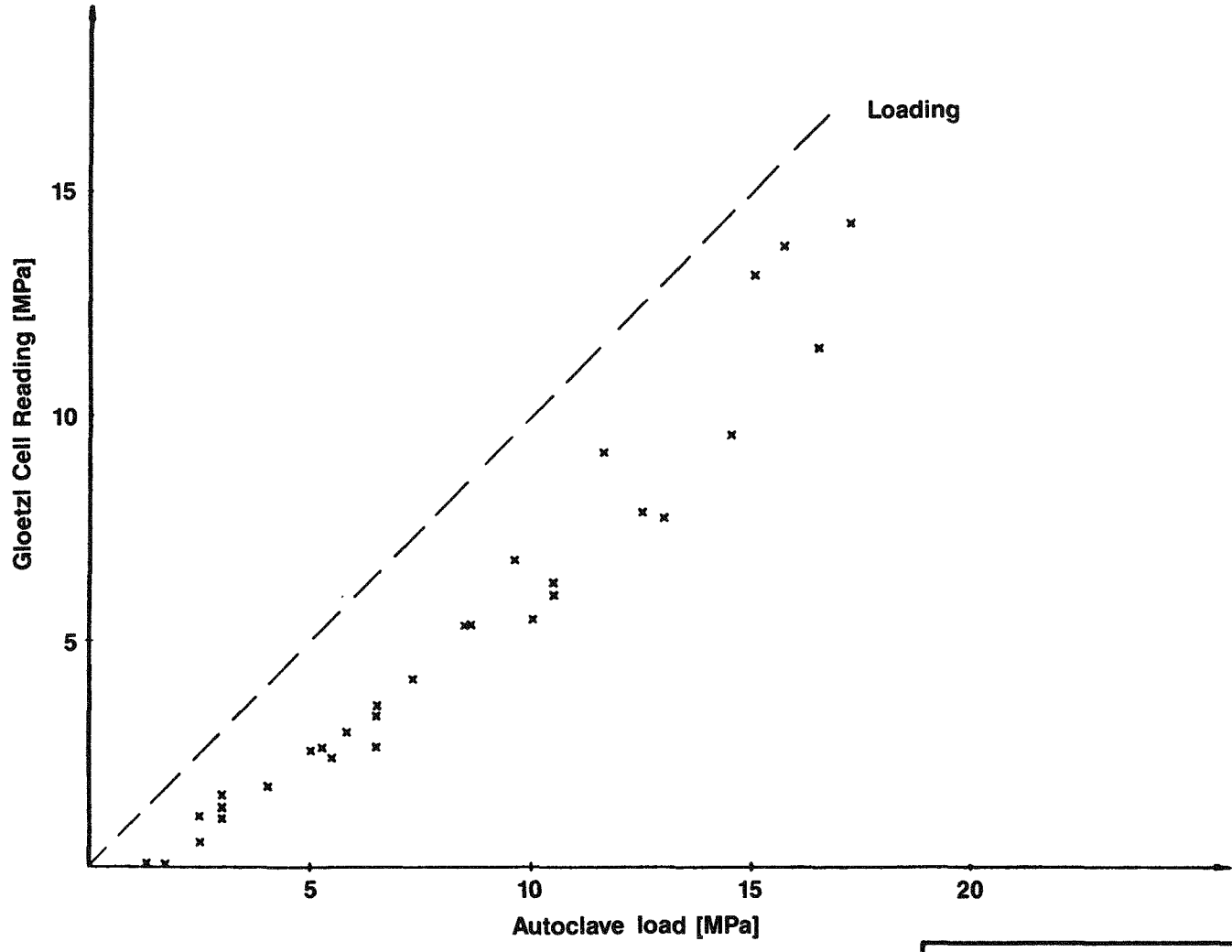

Calibration of a Sandwich System Polyurethane/Mortar/Flat Cell — Loading (the line indicates direct reading of the flat cell; conversion factor: 1MPa = 145.0377 psi)

Figure 6-37

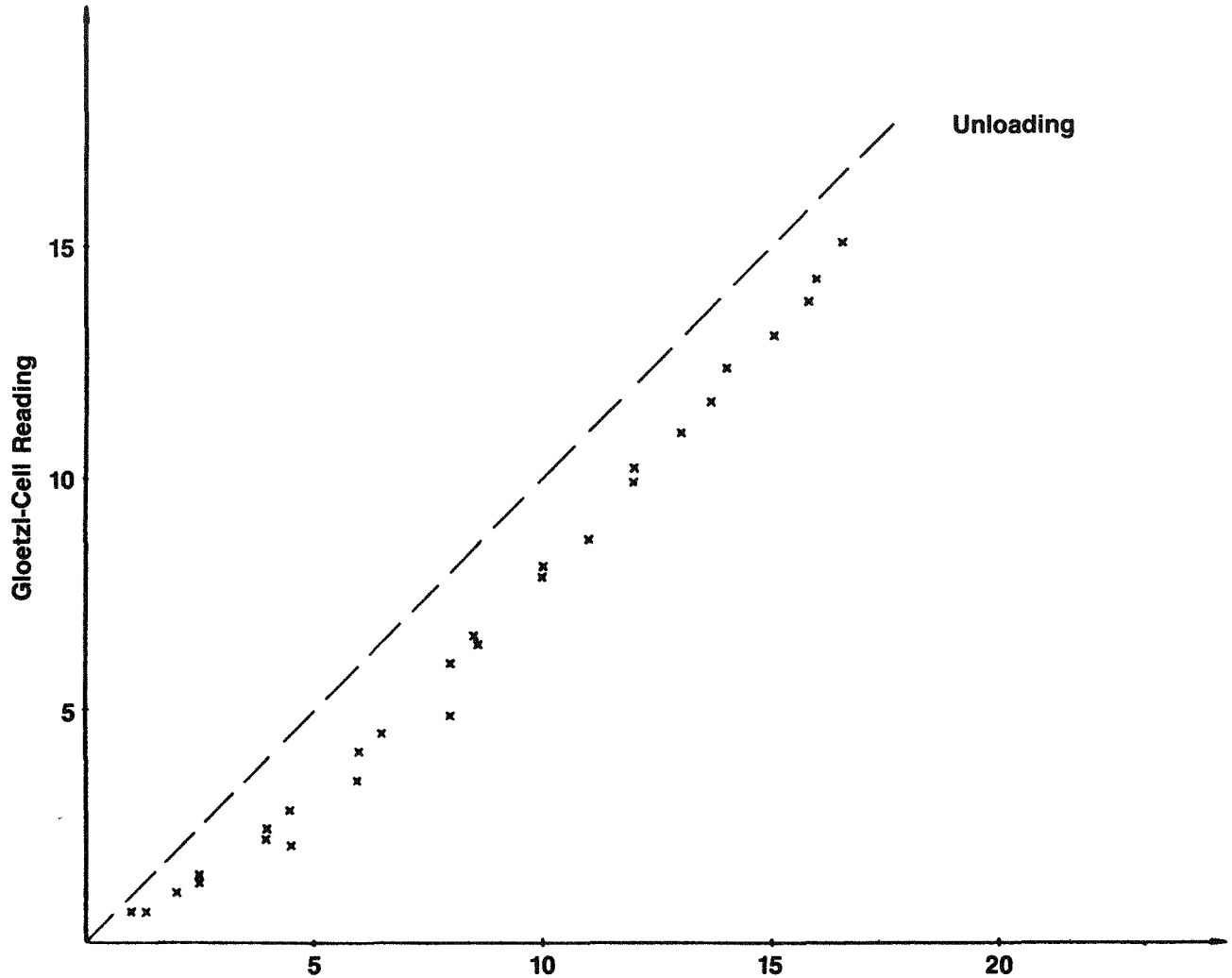

Calibration of a Sandwich System Polyurethane/Mortar/Flat Cell — Unloading (the line indicates direct reading of the flat cell; conversion factor: 1MPa = 145.0377 psi)

Figure 6-38

diameter cores and finished to the desired cube size of 20 cm by 20 cm by 20 cm (7.87 in by 7.87 in by 7.87 in). All calibrations were performed using the same stress meter (18.00 VDC excitation voltage). The general calibration procedure is described in the following paragraphs.

The strain-gaged stress meter is placed into a central borehole (48 mm [1.9 in] in diameter) and preloaded by wedging the gage against the borehole wall until the output reading registers a change of about 5 mV (amplified 50 times).

The machine load was applied to the salt block stepwise, increasing the load by 0.5 MPa (72.5 psi) and then keeping constant for five minutes. The maximum applied load was 11 MPa (1,595 psi). At this point the load was kept constant for a longer period to observe creep effects. The salt block was then unloaded at a rate of approximately 0.2 MPa/min (29 psi/min). The resulting calibration curves (Figures 6-39 through 6-41) show large differences in the output readings so that no reproducible curves were obtained. (Note: The same stress meter was used in all tests.) To evaluate the in situ data measured at test sites 1 and 2, further calibrations are needed. These tests will be performed using salt blocks taken from the test field. Also, the impact of temperature will be taken into account.

It was intended to evaluate the installed stress meters in test sites 1 and 2 using the results obtained from the large block. As the preloads of the stress meters in the field differ from the preloads selected in the laboratory, it was not possible to use these results for the evaluation of the stress meters in the test field. Using the calibration results of a small salt block (salt block K1-1U - 20 cm by 20 cm by 20 cm (7.87 in by 7.87 in by 7.87 in), one of the stress meters could be evaluated.

6.5.3 Measurement Results

The following two sections summarize the results from field measurements.

6.5.3.1 Central Borehole

The radial stress measured in the central borehole of test site 2 with azimuth of 0 degree and 270 degrees is given in Tables 6-35 and 6-36, respectively. The corresponding plots of radial stress versus time in the central borehole of test site 2 are presented in Figures 6-42 and 6-43. Radial stress was measured by Gloetzl cells positioned between the borehole wall and the lower sleeve. It was intended to get information on the pressure that acts on the sleeve. All three cells were emplaced at the upper, central, and lower level of the central borehole at two registered azimuths, making a total of six cells. The observed low pressures by the cells may be due to the mobility of the spherical alumina beads in the annulus.

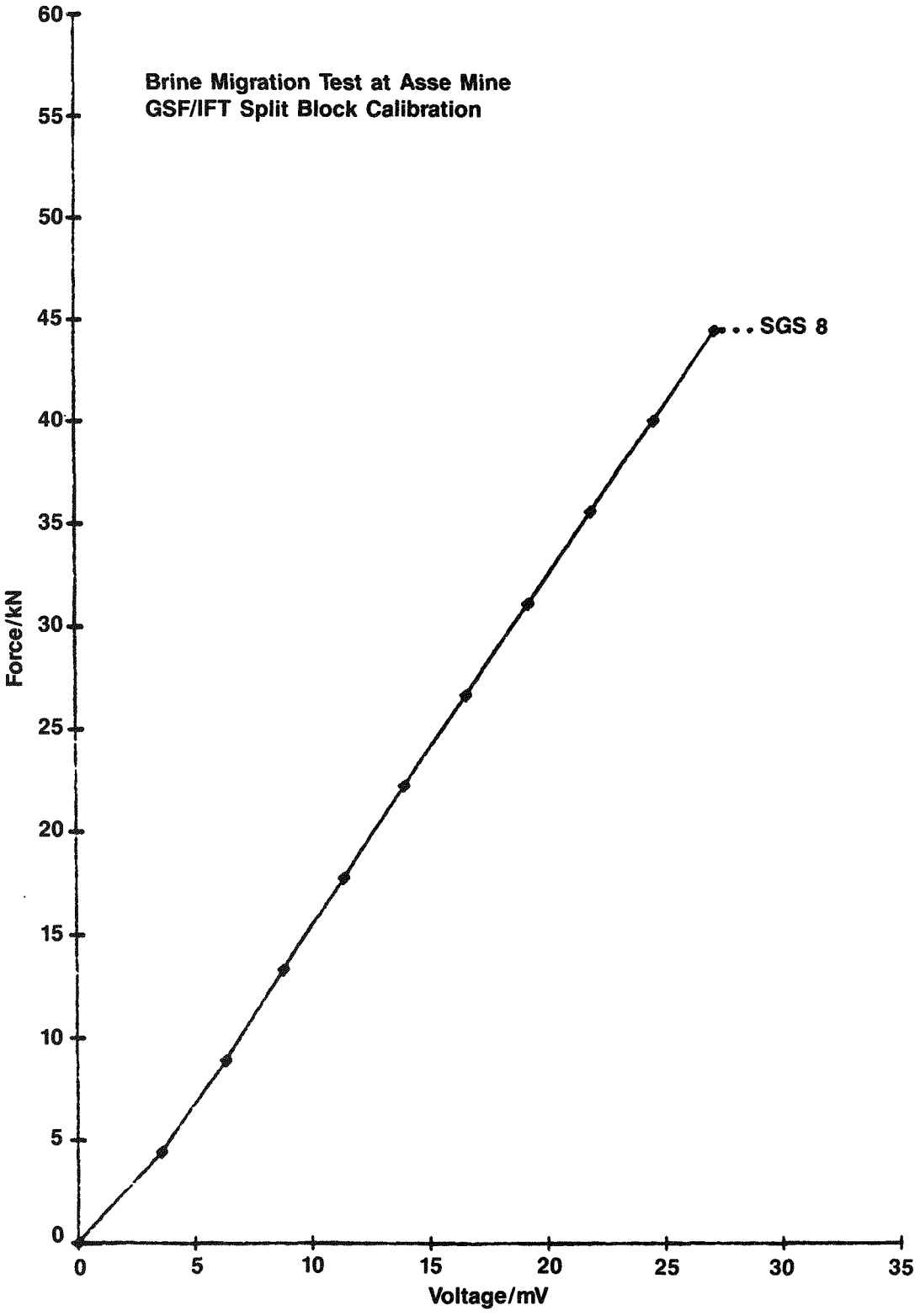

Split Block Calibration
Curve Gage No. 8
Located at 1S2-1

Figure 6-39

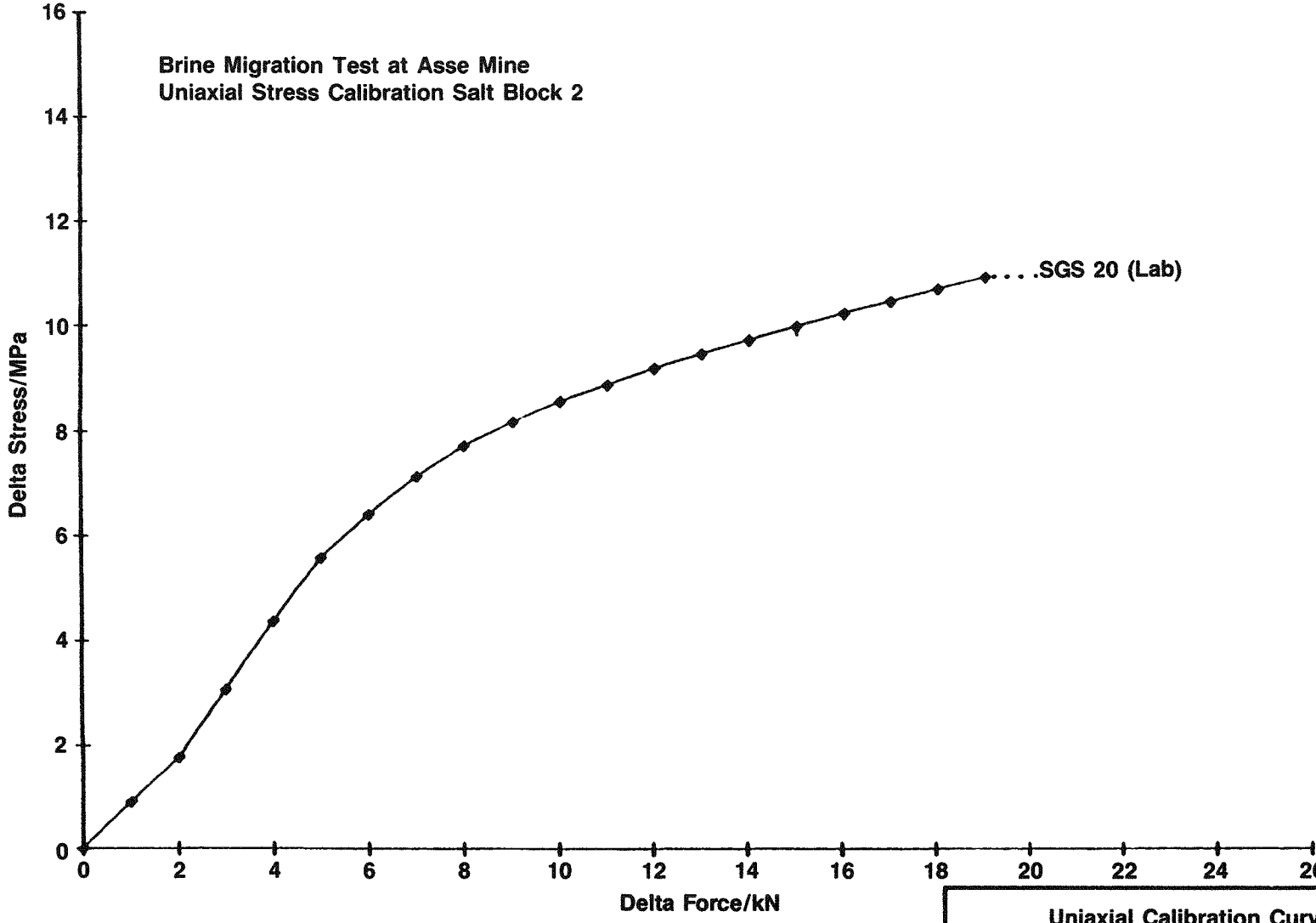

Uniaxial Calibration Curve in Large Salt Block 2, Gage No. 20 (Lab) as Reference Stress Meter

Figure 6-40

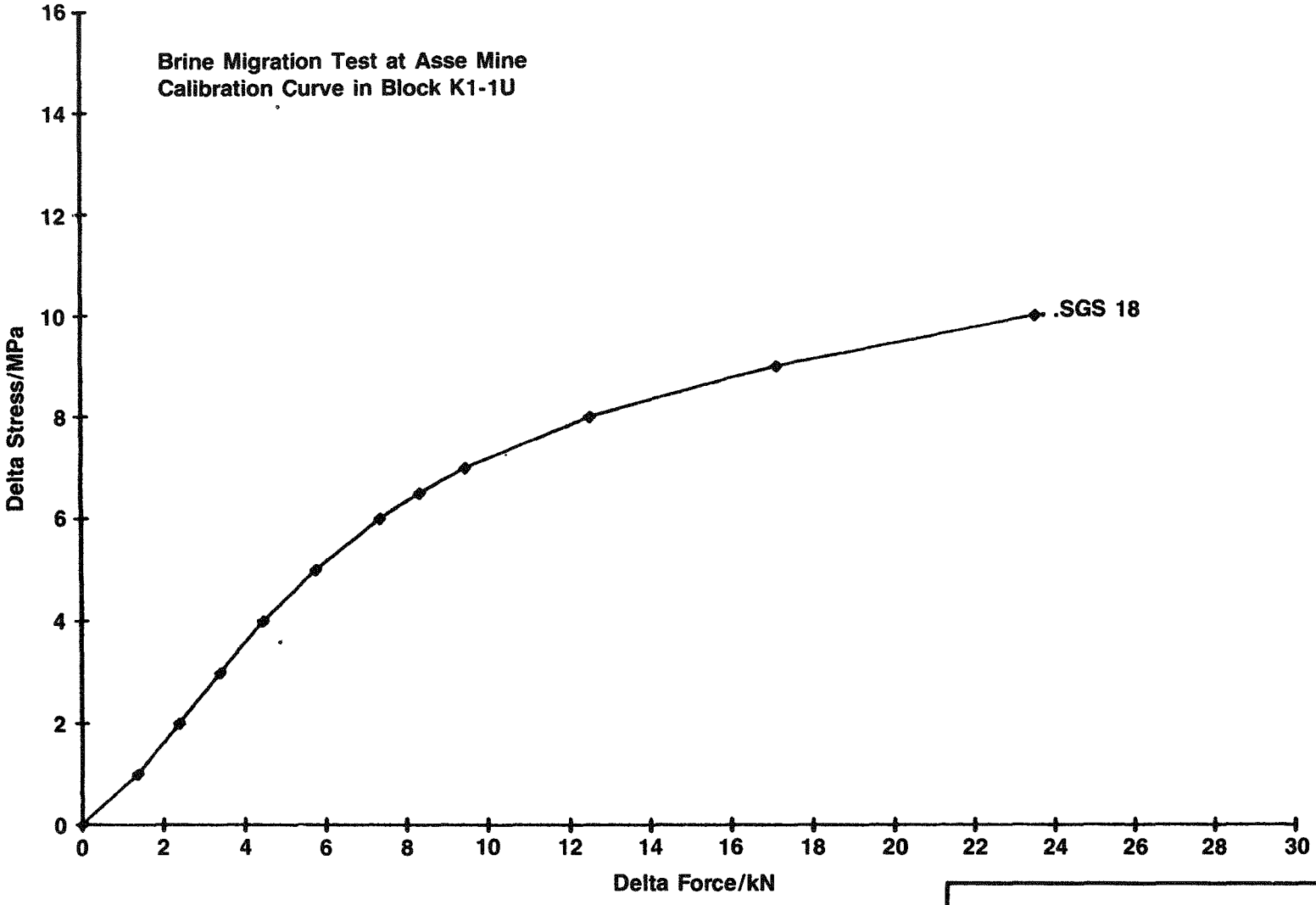

Uniaxial Calibration Curve
in Small Salt Block, Gage No. 18

Figure 6-41

Table 6-35. Radial Stress (Gloetzl Cell) Measurements (in Bars) in Central Borehole for Test Site 2 With Azimuth of 0 Degree

Date	Cell Location		
	Lower	Central	Upper
5/24/83	0.20	0.30	1.00
6/1/83	0.70	1.50	1.50
7/5/83	1.60	2.80	1.40
8/3/83	1.80	3.00	1.10
9/6/83	2.00	2.80	0.70
10/4/83	2.40	3.00	0.70
11/8/83	2.50	3.00	0.50
12/5/83	2.55	2.90	0.50
1/9/84	2.60	3.00	0.40
2/6/84	2.60	3.00	0.45
3/5/84	2.60	3.00	0.40
4/2/84	2.45	3.00	0.40
5/2/84	2.45	3.00	0.50
6/4/84	2.40	3.00	0.50
7/17/84	2.40	3.10	0.60
8/9/84	2.40	3.00	0.60
9/10/84	2.70	3.10	0.70
10/1/84	2.75	3.10	0.80
11/12/84	2.60	3.15	0.80
12/10/84	2.60	3.10	0.80
1/7/85	2.60	3.00	0.85
2/4/85	2.40	3.00	0.85
3/4/85	2.00	3.00	0.90
4/15/85	1.00	2.50	0.30
5/14/85	1.00	2.50	0.40
6/14/85	1.00	3.00	0.50
7/15/85	1.00	3.00	0.50
8/14/85	1.00	3.00	0.50
9/23/85	1.00	3.00	0.50

Table 6-36. Radial Stress (Gloetzl Cell) Measurements (in Bars) in Central Borehole for Test Site 2 With Azimuth of 270 Degrees

Date	Cell Location		
	Lower	Central	Upper
5/24/83	2.00	1.20	1.30
6/1/83	2.50	1.50	1.50
7/5/83	3.50	1.60	1.60
8/3/83	3.60	1.40	1.60
9/6/83	3.60	1.10	1.30
10/4/83	3.60	1.00	1.30
11/8/83	3.50	0.90	1.20
12/5/83	3.50	0.85	1.10
1/9/84	3.50	0.80	1.00
2/6/84	3.40	0.70	1.00
3/5/84	3.30	0.60	1.00
4/2/84	3.25	0.60	0.90
5/2/84	3.20	0.60	0.80
6/4/84	3.20	0.60	0.80
7/17/84	3.10	0.60	0.90
8/9/84	3.00	0.60	0.90
9/10/84	2.80	0.60	0.80
10/1/84	2.30	0.60	0.80
11/12/84	1.80	0.50	0.70
12/10/84	1.90	0.50	0.70
1/7/85	1.20	0.50	0.70
2/4/85	1.00	0.50	0.60
3/4/85	0.80	0.50	0.60
4/15/85	0.00	0.50	0.50
5/14/85	0.00	0.50	0.50
6/14/85	0.00	0.50	0.50
7/15/85	0.00	0.50	0.50
8/14/85	0.00	0.50	0.50
9/23/85	0.00	0.50	0.50

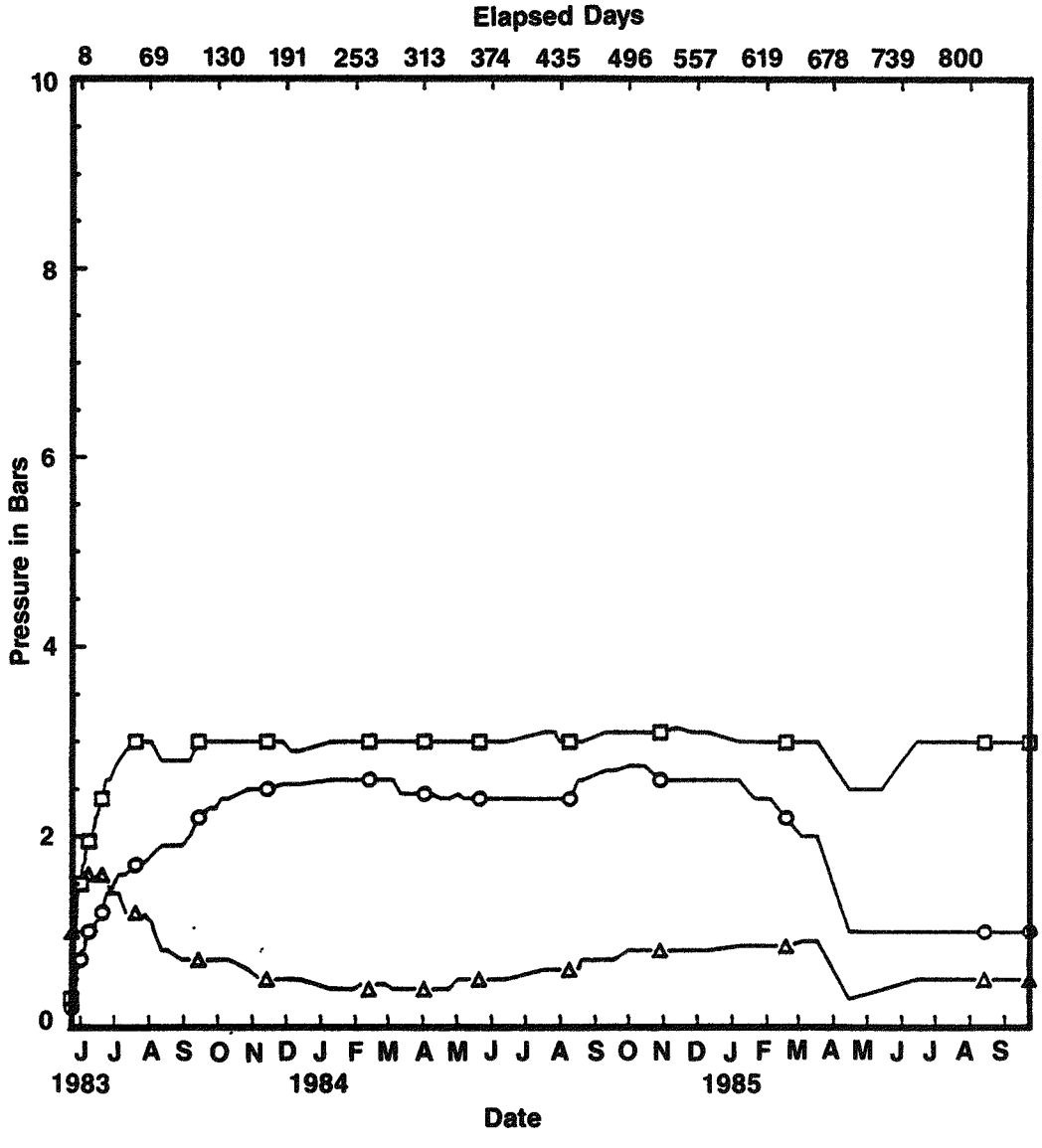

LEGEND:
Azimuth 0°
Radial Cell Location
- ○ Lower
- □ Central
- △ Upper

Radial Stress (Gloetzl Cell) in Central Borehole Versus Time for Test Site 2, Azimuth 0 Degree

Figure 6-42

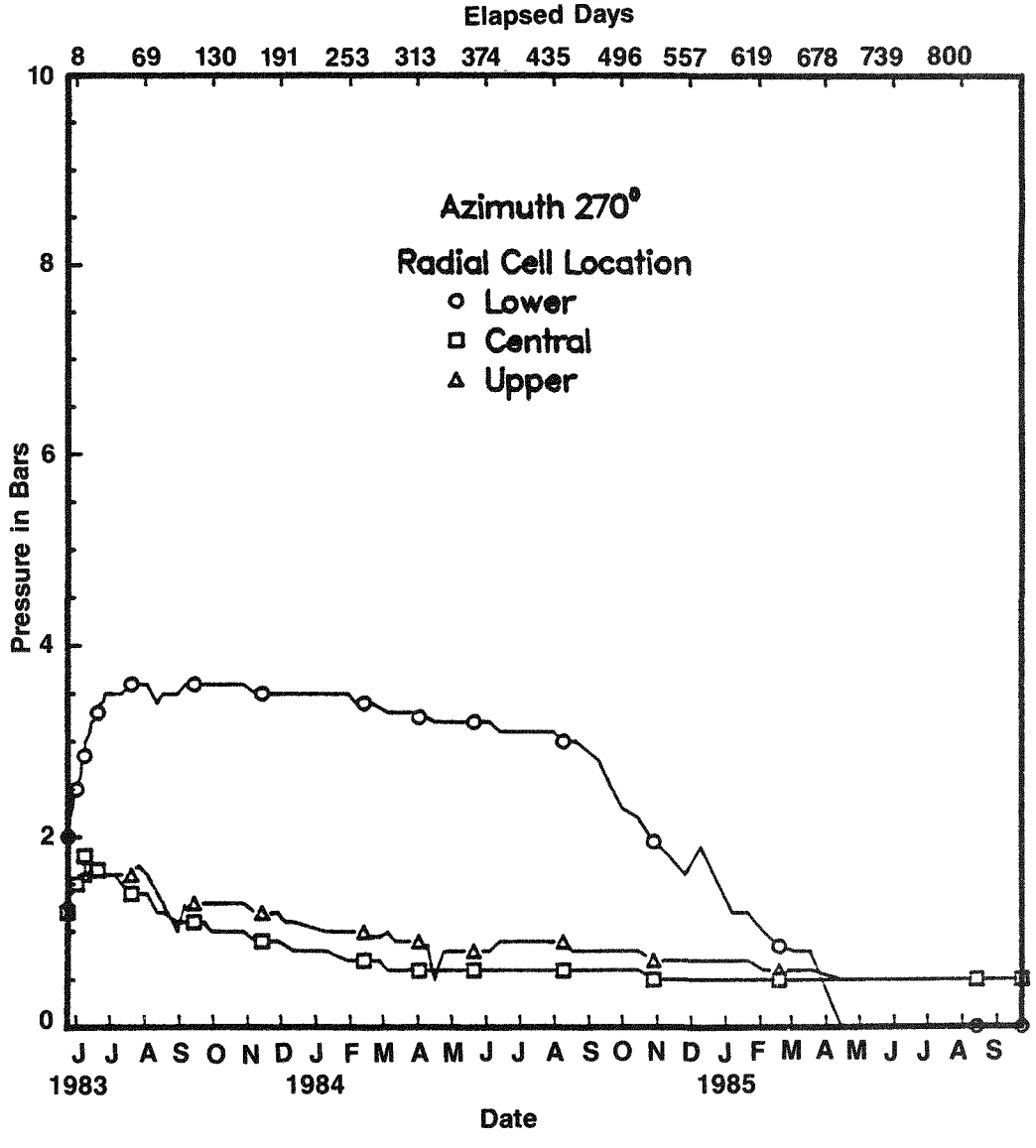

LEGEND:
Azimuth 270°
Radial Cell Location
- **Lower**
- **Central**
- **Upper**

Radial Stress (Gloetzl Cell) in Central Borehole Versus Time for Test Site 2, Azimuth 270 Degrees

Figure 6-43

6.5.3.2 Conditions at 2.2-m (7.2-ft) Radius

Tables 6-37 and 6-38 respectively list the radial and tangential salt pressure measured at test site 2 at a radius of 2.2 m (7.2 ft). The corresponding plots of the time-dependent variations of the stresses are presented in Figures 6-44 and 6-45. These flat cell (Gloetzl) measurements are provided without corrections for the outputs. The maximum radially induced stress at 2.2 m (7.2 ft) was expected to occur 10 days after start of heating. With exception of one flat cell (located at azimuth 270 degrees), the cells' reaction was delayed, probably due to differences in the installation techiques. Unfortunately, five out of the six flat cells installed failed 500 days after heating was started in test site 2. A possible cause may be that mercury penetrated the grain boundaries of the steel plates, causing them to become brittle and leading to failures by cracking. This will be investigated in the posttest phase.

The following observations were made for the strain-gaged stress meters. (Figures 6-46 and 6-47 show the electrical output of the stress in volts. Tables 6-39 and 6-40 give the measurements.)

1. The radial stresses at 2.2 m (7.2 ft) from the heater centerline increased rapidly during the early period of heating and then relaxed gradually as expected. Calculated stress changes for the total test period are given in Figure 6-48 for test site 2. To convert the output reading of this gage, calibration results from a small salt cube were used. The maximum radial stress change at this location is about 8 MPa (1,160 psi).

2. The tangential stresses at 2.2 m (7.2 ft) from the heater centerline also increased rapidly initially, but at a lower rate, followed by a gradual relaxation. The tangential stress increases are generally lower than the radial stress increases. It should be noted that the strain-gaged stress meters are very sensitive to small variations of the stress field in the surrounding rock mass. This can be readily observed by the immediate response to a small increase in borehole power input (300 W) on September 12, 1983 (109 days after start-up of heating). The radial stresses increased and the tangential stresses decreased, and then the stresses returned to normal.

6.6 FLOOR CRACKING

The pretest rock mechanical calculations performed indicate that tensile stresses would occur in the test room floor down to a depth of 1 m (3.28 ft). They were expected to occur within the first 2 months of running the tests. At test sites 1 and 2, small cracks were found in the floor during the first and second months of heating. The largest crack has a length of about 2 m (6.6 ft) and a vertical depth of 0.9 m (3.0 ft) measured at the top of the borehole. To gather information on the behavior of crack development, two additional horizontal extensometers were installed on the floor near the sliding shield systems at test sites 3 and 4 before the start-up of these tests. Floor crack growth measurements for test sites 3 and 4 are listed in

Table 6-37. Radial Salt Pressure (Gloetzl Cell) Measurements (in Bars) for Test Site 2 at a Radius of 2.2 m (7.2 ft)

Date	Azimuth in Degrees		
	0	135	270
5/24/83	1.20	0.20	1.30
6/1/83	1.20	0.20	12.90
7/5/83	1.40	0.20	15.20
8/3/83	4.40	0.20	20.20
9/6/83	5.70	0.20	31.00
10/4/83	10.70	0.20	47.00
11/8/83	17.00	0.20	68.00
12/5/83	23.60	0.20	74.00
1/9/84	35.20	0.30	96.50
2/6/84	45.00	0.50	98.70
3/5/84	47.00	0.60	97.00
4/2/84	49.00	0.65	95.90
5/2/84	47.50	0.70	96.70
6/4/84	47.50	0.70	96.50
7/17/84	48.20	0.70	96.00
8/9/84	51.50	3.50	180.00
9/10/84	52.50	0.70	0.50
10/1/84	54.00	0.70	0.50
11/12/84	53.50	0.70	0.50
12/10/84	52.50	0.70	0.60
1/7/85	52.00	0.70	0.50
2/4/85	49.00	0.70	0.60
3/4/85	0.85	0.70	0.60
4/15/85	1.50	0.50	0.50
5/14/85	1.60	0.50	0.50
6/14/85	0.00	0.50	0.50
7/15/85	0.00	0.50	0.50
8/14/85	0.00	0.50	0.50
9/23/85	0.00	0.50	0.50

Table 6-38. Tangential Salt Pressure (Gloetzl Cell) Measurements (in Bars) for Test Site 2 at a Radius of 2.2 m (7.2 ft)

Date	Azimuth in Degrees		
	0	135	270
5/24/83	0.20	0.20	0.20
6/1/83	0.30	0.20	0.30
7/5/83	0.20	0.20	0.20
8/3/83	0.40	0.60	0.30
9/6/83	0.70	6.40	0.60
10/4/83	0.90	21.80	1.90
11/8/83	1.40	29.00	54.00
12/5/83	1.30	32.80	62.00
1/9/84	2.00	37.50	52.00
2/6/84	4.80	42.30	69.50
3/5/84	6.50	0.80	75.00
4/2/84	8.70	0.60	73.10
5/2/84	10.00	0.60	77.20
6/4/84	10.40	0.60	71.50
7/17/84	12.00	1.40	70.00
8/9/84	1.00	0.60	84.00
9/10/84	0.20	0.60	46.00
10/1/84	0.20	0.60	8.50
11/12/84	0.30	0.60	19.40
12/10/84	0.30	0.60	19.50
1/7/85	0.30	0.60	12.20
2/4/85	0.30	0.60	10.40
3/4/85	0.30	0.60	6.50
4/15/85	0.00	0.50	7.10
5/14/85	0.00	0.50	7.00
6/14/85	0.00	0.50	9.00
7/15/85	0.00	0.50	7.00
8/14/85	0.00	0.50	6.50
9/23/85	0.00	0.50	7.00

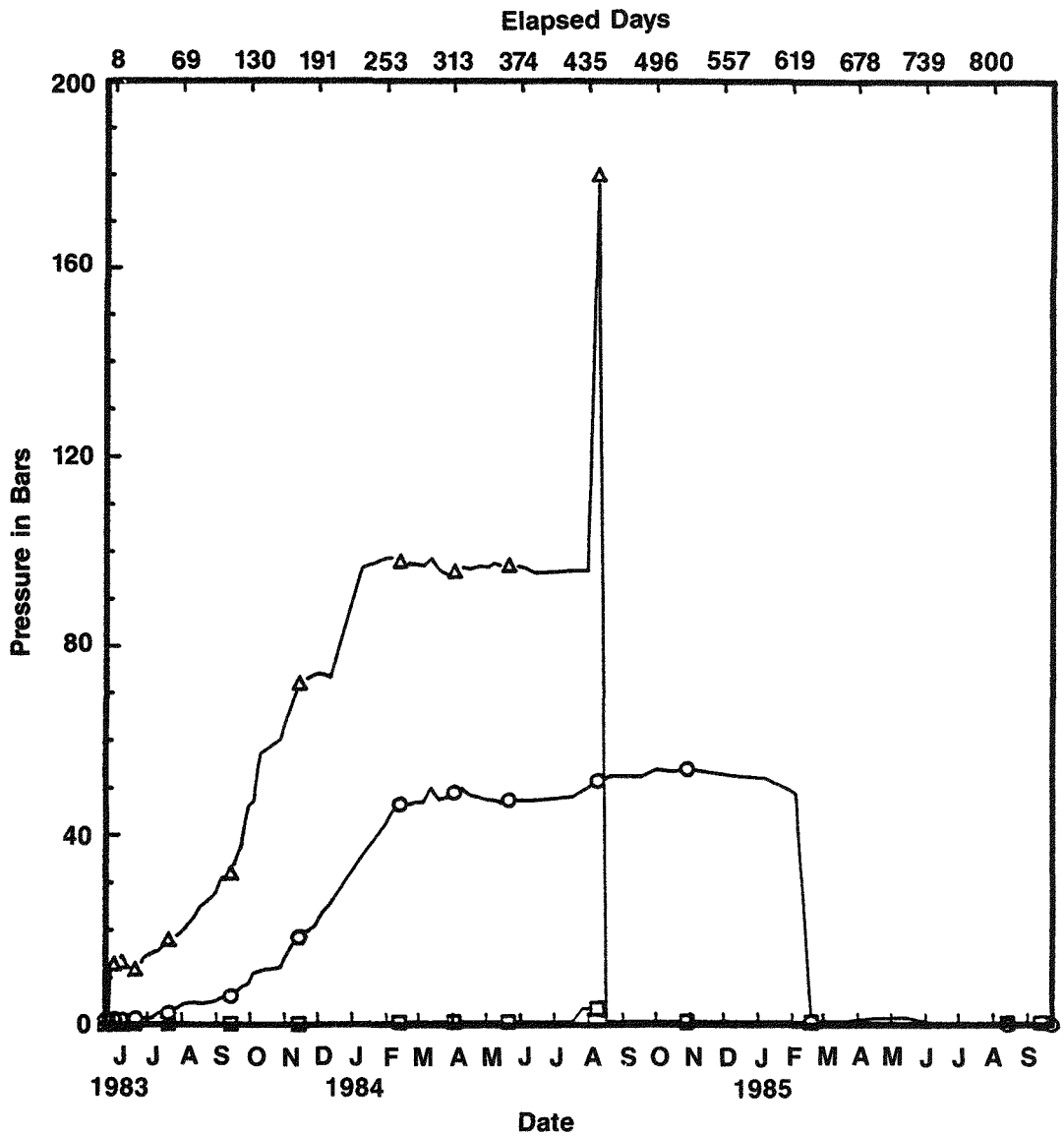

LEGEND:

- ○ 0° Azimuth
- □ 135° Azimuth
- △ 270° Azimuth

Radial Salt Pressure (Gloetzl Cell) Versus Time for Test Site 2

Figure 6-44

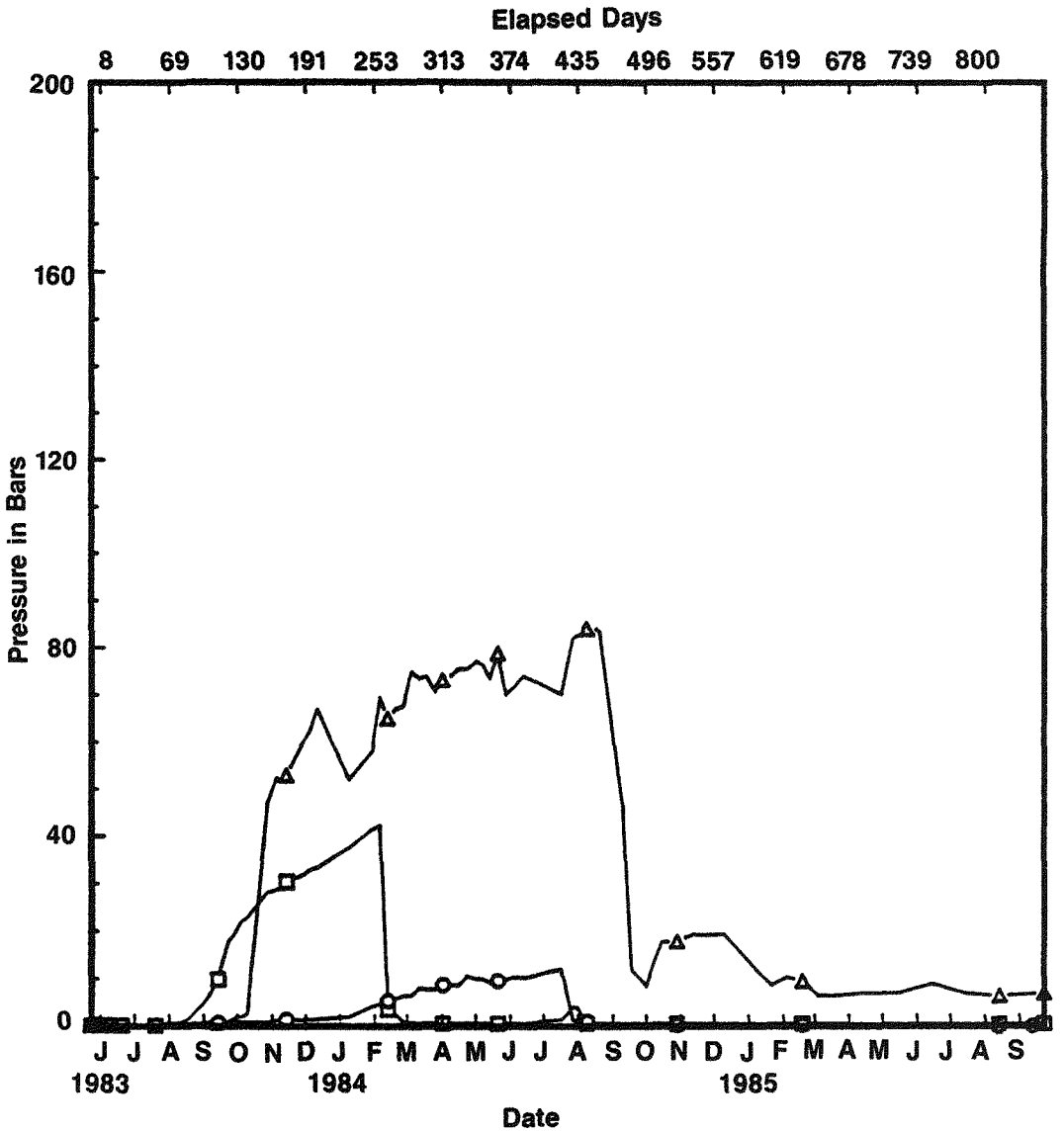

LEGEND:

- ○ 0° Azimuth
- □ 135° Azimuth
- △ 270° Azimuth

Tangential Salt Pressure (Gloetzl Cell) Versus Time for Test Site 2

Figure 6-45

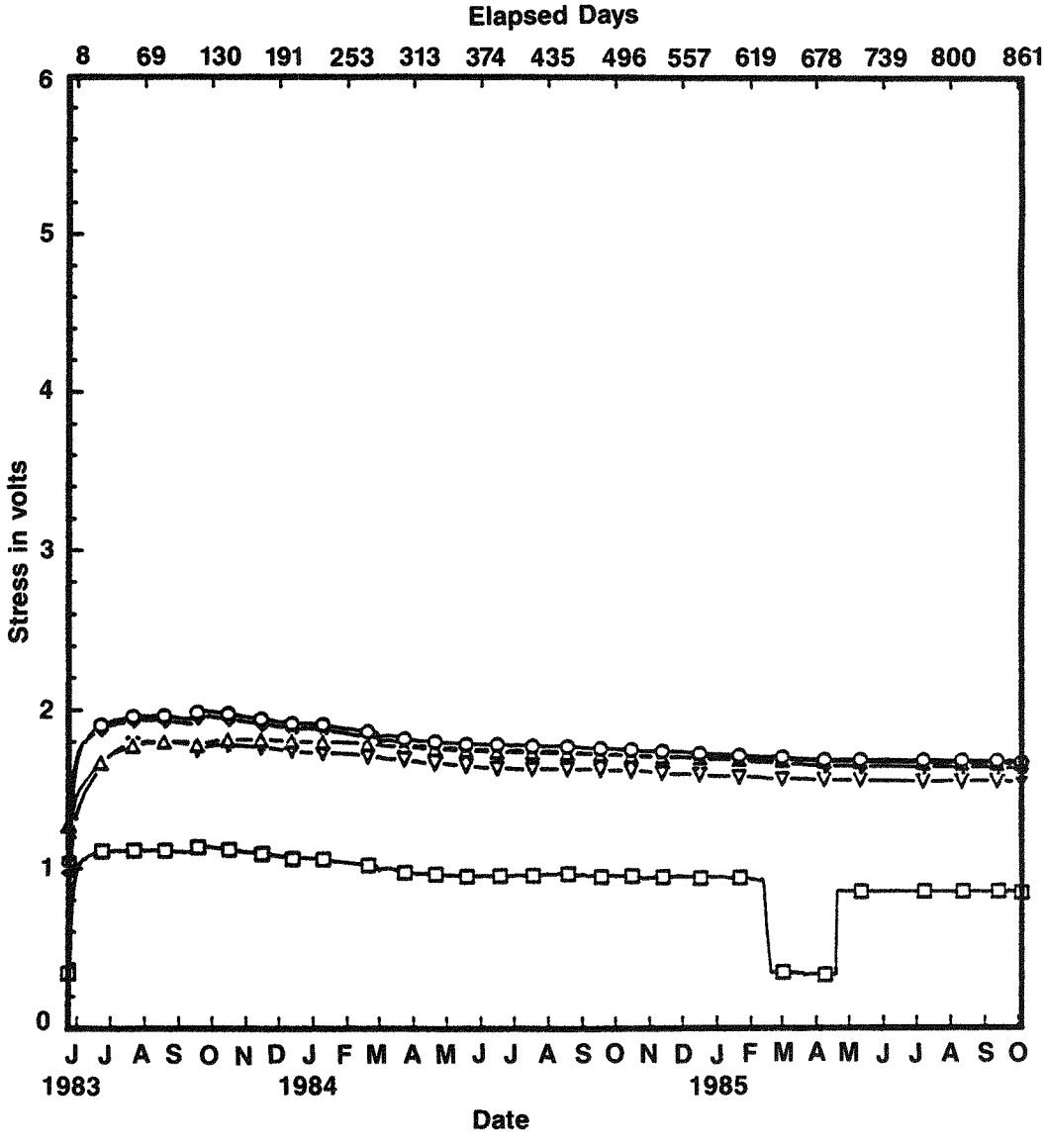

LEGEND:

- ○ Azimuth—90°
- □ Azimuth—180°
- △ Azimuth—180°
- ◇ Azimuth—315°
- ▽ Azimuth—315°

Stress Measurement Versus Time for Test Site 1

Figure 6-46

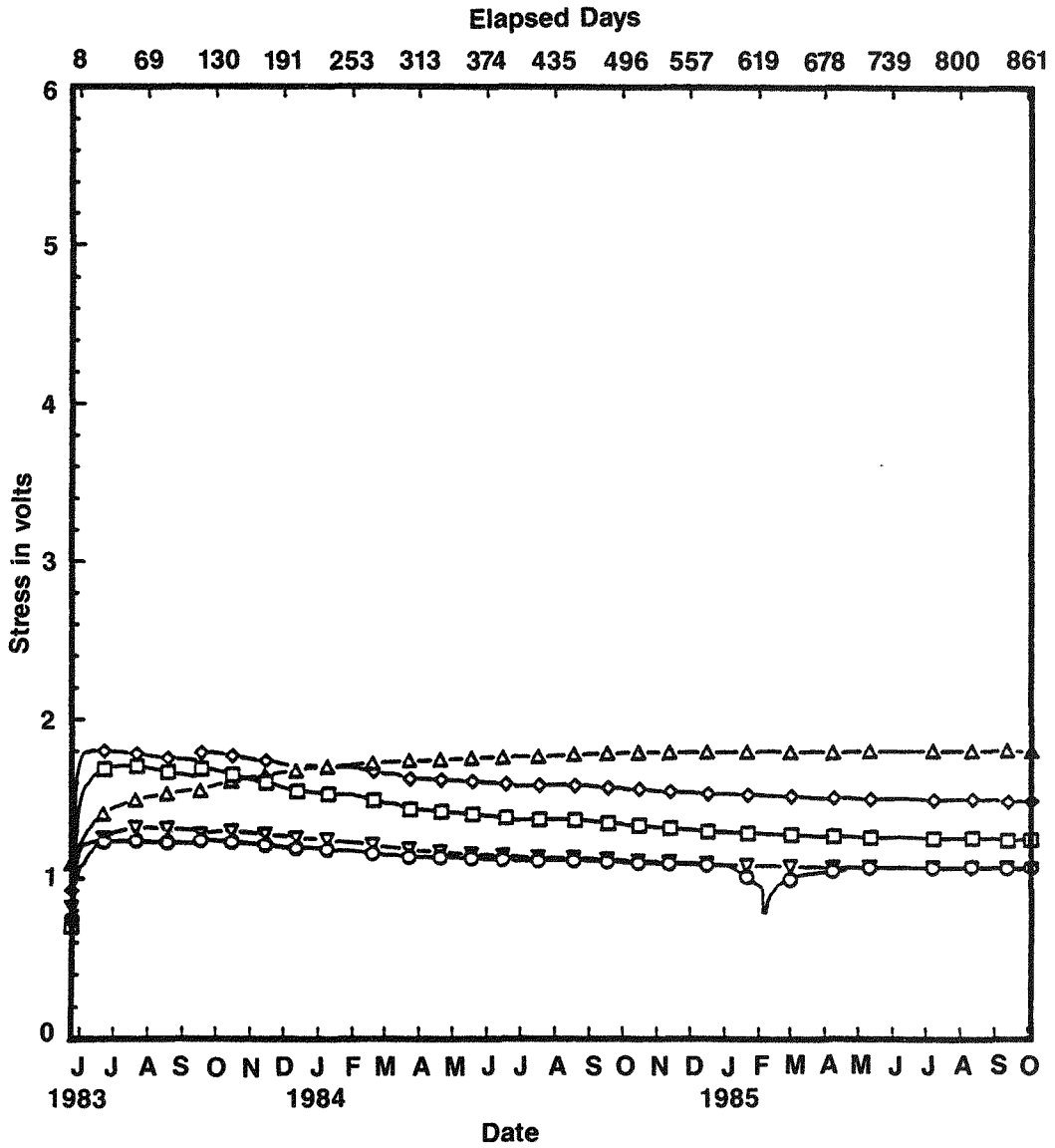

LEGEND:

- ○ Azimuth—90°
- □ Azimuth—180°
- △ Azimuth—180°
- ◇ Azimuth—315°
- ▽ Azimuth—315°

Stress Measurement
Versus Time for Test Site 2

Figure 6-47

Table 6-39. Stress Readings (in Volts) for Test Site 1

Date	Elapsed Days	Azimuth in Degrees				
		90	180	180	315	315
5/24/83	0	1.04	0.34	1.28	0.98	1.03
6/23/83	30	1.91	1.11	1.67	1.88	1.66
7/23/83	60	1.96	1.12	1.78	1.93	1.79
8/22/83	90	1.96	1.11	1.80	1.93	1.80
9/21/83	120	1.99	1.14	1.79	1.96	1.76
10/21/83	150	---	---	---	---	---
11/20/83	180	1.94	1.09	1.81	1.91	1.76
12/20/83	210	1.91	1.07	1.80	1.88	1.73
1/19/84	240	---	---	---	---	---
2/18/84	270	1.86	1.02	1.78	1.83	1.71
3/19/84	300	1.82	0.98	1.77	1.79	1.69
4/18/84	330	1.80	0.97	1.75	1.77	1.66
5/18/84	360	1.78	0.95	1.75	1.75	1.65
6/17/84	390	---	---	---	---	---
7/17/84	420	1.77	0.96	1.73	1.74	1.63
8/16/84	450	1.77	0.97	1.73	1.74	1.63
9/15/84	480	1.76	0.95	1.72	1.72	1.63
10/15/84	510	1.75	0.96	1.71	1.72	1.62
11/14/84	540	1.74	0.95	1.71	1.70	1.61
12/14/84	570	1.73	0.95	1.70	1.70	1.60
1/13/85	600	1.72	0.94	1.70	1.68	1.59
2/12/85	630	1.71	0.94	1.69	1.67	1.57
3/13/85	660	1.70	0.35	1.68	1.66	1.57
4/12/85	690	1.68	0.32	1.68	1.65	1.56
5/12/85	720	1.69	0.86	1.67	1.64	1.56
6/11/85	750	---	---	---	---	---
7/11/85	780	1.68	0.86	1.67	1.64	1.55
8/10/85	810	1.68	0.86	1.67	1.64	1.55
9/9/85	840	1.68	0.85	1.67	1.64	1.56

Table 6-40. Stress Readings (in Volts) for Test Site 2

Date	Elapsed Days	Azimuth in Degrees				
		90	180	180	315	315
5/24/83	0	0.75	0.70	1.10	0.93	0.82
6/23/83	30	1.23	1.69	1.41	1.80	1.26
7/23/83	60	1.24	1.71	1.50	1.79	1.32
8/22/83	90	1.23	1.67	1.54	1.76	1.31
9/21/83	120	1.24	1.69	1.57	1.80	1.28
10/21/83	150	---	---	---	---	---
11/20/83	180	1.21	1.60	1.66	1.74	1.27
12/20/83	210	1.19	1.55	1.69	1.71	1.25
1/19/84	240	---	---	---	---	---
2/18/84	270	1.16	1.49	1.73	1.67	1.21
3/19/84	300	1.14	1.44	1.74	1.63	1.19
4/18/84	330	1.13	1.42	1.75	1.62	1.17
5/18/84	360	1.13	1.40	1.76	1.61	1.15
6/17/84	390	---	---	---	---	---
7/17/84	420	1.12	1.37	1.77	1.59	1.13
8/16/84	450	1.12	1.37	1.78	1.59	1.13
9/15/84	480	1.11	1.35	1.79	1.58	1.12
10/15/84	510	1.10	1.34	1.79	1.56	1.11
11/14/84	540	1.10	1.32	1.80	1.55	1.11
12/14/84	570	1.09	1.30	1.80	1.54	1.10
1/13/85	600	1.05	1.29	1.80	1.53	1.09
2/12/85	630	0.92	1.28	1.80	1.52	1.09
3/13/85	660	1.03	1.27	1.80	1.52	1.08
4/12/85	690	1.05	1.27	1.80	1.51	1.07
5/12/85	720	1.07	1.26	1.81	1.50	1.07
6/11/85	750	---	---	---	---	---
7/11/85	780	1.07	1.25	1.81	1.50	1.07
8/10/85	810	1.08	1.25	1.81	1.50	1.07
9/9/85	840	1.07	1.25	1.81	1.49	1.07

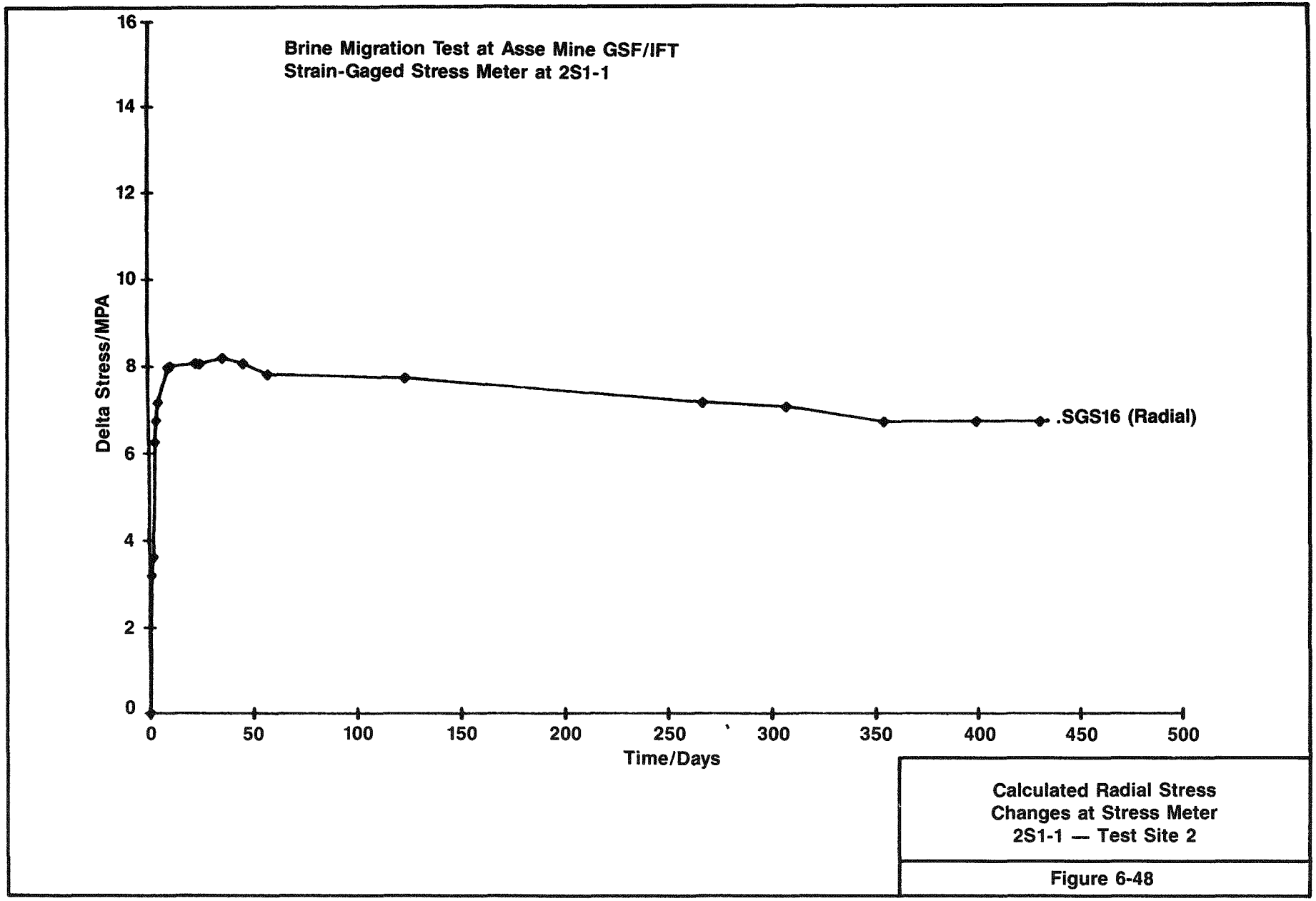

Calculated Radial Stress Changes at Stress Meter 2S1-1 — Test Site 2

Figure 6-48

Tables 6-41 and 6-42, respectively. The measured deformation curves representing floor strain at test sites 3 and 4 are shown in Figures 6-49 and 6-50. Extensometers xE3 and xE4 measure the east-west and north-south directions respectively. During the period of 660 days of heating, the curves do not indicate any unsteady conditions in the crack development. However, small cracks approximately perpendicular to the test room axis were found in the floor at test sites 3 and 4 after about 60 days of heating. These cracks run from the central borehole in radial directions having a detectable length of about 2 m (6.6 ft) and a depth of approximately 1 m (3.28 ft).

6.7 LABORATORY INVESTIGATIONS

After mining the test area, about 65 boreholes were drilled for equipment installation. The boreholes for the test assembly (C-boreholes) and for three field probes (T-boreholes) at each test site were obtained by core drilling. Several samples were taken from each borehole to determine the chemical-mineralogical composition and the water content of the salt.

6.7.1 Chemical-Mineralogical Examination

After retrieving the samples out of the boreholes, the samples were protected from air humidity by sealing them immediately in gas-tight plastic bags. They were brought to the laboratory for chemical and water content analysis. Table 6-43 gives a summary of the results obtained in 1984.

The data obtained for test sites 1 through 3 are comparable to those normally obtained from the main halite ($Na_2\beta$) at Asse. Here, the average water content is known to be about 0.25 wt %. The water content analyzed for test site 4 is much lower with only 0.14 wt %. A reason for this could be that the boundary to the pure halite (Na_2S) is only 2 to 3 m (6.6 to 9.8 ft) from this test site and that there is a certain transition zone between the main halite formation and the pure halite layer characterized by a decreasing water content. Table 6-43 shows that a higher water content corresponds with a higher concentration of anhydrite and polyhalite. Since only polyhalite ($K_2MgCa_2CSO_4 \cdot 2H_2O$) contains crystalline water (6.0 wt %), it can be concluded that most of the water found in the samples is due to this mineral. However, there is a small amount of water in several samples that cannot be due to the polyhalite, because their total water content is higher than the 6.0 wt % of polyhalite. It is assumed that this water is adsorbed at the salt crystal boundaries. If the crystalline water of polyhalite is only released at temperatures higher than 235°C (455°F) (Jockwer, 1981), then only the smaller content of adsorbed water would migrate toward the heat source in these experiments.

6.7.2 Rock Mechanics Laboratory Tests

Geomechanical laboratory tests were conducted with samples from main halite $Na_2\beta$ cores taken from core drills in the brine migration test field. The first test matrix related as well to elastic material properties and

Table 6-41. Floor Crack Growth Measurements (mm) for Test Site 3

Date	Elapsed Days	Longitudinal	Transverse
12/15/83	0	0.51	-0.25
1/14/84	30	---	---
2/13/84	60	2.04	3.22
3/14/84	90	---	---
4/13/84	120	2.25	3.80
5/13/84	150	2.33	3.99
6/12/84	180	2.32	4.14
7/12/84	210	2.35	4.22
8/11/84	240	2.37	4.24
9/10/84	270	---	---
10/10/84	300	2.44	4.33
11/9/84	330	2.48	4.43
12/9/84	360	2.46	4.44
1/8/85	390	2.49	4.51
2/7/85	420	2.49	4.57
3/8/85	450	---	---
4/7/85	480	2.50	4.61
5/7/85	510	2.50	4.65
6/6/85	540	2.50	4.64
7/6/85	570	2.51	4.70
8/5/85	600	2.53	4.72
9/4/85	630	2.53	4.70
10/4/85	660	2.54	4.89

Table 6-42. Floor Crack Growth Measurements (mm) for Test Site 4

Date	Elapsed Days	Longitudinal	Transverse
12/15/83	0	0.14	---
1/14/84	30	---	---
2/13/84	60	1.28	3.50
3/14/84	90	---	---
4/13/84	120	1.49	4.28
5/13/84	150	1.58	4.55
6/12/84	180	1.60	4.75
7/12/84	210	1.64	4.91
8/11/84	240	1.68	4.92
9/10/84	270	---	---
10/10/84	300	1.76	5.01
11/9/84	330	1.78	5.14
12/9/84	360	1.79	5.24
1/8/85	390	1.81	5.32
2/7/85	420	1.83	5.40
3/8/85	450	---	---
4/7/85	480	1.82	5.41
5/7/85	510	1.84	5.44
6/6/85	540	1.83	5.41
7/6/85	570	1.85	5.46
8/5/85	600	1.86	5.42
9/4/85	630	1.87	5.43
10/4/85	660	1.87	5.45

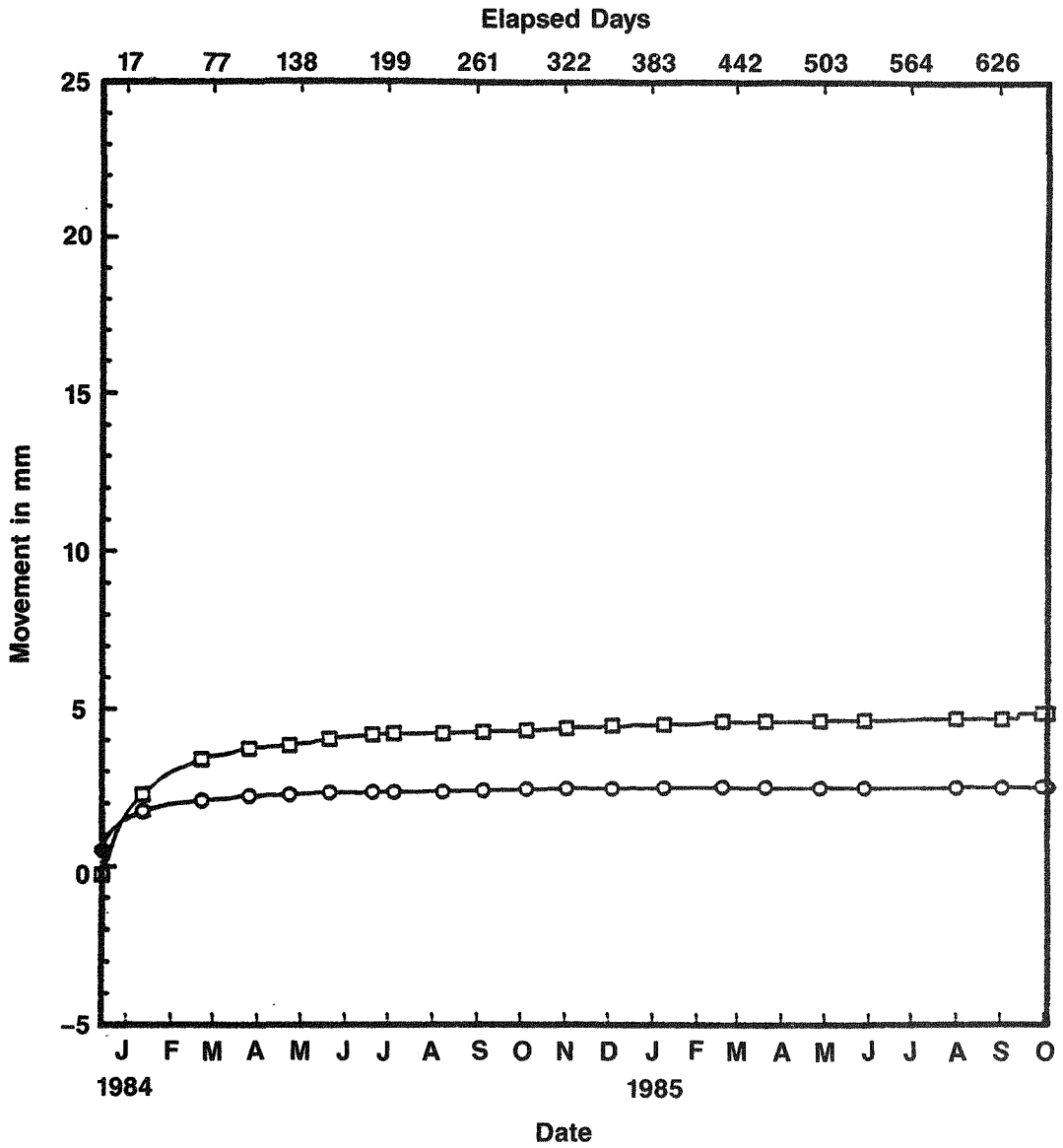

LEGEND:
- ○ 3E3—Longitudinal
- □ 3E4—Transverse

Floor Surface Crack Growth Measurements for Test Site 3

Figure 6-49

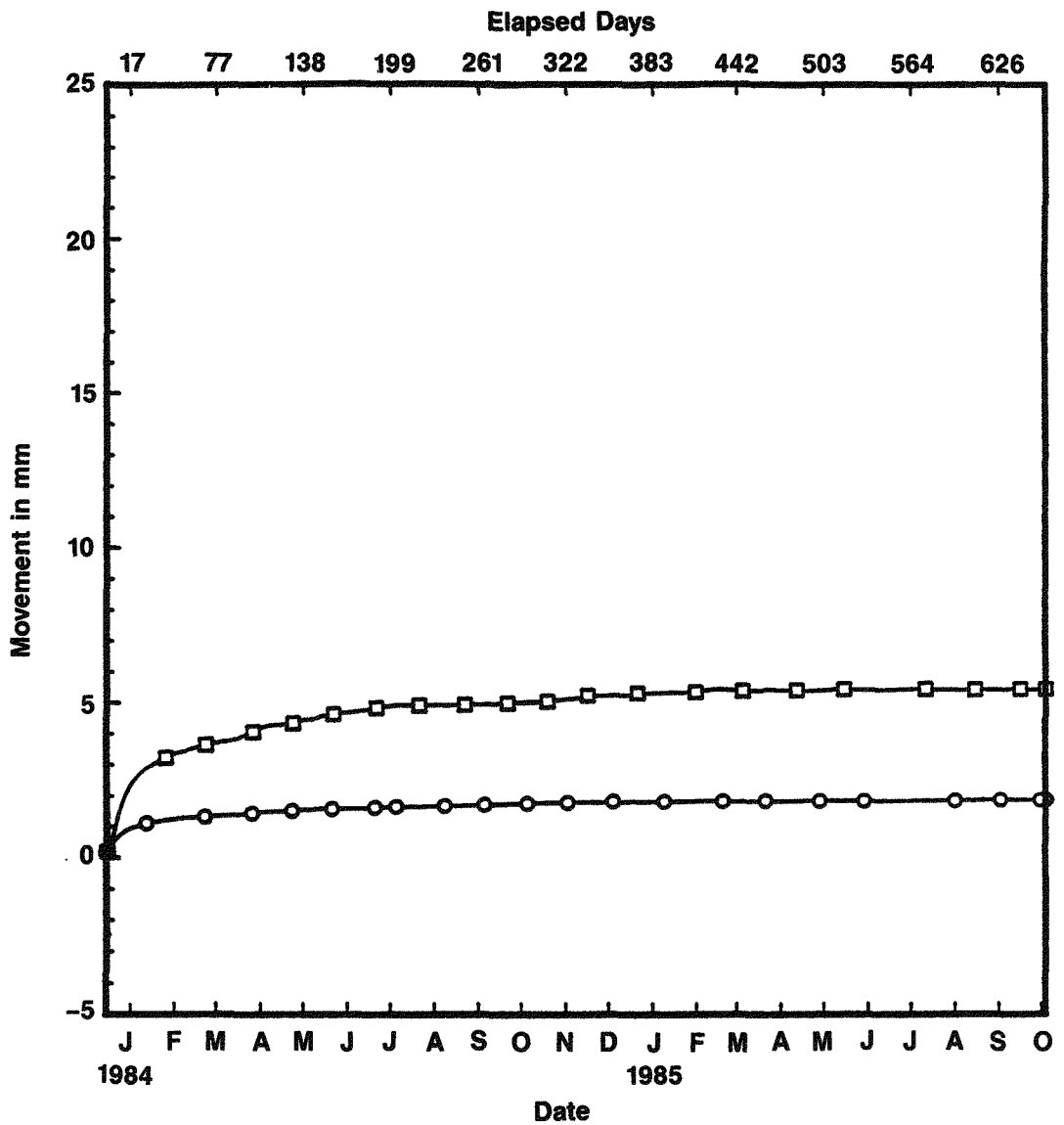

LEGEND:
○ 4E3—Longitudinal
□ 4E4—Transverse

Floor Surface Crack Growth Measurements for Test Site 4

Figure 6-50

Table 6-43. Average Mineralogical Composition and Water Content of Core Samples

Test Site	Borehole	Mineralogical Component (Wt %) Halite	Polyhalite	Anhydrite	Total Water Content (Wt %)	Adsorbed Water (Wt %)
1	1C	94.99 ± 5.3	2.93 ± 1.43	2.58 ± 4.17	0.23 ± 0.22	0.05
	1T1	94.0 ± 6.6	3.27 ± 2.88	2.73 ± 4.15	0.22 ± 0.17	0.02
	1T2	96.58 ± 2.87	2.95 ± 2.34	0.47 ± 0.77	0.28 ± 0.27	0.10
	1T3	92.47 ± 7.03	3.01 ± 1.48	4.52 ± 5.80	0.21 ± 0.10	0.03
2	2C	95.13 ± 4.88	4.12 ± 3.86	0.75 ± 1.18	0.23 ± 0.21	-
	2T1	92.85 ± 5.81	6.68 ± 5.22	0.47 ± 0.90	0.44 ± 0.35	0.04
	2T2	93.01 ± 7.32	6.28 ± 5.77	0.71 ± 2.04	0.31 ± 0.25	-
	2T3	93.41 ± 8.30	3.52 ± 2.56	1.77 ± 3.09	0.20 ± 0.15	-
3	3C	94.85 ± 2.77	2.90 ± 2.8	2.20 ± 2.02	0.18 ± 0.18	0.01
	3T1	94.13 ± 3.68	2.44 ± 0.63	3.43 ± 3.45	0.13 ± 0.04	-
	3T2	94.99 ± 3.39	2.26 ± 1.48	2.85 ± 1.97	0.16 ± 0.11	0.02
	3T3	94.87 ± 5.36	4.10 ± 3.23	1.11 ± 2.26	0.26 ± 0.24	0.01
4	4C	95.73 ± 3.62	1.88 ± 1.41	2.34 ± 2.81	0.12 ± 0.10	0.01
	4T1	96.16 ± 2.21	2.07 ± 1.24	1.97 ± 1.30	0.14 ± 0.14	0.02
	4T2	95.26 ± 4.63	2.33 ± 1.95	2.41 ± 3.06	0.16 ± 0.11	0.02
	4T3	92.00 ± 9.68	2.52 ± 1.98	5.48 ± 7.99	0.13 ± 0.09	-

uniaxial short-term compressive, tensile, and torsional material data as to time-dependent creep behavior. The matrix consisted of the following:

- Ultrasonic longitudinal and transverse wave velocities used to derive dynamic elastic moduli
- Uniaxial compressive strength from stress-controlled, short-term tests
- Tensile strength orthogonal and parallel to stratification from Brazilian tests (indirect tension)
- Shear strength and modulus of rigidity from torsional shear tests
- Failure envelope according to the theory of Huber and Von Mises, derived from results with different test methods
- Coulomb's failure criterion
- Time-dependent creep properties from two-stage uniaxial creep experiments for three different constant stress levels ($12.7 < \sigma_1 < 15.3$ MPa) ($1{,}843 < \sigma_1 < 2{,}219$ psi) at room temperature (298°F) (25°C) and for the 12.7 MPa (1,843 psi) stress level at temperatures between 323 and 423°F (50 and 150°C) respectively.

The stress exponent n, the energy of activation Q, and the structural coefficient A in the exponential secondary creep law were derived from the creep experiments (Section 6.4.5).

7.0 POSTTEST ACTIVITIES

In August 1985, a Joint U.S./FRG Posttest Plan was finalized. This plan called for obtaining core samples prior to, as well as after, salt field cooldown. It was believed that such cores would be more representative and would exhibit the properties of salt under repository conditions. However, considerable doubt about the viability of obtaining core samples prior to cooldown ("hot coring method") led to the need for a test. Accordingly, on September 10 and 11, 1985, a 110-mm- (4.33-in-) diameter by 5.21-m- (17.1-ft-) long core was obtained 0.6 m (2.0 ft) away from the borehole centerline of Test Site 1. The maximum salt temperature [170°C (338°F)] was as expected at the depth of 4.57 m (15.0 ft) (the midheight of the central borehole heater). The core was obtained in 1.2-m (3.9-ft) lengths and air coring was utilized causing considerable cooling of the salt. For instance, the highest temperature dropped from 170°C (338°F) to 113°C (235°F) immediately after drawing the cores. The cores were considered to be in excellent condition when they were sealed and stored for later tests. However, on the following day, when the cores were removed for inspection and testing they were found to be extensively cracked and could be easily broken by finger pressure. Therefore, the hot coring method for obtaining suitable samples was abandoned.

On October 4, 1985, the phased reduction in electric power to all heaters was started and was completed in seven steps over a period of 1 month. At this time, test site 1 was depressurized and borehole gases and vapors from all the test sites were being circulated through the cold trap. During the first 4 days of cooldown, nothing of note was observed; however, on the following day approximately 20 cm^3 (1.2 in^3) of condensate was collected until the total collected leveled out in November to the following quantities:

Site	Prior to Cooldown	After Cooldown
1	-	1,500 cm^3
2	122 cm^3	1,775 cm^3
3	100 cm^3	725 cm^3
4	135 cm^3	1,320 cm^3

This dramatic inflow of brine after more than 2 years of very little migration has also been observed after cooldown in heater tests at Avery Island and other sites. Thermal cracking of the salt caused by rapid cooling probably released this brine, which could not migrate to the boreholes because of increased impermeability caused by heating, or possibly because recrystallization closed off natural pathways of brine migration. The total collected at test site 3 is obviously in error. The diaphragm pump could not circulate the borehole vapor and gases through the cold trap, probably because salt had crystallized in the spaces between the alumina beads, not allowing the gases to pass through. A true reading cannot be obtained until after the borehole is opened.

In addition, since a seismic monitoring system was installed in the test gallery prior to cooldown, it will be interesting to see if microcracking can be monitored and possibly correlated with changing thermal and mechanical stresses in the field.

After the central test assemblies cooled down to 100°C (212°F), the retrieval of the cobalt-60 sources commenced on October 31, 1985, and the last canister was shipped to the manufacturer on November 26th. The canisters were in excellent condition and showed no signs of corrosion or wear.

The central test assemblies were removed from sites 1, 2, and 4 between November 21 and December 6, 1985. The test assembly in borehole 3 cannot be removed to date. Stronger jacking tools were being prepared for another attempt to break this assembly free. It is believed that this difficulty is the result of pumping urethane elastomer into the seal area to stop leakage from this site. And since this site is a radioactive one, the intense gamma field polymerized this elastomer causing it to become stiff and brittle.

Removal of the test assemblies revealed that the test assemblies were in excellent condition. The Inconel 600-sheathed active sections were completely coated with a black substance believed to be caused by the hydrogen sulfide gas found in Asse salt. The test assembly was covered with dimples caused by salt pressing the alumina beads into the soft but tough Inconel. The dimples were 1 mm (0.04 in) in diameter and about 0.3 mm (0.01 in) deep.

The alumina beads fell back into the boreholes, which appeared to be in excellent condition. Representative samples of the beads and any products of corrosion or scum will be collected for laboratory analyses.

The gases from the test site 1 smelled very bad and very acrid. A sample of the gas was analyzed and found to contain about 3 ppm of hydrogen chloride (HCl) gas as well as other gases. Since this is not a radioactive test site, this HCl is not the result of radiolysis. The gases from the other tests will also be analyzed to look for variances and to determine why HCl was not found in the monthly test samples over the past two years.

All of the posttest coring has been completed. The cores are all 131 mm (5.16 in) in diameter and about 0.5 m (1.6 ft) in length. Most of the cores are in excellent condition and should provide the necessary integrity and strength for comprehensive laboratory tests and analyses. However, the cores obtained closest to the boreholes (5.0 cm [2.0 in]) exhibited thermal cracks and some crumbling. These cores are still expected to provide sufficient intact core for mechanical testing of this salt.

Cores obtained from radioactive test sites 3 and 4 at a radius of 58.3 cm (23.0 in) and 28.3 cm (11.1 in) from the boreholes were of particular interest. Physical appearance and grain structure did not differ to any marked degree from the nonradioactive samples. However, the samples at the radius of 58.3 cm showed an occasional blue-centered crystal, whereas those from the radius of 23 cm (only about 5.0 cm or 2.0 in) from the borehole wall were almost completely dark blue with an occasional yellow crystal.

When the core is removed, it is separated into samples for different tests, specifically for water content, for chemical analyses, and for rock mechanics tests. Chemical analyses include determination of mineralogy (by thin section and by X-ray spectography). Thin sections will also be used to investigate the microstructural aspects such as grain boundaries, microcracks, the nature of fluid content, etc. However, it is not clear at present how to best investigate the effects of radiation, e.g., colloidal sodium.

8.0 FUTURE WORK

At the conclusion of the tests, which were planned to be shut off after at least 2 years of operation (by the end of 1985), additional posttest analyses are to be performed for final data evaluation. A detailed posttest analyses plan (PTAP) was developed in August 1985. Preliminary planning is summarized in the following sections.

8.1 SHUTDOWN AND DISASSEMBLY

Figure 8-1 shows a detailed block diagram of the sequence of activities planned during shutdown and disassembly of the four test sites. The PTAP will include detailed instructions for each step shown in Figure 8-1.

In order to avoid salt cracking, it was decided to reduce the heater power stepwise over 28 days having seven identical reduction phases of 4 days each. It was determined by temperature calculations that the temperature of the central test assembly will have dropped to 100°C at the end of this power reduction phase.

8.2 RETRIEVING OF TEST ASSEMBLY

The cooldown is expected to reduce the compressive loads on the test assembly and thus facilitate removal. The test assembly will be removed by installing jacking screws to push down on the salt surrounding the test assembly. After breaking the assembly free, it will be lifted from the salt, either by a hoist installed in the mine ceiling or by a portable hoist. The caisson will remain installed in the borehole. The assembly will be inspected to determine whether it is encrusted with deposits that may contain significant amounts of moisture. If so, the material will be collected quickly to avoid exchange of water with mine air. Then, the assembly will be protected by sealing the active region in plastic. If desired, parts of the test assembly will be distributed to different corrosion experts in the United States and in the FRG for corrosion investigations.

8.3 RECOVERY OF INSTALLATIONS

The remaining equipment need not be disassembled to satisfy test requirements. However, the heater power control racks, the moisture collection system racks, and the central console containing the data logger will be removed from the test gallery and stored in an underground storage room. It was decided to keep the equipment at the Asse mine because all parts are contaminated by salt dust and would corrode rapidly if brought out of the mine to the surface.

8.4 POSTTEST EVALUATIONS

The primary purpose of this test is to measure brine migration rates, quantities of brine collected, and the chemical constituents of brine in tests simulating the heat and gamma radiation output of conceptual waste packages.

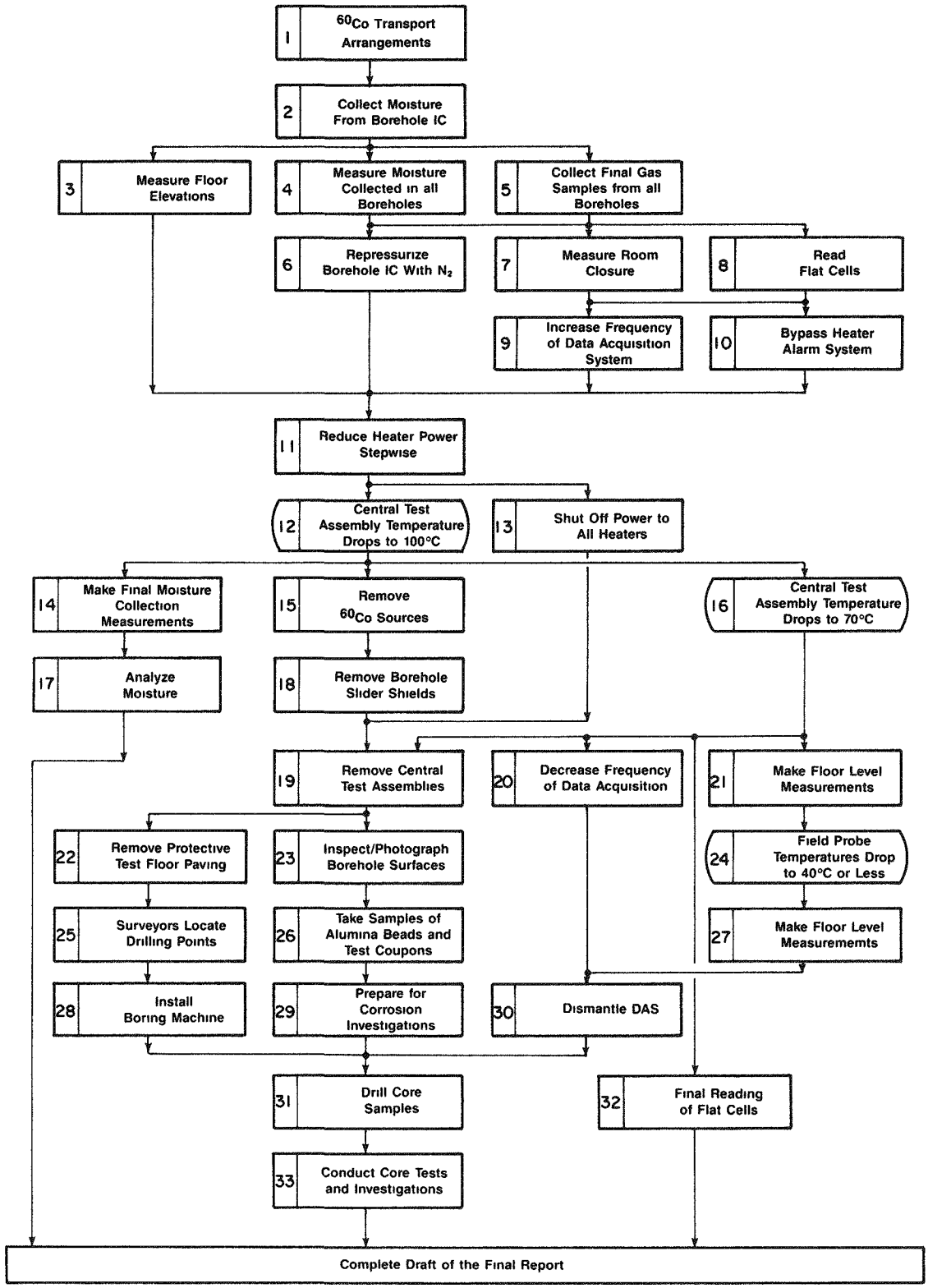

Block Diagram of Posttest Activities

Figure 8-1

These analyses will include a comparison of predicted brine migration (using various models) versus the actual quantities collected during these tests.

Evaluation of the information generated by the posttest activities will be started by observing the condition of the contents of the borehole. The borehole will be observed and photographed. If the alumina beads maintain their annular configuration, attempts should be made to collect bead samples from various locations. It is more likely that the beads will slump into a pile in the hole. In that case, only averaging samples can be taken and analyzed. The borehole walls should be scraped to remove beads and corrosion samples that are attached to the thermocouple cage. Evidence of salt flowing around the beads, salt cracking, dissolution, or other changes should be noted and photographed. Salt samples should be obtained from the borehole bottom.

Figures 8-2 and 8-3 show an overview of boreholes that are to be drilled around the test site for core sampling. Figure 8-3 also identifies types of analyses to be carried out with the samples.

With the caisson still installed in the borehole, it would not be easy to overcore the test site. Instead, cores will be taken adjacent to the borehole, possibly at a slight angle to intersect the borehole wall in the test zone. The objective is to obtain samples of salt from different radial distances and different depths below the floor. The samples are to be analyzed for water content, and for petrographic, rock mechanical, and mineralogical properties, and the results will be compared with those obtained by pretest investigations.

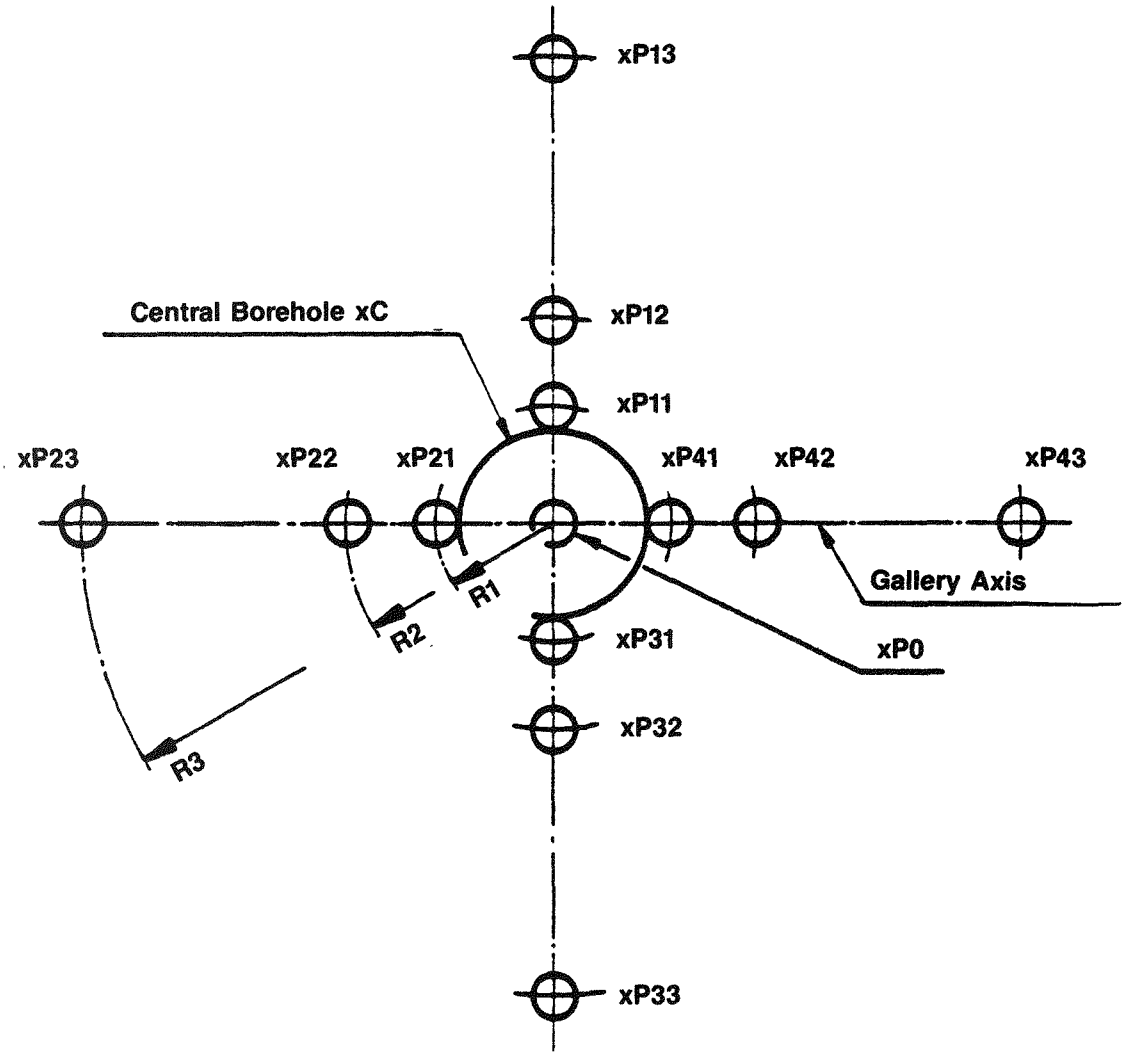

R1 = 283 mm
R2 = 583 mm
R3 = 1283 mm
x = Number of Test Site

Core Borehole
Diameter 131 mm

Overview of Core Drillings at a Single Test Site

Figure 8-2

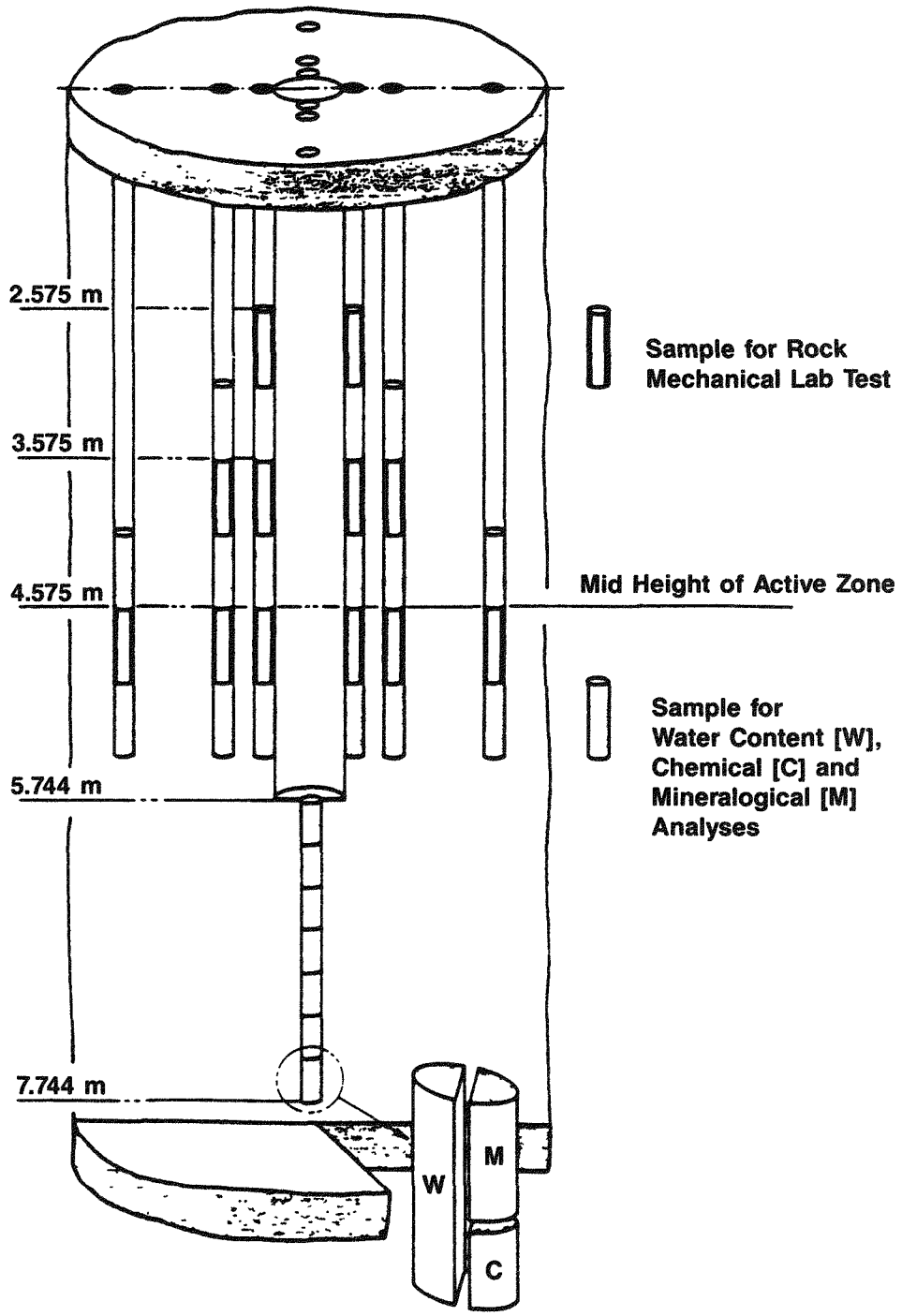

Overview of a Single Test Site Showing Location

Figure 8-3

9.0 REFERENCES

Blankenship, D. A., and R. G. Stickney, 1983. Nitrogen Gas Permeability Tests at Avery Island, ONWI-190(3), prepared by RE/SPEC Inc. for Office of Nuclear Waste Isolation, Battelle Memorial Institute, Columbus, OH.

Jenks, G. H., 1979. Effects of Temperature, Temperature Gradients, Stress, and Irradiation on Migration of Brine Inclusions in a Salt Repository, ORNL-5526, prepared for U.S. Department of Energy by Oak Ridge National Laboratory, Union Carbide Corporation, Oak Ridge, TN.

Jockwer, N., 1981. Studies on the Type and Amount of Water Contained in the Rock Salt of the Zechstein, and Its Release and Migration in the Temperature Field of Buried Radioactive Wastes, GSF-T 119, Gesellschaft für Strahlen- und Umweltforschung mbH München, Braunschweig, FRG.

Office of Nuclear Waste Isolation and Gesellschaft für Strahlen- und Umweltforschung, 1981. Asse Salt Mine Brine Migration Test Program, ONWI-245, GSF-118, Office of Nuclear Waste Isolation, Battelle Memorial Institute, Columbus, OH.

ONWI and GSF, see Office of Nuclear Waste Isolation and Gesellschaft für Strahlen- und Umweltforschung, 1981.

Rothfuchs, T., D. Lübker, A. Coyle, and H. Kalia, 1984. Nuclear Waste Repository Simulation Experiments, Asse Salt Mine, Federal Republic of Germany: Annual Report 1983, BMI/ONWI-539, prepared by Gesellschaft für Strahlen- und Umweltforschung mbH München and Office of Nuclear Waste Isolation for Battelle Memorial Institute, Columbus, OH.

Rothfuchs, T., D. Lübker, A. Coyle, and H. Kalia, 1986. Nuclear Waste Repository Simulation Experiments - Asse Salt Mine, Federal Republic of Germany: Annual Report 1984, BMI/ONWI-616, prepared by Gesellschaft für Strahlen- und Umweltforschung mbH München and Office of Nuclear Waste Isolation, Battelle Memorial Institute, Columbus, OH.

DISTRIBUTION LIST

ACRES INTERNATIONAL CORP
STEWART N. THOMPSON
AEROSPACE CORP
R. L. JOHNSON
KENNETH W. STEPHENS
ALABAMA STATE GEOLOGICAL SURVEY
THORNTON L. NEATHERY
AMARILLO PUBLIC LIBRARY
AMERICAN ROCK WRITING RESEARCH
JOHN NOXON
APPLIED RESEARCH ASSOCIATES
STEVEN WOOLFOLK
ARGONNE NATIONAL LABORATORY
DORLAND E. EDGAR
DOUGLAS F. HAMBLEY
WYMAN HARRISON
WILLIAM METZ
MARTIN SEITZ
MARTIN J. STEINDLER
YU CHIEN YUAN
ARIZONA NUCLEAR POWER PROJECT
HENRY W. RILEY, JR.
ARIZONA STATE UNIVERSITY
PAUL KNAUTH
ARTHUR D. LITTLE INC
CHARLES R. HADLOCK
ATOMIC ENERGY CONSULTANTS
DONALD G. ANDERSON
ATOMIC ENERGY CONTROL BOARD—CANADA
KEN SHULTZ
ATOMIC ENERGY OF CANADA LTD
T. CHAN
SIEGRUN MEYER
ATOMIC ENERGY RESEARCH ESTABLISHMENT—UNITED KINGDOM
D. P. HODGKINSON
B & D ENTERPRISES
WILLIAM K. DINEHART
BATTELLE MEMORIAL INSTITUTE
JAMES DUGUID
JOHN T. MCGINNIS
JEFFREY L. MEANS
CARL SPILKER
BCM CONVERSE INC
ROBERT J. MANUEL
BECHTEL NATIONAL INC
BEVERLY S. AUSMUS
LESLIE J. JARDINE
T. R. MONGAN
BENDIX FIELD ENGINEERING CORP
LARRY M. FUKUI
CHARLES A. JONES
ANTHONY ZAIKOWSKI
BERKELEY GEOSCIENCES/HYDROTECHNIQUE ASSOCIATES
BRIAN KANEHIRO
BHABHA ATOMIC RESEARCH CENTRE—INDIA
V. SUKUMORAN
BOEING ENGINEERING COMPANY SOUTHEAST INC
O. R. SANDERS
BOWDOIN COLLEGE
EDWARD P. LAINE
BRENK SYSTEMPLANUNG—W. GERMANY
H. D. BRENK
BRIGHAM YOUNG UNIVERSITY
STAN L. ALBRECHT
WILLIAM M. TIMMINS
BRITISH GEOLOGICAL SURVEY
DAVID MICHAEL MCCANN
BROOKHAVEN NATIONAL LABORATORY
M. S. DAVIS
PETER SOO
HELEN TODOSOW (2)
BROOME COMMUNITY COLLEGE
BRUCE OLDFIELD
BROWN UNIVERSITY
MICHELE BURKE
BUNDESANSTALT FUR GEOWISSENSCHAFTEN UND ROHSTOFFE—W. GERMANY
MICHAEL LANGER
HELMUT VENZLAFF
BUREAU DE RECHERCHES GEOLOGIQUES ET MINIERES—FRANCE
BERNARD FEUGA
PIERRE F. PEAUDECERF
BUTTES GAS & OIL COMPANY
ROBERT NORMAN
CALIFORNIA DEPT OF CONSERVATION
PERRY AMIMITO
CANVIRO CONSULTANTS
DOUG METCALFE
CAPITAL UNIVERSITY
VICTOR M. SHOWALTER
CAYUGA LAKE CONSERVATION ASSOCIATION INC
D. S. KIEFER
CELSIUS ENERGY COMPANY
NICK THOMAIDIS
CENTER FOR ENVIRONMENTAL HEALTH
CAMERON MCDONALD VOWELL
CENTER FOR ENVIRONMENTAL INFORMATION INC
FREDERICK W. STOSS
CENTER FOR INTERDISCIPLINARY STUDIES
DAVID M. ARMSTRONG
CER CORP
ELLA JACKSON
CHEVRON OIL FIELD RESEARCH COMPANY
BJORN PAULSSON
CITIZENS AGAINST NUCLEAR DISPOSAL INC
STANLEY D. FLINT
CITY OF MONTICELLO
RICHARD TERRY
CLARK UNIVERSITY
JEANNE X. KASPERSON
CLIFFS ENGINEERING INC
GARY D. AHO
COLBY COLLEGE
BRUCE F. RUEGER
COLORADO GEOLOGIC INC
MIKE E. BRAZIE
COLORADO GEOLOGICAL SURVEY
JOHN W. ROLD
COLORADO SCHOOL OF MINES
W. HUSTRULID
COLORADO STATE UNIVERSITY
FRANK A. KULACKI
COLUMBIA UNIVERSITY
M. ASHRAF MAHTAB
CONGRESSIONAL INFORMATION SERVICE
PHYLLIS KLUN
CONNECTICUT DEPT OF ENVIRONMENTAL PROTECTION
KEVIN MCCARTHY
CORNELL UNIVERSITY
ARTHUR L. BLOOM
DUANE CHAPMAN
FRED H. KULHAWY
ROBERT POHL
COUNCIL OF ENERGY RESOURCE TRIBES
WYATT M. ROGERS, JR.
DAMES & MOORE
RON KEAR
ROBERT W. KUPP
CHARLES R. LEWIS
DANIEL B. STEPHENS AND ASSOCIATES
ROBERT G. KNOWLTON, JR.
DEAF SMITH COUNTY LIBRARY
DEPARTMENT OF THE NAVY
GENNARO MELLIS
DEPT OF ENERGY, MINES AND RESOURCES—CANADA
A. S. JUDGE
DESERET NEWS
JOSEPH BAUMAN
DEUTSCHE GESELLSCHAFT ZUM BAU UND BETRIEB VON ENDLAGERN
GERNOT GRUBLER
DISPOSAL SAFETY INC
BENJAMIN ROSS
DMGA, IPT—BRAZIL
C. DINIS DA GAMA
DUNN GEOSCIENCE CORP
WILLIAM E. CUTCLIFFE
DYNATECH RESEARCH/DEVELOPMENT COMPANY
STEPHEN E. SMITH
E.I. DU PONT DE NEMOURS & CO
A. B. MILLER
E.R. JOHNSON ASSOCIATES INC
G. L. JOHNSON
EAL CORP
LEON LEVENTHAL
EARTH RESOURCE ASSOCIATES INC
SERGE GONZALES
EARTH SCIENCE AND ENGINEERING INC
LOU BLANCK
EARTH SCIENCES CONSULTANTS INC
HARRY L. CROUSE
EAST TENNESSEE STATE UNIVERSITY
ALBERT F. IGLAR
EBASCO SERVICES INC
KATHLEEN E. L. HOWE
GARRY MAURATH
ECOLOGY & ENVIRONMENT INC
MICHAEL BENNER
EDISON ELECTRIC INSTITUTE
LORING E. MILLS
EG & G IDAHO INC
BRENT F. RUSSELL
ELEKTRIZITAETS-GES. LAUFENBURG—SWITZERLAND
H. N. PATAK
ELSAM—DENMARK
ARNE PEDERSEN
ENERGY FUELS NUCLEAR INC
DON M. PILLMORE
ENERGY RESEARCH GROUP INC
MARC GOLDSMITH
ENGINEERING ANALYSIS INC
WILLIAM MULLEN
ENGINEERS INTERNATIONAL INC
ROBERT A. CUMMINGS
LIBRARY
MADAN M. SINGH
ENVIRONMENTAL DEFENSE FUND
JAMES B. MARTIN
ENVIRONMENTAL POLICY INSTITUTE
DAVID M. BERRICK

ENVIROSPHERE COMPANY
ROGER G. ANDERSON
EXXON COMPANY
MICHAEL FARRELL
F.J. SCHLUMBERGER
PETER ALEXANDER
FENIX & SCISSON INC
CHARLENE U. SPARKMAN
FERRIS STATE COLLEGE
MICHAEL E. ELLS
FINNISH CENTRE FOR RADIATION AND NUCLEAR SAFETY
KAI JAKOBSSON
FLORIDA INSTITUTE OF TECHNOLOGY
JOSEPH A. ANGELO, JR.
FLORIDA STATE UNIVERSITY
JOSEPH F. DONOGHUE
FLUID PROCESSES RESEARCH GROUP BRITISH GEOLOGICAL SURVEY
NEIL A. CHAPMAN
FLUOR TECHNOLOGY INC
WILLIAM LEE (F2X)
THOMAS O. MALLONEE, JR (F2X)
FOUR CORNERS COMMUNITY MENTAL HEALTH CENTER
BOB GREENBERG
FUTURE RESOURCES ASSOCIATES INC
ROBERT J. BUDNITZ
GA TECHNOLOGIES INC
MICHAEL STAMATELATOS
GARTNER LEE ASSOCIATES LTD—CANADA
ROBERT E. J. LEECH
GEOLOGICAL SURVEY OF CANADA
JEFFREY HUME
LIBRARY
GEOLOGICAL SURVEY OF NORWAY
SIGURD HUSEBY
GEOMIN INC
J. A. MACHADO
GEORGIA INSTITUTE OF TECHNOLOGY
GEOFFREY G. EICHHOLZ
ALFRED SCHNEIDER
CHARLES E. WEAVER
GEOSTOCK—FRANCE
CATHERINE GOUGNAUD
GEOSYSTEMS RESEARCH INC
RANDY L. BASSETT
GEOTHERMAL ENERGY INSTITUTE
DONALD F. X. FINN
GEOTRANS INC
JAMES MERCER
GOLDER ASSOCIATES
MELISSA MATSON
J. W. VOSS
GOLDER ASSOCIATES—CANADA
CLEMENT M. K. YUEN
GRAND COUNTY PUBLIC LIBRARY
GRIMCO
DONALD H. KUPFER
GRUPPE OKOLOGIE (GOK)
JURGEN KREUSCH
GUSTAVSON ASSOCIATES
RICHARD M. WINAR
H. LAWROSKI & ASSOCIATES P.A.
HARRY LAWROSKI
H-TECH LABORATORIES INC
BRUCE HARTENBAUM
HANFORD OVERSIGHT COMMITTEE
LARRY CALDWELL
HART-CROWSER AND ASSOCIATES
MICHAEL BAILEY
HARVARD UNIVERSITY
CHARLES W. BURNHAM
DADE W. MOELLER
RAYMOND SIEVER
HARZA ENGINEERING COMPANY
PETER CONROY
HEALTH & ENERGY INSTITUTE
ARJUN MAKHIJAN
HEREFORD NUCLEAR WASTE INFORMATION OFFICE
MARTHA SHIRE
HIGH LEVEL NUCLEAR WASTE OFFICE
PATRICK D. SPURGIN (5)
HIGH PLAINS WATER DISTRICT
DON MCREYNOLDS
A. WAYNE WYATT
HITACHI WORKS, HITACHI LTD
MAKOTO KIKUCHI
HOUGH-NORWOOD HEALTH CARE CENTER
GEORGE H. BROWN, M.D.
HUMBOLDT STATE UNIVERSITY
JOHN LONGSHORE
ILLINOIS DEPT OF NUCLEAR SAFETY
JOHN COOPER
ILLINOIS STATE GEOLOGICAL SURVEY
KEROS CARTWRIGHT
MORRIS W. LEIGHTON
E. DONALD MCKAY, III
INDIANA GEOLOGICAL SURVEY
MAURICE BIGGS
INDIANA UNIVERSITY
CHARLES J. VITALIANO
INSTITUT FUR TIEFLAGERUNG—W. GERMANY
WERNT BREWITZ
H. GIES
E. R. SOLTER
INSTITUTE OF GEOLOGICAL SCIENCES—ENGLAND
STEPHEN THOMAS HORSEMAN
INSTITUTE OF PLASMA PHYSICS
H. AMANO
INSTITUTO DE INVESTIGACIONES FISCOQUIMICAS TEORICAS Y APLICADAS
J. R. VILCHE
INTER/FACE ASSOCIATES INC
RON GINGERICH
INTERA TECHNOLOGIES INC
JAMES E. CAMPBELL
F. J. PEARSON, JR.
JOHN F. PICKENS
MARK REEVES
INTERNATIONAL ENGINEERING COMPANY INC
MAX ZASLAWSKY
INTERNATIONAL GROUND WATER MODELING CENTER
PAUL K. M. VAN DER HEIJDE
INTERNATIONAL RESEARCH AND EVALUATION
R. DANFORD
INTERNATIONAL SALT COMPANY
JOHN VOIGT
IRAD-GAGE
R. BOYD MONTGOMERY
ISTITUTO SPERIMENTALE MODELLI E STRUTTURE S.P.A.—ITALY
FERRUCCIO GERA
IT CORP
MORRIS BALDERMAN
PETER C. KELSALL
LIBRARY
CARL E. SCHUBERT
ITASCA CONSULTING GROUP INC
CHARLES FAIRHURST
ROGER HART
J.F.T. AGAPITO & ASSOCIATES INC
MICHAEL P. HARDY
CHRISTOPHER M. ST. JOHN
J.L. MAGRUDER & ASSOCIATES
J. L. MAGRUDER
JACOBY & COMPANY
CHARLES H. JACOBY
JAMES MADISON UNIVERSITY
STEPHEN B. HARPER
JAY L. SMITH COMPANY INC
JAY L. SMITH
JGC CORPORATION—JAPAN
MASAHIKO MAKINO
JOHNS HOPKINS UNIVERSITY
JARED L. COHON
JOINT STUDY COMMITTEE ON ENERGY
T. W. EDWARDS, JR.
KALAMAZOO COLLEGE
RALPH M. DEAL
KANSAS DEPT OF HEALTH AND ENVIRONMENT
GERALD W. ALLEN
KANSAS STATE GEOLOGICAL SURVEY
WILLIAM W. HAMBLETON
KEARNS & WEST INC
LEXINGTON SQUARE
KELLER WREATH ASSOCIATES
FRANK WREATH
KERNFORSCHUNGSZENTRUM KARLSRUHE GMBH—W. GERMANY
K. D. CLOSS
R. KOESTER
KETTERING FOUNDATION
ESTUS SMITH
KIERSCH ASSOCIATES GEOSCIENCES/RESOURCES CONSULTANTS INC
GEORGE A. KIERSCH, PH.D.
KIHN ASSOCIATES
HARRY KIHN
KILLGORES INC
CHARLES KILLGORE
KIMBERLY MECHANICAL CONSULTANTS
KENNETH CROMWELL
KLM ENGINEERING INC
B. GEORGE KNIAZEWYCZ
KUTA RADIO
KUTV-TV
ROBERT LOY
LACHEL HANSEN & ASSOCIATES INC
DOUGLAS E. HANSEN
LAKE SUPERIOR REGION RADIOACTIVE WASTE PROJECT
C. DIXON
LATIR ENERGY CONSULTANTS
JOHN GERVERS
LAW ENGINEERING TESTING COMPANY
JOSEPH P. KLEIN III
LAWRENCE BERKELEY LABORATORY
JOHN A. APPS
EUGENE P. BINNALL
NORMAN M. EDELSTEIN
M. S. KING
E. MAJER
CHIN FU TSANG
J. WANG
LAWRENCE LIVERMORE NATIONAL LABORATORY
EDNA M. DIDWELL
HUGH HEARD
FRANCOIS E. HEUZE
NAI-HSIEN MAO
LAWRENCE MCKAGUE
THOMAS E. MCKONE
ABELARDO RAMIREZ

LAWRENCE D. RAMSPOTT (2)
DAVID B. SLEMMONS
TECHNICAL INFORMATION DEPARTMENT
WASTE PACKAGE TASK LIBRARY
JESSE L. YOW, JR.

LEAGUE OPPOSING SITE SELECTION
LINDA S. TAYLOR

LEGISLATIVE COMMISSION ON SCIENCE & TECHNOLOGY
DALE M. VOLKER

LEIGHTON AND ASSOCIATES INC
BRUCE R. CLARK

LIBRARY OF MICHIGAN
RICHARD J. HATHAWAY

LOCKHEED ENGINEERING & MANAGEMENT COMPANY
STEVE NACHT

LOS ALAMOS NATIONAL LABORATORY
ERNEST A. BRYANT
B. CROWE
AREND MEIJER
C. W. MYERS
DONALD T. OAKLEY

LOUISIANA GEOLOGICAL SURVEY
RENWICK P. DEVILLE
JAMES J. FRILOUX
SYED HAQUE

LOUISIANA GOVERNORS OFFICE
JUNE TAYLOR

LOUISIANA STATE UNIVERSITY
JEFFREY S. HANOR

LOUISIANA TECHNICAL UNIVERSITY
LIBRARY
R. H. THOMPSON

LOWENBERG ASSOCIATES
HOMER LOWENBERG

LYLE FRANCIS MINING COMPANY
LYLE FRANCIS

M.J. OCONNOR & ASSOCIATES LTD
M. J. OCONNOR

MARTIN MARIETTA
CATHY S. FORE

MARYLAND DEPT OF HEALTH & MENTAL HYGIENE
MAX EISENBERG

MASSACHUSETTS INSTITUTE OF TECHNOLOGY
MARSHA LEVINE
DANIEL METLAY

MATERIALS RESEARCH LABORATORY LTD—CANADA
S. SINGH

MCDERMOTT INTERNATIONAL
KAREN L. FURLOW

MCMASTER UNIVERSITY—CANADA
L. W. SHEMILT

MELLEN GEOLOGICAL ASSOCIATES INC
FREDERIC F. MELLEN

MEMBERS OF THE GENERAL PUBLIC
ROGER H. BROOKS
LAWRENCE CHASE, PH.D.
TOM & SUSAN CLAWSON
VICTOR J. COHEN
ROBERT DEADMAN
GHISLAIN DEMARSILY
GERALD A. DRAKE, M.D.
ROBERT EINZIGER
WARREN EISTER
GERALDINE A. FERRARO
DUNCAN FOLEY
CARL A. GIESE
OSWALD H. GREAGER
KENNETH GUSCOTT
C. F. HAJEK
A. M. HALE
MICHAEL T. HARRIS
MICHAEL R. HELFERT
JOSEPH M. HENNIGAN
B. JEANINE HULL
CHARLES B. HUNT
YOZO ISOGAI
HAROLD L. JAMES
KENNETH S. JOHNSON
THOMAS H. LANGEVIN
LINDA LEHMAN
GEORGE LOUDDER
CLIVE MACKAY
DUANE MATLOCK
W. D. MCDOUGALD
MAX MCDOWELL
A. ALAN MOGHISSI
F. L. MOLESKI
TONY MORGAN
CAROLINE PETTI
L. M. PIERSON
MARTIN RATHKE
PETER J. SABATINI, JR.
ZUBAIR SALEEM
OWEN SEVERANCE
LEWIS K. SHUMWAY
HARRY W. SMEDES
FRANK STEINBRUNN
P. E. STRALEY-GREGA
M. J. SZULINSKI
EBIMO D. UMBU
A. E. WASSERBACH
SUSAN D. WILTSHIRE

MERRIMAN AND BARBER CONSULTING ENGINEERS INC
GENE R. BARBER

MICHAEL BAKER, JR. INC
C. J. TOUHILL

MICHIGAN DEPT OF PUBLIC HEALTH
ARTHUR W. BLOOMER

MICHIGAN DISTRICT HEALTH DEPT NO. 4
EDGAR KREFT

MICHIGAN ENVIRONMENTAL COUNCIL
ROOM 305

MICHIGAN GEOLOGICAL SURVEY
ROBERT C. REED

MICHIGAN PUBLIC SERVICE COMMISSION
RON CALLEN

MICHIGAN TECHNOLOGICAL UNIVERSITY
DAE S. YOUNG

MICHIGAN UNITED CONSERVATION CLUBS
WAYNE SCHMIDT

MIDDLETON LIBRARY
M. S. BOLNER

MINDEN NUCLEAR WASTE INFORMATION OFFICE
SHIRLEY JOHNSON

MINE CRAFT INC
NORBERT PAAS

MINNESOTA DEPT OF ENERGY AND DEVELOPMENT

MINNESOTA DEPT OF HEALTH
ALICE T. DOLEZAL-HENNIGAN

MINNESOTA F.A.I.R.
DELORES SWOBODA

MINNESOTA GEOLOGICAL SURVEY
MATT S. WALTON

MISSISSIPPI ATTORNEY GENERALS OFFICE
LISA A. SPRUILL

MISSISSIPPI BUREAU OF GEOLOGY
MICHAEL B. E. BOGRAD

MISSISSIPPI DEPT OF ENERGY AND TRANSPORTATION
DON CHRISTY
RONALD J. FORSYTHE (3)

MISSISSIPPI DEPT OF NATURAL RESOURCES
ALVIN R. BICKER, JR.
CHARLES L. BLALOCK

MISSISSIPPI DEPT OF WILDLIFE CONSERVATION
KENNETH L. GORDON

MISSISSIPPI LIBRARY COMMISSION
SARA TUBB

MISSISSIPPI MINERAL RESOURCES INSTITUTE

MISSISSIPPI STATE DEPT OF HEALTH
EDDIE S. FUENTE
GUY R. WILSON

MISSISSIPPI STATE UNIVERSITY
JOHN E. MYLROIE

MITRE CORP
LESTER A. ETTLINGER

MONTICELLO HIGH SCHOOL LIBRARY
MEDIA CENTER

MONTICELLO NUCLEAR WASTE INFORMATION OFFICE
CARL EISEMANN (2)

MORRISON-KNUDSEN COMPANY INC
BILL GALE
MICHELLE L. PAURLEY

NAGRA—SWITZERLAND
CHARLES MCCOMBIE

NATIONAL ACADEMY OF SCIENCES
JOHN T. HOLLOWAY

NATIONAL BOARD FOR SPENT NUCLEAR FUEL, KARNBRANSLENAMDEN—SWEDEN
NILS RYDELL

NATIONAL GROUND WATER INFORMATION CENTER
JANET BIX

NATIONAL PARK SERVICE
CECIL D. LEWIS, JR.
L. L. MINTZMEYER
PETER L. PARRY

NATIONAL PARKS & CONSERVATION ASSOCIATION
TERRI MARTIN

NATIONAL SCIENCE FOUNDATION
ROYAL E. ROSTENBACH

NATIONAL WATER WELL ASSOCIATION
VALERIE ORR

NEW HAMPSHIRE HOUSE OF REPRESENTATIVES
M. ARNOLD WIGHT, JR.

NEW MEXICO BUREAU OF GEOLOGY
BILL HATCHELL

NEW MEXICO ENVIRONMENTAL EVALUATION GROUP
ROBERT H. NEILL

NEW MEXICO INSTITUTE OF MINING AND TECHNOLOGY
JOHN L. WILSON

NEW YORK ENERGY RESEARCH & DEVELOPMENT AUTHORITY
JOHN P. SPATH (8)

NEW YORK STATE ASSEMBLY
WILLIAM B. HOYT

NEW YORK STATE ATTORNEY GENERALS OFFICE
PETER SKINNER

NEW YORK STATE DEPT OF ENVIRONMENTAL CONSERVATION
PAUL MERGES

NEW YORK STATE ENVIRONMENTAL FACILITIES CORP
PICKETT T. SIMPSON

NEW YORK STATE GEOLOGICAL SURVEY
JAMES R. ALBANESE
ROBERT H. FICKIES
NEW YORK STATE HEALTH DEPT
JOHN MATUSZEK
NEW YORK STATE PUBLIC SERVICE COMMISSION
FRED HAAG
NEYER, TISEO, & HINDO LTD
KAL R. HINDO
NIAGARA MOHAWK POWER CORP
GERALD K. RHODE
NORTH CAROLINA STATE UNIVERSITY
M. KIMBERLEY
NORTH DAKOTA GEOLOGICAL SURVEY
DON L. HALVORSON
NORTHEAST LOUISIANA UNIVERSITY
ROBERT E. DOOLEY
NORTHWESTERN UNIVERSITY
BERNARD J. WOOD
NUCLEAR ASSURANCE CORP
JOHN V. HOUSTON
NUCLEAR SAFETY RESEARCH ASSOCIATION
HIDETAKA ISHIKAWA
NUCLEAR WASTE CONSULTANTS
ADRIAN BROWN
NUCLEAR WASTE INFORMATION CENTER MISSISSIPPI STATE LAW LIBRARY
JUDITH HUTSON
NUCLEAR WASTE WATCHERS
HELEN LETARTE
NUS CORP
W. G. BELTER
DOUGLAS D. ORVIS
YONG M. PARK
NWT CORP
W. L. PEARL
OAK RIDGE NATIONAL LABORATORY
J. O. BLOMEKE
H. C. CLAIBORNE
ALLEN G. CROFF
DAVID C. KOCHER
T. F. LOMENICK
E. B. PEELLE
FRANCOIS G. PIN
ELLEN D. SMITH
SUSAN K. WHATLEY
OHIO DEPT OF HEALTH
ROBERT M. QUILLIN
ONR DETACHMENT
DAVID EPP
ONTARIO DEPT OF CIVIL ENGINEERING
F. SYKES
ONTARIO HYDRO—CANADA
K. A. CORNELL
C. F. LEE
ONTARIO RESEARCH FOUNDATION—CANADA
LYDIA M. LUCKEVICH
ORANGE COUNTY COMMUNITY COLLEGE
LAWRENCE E. OBRIEN
OREGON STATE UNIVERSITY
JOHN C. RINGLE
ORGANIZATION FOR ECONOMIC COOPERATION AND DEVELOPMENT—FRANCE
STEFAN G. CARLYLE
PACIFIC NORTHWEST LABORATORY
DON J. BRADLEY
CHARLES R. COLE
WILLIAM CONBERE
PAUL A. EDDY
FLOYD N. HODGES
J. H. JARRETT
CHARLES T. KINCAID
J. M. LATKOVICH
J. E. MENDEL
J. M. RUSIN
R. JEFF SERNE
STEVEN C. SNEIDER
R. E. WESTERMAN
PARSONS BRINCKERHOFF QUADE & DOUGLAS INC
T. R. KUESEL
ROBERT PRIETO
PARSONS BRINCKERHOFF/PB-KBB
KAROLYN KENNEDY
PARSONS-REDPATH
KRISHNA SHRIYASTAVA
GLEN A. STAFFORD
PB-KBB INC
JUDITH G. HACKNEY
PENNSYLVANIA STATE UNIVERSITY
MICHAEL GRUTZECK
DELLA M. ROY
WILLIAM B. WHITE
PERRY COUNTY CITIZENS AGAINST NUCLEAR WASTE DISPOSAL
DOROTHY G. COLE
DURLEY HANSEN
PHYSIKALISCH-TECHNISCHE BUNDESANSTALT—W. GERMANY
PETER BRENNECKE
POBERESKIN INC
MEYER POBERESKIN
POTASH CORPORATION OF SASKATCHEWAN—CANADA
GRAEME G. STRATHDEE
POTASH CORPORATION OF SASKATCHEWAN MINING LIMITED
PARVIZ MOTTAHED
POWER REACTOR AND NUCLEAR FUEL DEVELOPMENT CORP—JAPAN
PRESEARCH INC
MARTIN S. MARKOWICZ
PUBLIC SERVICE ELECTRIC & GAS
JOHN J. MOLNER
R.J. SHLEMON AND ASSOCIATES INC
R. J. SHLEMON
RADIAN CORP
RICHARD STRICKERT
RANDALL COUNTY LIBRARY
RAYMOND KAISER ENGINEERS
W. J. DODSON
RE/SPEC INC
GARY D. CALLAHAN
PAUL F. GNIRK
RENEWABLE ENERGY COUNCIL OF NORTH CAROLINA
JANE SHARP
RENSSELAER POLYTECHNIC INSTITUTE
BRIAN BAYLY
RHODE ISLAND OFFICE OF STATE PLANNING
BRUCE VILD
RICHTON NUCLEAR WASTE INFORMATION OFFICE
BOB FREEMAN
RISO NATIONAL LABORATORY—DENMARK
LARS CARLSEN
ROCKWELL HANFORD OPERATIONS
RONALD C. ARNETT
HARRY BABAD
G. S. BARNEY
KUNSOO KIM
KARL M. LA RUE
STEVEN J. PHILLIPS
NORMAN A. STEGER
ROCKWELL INTERNATIONAL ENERGY SYSTEMS GROUP
HARRY PEARLMAN
ROGERS & ASSOCIATES ENGINEERING CORP
ARTHUR A. SUTHERLAND
ROBERT E. WILEMS
ROY F. WESTON INC
MICHAEL CONROY
DAVID F. FENSTER
MARTIN HANSON
WILLIAM IVES
MICHAEL V. MELLINGER
VIC MONTENYOHL
SAM PANNO
JILL RUSPI
STEVE SMITH
KAREN ST. JOHN
LAWRENCE A. WHITE
ROYAL INSTITUTE OF TECHNOLOGY—SWEDEN
IVARS NERETNIEKS
ROGER THUNVIK
ROYCES ELECTRONICS INC
ROYCE HENNINGSON
RPC INC
LIBRARY
SALT LAKE CITY TRIBUNE
JIM WOOLF
SAN DIEGO GAS & ELECTRIC COMPANY
STEPHEN B. ALLMAN
SAN JOSE STATE UNIVERSITY SCHOOL OF ENGINEERING
R. N. ANDERSON
SAN JUAN RECORD
JOYCE MARTIN
SANDIA NATIONAL LABORATORIES
JOY BEMESDERFER
SHARLA BERTRAM
ROBERT M. CRANWELL
JOE A. FERNANDEZ
ROBERT GUZOWSKI
THOMAS O. HUNTER
A. R. LAPPIN
R. W. LYNCH
RUDOLPH V. MATALUCCI
JAMES T. NEAL
E. J. NOWAK
SCOTT SINNOCK
LYNN D. TYLER
WOLFGANG WAWERSIK
WENDELL WEART
SARGENT & LUNDY ENGINEERS
LAWRENCE L. HOLISH
SAVANNAH RIVER LABORATORY
CAROL JANTZEN
WILLIAM R. MCDONELL
DONALD ORTH
SCIENCE APPLICATIONS INTERNATIONAL CORP
MARY LOU BROWN
JERRY J. COHEN
BARRY DIAL
ROBERT R. JACKSON
DAVID H. LESTER
JOHN E. MOSIER
ANTHONY MULLER
DOUGLAS A. OUTLAW
HOWARD PRATT
MICHAEL E. SPAETH
ROBERT T. STULA
M. D. VOEGELE
KRISHAN K. WAHI

SENECA COUNTY DEPT OF PLANNING & DEVELOPMENT
SHAFER EXPLORATION COMPANY
WILLIAM E SHAFER
SHANNON & WILSON INC
HARVEY W PARKER
FRANK S SHURI
SHIMIZU CONSTRUCTION COMPANY LTD—JAPAN
TAKASHI ISHII
SIERRA CLUB
MARVIN RESNIKOFF
SIERRA CLUB—COLORADO OPEN SPACE COUNCIL
ROY YOUNG
SIERRA CLUB—MISSISSIPPI CHAPTER
SIERRA CLUB LEGAL DEFENSE FUND
H ANTHONY RUCKEL
SIMECSOL CONSULTING ENGINEERS—FRANCE
MATTHEW LEONARD
SKBF/KBS—SWEDEN
C THEGERSTROM
SOGO TECHNOLOGY INC
TIO C CHEN
SOKAOGON CHIPPEWA COMMUNITY
ARLYN ACKLEY
SOUTH DAKOTA GEOLOGICAL SURVEY
MERLIN J TIPTON
SOUTH DAKOTA OFFICE OF ENERGY POLICY
STEVEN M WEGMAN
SOUTHERN CALIFORNIA EDISON CO
JOHN LADESICH
SOUTHERN STATES ENERGY BOARD
J F CLARK
SOUTHWEST RESEARCH AND INFORMATION CENTER
DON HANCOCK
SPRING CREEK RANCH
DALTON RED BRANGUS
SPRINGVILLE CITY LIBRARY
SRI INTERNATIONAL (PS 285)
DIGBY MACDONALD
ST & E TECHNICAL SERVICES INC
STANLEY M KLAINER
STANFORD UNIVERSITY
KONRAD B KRAUSKOPF
GEORGE A PARKS
IRWIN REMSON
STATE PLANNING AGENCY
BILL CLAUSEN
STATE UNIVERSITY OF NEW YORK AT CORTLAND
JAMES E BUGH
STATE UNIVERSITY OF NEW YORK AT STONY BROOK
S REAVEN
STEARNS CATALYTIC CORP
VERYL ESCHEN
STONE & WEBSTER ENGINEERING CORP
JOHN PECK
ARLENE C PORT
EVERETT M WASHER
STUDIO GEOLOGICO FOMAR—ITALY
A MARTORANA
SWEDISH GEOLOGICAL
LEIF CARLSSON
SWISHER COUNTY LIBRARY
SYRACUSE UNIVERSITY
WALTER MEYER
J E ROBINSON
SYSTEMS SCIENCE AND SOFTWARE
PETER LAGUS
TECHNICAL INFORMATION PROJECT
DONALD PAY
TERRAFORM ENGINEERS INC
FRANCIS S KENDORSKI
TEXAS A & M UNIVERSITY
JOHN HANDIN
STEVE MURDOCK
JAMES E RUSSELL
TEXAS BUREAU OF ECONOMIC GEOLOGY
WILLIAM L FISHER
TEXAS DEPT OF AGRICULTURE
GARY KEITH
TEXAS DEPT OF HEALTH
DAVID K LACKER
TEXAS DEPT OF WATER RESOURCES
W KLEMT
T KNOWLES
TEXAS GOVERNORS OFFICE
STEVE FRISHMAN
TEXAS STATE HOUSE OF REPRESENTATIVES
JULIE CARUTHERS
TEXAS TECHNICAL UNIVERSITY
C C REEVES, JR
TEXAS WORLD OPERATIONS INC
DAVID JEFFERY
THE ANALYTIC SCIENCES CORP
JOHN W BARTLETT
THE BENHAM GROUP
KEN SENOUR
THE DAILY SENTINEL
JIM SULLIVAN
THE EARTH TECHNOLOGY CORP
DANIEL D BUSH
FRED A DONATH (2)
JOSEPH G GIBSON
DAN MELCHIOR
JAMES R MILLER
FIA VITAR
MATT WERNER
KENNETH L WILSON
THE RADIOACTIVE EXCHANGE
EDWARD L HELMINSKI
THE SEATTLE TIMES
ELOUISE SCHUMACHER
THOMSEN ASSOCIATES
C T GAYNOR, II
TIMES-PICAYUNE
MARK SCHLEIFSTEIN
TIOGA COUNTY PLANNING BOARD
THOMAS A COOKINGHAM
TRINITY EPISCOPAL CHURCH
BENJAMIN F BELL
TULIA NUCLEAR WASTE INFORMATION OFFICE
NADINE SMITH
U.S. ARMY CORPS OF ENGINEERS
DON BANKS
ALAN BUCK
U.S. BUREAU OF LAND MANAGEMENT
GENE NODINE
GREGORY F THAYN
U.S. BUREAU OF MINES
ANTHONY IANNACCHIONE
U.S. BUREAU OF RECLAMATION
JOHN BROWN
REGE LEACH
UC 150 & UC 760
U.S. DEPT OF COMMERCE
PETER A RONA
U.S. DEPT OF ENERGY
RICHARD BLANEY
REBECCA BOYD
CHED BRADLEY
C R COOLEY (2)
R COOPERSTEIN
NEAL DUNCAN
JIM FIORE
MARK W FREI
LAWRENCE H HARMON
D L HARTMAN
ROGER MAYES
MICHAELENE PENDLETON (2)
PUBLIC READING ROOM
JANIE SHAHEEN
HENRY F WALTER
U.S. DEPT OF ENERGY—ALBUQUERQUE OPERATIONS OFFICE
LORETTA HELLING
U.S. DEPT OF ENERGY—CHICAGO OPERATIONS OFFICE
NURI BULUT
BARRETT R FRITZ
VICKI PROUTY
PUBLIC READING ROOM
R SELBY
U.S. DEPT OF ENERGY—ENGINEERING AND LICENSING DIVISION
RALPH STEIN
U.S. DEPT OF ENERGY—IDAHO OPERATIONS OFFICE
JAMES F LEONARD
PUBLIC READING ROOM
U.S. DEPT OF ENERGY—OAK RIDGE OPERATIONS OFFICE
PUBLIC READING ROOM
U.S. DEPT OF ENERGY—OFFICE OF ENERGY RESEARCH
FRANK J WOBBER
U.S. DEPT OF ENERGY—OSTI (317)
U.S. DEPT OF ENERGY—RICHLAND OPERATIONS OFFICE
D H DAHLEM
U.S. DEPT OF ENERGY—SALT REPOSITORY PROJECT OFFICE
J O NEFF
U.S. DEPT OF ENERGY—SAN FRANCISCO OPERATIONS OFFICE
PUBLIC READING ROOM
U.S. DEPT OF ENERGY—WIPP
ARLEN HUNT
U.S. DEPT OF LABOR
KELVIN K WU
U.S. DEPT OF THE INTERIOR
MATTHEW JAMES DEMARCO
F L DOYLE
PAUL A HSIEH
U.S. ENVIRONMENTAL PROTECTION AGENCY
JAMES NEIHEISEL
U.S. ENVIRONMENTAL PROTECTION AGENCY—DENVER REGION VIII
PHIL NYBERG
U.S. ENVIRONMENTAL PROTECTION AGENCY—REGION II
JOYCE FELDMAN
U.S. GEOLOGICAL SURVEY
GEORGE A DINWIDDIE
VIRGINIA M GLANZMAN
DARWIN KNOCHENMUS
GERHARD W LEO
EDWIN ROEDDER
RAYMOND D WATTS
U.S. GEOLOGICAL SURVEY—DENVER
M S BEDINGER
JESS M CLEVELAND
ROBERT J HITE

FREDERICK L. PAILLET
WILLIAM WILSON

U.S. GEOLOGICAL SURVEY—JACKSON
GARALD G. PARKER, JR.

U.S. GEOLOGICAL SURVEY—MENLO PARK
MICHAEL CLYNNE

U.S. GEOLOGICAL SURVEY—RESTON
I-MING CHOU
NEIL PLUMMER
EUGENE H. ROSEBOOM, JR.
DAVID B. STEWART
NEWELL J. TRASK, JR.

U.S. NUCLEAR REGULATORY COMMISSION
R. BOYLE
EILEEN CHEN
DOCKET CONTROL CENTER
GEOSCIENCES BRANCH
PAUL F. GOLDBERG
BANAD N. JAGANNATH
CLYDE JUPITER
PHILIP S. JUSTUS
WALTON R. KELLY
WILLIAM D. LILLEY
JOHN C. MCKINLEY
NRC LIBRARY
EDWARD OCONNELL
JEROME R. PEARRING
JACOB PHILIP
FREDERICK W. ROSS
R. JOHN STARMER
NAIEM S. TANIOUS
JOHN TRAPP
TILAK R. VERMA
MICHAEL WEBER

U.S. SENATE
CARL LEVIN
BILL SARPALIUS

UNION OF CONCERNED SCIENTISTS
MICHAEL FADEN

UNITED KINGDOM ATOMIC ENERGY AUTHORITY
A. B. LIDIARD

UNITED KINGDOM DEPT OF THE ENVIRONMENT
F. S. FEATES

UNIVERSITE DU QUEBEC EN ABITIBI-TEMISCAMINGUE
AUBERTIN MICHEL

UNIVERSITY COLLEGE LONDON
B. K. ATKINSON

UNIVERSITY OF ALBERTA—CANADA
F. W. SCHWARTZ

UNIVERSITY OF ARIZONA
JAAK DAEMEN
STANLEY N. DAVIS
I. W. FARMER
KITTITEP FUENKAJORN
AMITAVA GHOSH
JAMES G. MCCRAY
SHLOMO P. NEUMAN

UNIVERSITY OF BRITISH COLUMBIA—CANADA
R. ALLAN FREEZE

UNIVERSITY OF CALIFORNIA AT BERKELEY
RICHARD E. GOODMAN
TODD LAPORTE

UNIVERSITY OF CALIFORNIA AT RIVERSIDE
LEWIS COHEN

UNIVERSITY OF CONNECTICUT
GARY ROBBINS

UNIVERSITY OF DAYTON RESEARCH LAB
NACHHATTER S. BRAR

UNIVERSITY OF ILLINOIS AT URBANA—CHAMPAIGN
ALBERT J. MACHIELS
MAGDI RAGHEB

UNIVERSITY OF LOWELL
JAMES R. SHEFF

UNIVERSITY OF MARYLAND
AMERICAN NUCLEAR SOCIETY
LUKE L. Y. CHUANG
MARVIN ROUSH

UNIVERSITY OF MASSACHUSETTS
GEORGE MCGILL

UNIVERSITY OF MISSOURI AT COLUMBIA
W. D. KELLER

UNIVERSITY OF MISSOURI AT KANSAS CITY
EDWIN D. GOEBEL
SYED E. HASAN

UNIVERSITY OF MISSOURI AT ROLLA
ALLEN W. HATHEWAY

UNIVERSITY OF NEVADA AT RENO
BECKY WEIMER-MCMILLION

UNIVERSITY OF NEW MEXICO
DOUGLAS G. BROOKINS
RODNEY C. EWING

UNIVERSITY OF OKLAHOMA
DANIEL T. BOATRIGHT

UNIVERSITY OF OTTAWA—CANADA
TUNCER OREN

UNIVERSITY OF ROCHESTER
DAVID ELMORE

UNIVERSITY OF SOUTHERN MISSISSIPPI
CHARLES R. BRENT
DANIEL A. SUNDEEN

UNIVERSITY OF TEXAS AT AUSTIN
BUREAU OF ECONOMIC GEOLOGY
CAROLYN E. CONDON
PRISCILLA P. NELSON
JOHN M. SHARP, JR.
THE GENERAL LIBRARIES

UNIVERSITY OF TEXAS AT SAN ANTONIO
DONALD R. LEWIS

UNIVERSITY OF TOLEDO
DON STIERMAN

UNIVERSITY OF UTAH
THURE CERLING
STEVEN J. MANNING
MARRIOTT LIBRARY
JAMES A. PROCARIONE
GARY M. SANDQUIST
LEE STOKES

UNIVERSITY OF UTAH RESEARCH INSTITUTE
LIBRARY
HOWARD P. ROSS

UNIVERSITY OF WASHINGTON
DAVID BODANSKY
M. A. ROBKIN

UNIVERSITY OF WATERLOO
CHRIS FORDHAM

UNIVERSITY OF WISCONSIN—MADISON
B. C. HAIMSON

UNIVERSITY OF WISCONSIN—MILWAUKEE
HOWARD PINCUS

UNIVERSITY OF WISCONSIN CENTER—JANESVILLE

UNIVERSITY OF WYOMING
PETER HUNTOON

USGS NATIONAL CENTER
JIM ROLLO

UTAH DEPT OF HEALTH
LARRY F. ANDERSON

UTAH DEPT OF NATURAL RESOURCES & ENERGY
MARK P. PAGE

UTAH DEPT OF TRANSPORTATION
DAVID LLOYD

UTAH DIVISION OF PARKS & RECREATION
PARK MANAGER
GORDON W. TOPHAM

UTAH ENERGY OFFICE
ROD MILLAR

UTAH GEOLOGICAL AND MINERAL SURVEY
MAGE YONETANI

UTAH SOUTHEASTERN DISTRICT HEALTH DEPT
ROBERT L. FURLOW

UTAH STATE GEOLOGIC TASK FORCE
DAVID D. TILLSON

UTAH STATE UNIVERSITY
DEPT OF GEOLOGY 07

V. RAJARAM, P.E.
V. RAJARAM

VANDERBILT UNIVERSITY
FRANK L. PARKER

VEGA NUCLEAR WASTE INFORMATION OFFICE
EFFIE HARLE

VERMONT STATE NUCLEAR ADVISORY PANEL
VIRGINIA CALLAN

VIRGINIA DEPT OF HEALTH
ROBERT G. WICKLINE

VIRGINIA POLYTECHNICAL INSTITUTE AND STATE UNIVERSITY
JOHN M. HALSTEAD

VIRGINIA POWER COMPANY
B. H. WAKEMAN

WASHINGTON HOUSE OF REPRESENTATIVES
RAY ISAACSON

WASHINGTON STATE DEPT OF ECOLOGY
TERRY HUSSEMAN

WATER INDUSTRIES
STEVE CONEWAY

WATTLAB
BOB E. WATT

WEST VALLEY NUCLEAR SERVICES COMPANY INC
LARRY R. EISENSTATT

WESTERN MICHIGAN UNIVERSITY
ROBERT KAUFMAN
W. THOMAS STRAW

WESTERN STATE COLLEGE
FRED R. PECK

WESTINGHOUSE ELECTRIC CORP
JAMES H. SALING
WIPP PROJECT

WESTINGHOUSE HANFORD COMPANY
C. R. ALLEN

WESTINGHOUSE IDAHO NUCLEAR COMPANY INC
NATHAN A. CHIPMAN

WESTON GEOPHYSICAL CORP
CHARLENE SULLIVAN

WEYER CORP INC
K. U. WEYER

WILLIAMS AND ASSOCIATES INC
GERRY WINTER

WISCONSIN DEPT OF NATURAL RESOURCES
DUWAYNE F. GEBKEN

WISCONSIN DIVISION OF STATE ENERGY
ROBERT HALSTEAD

WISCONSIN ELECTRIC POWER CO.
DAVID K. ZABRANSKY

WISCONSIN STATE SENATE
JOSEPH STROHL

WISCONSIN WATER RESOURCES MANAGEMENT
SALLY J. KEFER

WITHERSPOON, AIKEN AND LANGLEY
RICHARD FORREST

WOODWARD-CLYDE CONSULTANTS
RANDALL L. LENTELL
ASHOK PATWARDHAN
WESTERN REGION LIBRARY

YALE UNIVERSITY
G. R. HOLEMAN
BRIAN SKINNER

YORK COLLEGE OF PENNSYLVANIA
JERI LEE JONES

U.S. GOVERNMENT PRINTING OFFICE:1986-748-075/40073